An analysis of FGF-regulated genes during *Xenopus* neural development

Hannah Rebecca Brunsdon

PhD

University of York

Biology

July 2015

Abstract

FGF signalling is pivotal in early vertebrate development and is involved in cell movements, germ layer induction and organogenesis. There is also evidence of an important role of FGF signalling in the specification and patterning of posterior neural tissues. Transcriptional targets of FGF signalling during germ layer specification have been identified recently by previous lab members. However, less is known about FGF targets active during neural development.

The aim of this project was to investigate proximal downstream targets of FGF signalling in the context of early neural development by using drug-inducible forms of *Xenopus* FGF receptors, iFGFRs 1-4. The effect of iFGFR 1-4 induction in *Xenopus laevis* during gastrulation was initially investigated through analysis of a microarray dataset. This, and investigation of phenotypes of embryos expressing iFGFRs, found that each iFGFR had distinct effects upon the *Xenopus* transcriptome and embryonic development.

An RNA-seq based screen was performed to investigate proximal changes to the *Xenopus laevis* transcriptome in the context of neural development, as a result of iFGFR1 or iFGFR4 activation during a period of early neural specification. After filtering the data, 188 genes were found to be affected by iFGFR1 and 274 genes affected by iFGFR4. As well as genes known to regulate posterior neural development, a number of genes regulating laterality, cell cycle and anterior neural development were also identified as being regulated by both receptors. Functional characterisation of a few novel FGF targets identified from the microarray and/or RNA-seq screens was performed using genome editing approaches. TALEN-mediated knockout of one of these targets, *Nek6,* was shown to affect the expression of mesodermal and neuroectodermal genes, as well as affecting FGF signalling itself. This work shows that FGFR1 and FGFR4 have distinct signalling outputs during neural development, but cooperate to specify and pattern the developing *Xenopus* CNS.

Table of Contents

List of Figures

List of Tables

List of Accompanying Materials

CD containing

Movies of Nek6 and Dynll1 movement phenotypes:

1. Nek6 Uninjected control
2. 2ng Nek6 Right TALEN control
3. 2ng Nek6 TALEN
4. Dynll1 uninjected control
5. 15ng Dynll1 morpholino

Supplementary Tables:

Microarray Genelists

1. Genes upregulated by iFGFR1
2. Genes downregulated by iFGFR1
3. Genes upregulated by iFGFR2
4. Genes downregulated by iFGFR2
5. Genes upregulated by iFGFR3
6. Genes downregulated by iFGFR3
7. Genes upregulated by iFGFR4
8. Genes downregulated by iFGFR4

9. List of microarray overlapping genes

RNA-seq Genelists

10. Genes upregulated by iFGFR1
11. Genes downregulated by iFGFR1
12. Genes upregulated by iFGFR4
13. Genes downregulated by iFGFR4

Acknowledgements

I would like to thank those who work in the University of York Technology Facility, particularly Celina Whalley and Toby Hodges for their advice and help with RT-qPCR and RNA seq data analysis. Thanks also go to those who ran my RNA-seq experiment and responded to questions in the University of Liverpool Centre for Genomic Research. I would also like to thank my TAP panel members for their advice and feedback.

I would like to thank my supervisor Harv for the many hours he spent supervising me, reading and re-reading various TAP reports and bits of thesis, providing useful advice and high levels of enthusiasm/commiserations throughout this project! Thanks also to Betsy Pownall for providing a lot of helpful lab tips, advice and biscuits. I could not have asked for a friendlier and more helpful group of fellow frog squadders, and there have been a lot of them during my time in York that have all helped me with blank gels, XXL frogs and degraded RNA. In particular I would like to thank Richard and Simon for being so patient when I started, for continuing to respond to questions and giving so much time to help me well after I should have achieved competency, and they left. I would also like to thank Di for generally being great, knowing everything about any protocol and putting up with my untidiness. I would not have been able to do this PhD without them, and their jokes, tales of Simon's amusing lab injuries and bickering amongst themselves made for a happy lab experience. Thanks also to the Arabidopsis people for fun conversational distractions, being the recipients of occasional neurotic rants about experiments, and donors of philosophical/arty ramblings (mainly Joe).

A very large thank you is in order to Mum, Dad, Emily and Grandparents who have been so supportive (emotionally and financially!) during my degree, masters and this PhD. I am very fortunate to be their progeny/sibling!

Endelig, men viktigst, jeg vil kjempetusenhjertelig takke min fantastisk kjæreste Øyvind. He's always been there on both good days and bad days, has always managed to make me smile, and has never doubted I could do this. Also, his horrible physics symbols and equations have served as a constant reminder of how great developmental biology is.

Author's Declaration

I declare that this is an original piece of work conducted under the supervision of H.V. Isaacs at the University of York. All the data presented is my own work, apart from the following: Injections for the microarray screen were undertaken by HVI and processed by the University of York Biology Technology Facility (with subsequent analysis by myself). Processing and running of samples I collected for RNA-seq was undertaken by staff at the Centre for Genomic Research at the University of Liverpool. Processing of this raw data into FPKM values was undertaken by Toby Hodges of the University of York Biology Technology Facility.

None of the work presented in this thesis has been previously published or submitted for a qualification either at the University of York or at any other institution. However, some parts of this work have been presented in posters at the 14th (2012)/15th (2014) International *Xenopus* conferences.

1 General Introduction

1.1 Introduction

The focus of this project is to identify and characterise FGF signalling targets during *Xenopus* neural development. FGFs are important signalling molecules and essential for a range of diverse processes in development including mesoderm and neural induction, patterning in neural and limb tissues, somitogenesis, myogenesis and left/right asymmetry (Slack et al. 1987; Lamb & Harland 1995; del Corral et al. 2003; Niswander et al. 1993; Dubrulle et al. 2001; Fisher et al. 2002; Meyers & Martin 1999). After embryonic life, FGF signalling is important for regulating cell proliferation, differentiation and survival in the adult, so it is not surprising that abnormal FGF signalling during development is implicated in many disorders including the skeletal abnormalities achondroplasia and Apert syndrome, and cancer (Webster & Donoghue 1997; Turner & Grose 2010).

1.2 FGF Ligands

1.2.1 FGF ligands are organised into subfamilies

FGFs were discovered when they were isolated from the bovine brain and found to have mitogenic properties when added to cultured fibroblasts (Gospodarowicz 1975). FGFs have since been found to be well conserved throughout evolution as orthologues can be found in all metazoans (Böttcher & Niehrs 2005). Two FGF orthologues have been identified in *Caenorhabditis elegans* – *Egl17* and *Let756*. The ascidian *Ciona intestinalis,* which is studied as a model of an ancestral chordate, has 6 FGF-like genes. This suggests numerous duplication events occurred during early metazoan evolution after the divergence of protostomes and deuterosomes (Itoh & Ornitz 2008). These *Ciona* FGFs are known as FGF4-like, FGF5-like, FGF8-like, FGF9-like, FGF10-like and FGF 13-like, indicating that the precursors of these subfamilies were present in the chordate lineage ancestral to modern vertebrates (Itoh & Ornitz 2004; Itoh & Ornitz 2011).

22 FGF ligands have been identified in higher vertebrates and are functionally divided into three groups – paracrine, endocrine and intracrine. The evolutionary progression of the mammalian FGFs was proposed as follows: FGFs derived from FGF5, 8 and 10-like conserved their secreted signalling sequence and heparin-binding sites and became paracrine FGFs. FGF9 subfamily FGFs also arose in this way but also evolved an uncleaved bipartite signal sequence. There is no ancestral gene of the endocrine FGF15/19 family in *Ciona*, but it is thought that these arose from FGF4 by local gene duplication in vertebrate evolution (Itoh & Ornitz 2011). Two further genome duplications during vertebrate evolution resulted in families of FGF ligands with three or four members (Itoh & Ornitz 2004). Therefore, the FGF family has undergone considerable expansion during evolution from simple metazoan to vertebrate.

On the basis of Itoh and Ornitz's (2008) phylogenetic analyses, human and mouse FGFs have been organised into the families as outlined in Table 1.1. However, after studying the location of FGF genes within the genome rather than just phylogenetic analysis, there is a slightly different interpretation of grouping the FGFs into 6 subfamilies shown in Table 1.2. This is based upon the analysis of gene loci on chromosomes that is thought to indicate more precise evolutionary relationships (Itoh & Ornitz 2008).

Table 1.1 – Phylogenetic-based grouping of FGF ligands

FGF subfamily	Ligands	Receptor Preference
FGF1	FGF1, FGF2 (aka bFGF)	Fgf1 activates all FGFRs, FGF2 – FGFR1c, 3c>2c, 1b, 4
FGF4	FGF4 (aka eFGF),5,6	FGFR1c, 2c>3c, 4
FGF7	FGF3,7,10,22	FGFR2b>1b
FGF8	FGF8, 17*, 18*	FGFR3c>4>1c
FGF9	FGF9,FGF16,FGF20	FGFR3c>2c>1c, 3b>>4
FGF19 – Hormone class	FGF15/19†, FGF21, FGF23**	Hormone class, weakly activate FGFR1c, 2c,3c, 4
FGF11 - iFGFs	FGF11,12,13,14	No known activity

Table 1.2 – Gene location based grouping of FGF ligands

FGF subfamily	Ligands
1	FGF1, FGF2 (aka bFGF), 5
2	FGF3,4 (aka eFGF),6, 15/19, 21, 23**
3	FGF 7,10,22
4	FGF8, 17*, 18*
5	FGF9, 16, 20
6	FGF11, 12, 13, 14

Table 1.1 and 1.2 *FGFs 17 and 18 have not been identified in *Xenopus.* ** FGF23 is duplicated in *Xenopus* † FGF15 has not been identified in humans or *Xenopus* and are likely orthologues. FGF19 has not been identified in mice/rats. Adapted from (Zhang et al. 2006; Pownall & Isaacs 2010)

The FGF ligands have varying affinities to each FGFR and receptor variants. FGF1 is the only ligand that interacts with all four FGFRs, and the other ligands are less promiscuous (Zhang et al. 2006). The binding properties of FGF ligands tend to group within families. For example FGF8 family members only bind FGFRc subforms and FGFR4, and FGF7 family members only bind FGFR1/2b.

There are some small differences between the *Xenopus* and the mammalian FGF repertoire listed in Table 1.1. Recently Lea et al (2009) identified and annotated the *Xenopus tropicalis* orthologues of human and mouse FGF genes. 19 out of the 22 mammalian FGFs were found in *Xenopus.* They found that synteny was largely conserved and upon phylogenetic analysis, the *tropicalis* FGF ligands group into the same subfamilies as mouse and human. However, orthologues for FGF21, FGF18 and FGF17 were not found in *Xenopus* in areas expected to contain them based on synteny. This was partially due to the poor quality of the frog genome in the regions expected to contain those FGFs. Interestingly, there are two paralogues of FGF23 present next to each other, meaning that this gene must have undergone a duplication event during *Xenopus* evolution. Nevertheless, FGFs have been remarkably conserved throughout vertebrate evolution, making *Xenopus* a viable organism in which to study FGF signalling and apply it to mammalian systems.

1.2.2 Structure of FGF ligands

1.2.2.1 Paracrine FGFs

The paracrine FGFs 3-8, 10, 15/19, 17, 18, 21, 22 are secreted proteins with cleavable amino terminal signal peptides for transport through the secretory pathway (Ornitz & Itoh 2001). FGFs 9, 16 and 20 are also secreted proteins but in place of the cleavable regions have an uncleavable bipartite signal sequence (Revest 2000). FGF1 and 2 do not have identifiable signalling sequences but nevertheless are secreted (Itoh & Ornitz 2008). FGFs 1-9 range in size from 150-260 amino acids and have a conserved core region of 120 amino acids. These core regions have between 30 and 70% sequence identity (Ornitz & Itoh 2001; Itoh & Ornitz 2004). FGF10-22 range from 160-250 amino acid residues and again have a conserved 120 amino acid core (Itoh & Ornitz 2004). The core homology domain of FGF ligand folds into a globular trefoil. Paracrine FGFs have a regular trefoil domain of 12 β-strands in contrast to the endocrine FGFs which have an atypical trefoil domain lacking the β11 strand (Mohammadi et al. 2005; Goetz et al. 2007). Paracrine FGFs are secreted proteins that contain binding sites for glycosaminoglycans such as heparan sulphate as well as FGF receptors. Ligands, heparan sulphate chains and the FGFR bind each other in a 2:2:2 configuration on the cell surface to activate FGF signalling (Figure 1.1) (Mohammadi et al. 1997).

1.2.2.2 Intracrine FGFs

The FGF11 subfamily – FGF11-14 – comprises the intracrine FGFs. They are also secreted proteins and contain a nuclear localisation signal, but are unable to bind FGFRs. On this basis it has been debated whether they should be considered 'true' FGFs and so are sometimes referred to as FGF homologous factors (FHFs). FHFs interact with intracellular domains of voltage gated sodium channels as well as the neuronal MAPK scaffold protein Islet-brain-2. Their only known role is to regulate neuronal excitability (Itoh & Ornitz 2011). FGF12-/- FGF14-/- double-knockout mice suffer from severe ataxia and their neurons fire much less readily, with higher voltage thresholds than wild types due to altered sodium channel physiology (Goldfarb et al. 2007).

1.2.2.3 Endocrine FGFs

The FGF19 family is known as the hormone class of FGFs and act in an endocrine manner. Instead of binding to heparan sulphate they use Klotho as a co-receptor to increase affinity between ligand and receptor (Goetz et al. 2007). Hormonal FGFs

are not expressed early during development and mainly function in the adult organism to control metabolism. Examples include FGF19 involved in bile acid metabolism, FGF23 necessary for vitamin D metabolism and FGF21 required for correct carbohydrate and lipid metabolism (Inagaki et al. 2005; Shimada et al. 2004; Kharitonenkov et al. 2005).

1.2.3 Regulation of FGF ligands

FGFs can be regulated by heparin sulphate binding, N-terminal alternative splicing, homeodimerisation and proteolytic cleavage (Goetz & Mohammadi 2013). FGF9 and its family member FGF20 are unique among the FGFs as they can reversibly homodimerise which buries their receptor binding sites – thereby providing a means of auto-inhibition of signalling (Plotnikov et al. 2001). Proteolytic cleavage of the N-terminus of FGF23 has been shown to occur *in vitro*. The truncated FGF23 can no longer bind to the FGFR or Klotho, providing another mode of autoinhibition (Goetz & Mohammadi 2013). Members of the FGF8 subfamily can be alternatively spliced. In the chick, FGF8 is alternatively spliced into an FGF8a and FGF8b form. FGF8b induces the MAPK pathway to a much greater extent than FGF8a. Ectopic expression of FGF8a in the chick neural plate caused posterior transformation of the presumptive diencephalon to mesencephalon. In contrast, ectopic expression of FGF8b changed the fate of the mesencephalon to cerebellum, thus more severely posteriorising the developing brain (Sato et al. 2001). This result was also seen in the mouse model, suggesting the regulation and balance of FGF8 splicing is required for correct mesencephalon and hindbrain development (Liu et al. 2003).

1.2.4 Heparan Sulphate Proteoglycans

Heparan Sulphate Proteoglycans (HSPGs) are located in the plasma membrane and are required as cofactors for a number of signalling pathways including FGF. Heparan sulphates consist of repeating disaccharide units composed of a *N*-uronic acid and a derivative of *N*-glucosamine, the latter of which is variably O-sulphated (Esko & Selleck 2002). The stability of paracrine FGF ligands bound to FGF receptor and thereby the ability of this complex to signal depends on the interaction of both ligand and receptor with HS chains. This interaction therefore forms a tripartite complex by contacting both the receptor and the ligand simultaneously in a 2:2:2 ratio (Pellegrini et al. 2000; Schlessinger et al. 2000). The interaction between HSPG and paracrine FGFs enhances ligand stability. It also sequesters

ligands near FGFRs providing a reservoir for ligand storage, in doing so limiting the dispersion of ligand signalling (Goetz & Mohammadi, 2013).

This requirement of HSPGs for FGF signalling has been demonstrated, as prior digestion of HSPGs by heparanase inhibits the ability of FGF to induce mesodermal genes such as *Xbra* in *Xenopus* animal cap explants (Itoh & Sokol 1994). *In vitro*, the mitogenic property of FGFs is only activated in BaF3 cells transfected with a soluble form of FGFR1 when heparan is also present in cell medium (Ornitz et al. 1992). There are differences in affinities of FGF ligands for HSPGs which affects their signalling. FGF10 has a greater affinity for HS than its sub-family member FGF7. When these FGFs emanate from a source, the varying affinities for HS result in a short steep gradient of FGF10 and a long shallow gradient of FGF7. These different affinities are utilised in the context of branching morphogenesis of ureteric gland buds during murine development. Mutation of Arg^{178} of FGF10 to valine, the corresponding amino acid in FGF7, caused a reduction of FGF10 binding to HS. This caused mutant FGF10 to induce branching rather than elongation of epithelial buds (Makarenkova et al. 2009).

The formation of a tripartite signalling complex is dependent on the pattern of sulphation on 2- and 6-O-sulphate groups (Pellegrini et al. 2000). HS chains containing tri-sulphated disaccharide units for example greatly promote FGF2-FGFR1 interactions (Lundin et al. 2000). Differential signal transduction through FGF1 and FGF2 was found to be mediated by oligosaccharide length and sulphation pattern in cell culture. This suggests that as well as being required for FGF ligand to receptor binding, HSPGs can also influence the affinities of specific ligands to receptors thereby introducing another level of signal modulation (Pye et al. 2000).

These sulphation patterns are partially controlled by the actions of 6-O-sulfatases Sulf1 and Sulf2. The removal of sulphate groups from heparan sulphate (HS) changes the nature of the interaction of HS to FGFs and consequently the ability of FGF to signal. Loss of HS sulphation in the *Drosophila* mutant *sulfateless* leads to defects in the Wg and FGF signalling pathways (Lin & Perrimon 1999; Lin et al. 1999). The *Drosophila slalom* mutant, characterised by unsulphated HSPGs, has defects in FGF and Hedgehog signal transduction (Lüders et al. 2003). This is true in *Xenopus,* as overexpression of *Sulf1* mRNA in ectodermal explants prevented FGF2 and FGF4-dependent mesoderm induction (Wang et al. 2004). This was also

observed in whole embryos, where ectopic *Sulf1* resulted in downregulation of dpERK and the mesodermal FGF targets *Xbra* and *MyoD*. Conversely, Sulf1 morphant embryos exhibited an increase in MAPK signalling and levels of *Cdx4*, suggesting a role for Sulf1 of restricting FGF signalling in the presomitic mesoderm (PSM) (Freeman et al. 2008).

1.2.5 Expression of FGF ligands in the *Xenopus* embryo

Lea et al. (2009) performed a comprehensive *in situ* hybridisation screen using probes for all the *Xenopus tropicalis* FGF ligands to investigate differences in their expression patterns. Interesting variations in expression patterns and timings of ligand expression, even within FGF ligand families, was discovered. Even though FGF1 and FGF2 are in the same family, they have distinct expression patterns within the nervous system. FGF1 is expressed in the brain whereas FGF2 is expressed in the extreme posterior central nervous system (CNS) of the embryo and branchial arches. Other paracrine FGFs family have quite similar expression patterns in the head, somites and branchial arches. The intracrine FGF11 family members FGF12 and FGF13 are expressed in the brain, neural tube and somites, showing that although they do not activate FGF signalling through FGFRs, they are co-expressed in the same places as paracrine FGFs. The hormonal class FGFs in contrast are expressed globally at all stages, lacking distinct expression domains (Lea et al. 2009).

There is also variation between and within ligand families of when FGF ligands are expressed during development. FGF1 and 2 are expressed throughout development, whereas other paracrine FGFs such as FGF3 and FGF7 are expressed only after the onset of neurulation, and FGF6 after stage 30. FGF8 expression peaks in gastrulation and neurulation and then levels sharply decrease. Intracrine FGFs are only expressed past tailbud stage 30 and endocrine FGFs 19 and 22 are expressed only for a brief window during neurulation.

This variety in FGF ligands, their affinities to different FGFRs, as well as spatial and temporal regulation of ligand expression during development points towards a very complicated and nuanced signalling system. This complexity is further increased as there is also variation in FGFRs.

1.3 FGF Receptors (FGFRs)

1.3.1 Structure of FGFRs

There are four main subtypes of FGFR, FGFR1-4. FGFRs consist of an extracellular domain – containing an amino terminal signal sequence and three immunoglobulin-like domains – a single membrane transmembrane spanning domain, and an intracellular domain (Figure 1.1).

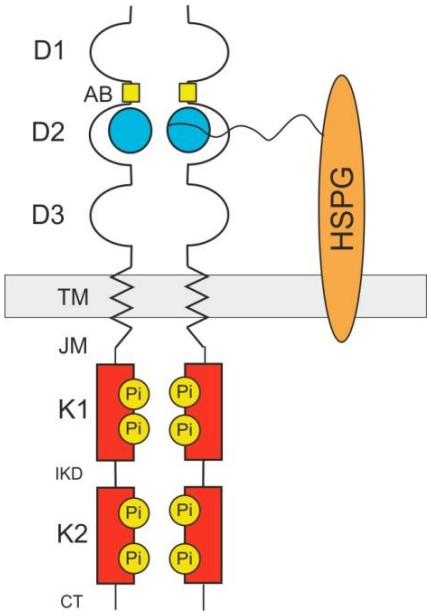

Figure 1.1 Schematic diagram of a FGFR
The extracellular domain of the FGFR contains three immunoglobulin-like domains D1-3. Between D1 and D2 is an acid box region (AB). Ligands bind to D2 and D3, shown in blue, and dimerise the receptor. This interaction is stabilised through interaction between the ligand and receptor with Heparan sulphate chains in HSPGs in the plasma membrane. The extracellular domain of the FGFR is connected to the intracellular via a single pass transmembrane domain (TM). The intracellular domains contain the juxtamembrane region (JM), and two kinase domains (K1 and 2) split by a 14 amino acid interkinase domain (IKD) and finally the carboxy terminal tail (CT). These kinase domains are phosphorylated (Pi) at several tyrosine residues to activate the receptor.

The intracellular domain contains a juxtamembrane domain, a split tyrosine kinase domain and a short carboxy terminus (Gong 2014). The sequence and structural homology between FGFR1 and FGFR2-4 varies. FGFR1 and FGFR2 have a relatively high similarity, as they share 72% amino acid identity. The least similarity is seen between FGFR1 and FGFR4 with only 55% of the amino acid sequence in common. The variability between FGFRs is mainly between extracellular domains, although FGFR4 shares 66-73% sequence identity in the first kinase domain (Kostrzewa & Müller 1998). Perhaps the greatest difference between extracellular domains is due to FGFR1-3 containing 19 exons, whereas FGFR4 contains 18.

The extracellular domain of the FGFR contains three immunoglobulin-like domains designated D1-D3 (also known as Ig1-3). Between the D1 and D2 domains is a 7-8 acidic amino acid motif known as the acid box which electrostatically interacts with a heparan-binding region within the D2 domain. This prevents HSPG binding to the FGFR, and therefore provides a mode of FGFR autoinhibition (Kalinina et al. 2012; Eswarakumar et al. 2005). FGF ligands bind to the D2 and linker region between D2 and D3 via a network of hydrogen bonds, which stabilise the interactions between ligand, receptor and HS chains contacting both ligand and receptor, stabilise the interaction (Goetz & Mohammadi 2013). The tripartite complex of ligand, receptor and HS chain brings the intracellular domains of the FGFR into close proximity. The kinase domains transphosphorylate each other on certain tyrosine residues. Tyrosine residues 463, 583, 585, 653, 654, 730 and 766 are the major autophosphorylation sites for FGFR1 *in vitro*, with Y766 being a binding site exclusively for the SH2 domain of PLCγ (Mohammadi et al. 1996). Mass spectrometry analysis showed that 5 tyrosine sites in the catalytic core of the FGFR1 kinase domain are phosphorylated in a precise order, with Y653 in the activation loop being phosphorylated first. This is sufficient for the subsequent autophosphorylation of the other tyrosines; however the second phosphorylation event of Y654 increases the signal transduction efficiency of FGFR1 1000-fold.The phosphorylated tyrosines are then able to act as docking sites for signalling proteins (Furdui et al. 2006). The signalling proteins are activated by phosphorylation and go on to activate other downstream signalling components.

1.3.2 Alternate splicing of FGFRs produce different variants

1.3.2.1 FGFRIIIb and FGFRIIIc

Alternate splicing of the D3 domain through differential usage of exon 8 and 9 generates different isoforms of FGFR1-3 with distinct ligand binding properties, known as IIIb and IIIc isoforms (Zhang et al. 2006). There is also an IIIa spliceform possible when exon 7 is spliced out, but it has no known function (Duan et al. 1992). FGFR4, with only one exon encoding the c-terminal region of IgIII, does not have this property, and only the IIIb form is translated (Kostrzewa & Müller 1998). IIIb forms are generally restricted to epithelial cell lineages and preferentially bind ligands secreted from mesenchymal tissues, and the reverse is true for IIIc FGFR isoform (Goetz & Mohammadi 2013). This reciprocal expression creates paracrine FGF signalling loops between the epithelium and mesenchyme which are important for developmental processes and homeostasis. For example, during murine lung

development FGF9 secreted by the developing lung epithelium stimulates the proliferation of the mesenchyme while FGF10 secreted from the mesenchyme stimulates budding and branching of the epithelium. FGF9-null mice not only exhibit reduced mesenchyme proliferation in lungs, but also decreased branching of airways. Therefore, bidirectional signalling loops between FGFRIIIb and IIIc isoforms are an important developmental mechanism for coordinating the development of very complex structures (Colvin et al. 2001).

1.3.2.2 FGFR VT+ and VT-

As well as alternative splicing in the extracellular domain of FGFRs, another variant of FGFR1-3 excludes a Valine^{423} and Threonine^{424} (VT) from the juxtamembrane region. These isoforms are known as FGFR VT- and arise from use of an alternative 5' donor splice site (Gillespie et al. 1995). The threonine^{424} is a conserved phosphorylation site, and the VT+ but not VT- form can be phosphorylated by PKC *in vitro* suggesting the two isoforms have different signalling properties (Gillespie et al. 1995).

RNase protection analysis in *Xenopus* blastulae showed the FGFR1 (VT-) is restricted to marginal zones, whereas the VT+ form is present in animal, marginal and vegetal areas (Paterno et al. 2000). This lead to the hypothesis that FGFR1 (VT-) is particularly important for mesoderm development and indeed, the mesodermal marker *Xbra* was expressed as controls in embryos overexpressing FGFR1(VT-) compared to those overexpressing FGFR1(VT+) where *Xbra* was almost non-detectable (Paterno et al. 2000). In *Xenopus*, the VT- isoform of FGFR1 is expressed at very low levels relative to the VT+ isoform except during the mid-blastula transition when it increases in abundance to become the predominant form, before returning to basal levels in later developmental stages. The biological significance of this is unclear as overexpression of VT- did not produce a detectable phenotype (Paterno et al. 2000). Later experiments in 293T cells revealed that the VT region is required for the binding of FRS2 to the FGFR kinase domain. FGFR1 VT- was unable to activate MAPK in mouse embryos suggesting that the inclusion of the VT motif in FGFRs is important for controlling the formation of the FRS2-dependent signalling complex (Burgar et al. 2002).

1.3.3 Expression of FGFRs in *Xenopus*

As with FGF ligands, the four main *Xenopus* FGFR subtypes are expressed in a range of locations and developmental stages in the developing embryo. RT-PCR

using primers against the four receptors in *Xenopus* showed that FGFR1,2 and 4 are expressed throughout development, whereas FGFR3 is first detectable at stage 12 and increased in levels most noticeably after neurulation (Lea et al. 2009). During gastrula stages, ISH on sagittal sections through *Xenopus* embryos showed that FGFR1 is distributed over the ectoderm and mesoderm, including the involuting leading edge. FGFR4 however is confined within, and anterior to, the prospective midbrain/hindbrain boundary in the neural tube (Yamagishi & Okamoto 2010). During *Xenopus* neurulation, FGFR1 is expressed throughout the embryo and FGFR2 throughout the neural plate. FGFR3 is expressed in the anterior neural border (ANB) and the presomitic mesoderm, in contrast to FGFR4 which is expressed in a complementary pattern around the ANB, as well as in the somitic mesoderm and neural plate. By tailbud stages though, the expression patterns of FGFRs are very similar. FGFR1, 3 and 4 are expressed strongly in the brain and eyes, and FGFR2 is less abundant in these areas. FGFR1 and 2 are expressed in the pronephros. All four receptors are expressed in the neural tube, with FGFR1 having a burst of strong expression in the posterior extremity of the developing CNS (Lea et al. 2009).

1.3.3.1 FGFRL1

FGFR-like 1 (FGFRL1) is known as 'the fifth FGFR' and is the most recently discovered member of the FGF signalling family. Its extracellular domain displays up to 50% amino acid sequence similarity to canonical FGFRs (Steinberg et al. 2010). Experiments in cell culture showed that these extracellular domains are able to bind FGF ligands, in particular FGF2, and bind to heparan. In *Xenopus*, *FGFRL1* is expressed in the forebrain, midbrain-hindbrain boundary, neural tube, somites and branchial arches (Hayashi et al. 2004). The FGFRL1-null phenotype is embryonic lethal in mice, which display craniofacial, heart valve and kidney defects, and a hypoplastic diaphragm (Catela et al. 2009).

The intracellular domain of FGFRL1 lacks the FGFR kinase domain required for signal transduction (Trueb et al. 2003). On this basis it was hypothesised that FGFRL1 would interfere with FGF signalling, either by heterodimerising with other receptors and forming non-functional FGFR heterodimers or by competing with FGFRs for ligands (Steinberg et al. 2010). Experiments in cell culture showed the extracellular domain of FGFRL1 was shed from the membranes of HEK293 cells, generating soluble FGF receptors able to scavenge ligands away from canonical FGFRs. Support for FGFRL1 having a detrimental impact on FGF signalling was

shown *in vivo* when FGFRL1 mRNA was overexpressed in *Xenopus* embryos and caused developmental defects very similar to those caused by injection of a dominant negative form of FGFR1 (dnFGFR1) (Amaya et al. 1991; Steinberg et al. 2010). These defects could be partially rescued by injecting FGFR1 mRNA (Steinberg et al. 2010).

1.4 FGF signal Transduction

1.4.1 FGFRs transduce signalling through MAPK, PLCγ and AKT

Following ligand-induced dimerisation and activation of the FGFR, a number of downstream signalling pathways are activated including mitogen activated protein kinase (MAPK), phospholipase C gamma (PLCγ) and rac-alpha serine/threonine-protein kinase (AKT) as illustrated in Figure 1.2.

1.4.1.1 MAPK

An important first step in the MAPK and AKT branches of FGF signalling is the association of FGFR substrate 2 (FRS2) to phosphorylated tyrosines on the activated FGFR intracellular kinase domains (Kouhara et al. 1997). FRS2 associates with Grb2, an adaptor protein, which itself associates with Son of Sevenless (SOS) (Ong et al. 2000). SOS is a nucleotide exchange factor which in combination with Grb2 activates Ras by catalysing the exchange of GDP to GTP. Ras is a GTPase which hydrolyses GTP to GDP, inactivating itself, but it activates Raf by an unknown mechanism. Raf in turn activates by phosphorylation the MAP kinase kinase MEK. MEK then phosphorylates and activates the MAP kinase ERK. ERK is a serine/threonine kinase, which is able to phosphorylate and regulate the activity of transcription factors, such as ETS, which modulate the transcription of FGF target genes. ETS-domain transcription factors, of which there are 22 types in humans, have a winged helix-turn-helix DNA binding domain which allows monomeric binding to sequences with a GGA(A/T) motif (Hollenhorst et al. 2011). Phosphorylation of ETS proteins by MAPK classes such as ERK, JNK and p38 changes their transcriptional functions and therefore their affinities to DNA, co-activator recruitment properties and their subcellular localisation (Selvaraj et al. 2015). A number of ETS transcription factors have been found to be targets for FGF/MAPK signalling (Willardsen et al. 2014). Examples of these include Etv1, Etv4 and Etv5 which are required to regulate the initiation of neurogenesis in the

developing *Xenopus* retina, and induction of atonal-related proneural bHLH transcription factors downstream of MAPK (Willardsen et al. 2014).

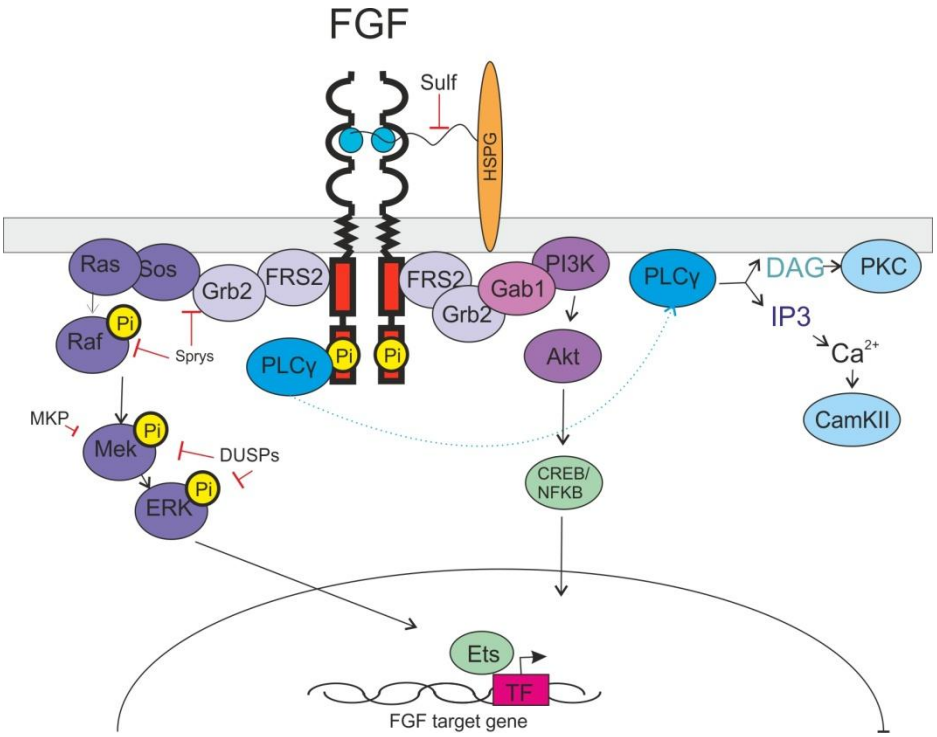

Figure 1.2. Schematic diagram of some aspects of FGF signalling
This is a schematic diagram of FGF signalling based upon figures in Pownall & Isaacs (2010) and Dorey & Amaya (2010). FGFRs dimerise when ligands (blue circles) bind to their extracellular domains. This complex is stabilised by interactions with heparan sulphate chains on HSPGs in the cell membrane. Phosphorylated receptor kinase domains provide docking sites for PLCγ, which then localises at the membrane and hydrolyses phosphatidylinositol 4, 5 diphosphate into IP3 and DAG which provoke a calcium response and activate protein kinase C (PKC) respectively. FRS2 also binds to active FGFRs, and bind to Grb2. To activate the MAPK pathway, Grb2 activates Sos, then Ras, which then phosphorylates and activates MAPK kinases, resulting in phosphorylation and activation of ERK/MAPK. ERK can influence gene expression in the nucleus, usually through ETS transcription factors. Grb2 also interacts with the scaffolding protein Gab1, which associates with PI3K, which phosphorylates and activates Akt (also known as PKB), which transduces signals to the nucleus via CREB and NFκB transcription factors. The MAPK pathway is negatively regulated by Map kinase phosphatases (MKP), Sprys, Dusps, and FGF signalling by Sulf.

1.4.1.2 PI3K/Akt

GRB2 also associates with a scaffolding protein GAB1 to activate the phosphoinositide-3 kinase pathway, which in conjunction with the serine/threonine kinase Akt (also known as PKB) regulates cell survival and growth in normal development (Cheng et al. 1997; Nicholson & Anderson 2002). FGFRs and other receptor tyrosine kinases activate PI-3K, which is recruited to the plasma membrane. Following this, PI-3K phosphorylates phosphatidylinositol-4, 5-bisphosphate (PIP_2) generating phosphatidylinositol-3, 4, 5-trisphosphate (PIP_3). PIP_3 recruits Akt to the plasma membrane and alters its confirmation to allow

phosphorylation and activation by phosphoinositide-dependent kinase 1 (PDK1). Activated Akt regulates several cellular processes, including cell survival and growth (reviewed in Nicholson & Anderson (2002).

1.4.1.3 PLCγ

PLCγ pathway activation is different from that of MAPK and Akt as Grb2 is not required. The Src homology region 2 (SH2) domain of PLCγ binds directly to a conserved phosphotyrosine residue, Y766 in FGF kinase domains (Mohammadi et al. 1991). PLC then hydrolyses phosphatidylinositol-4, 5-diphosphate to inositol-1, 4, 5-triphosphate (IP3) and diacylglygerol (DAG). DAG activates PKC, and IP3 stimulates intracellular calcium release, which activates CamKII, a calcium/calmodulin-dependent protein kinase. This branch of FGF signalling is important for regulation of morphology and cell migration (Dorey & Amaya 2010).

1.4.2 Regulation of FGF signalling

As well as regulation of FGF signalling at the level of the receptor through modifications of HSPG interactions, there are also numerous negative regulators of FGF signalling that act post-translationally to quickly and effectively modulate FGF signalling. Those important for regulating the MAPK pathway, which is the predominant pathway active during neural development, are detailed below (Pera & Ikeda 2003).

1.4.2.1 MAPK phosphatases (MKPs) and DUSPs

The series of phosphorylation events undertaken by the MAP kinase pathway culminating in the phosphorylation of ERK are reversible, and there is a balance between the actions of kinases and MAPK phosphatases (MKPs) rapidly modulating MAPK signal transduction. MKPs are dual-specificity phosphatases and so sometimes known as DUSPs. There is a well-documented negative feedback loop conserved from *Drosophila* to mammals as FGF signalling is required for MKP/DUSP expression (Gómez et al. 2005). Furthermore, MKPs and DUSPs are expressed in overlapping expression domains to FGFs suggesting a close functional link (Gómez et al. 2005; Eblaghie et al. 2003). Some DUSPs, such as DUSP6, only dephosphorylate one MAPK kinase, in this case ERK. This keeps ERK from translocating into the nucleus and affecting gene expression (Pownall & Isaacs 2010).

Application of an FGF4-soaked bead to a chick embryo induced *Dusp6* expression within 1 hour in the chick embryo, whereas beads soaked in the FGF inhibitor SU5402 severely reduced *Dusp6* expression. Furthermore, overexpression of *Dusp6* caused depletion of MAPK signalling, showing that *Dusp6* expression is dependent on FGF signalling and acts via a negative feedback loop to control FGF signalling (Eblaghie et al. 2003). This is also the case in mice, where targeted inactivation of *Dusp6* increased levels of phosphorylated ERK (dpERK) and embryos displayed penetrant phenotypes including dwarfism and coronal craniosyntosis reminiscent of those caused by over-active FGF signalling during development (Li et al. 2007). *Dusp1*, *Dusp5* and *Dusp6* were also shown to have a requirement of FGF signalling in *Xenopus* and repress FGF signalling, with *Dusp6* overexpression blocking FGF-mediated mesoderm induction (Branney et al. 2009; Umbhauer et al. 1995).

1.4.2.2 Sproutys (Sprys)

Spry1 and 2 translocate to the plasma membrane and become phosphorylated on a conserved tyrosine after stimulation by growth factors such as FGFs. They then antagonise MAPK signalling. Therefore, like MKPs, they are dependent on FGF activity. Co-immunoprecipitation experiments in HeLa cells showed Sproutys bind to Grb2 and inhibit its recruitment with Sos to FRS2. *Spry4* has also been shown to bind to Raf to inhibit the MAPK pathway (Sasaki et al. 2003). Overexpression of *Spry1* mRNA in *Xenopus* blocked activation of ERK in cells treated with FGF2 protein in *Xenopus* embryos (Hanafusa et al. 2002).

FGF signalling also feeds into *Spry2* expression by increasing the levels of protein phosphatase 2A (PP2A) *in vitro*. PP2A binding to Spry2 on certain tyrosine residues causes the dephosphorylation of two serine residues in 293T cells. The dephosphorylation results in a conformational change in Spry2, revealing a Grb2-binding motif, necessary for Spry2's subsequent inhibitory activity to the FGF signalling pathway. Interestingly The PP2A binding site is also competed for by c-Cbl which likely targets Spry2 for ubiquitin-mediated decay. Therefore, as well as inducing *Spry2* expression, FGF activation is also needed for Spry2's negative feedback function (Olsen et al. 2006).

1.4.2.3 Spreds

Two Spreds, Spred1 and Spred2 have been identified in *Xenopus.* Spreds are membrane associated proteins that like other negative FGF regulators are

expressed in very similar expression patterns to FGFs in the mouse, chick, rat and frog (Bundschu et al. 2007). Spred1 and 2 inhibit the MAPK pathway via association with Raf. Raf is able to associate with Ras in this complex, but these kinases cannot be phosphorylated and activated by FGFRs in this state, thus inhibiting the MAPK pathway (Wakioka et al. 2001). Overexpression of *Spred1* and *2* in *Xenopus* causes a loss of ERK activity and as a result, a loss of mesoderm specification (Sivak et al. 2005).

1.4.2.4 Sef

In the zebrafish, mouse, chick and rat, Similar Expression to FGF (SEF) is expressed in many sites overlapping with FGFs, hence its name (Grothe et al. 2008). *SEF* encodes a type 1 transmembrane protein. It has similarities with FGFR structurally as its extracellular domain contains an Ig-like segments and its intracellular domain contains tyrosine phosphorylation sites. *SEF* was first identified in zebrafish and found to be positively regulated by FGF, however ectopic *SEF* expression specifically inhibited FGF – therefore SEF is another example of an FGF negative feedback antagonist (Tsang et al. 2002; Grothe et al. 2008). It is thought that SEF interacts with the FGFR itself at the plasma membrane and prevents receptor tyrosine phosphorylation and thus downstream signalling *in vitro.* In zebrafish SEF was found to directly associate with FGFR1, but its exact methods of FGF and inhibition remain unclear (Kovalenko et al. 2003; Ren et al. 2007).

1.4.2.5 FLRT3

The transmembrane protein FLRT3 is an example of an FGF signal modulator that functions in a positive feedback loop with FGF signalling. It is co-expressed with FGFs. Overexpression of FLRT3 in *Xenopus* caused posteriorisation of the embryo resembling embryos injected with FGFR1 or Ras mRNA (Böttcher et al. 2004). In the context of neural development, BMP signalling was shown to inhibit expression of *FLRT3*. Injection of a *FLRT3* morpholino into the anterior neural tissue *Xenopus* embryo resulted in expansion of anterior neural markers *Otx2* and *FoxG1,* and decreased the expression of more posterior markers *En2* and *Krox20* (Cho et al. 2013).

1.4.3 Conclusion

FGF signalling is a very complicated process, with many different signalling outputs possible through variable ligand:receptor interactions, and activation of multiple downstream signalling pathways. FGF signalling is rapidly regulated post-

translationally through the action of kinases and phosphatases, as well as modification of HSPGs. The variety of these responses are very important to safeguard against aberrant cellular behaviour such as uncontrolled proliferation or differentiation that could lead towards pathologies or cell death. In the embryo, FGF signalling is also important for numerous developmental processes, including mesoderm induction, neural induction and patterning.

1.5 Mesoderm Induction

In the classic Spemann Mangold experiments, cells from a region in the dorsal blastopore lip of one newt embryo was transplanted to a ventral region of another embryo. Although the graft cells themselves gave rise to an ectopic neural tube, the surrounding cells formed a complete secondary axis, including mesodermal tissue. Another early experiment by Peter Nieukwoop involved taking animal cap explants from newt embryos, which would ordinarily become surface ectoderm, and combining them with explants from the vegetal endodermal region. This resulted in the spontaneous formation of mesodermal cells formed from the conversion of the ectodermal cells to a mesodermal fate, suggesting that during early development, the endoderm signals to the overlying marginal zone cells, specifying them as mesodermal (reviewed in Pownall & Isaacs, (2010)).

The signal responsible for this induction was hypothesised to be FGFs, as they were the first purified proteins shown to mimic endogenous mesoderm-inducing signals. Slack et al. (1987), found that the addition of FGF2 protein to animal cap explants caused the induction of mesodermal tissues, with lower concentrations of FGF2 inducing mesoderm characteristic of the ventral vegetal region (Slack et al. 1987). This was also found by Kimelman and Kirschner, (1987) who showed that FGF2 was expressed in the *Xenopus laevis* oocyte, as well as throughout early embryonic development (Kimelman & Kirschner 1987). In addition to FGF2, FGF4 was shown by Isaacs et al. (1992) to be an inducer of mesoderm, as *Xenopus* animal cap explants cultured with FGF4 developed a central core of muscle tissue surrounded by mesenchyme (Isaacs et al. 1992). FGF4 was later found to be necessary for the activation and maintenance of the mesodermal marker gene *Xbra*, with *Xbra* activating FGF4 expression itself in a positive feedback loop (Figure 1.3) (Isaacs et al. 1994; Fletcher & Harland 2008). Evidence that FGF signalling was required for mesoderm induction came after the first injections into *Xenopus laevis* embryo with a dominant negative form of FGFR1, dnFGFR1. Embryos expressing

dnFGFR1 displayed a loss of mesodermal tissue (Amaya et al. 1991). These embryos showed a loss of *Xbra* expression, and a lack of muscle differentiation and somitogenesis (Amaya et al. 1993). As well as the requirement for FGF signalling for *Xbra* activation, intact FGF signalling was shown to be required for activation of *MyoD* (Fisher et al. 2002).

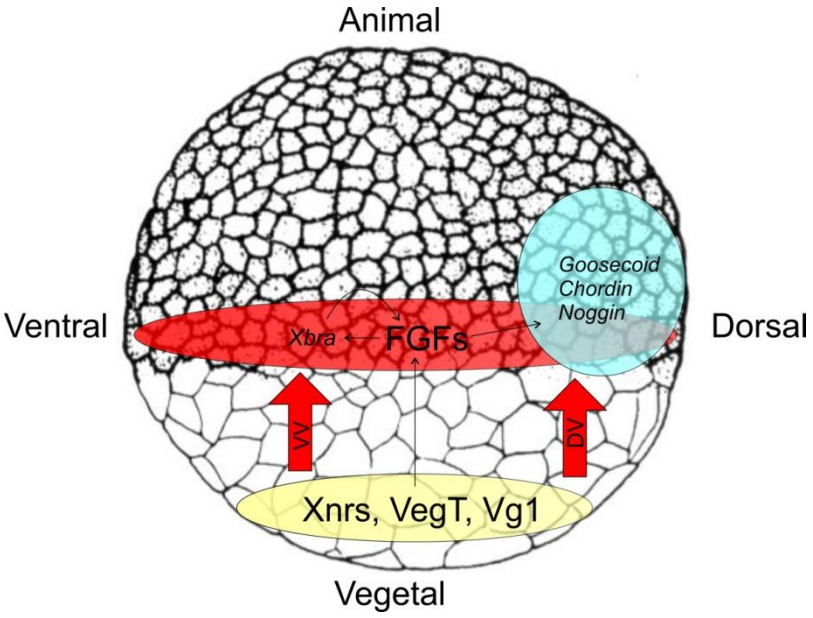

Figure 1.3 – Schematic diagram showing signalling during *Xenopus* mesoderm induction
This is a schematic diagram of a late blastula *Xenopus* embryo (from (Nieukwoop and Faber, 1994)), with the dorsal region to the right and ventral to the left. Activation of *Xnrs*, *VegT* and *Vg1* in the vegetal endoderm region (yellow) converts ectodermal cells in the marginal zone region of the animal pole (red) to mesoderm. These can be divided broadly into ventrovegetal signals (VV, arrowed) and dorsovegetal signals (DV, arrowed). FGF signals in the marginal zone (red) are activated by VV signals. FGF4 activates and maintains the expression of the mesodermal marker *Xbra,* and also activates BMP antagonists in the presumptive Organiser region (blue).

FGFs are not localised at the vegetal pole during blastula stages and are instead present in a characteristic band around the marginal zone where the mesoderm will eventually be specified. This means they are probably not the primary inducers of mesoderm, although they are required for its maintenance and propagation. Such vegetally-located factors have been identified as TGFβ family members, Nodal-related Xnr1, Xnr2 and Xnr4 as well as Vg1 and the T-box transcription factor VegT, the downstream signalling of which are often activated by the commercially-available ligand Activin (Figure 1.3) (Pownall & Isaacs 2010). The action of Activin is therefore routinely used to activate mesodermal tissues in *Xenopus,* particularly when added to animal caps. However, experiments on Activin-treated explants

expressing dnFGFR1 or a dominant negative form of Ras found that a loss of FGF signalling inhibited the ability of Activin to induce the mesodermal markers *Xbra, Mix1* and *Not-b* and *Actc1* (LaBonne & Whitman 1994). Some genes, such as the organiser gene *Goosecoid* and *Lhx1* were also diminished in dnFGFR1 and activin caps, however to a lesser extent, suggesting that some genes have a higher requirement for FGFs than others (Cornell & Kimelman 1994). This idea was expanded by other groups, who found that at low doses, *VegT* induced *Xbra* in *Xenopus* embryos, but a higher dose is needed to induce the its endodermal target *Sox17.* However, when FGF signalling was inhibited by the addition of SU5402 the expansion of *Xbra* was not seen, suggesting that intact FGF signalling is required for the action of VegT. *Sox17* levels however, were unchanged upon SU5402 treatment. Therefore FGF is required for the activation of *Xbra* by VegT, but is not responsible for all of its mesoderm-inducing effects and thus contributes to different kinds of mesoderm (Fletcher & Harland 2008). FGF4 has been shown to be a direct target of Activin (Fisher et al. 2002). Therefore, Nodal signalling from the vegetal pole of a blastula staged *Xenopus* embryo activates FGF4 and FGF8 in the marginal zone. FGFs then activate mesodermal genes such as *Xbra* and *MyoD* to specify and maintain a mesodermal fate (Fletcher & Harland 2008; Pownall & Isaacs 2010).

However, there is evidence to suggest that the FGF/Xbra feed-forward loop does not exist in other organisms, or may not be the sole mesoderm-inducing pathway in *Xenopus*. As well as FGF, *Xbra* is also a direct target of zygotic Wnt signalling in *Xenopus*. However, Wnt signalling may not be sufficient for *Xbra* expression as addition of FGF2 protein can bypass the requirement of intact Wnt signalling for *Xbra* expression upon Wnt inhibition (Vonica & Gumbiner 2002). In mouse embryos, the knockout phenotype for the Wnt transcription factors, *Lef1* and *Tcf1* has a very similar somitic phenotype to loss of *brachyury*, suggesting a functional link between *Brachyury* and Wnts in higher vertebrates (Galceran et al. 1999). In zebrafish, there are two *Xbra* orthologues - *Ntl* and *bra*. Loss-of-function experiments by Martin and Kimelman, (2009) using morpholinos against *Ntl* and *Bra* show that *Fgf8* expression is unchanged in paraxial mesoderm, whereas *Wnt3* and *Wnt8* gene expression was reduced. Conversely, overexpression of *Ntl* caused upregulation of *Wnt8*. Furthermore, a dominant-negative construct of *Tcf1* caused loss of both *Ntl* and *bra* in fish embryos, suggesting that in this organism, it is a feed-forward loop between *bra/Ntl* and Wnt signalling that is predominantly required for mesoderm induction and maintenance (Martin & Kimelman 2009). Therefore,

Wnt signalling may also be required with FGF signalling to induce and maintain the mesoderm.

A microarray-based screen of genes affected by FGF signalling during mesoderm induction was undertaken by Branney et al. (2009). This found 67 genes positively regulated, and 16 genes negatively regulated by FGF signalling at this time. Key findings were that negative regulators of the MAPK signalling pathway such as *Spry2, Dusp5* and *Mkp1* were downregulated, indicating multiple negative feedback loops operational during mesoderm induction to regulate FGF signalling output. Also, pluripotency genes such as *Lin28* and *FoxD3* were upregulated by FGFs. Importantly, during this period of mesodermal specification FGFs signalling was shown to be also active in the dorsal mesoderm activating *Chordin, Noggin* and *Goosecoid* in the Spemann's Organiser region. These genes encode BMP antagonists which are required for neural induction (Branney et al. 2009; Fletcher & Harland 2008).

1.6 Neural Induction

Neural induction is the process by which pluripotent cells in the early embryo receive particular signals that instruct them to adopt a neural fate. It is thought that this induction happens in the early gastrula, as birth of primary motor neurons and sensory neurons rapidly rises during gastrulation in *Xenopus* (Lamborghini 1980; Schlosser et al. 2002).

1.6.1 The Spemann Organiser

Neural induction has been extensively researched ever since the famous embryological experiments of Spemann and Mangold in 1923. The transplantation of cells from above the dorsal blastopore lip to the ventral side of another embryo resulted in antero-posterior axis duplication and the formation of an ectopic second head where the embryo would otherwise have formed epidermis. Cells surrounding the transplanted graft became axial mesoderm and neural tube (reviewed in Hemmati-Brivanlou & Melton 1997). Therefore cells from this region are not only following signalling pathways to become neural in nature, but are capable of signalling to surrounding cells to follow the same developmental program. There has since been decades of research into what exactly the nature of these signals are.

1.6.2 BMP inhibition causes neural induction by a default mechanism

It was hypothesised based on Spemann and Mangold's observations that cells of Spemann's organiser must secrete molecules to surrounding tissues to induce neural differentiation. This was supported by early work in using *Xenopus* ectodermal explants. If explants were dissociated for 5 hours, cells spontaneously differentiated into neural cells in the absence of any other treatment (Godsave & Slack 1989; Grunz & Tacke 1989). However, if these dissociated cells were allowed to re-aggregate within a period of 5 hours, epidermal differentiation would take place (Grunz & Tacke 1989). These experiments suggested that it was the cessation of signalling events between cells that induced a neural fate rather than a positive transforming substance that actively converted epidermal signals to neural.

Whilst screening for secondary axis inducers, Smith and Harland (1992) isolated Noggin which was secreted from the Organiser. *Noggin* mRNA injected into ventral cells of UV-irradiated *Xenopus* embryos, partially rescuing the loss of body axes (Smith & Harland 1992). Furthermore, *Noggin* overexpression in the direct-developing frog *Eleutherodactylus coqui* was sufficient to induce a secondary axis (Fang et al. 2000). Another molecule secreted from the Organiser – Chordin – was identified as a BMP4 antagonist and caused ectopic neural induction (Sasai et al. 1995). BMPs are part of the TGFβ family of signalling molecules, expressed ventrally and are required for epidermal differentiation. Both Noggin and Chordin bind BMP ligands extracellularly and prevent ligand association to BMP receptors, thus are BMP antagonists (Piccolo et al. 1996; Zimmerman et al. 1996). Therefore it was hypothesised that inhibition of the BMP signalling pathway in prospective neuroectoderm pushed cells surrounding the organiser to a neural fate. Repression of the BMP pathway by injection of mRNA coding cleavage mutants of *BMP7* and *BMP4* into naïve *Xenopus* ectodermal explants caused spontaneous expression of the neural tissue marker *NCAM* (Hawley et al. 1995). The presence of a dominant negative mutant of another member of the of the TGFβ signalling pathway *Activin*, or its antagonist *Follistatin*, both potently neuralised ectodermal explants (Hemmati-Brivanlou & Melton 1994). Furthermore, it was found in whole embryos triple knockdown of *Chordin, Noggin* and *Follistatin* caused complete ablation of the neural plate in *Xenopus* embryos, with a concurrent expansion of posterior and ventral fates (Khokha et al. 2005). Taking all this evidence together lead to the postulation of a 'default' model for neural induction - unless told otherwise, the

default inhibition of the BMP signalling pathway is necessary and sufficient for complete neural induction (Hemmati-Brivanlou & Melton 1997).

1.6.3 Problems with the default model

However, later experiments in amniotes and mammals challenged the default model. In chick embryos, blocking BMP signalling via electroporation of the BMP signalling inhibitor *Smad6* was not sufficient to induce the pan-neural marker *Sox3* in epiblasts. Furthermore, injection of *Smad6* mRNA into the ventral A4 blastomere of a *Xenopus* embryo also failed to induce the neural markers *Sox3* and *NCAM*, even though epidermal markers were not induced (Delaune et al. 2005; Linker & Stern 2004). These findings could be explained through Smad6 not adequately suppressing the BMP pathway, since in Khokha et al, (2005) only a triple knockdown of BMP antagonists was sufficient to stop neural induction in *Xenopus* (Khokha et al. 2005). Therefore, a more potent BMP inhibitor based on a dominant negative Smad5 in fish (Smad5-sbn), which forms a non-functional complex with Smad1/5 & 8, was used. Overexpression of *Smad5-sbn* in ventral epidermis was capable of inducing neural marker genes autonomously, however this induction required the maintenance of FGF signalling (Linker & Stern 2004).

Further research in the chick showed that, unlike in *Xenopus*, over-expression of BMP4 in the prospective neural plate at any stage of development did not prevent neural development, and ectopic expression of *Chordin* or *Noggin* could not induce an ectopic neural plate (Streit et al. 1998). Also in the chick, BMP4 overexpression caused inhibition of the neural marker *Sox2* but not its upstream activator *Sox3. Sox3* was therefore still able to influence neural induction - so BMP inhibition could be a later incomplete influence on neural induction and preceded by something else (Linker & Stern 2004). In mammals, mice lacking *Noggin, Chordin* or both of these still form a nervous system where all but the anterior-most structures are present (McMahon et al. 1998; Bachiller et al. 2000; Belo et al. 2000; Mukhopadhyay et al. 2001) Taken together, these experiments suggest that although BMP inhibition is necessary for neural induction, it is not sufficient and other factors must be required for complete neural induction.

1.6.4 FGF as a neural inducer in combination with BMP signalling

As alluded to by Linker and Stern (2004), research occurring in parallel in *Xenopus* and other model organisms pointed towards FGF signalling playing an important

role in neural induction. In ascidians, FGF signalling is the endogenous neural inducer, showing that there is a precedent in evolutionary history for FGF to be involved in neural induction – FGFs 8/16/20 induce neural tissue in the ectoderm via synergy with maternal response factors Ets1/2 and GATA (Bertrand et al. 2003). As with higher vertebrates, it is the MAPK pathway that is required for the acquisition of neural fates in otherwise epidermal cells, which further points to an evolutionary requirement for this pathway (Hudson et al., 2003). FGFs are expressed strongly in the posterior mesoderm – as are secreted BMP inhibitors – and so are present at the correct time and place to participate in neural induction. The addition of FGF2 to *Xenopus* ectodermal explants caused induction of posterior neural markers such as *HoxB9* independent of its role in mesoderm induction (Lamb & Harland 1995) In the chick, blocking FGF signalling activity using the FGFR1 inhibitor drug SU5402 inhibited the induction of *Sox2* and *Sox3* by Hensen's node (a homologous structure to Spemann's organiser) (Streit et al. 2000; Kuroda et al. 2005). However, FGF cannot be sufficient for neural induction because after addition of the FGF inhibitor drug SU5402, nodes still lengthen and express *Chordin* (Streit et al. 2000). In animal caps, it is only through a combination of FGF signalling and *Noggin* expression that the full range of anterior and posterior neural markers is expressed (Lamb & Harland 1995).

One way FGF can work through BMP inhibition is by mutual antagonism between FGF3 and BMP4/7. As FGF3 expression rises in the chick epiblast, BMP4 and 7 levels fall and are thereby restricted to areas fated to be epidermis (Wilson et al. 2000). Overexpression of FGF3 causes ectopic *Chordin* expression at the expense of BMP4 (Kudoh et al. 2004). This restriction of BMPs through FGF antagonism is also seen in the zebrafish, independent of the actions of Chordin and Noggin (Fürthauer et al. 2004). Furthermore, FGF signals are required for *Noggin* and *Chordin* expression, thus there a BMP antagonist/FGF feed forward loop to further promote neural induction (Branney et al. 2009; Delaune et al. 2005; Fletcher & Harland 2008). The ways in which FGF signalling affects the expression of proneural genes by itself or through interaction with the BMP or Wnt pathway is shown in Figure 1.4.

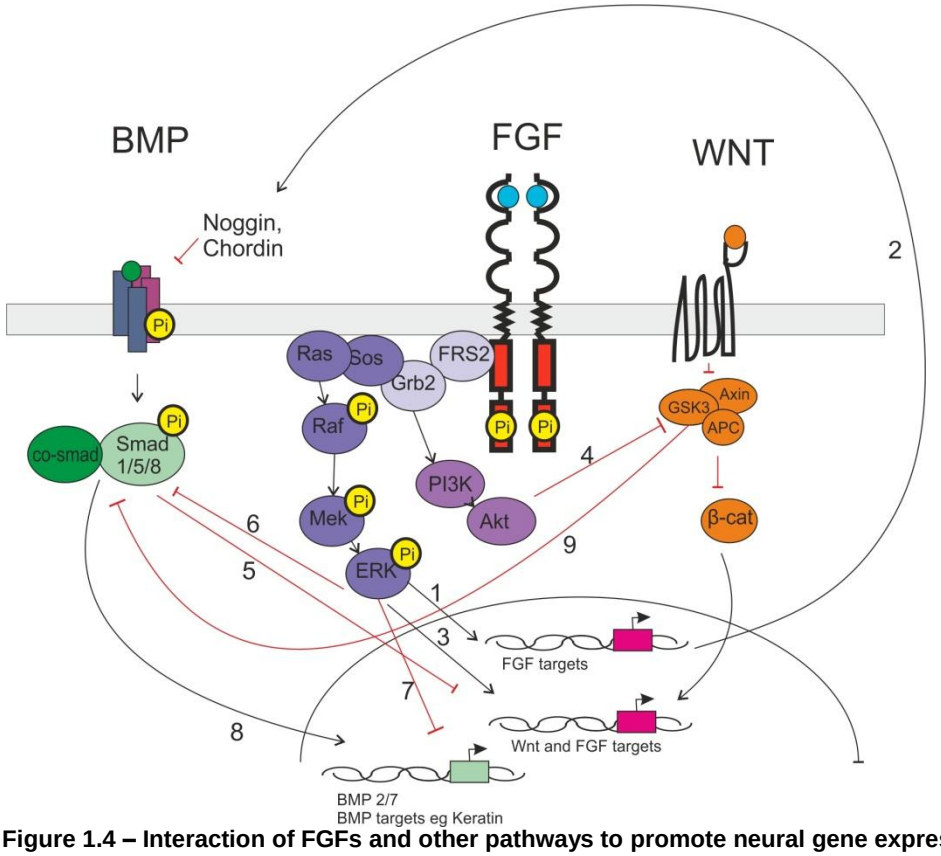

Figure 1.4 – Interaction of FGFs and other pathways to promote neural gene expression
This is a schematic diagram based upon those in Pownall & Isaacs (2010). 1)FGF activates some neural genes directly, such as *Dazap2, Zic3* and *Htra1* (Roche et al. 2009; Marchal et al. 2009; Hou et al. 2007). FGF also activates the BMP antagonists *Noggin* and *Chordin* which are required for anterior neural induction (2) (Kudoh et al. 2004; Branney et al. 2009). 3) Wnt and FGF cooperate to activate some posterior neural genes, such as *Cdx4* (Keenan et al. 2006), and Akt is thought to activate Wnt signalling by phosphorylating and inactivating GSKβ (4) (Hashimoto et al. 2002). 5) BMP signalling inhibits the expression of neural FGF targets. 6) active ERK phosphorylates BMP effector Smad1/5/8 sequestering it in the cytoplasm (Fuentealba et al. 2007; Kuroda et al. 2005) and also directly represses the activation of BMP2/7 ligands (7) (Fürthauer et al. 2004). This prevents BMP signal-mediated activation of epidermal genes (8). MAPK also primes GSK3 which marks Smad1 for ubiquitination (9) (Pera et al. 2014).

A site of convergence for FGF and BMP signalling is Smad1 (Kretzschmar et al. 1997; Pera & Ikeda 2003). When phosphorylated through BMP signalling, Smad1 translocates to the nucleus and activates BMP target genes. However, the FGF MAPK effector dpERK can phosphorylate the linker region of Smad1 at four conserved MAPK (PXS[PO3]P) sites (Fuentealba et al. 2007; Kuroda et al. 2005). This sequesters Smad1 in the cytoplasm, inhibiting activation of BMP target genes. The MEK inhibitor U0126 normally blocks neural differentiation in dissociated *Xenopus* explants. However, when a linker mutant *Smad1* (*LM-smad1*) lacking MAPK binding sites is expressed in the explants, *Sox2* and *NCAM* expression is lost and instead epidermal *cytokeratin*, is upregulated (Kuroda et al. 2005).

Therefore, although not sufficient, FGFs are necessary for neural induction. This is partially through their negative effects on BMP signalling which complement the BMP inhibition by BMP antagonists that is the essence of the default model.

1.6.5 FGFs work independently of BMPs

As well as inducing neural tissue through the direct or indirect inhibition of BMP signalling, FGFs have also been shown to promote a neural fate independent of BMP antagonism (Figure 1.4). Using a combination of the FGFR1 inhibitor SU5402 and/or knockdown of BMP antagonists showed that posterior neural markers are more susceptible to depletion upon FGF inhibition, whereas BMP activity was more likely to affect anterior neural tissue (Wills et al. 2010). The injection of dominant negative *FGFR1* mRNA into *Xenopus* did not prevent Noggin inducing the most anterior neural structures, however more posterior tissues such as the hindbrain and spinal cord were compromised (Ribisi et al. 2000). This splitting up of neural induction into anterior control by BMP antagonism and posterior induction by FGF activity is important for patterning the early nervous system and will be discussed later. Other research shows that FGF signalling targets overlap with BMP antagonist targets spatially and temporally but work independently. Work on early neural targets *Zic1, Zic3* and *FoxD5a* in *Xenopus* showed that *Zic3* and *FoxD5a* are FGF targets, whereas *Zic1* is an immediate-early target of BMP inhibition (Marchal et al. 2009). Morphants of both Zic1 and Zic3, although regulated by different signalling pathways, showed that both of these genes were required for neural fate acquisition, and therefore cooperation as well as separate signalling between the BMP and FGF targets are needed for correct progression through the neural program (Marchal et al. 2009). In the chick a similar result was found after a differential screen searching for genes induced by a Hensen's Node graft. One novel gene encoding an uncharacterised protein, *Asterix*, is dependent on FGF signalling for activation. FGFs can synergise with BMP signalling to activate the uncharacterised gene *Obelix* but is neither necessary nor sufficient for induction of the neural plate marker *TrkC* (Pinho et al. 2011). Other research has suggested that some early onset genes require a mixture of both FGFs and BMPs (Rogers et al. 2011). Therefore, FGFs are required for the acquisition of neural fate, particularly posterior neural fate. FGFs work independently or in cooperation with BMP antagonists to induce the full neural program of anterior and posterior neural markers.

1.6.6 Other Pathways as well as FGF signalling have roles in neural induction

Various research groups have found that signalling pathways other than BMP and FGF have important roles in neural induction. *Wnt* signalling is important for neural induction, as injection of *Wnt1* mRNA opposite the future Spemann Organiser in *Xenopus* embryos caused axial duplication and the formation of secondary head-like structures (McMahon & Moon 1989). As well as BMP antagonists, Wnt antagonists such as Cerberus and Dkk are also secreted from the Organiser. Co-injection of both Wnt and BMP inhibitors is more likely to induce forebrain compared to injection of BMP inhibitors alone (Niehrs & Feld 1999). Like FGFs, canonical Wnt signalling is mutually antagonistic to BMP4 expression and so can restrict BMP4 signalling to the anterior of the embryo (Baker et al. 1999). Insulin-like growth factor (IGF) signalling also phosphorylates the linker region of Smad1, thereby repressing BMP signalling, and injection of a dominant negative IGFR blocks neural induction by Chordin (Pera & Ikeda 2003). Finally, Hedgehog signalling can induce anterior neural markers in explants (Lai et al. 1995). This may be because a common target of Hh and Wnt, Suppression of Fused (Sufu) induces expansion of the epidermis at the expense of neural plate tissue in *Xenopus* (Min et al. 2011).

To summarise, FGF plays a pivotal role in neural induction by both contributing to BMP pathway repression and also by independently activating genes required for the onset of neural development. FGF manipulation has a larger influence on posterior neural development relative to anterior, and this is important for patterning the early CNS. Lastly, there is still much unknown about the roles and importance of other signalling pathways involved in neural induction, either in concert with or independent of FGFs. Induction of the complete neural program is probably much more complicated than the original default model would suggest.

1.7 Neural Patterning

As well as being important for neural induction, FGF signalling is also required for the patterning of neural tissue. FGF signalling emanating from the posterior of the embryo creates a gradient which patterns the spinal cord and posterior hindbrain along the antero-posterior axis.

1.7.1 FGF signalling promotes a posterior neural fate

In 1954, Nieuwkoop and Nigtevecht articulated an 'activation-transformation' model for antero-posterior patterning of the CNS. This proposed that the first patterning step is the activation of anterior neural fate with the specification of the forebrain. The next patterning step involves a 'transforming' signal, which converts some of the forebrain primordia into more posterior fates (Nieuwkoop & Nigtevecht 1954). The existence of this transforming signal was realised when folds of competent ectoderm were grafted to different locations along the antero-posterior axis of the *Xenopus* embryo. These graft cells took on the characteristics of the surrounding areas suggesting that both activation and transformation of cell fate had taken place in these explants. The activation transformation model has since been modified to describe an activation step generating a transient 'pre-neural state'. The transformation step requires signals to maintain an anterior neural fate for some stem cells, but for a sub-population of these cells caudalisation signals act to transform them into a more posterior fate (Stern 2001).

One of the candidates for the transformation signal was identified as FGFs, and FGFs were found to be necessary for both inducing neural development but they are also required for caudalising and patterning neural tissue. *Xenopus* prospective forebrain explants cultured with FGF2 caused them to become more posterior in character and express hindbrain and spinal cord markers (Cox & Hemmati-Brivanlou 1995). Conversely, upon transplantation of dnFGFR1-expressing cells to a zebrafish embryo to the dorsal neuroectoderm, it was observed that the dnFGFR1 cells incorporated themselves into more anterior neural structures as development progressed (Kudoh et al. 2004). In *Xenopus* embryos, overexpression of *FGF4* caused expansion of posterior neural tissue at the expense of anterior structures, whereas inhibition of FGF signalling caused posterior truncations and anteriorisation of the embryo (Pownall et al. 1996; Monsoro-Burq et al. 2003). This suggests that FGF signalling is required for specification of posterior neural fates, and conveys positional information along the antero-posterior body axis.

1.7.2 FGF signalling patterns the Antero-Posterior Axis through the regulation of *Cdx* and *Hox* genes

1.7.2.1 Evolution of *Cdx* and *Hox* genes

Cdx genes are part of the parahox family, which also includes the genes *Gsx* and *Pdx/Xlox*. The Parahox genes reside in a single genomic locus, unlike their

evolutionary sister family the Hox family. Parahox and Hox genes have a common 60 amino acid DNA-binding motif – the homeodomain – and act as transcription factors. There are two distinct classes of homeodomain in animals – ANTP and PRD – as well as more divergent classes LIM, POU SINE and TALE. The ANTP class is split into NK-like genes and the Hox/Parahox group. The Hox and Parahox gene families arose from a single Protohox gene cluster during the divergence of Cnidarians and bilatarian clades (Chourrout et al. 2006; Garcia-Fernàndez 2005). During vertebrate evolution, the Hox gene cluster underwent a series of duplications producing a number of sub-families and map to several chromosomes, however the Parahox cluster occupies a single genomic locus (Holland & Takahashi 2005).

There are three *Cdx* genes, *Cdx1*, *2* and 4 in mouse and *Xenopus* which have been well conserved throughout evolution. Most vertebrates have 39 *Hox* genes, organised into four separate chromosomal clusters A-D. Each subfamily contains 13 paralogues (Lappin et al. 2006). *Hox* family members have several unique properties. They display spatial collinearity as the 5' to 3' chromosomal arrangement of each *Hox* gene on its cluster corresponds to its expression pattern from posterior to anterior along the antero-posterior axis of the embryo. Secondly *Hox* genes display temporal collinearity as 3' Hox genes are activated earliest in development and more 5' genes activated successively afterwards (Montavon & Soshnikova 2014).

1.7.2.2 *Cdx* genes posteriorise the embryo and activate posterior Hox genes

FGFs regulate *Hox* genes in part through their regulation of *Cdx* genes (Pownall et al. 1996). *Cdx* genes were identified first as the *caudal* gene in *Drosophila,* and are required for normal posterior development and patterning (Mlodzik & Gehring 1987). Overexpression of *FGF4* in *Xenopus* embryos caused an anterior expansion of *Cdx4* and *HoxA7* expression domains, which was sufficient to cause development of posterior structures at the expense of the head (Isaacs et al. 1994; Pownall et al. 1996). On this basis, it was suggested that the pattern of *Hox* genes is regulated by the Cdx family expressed in posterior nascent tissues of the three germ layers in a posterior to anterior gradient (Isaacs et al. 1998; Bel-Vialar et al. 2002).

Evidence for this has been shown in a number of experiments in zebrafish. Zebrafish embryos homozygous for the autosomal recessive mutant *kugelig* are characterised by their tail defects as well as aberrant antero-posterior patterning (Davidson et al. 2003). This was found to be due to a mutation in *Cdx4,* and could

be rescued by *Cdx4* mRNA injection which restored the expression of *HoxA7*, *HoxB7* and *HoxB9* (Davidson et al. 2003). Later work by the same group involved injection of morpholinos for Cdx1 into heterozygous zebrafish Cdx4+/- embryos. This did not produce additional morphological defects relative to Cdx4-/- embryos, but doubly deficient Cdx1-MO/Cdx4-/- embryos displayed very severe posterior defects. This suggested that both Cdx1 and Cdx4 are required for correct posterior development, but act in a partially redundant fashion. This was supported by their individual and combinatorial effects upon *Hox* gene expression. *Cdx1* morphants and morphant/*Cdx4+/-* embryos both displayed shortened *HoxB7* and *HoxB9* expression domains which was even more severe in double mutants (Davidson & Zon 2006). Individual and combined knockdowns of *Cdx1*, *Cdx2* and *Cdx4* in *Xenopus* caused severe posterior truncations and a reduction in 5' *Hox* gene expression (Faas & Isaacs 2009). Conversely inactivation of *Cdx1* and *Cdx2* via homologous recombination in the mouse caused anterior homeotic transformations – that is, vertebra 7 resembled the more anterior vertebra 6 – and this corresponded to a reduction and posterior shift in *Hox* gene expression domain (Subramanian et al. 1995).

The posterior to anterior gradient of FGF and Cdx activity is sharpened by the decay of *Cdx* transcripts anteriorly as the embryo lengthens and grows which also defines *Hox* gene expression (Gaunt et al. 2003; Gaunt et al. 2005). This gradient is also opposed by a gradient of retinoic acid (RA) signalling, which is required for the specification of more 3' Hox genes in the hindbrain (del Corral et al. 2003). A mutually repressive relationship between Cdx activity and the anteriorising activity of retinoid signalling in the spinal cord has been demonstrated. Whereas *Cdx4* directly activates posterior *HoxC6*, *HoxA7*, *HoxB7* and *HoxB9* in a dose-dependent manner, it inhibits the expression of more anterior *HoxB1* or *HoxB3* (Isaacs et al. 1998). In zebrafish, *Cdx1* or *Cdx4* morphant zebrafish embryos were found to exhibit ectopic expression of hindbrain marker *Krox20* and hindbrain neurons more posteriorly than control embryos (Shimizu et al. 2006). As a result of this posterior expansion of hindbrain-fate, posterior-most tissue was responsive to RA treatment, which did not affect the fate of posterior neural tissue (Shimizu et al. 2006; Skromne et al. 2007). Therefore, *Cdx* genes promote a posterior neural fate, whilst also restricting the size of the hindbrain.

1.7.2.3 *Hox* genes pattern the hindbrain and spinal cord

Hox genes are activated and regulated within the elongating neural plate in regions overlapping the domains of the neural progenitors around the node in the chick and mouse. It has been shown that early Wnt signalling is crucial in the initial specification of prospective hindbrain and spinal cord progenitors, which is later refined by retinoid and FGF signals in the ventral neural tube (Liu et al. 2001; Dasen et al. 2003; Nordström et al. 2006). Although *Hox* genes, regulated by *Cdx* genes pattern all three germ layers, the role of *Hox* genes in specifying the neuroectoderm will be discussed below.

1.7.2.4 Hindbrain development and Patterning

The hindbrain or rhombocephalon consists of the cerebellum, pons and medulla and these oversee vital functions (Pownall & Isaacs 2010). During neurulation, the prospective hindbrain is divided into seven regions called rhombomeres. Rhombomeres are composed of discrete cell groups displaying heterochronic patterns of neurogenesis, which give rise to motor or sensory neurons depending on their position along the dorsoventral axis (Clarke & Lumsden 1993). At first the fate of each rhombomere is plastic, but after the onset of *Hox* gene expression cells are committed and do not mix. *Hox1-4* are expressed in the hindbrain and spinal cord, and *Hox4-13* in the spinal cord only (Nolte & Krumlauf 2000). *HoxA2* is the first and most anterior *Hox* gene expressed in the hindbrain, and is expressed in R2. *HoxA2* and *HoxB3* are expressed in R3, thus each rhombomere contains a certain combination of *Hox* genes (Trumpel et al. 2009). Other anterior Hox genes such as *HoxB1, HoxA4*, *HoxB4* and *HoxD4* are regulated by retinoid signalling and contain retinoic response elements in their promoters. For example, *HoxB1* is restricted to R4 through early induction by RA and later repression in R3 and R4 from the RA degradation enzyme Cyp26A1 (Sirbu et al. 2005).

Although FGF signalling does not activate anterior-most *Hox* genes in the rostral hindbrain, low FGF activity activates *Hox* genes indirectly in the caudal hindbrain. In zebrafish, the first rhombomere to appear is R4, and it expresses *FGF3* and *FGF8.* Mis-expression of *FGF3* and/or FGF8 causes the transformation of tissue to R5/R6 fate and ectopic expression of the R5 marker *Krox20*, showing that FGF signalling is needed in an organiser capacity in R4 (Maves et al. 2002). The R5 fate is also regulated by FGF's activation of the R3 and R5 marker gene *Krox20* (Marín & Charnay 2000). In mice, *Krox20* inhibits the more anterior *HoxB1* normally expressed in R1 and R2 to help specify R3 (Barrow et al. 2000). *Krox20* expression

in R5 is also dependent on the transcription factor Mafb, as in Mafb mutants it is restricted to R3 only (Manzanares et al. 1999). *Mafb* is also activated by FGFs and mouse Mafb mutants lack recognisable R5 and R6 (Maves et al. 2002; Giudicelli et al. 2003). Therefore, the actions of Krox20 and Mafb, mediated by FGF signalling are essential for correct caudal hindbrain development.

1.7.2.5 Development and patterning of the spinal cord

Spinal cord motor neurons (MNs) derive from progenitor cells located at a constant point along the dorso-ventral axis along the neural tube. Neurons are organised into columns in the CNS, and *Hox* genes specify their identification and connectivity. MNs acquire their distinct columnar identity depending on their position along the antero-posterior axis of the spinal cord (Dasen et al. 2003).

In the chick, the first step for spinal cord emergence has been proposed to be caudalisation of cells exhibiting forebrain characteristics through exposure to FGF signals from the primitive streak and the paraxial mesoderm (Jessell 2000). The posterior to anterior gradient of FGF signalling activates *Hox* genes at the anterior 3' of a cluster at very low levels of FGF, whereas those at the 5' end are activated at a much higher concentration and after exposure for a greater length of time (Dubrulle & Pourquié 2004).

This graded FGF signal induces the expression of 5' Hox genes at the brachial, thoracic and lumbar levels of the spinal cord in their correct order along the antero-posterior axis (Bel-Vialar et al. 2002). This is seen *in vitro* – explants taken at the thoracic level of chick embryos were cultured with beads soaked with FGF8. As the concentration of FGF was increased, progressively more 5' Hox genes were activated in cells around the bead (Liu et al. 2001). Dasen et al. (2003) studied *HoxC* genes further *in vivo*. *HoxC6* expression in chick MNs was shown to be confined to brachial levels, whereas *HoxC9* is expressed more posteriorly at the thoracic level. *In ovo* electroporation of FGF8 to brachial areas lead to the disappearance of *HoxC6* and ectopic anterior expression of *HoxC9*, indicating a switch from a brachial to thoracic fate. *HoxA9* and *HoxC9* expression domains were also expanded rostrally and neurons did not express *Raldh2*, suggesting an antagonistic relationship between RA pathway members and FGFs caudally (Dasen et al. 2003).

1.7.3 Opposing RA and FGF signals control neural differentiation

1.7.3.1 Retinoic acid signalling patterns more anterior neural differentiation

Retinoic acid and its metabolic products are required for patterning in the hindbrain and rostral spinal cord by regulating the expression of 3' *Hox* genes. Thoracic-level chick embryo explants cultured with retinoic acid receptor (RXR) inhibitor LG100815 caused a loss of *HoxC5* expression, and explants cultured with RA did not express *HoxC6-10* (Liu et al. 2001). Therefore, retinoid signalling promotes an anterior but not posterior neural fate. RA has also been shown to anteriorise caudal neural plate explants in the chick and impose a caudal character to hindbrain cells and rostral character to spinal cord cells – untreated cells expressed a combination of *HoxB4*, *HoxB8* and *HoxB9*, reminiscent of the caudal spinal cord. However, treatment with RA blocked the expression of *HoxB9*, resulting in cells reminiscent of the rostral spinal cord (Nordström et al. 2006). Other work showed that RA treatment could not affect posterior *Hox* genes, as treatment of chick embryos with RA lead to anteriorisation of *HoxB1-5* expression domains but did not affect the expression pattern of the posterior *HoxB6-9*, suggesting a posterior limit to retinoid signal responsiveness (Bel-Vialar et al. 2002).

1.7.3.2 FGF signalling promotes proliferation of neural progenitors, whereas RA promotes neuronal differentiation

In the chick, FGF activity in the posterior of the embryo maintains a proliferating pool of neural stem cells. As the embryo extends in an antero-posterior direction, the front of this gradient moves posteriorly. As the stem cells leave the influence of the FGFs in the 'stem zone' lateral inhibition causes a salt-and-pepper pattern of differentiating neural cells – therefore there is an inverse rostro-caudal gradient of neuronal differentiation (Akai et al. 2005; del Corral et al. 2002). Combinations of genes expressed outside of FGF-influenced areas, such as *NeuroD* and *Ngn1,* induce neurogenesis (Figure 1.5) (del Corral et al. 2003). Blocking FGFR function in the stem zone causes precocious movement of these cells out of the stem zone and into the spinal cord (Diez del Corral et al. 2003). The gradient of FGF proliferative activity is sharpened by a complimentary gradient of RA, which is required for neuronal differentiation and expression of key ventral neural patterning genes (Diez del Corral et al. 2003). Thus, FGF and retinoid signalling mutually antagonise each other to control the onset of neural differentiation.

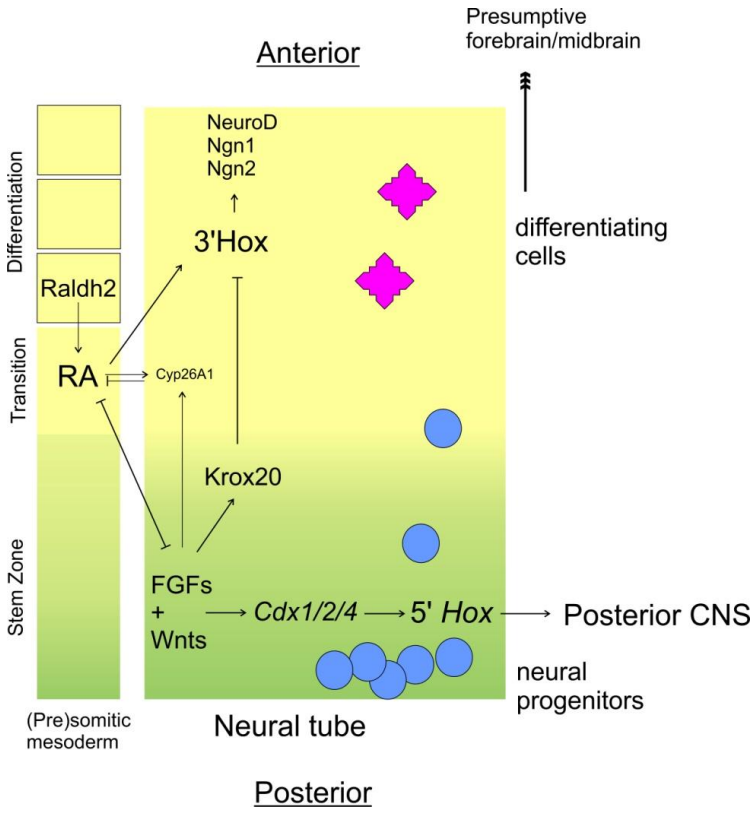

Figure 1.5 – Opposing gradient of FGF and RA pattern the neural tube
A schematic diagram of the presomitic mesoderm and the neural tube during neural development. In the posterior, FGF signalling in the stem zone promotes proliferation of neural progenitors. FGFs with Wnts activate *Cdx* genes, which activate 5' *Hox* genes. FGF signalling also activates *Krox20* which inhibits 3' *Hox* genes. Raldh in the somitic and presomitic mesoderm produces retinoic acid (RA), which mutually antagonizes FGF signalling and its targets. The RA degradation enzyme Cyp26A1 is activated by RA in a negative feedback loop, as well as by FGF signalling. RA signalling activates more 3' Hox genes and promotes differentiation of neural progenitors after they leave the stem zone into motor or sensory neurons depending on the combinations of *Hox* genes expressed in each cell. Neuron-specific markers such as *NeuroD, Ngn1* and *Ngn2* are then expressed.

Specifically, it was found that FGF8 inhibits the RA synthesis enzyme *Raldh2* (del Corral et al. 2003). FGF also activates *Cyp26A1,* an enzyme that triggers RA degradation. *Cyp26A1* is expressed in complementary patterns to RA and sharpens the gradient of RA at both anterior and posterior ends, resulting in a two tailed RA gradient that is highest at the midbrain-hindbrain boundary (Pera et al. 2014).

To summarize, a gradient of FGF signalling emanating from the posterior of the embryo activates *Cdx* and *Hox* genes caudally to pattern the posterior neural tube which later gives rise to the posterior hindbrain and spinal cord. The FGF gradient is opposed by an anterior gradient of RA, which sets the anterior limits of FGF's influence and specifies more anterior Hox genes. As the embryo grows, cells leaving the proliferative zone of FGF signalling are exposed to higher

concentrations of RA, which pushes them to differentiate into neurons based upon the combination of *Hox* genes they express.

1.7.4 FGFs also promote a posterior neural fate through other means, and cooperate with posterior Wnts

1.7.4.1 Htra1 and *Dazap2*

FGFs also promote posterior neural development through the regulation of other patterning genes. *Htra1* is a serine protease that is known to modulate IGF signalling and bind to members of the TGFβ family. Hou et al. (2007) showed *Htra1* also modulates FGF signals and transduces them over long range. Ectopic expression of *Htra1* lead to secondary tail formation and appearance of ectopic neurons over the whole epidermis. Anterior neural markers such as *Otx2* and *Krox20* were downregulated whilst the posterior *Cdx4* was upregulated. Long range transduction of FGF signals through *Htr1a* was shown by combining FGF4-injected ectodermal explants with *Htr1a*-injected explants. Explants injected with *Htra1* only did not extend as much as FGF4-injected caps, however combination explants extended on both sides and induced *Xbra* despite no cell mixing. Therefore genes such as *Htra1* may be important for expanding the range of FGF influence (Hou et al. 2007). FGF also works to pattern the posterior via a feed-forward loop with its target *Dazap2* which is required for patterning the spinal cord. When *Dazap2* was overexpressed in *Xenopus* through mRNA injection, anterior neural markers such as *Otx2* and *Pax6* were reduced. On the other hand, *HoxB9* expression was expanded anteriorly even in the presence of the antimorphic *Cdx4* construct *Cdx4-EnR* and in the presence of a dominant negative form of Wnt8. Therefore *Dazap2* regulates *Hox* gene expression independent of *Cdx* and other pathways (Roche et al. 2009).

1.7.4.2 Wnt signalling promotes posterior neural patterning

Wnts also have an important role to play in antero-posterior neural patterning, and cooperate with FGFs to induce and pattern the posterior neural tube (Figure 1.5). Wnt3a and Wnt8 are expressed dorsally in a posterior to anterior gradient, overlapping with FGFs (Kiecker & Niehrs 2001). *Wnt1*, *Wnt3a* and *Wnt8* are expressed in the CNS and their expression domains overlap in the forebrain, midbrain and hindbrain (Wolda et al. 1993; McGrew et al. 1997). The requirement for Wnt signalling for neural development was shown when disruption of *Wnt1* expression in the murine brain caused severe deformities in the midbrain and cerebellum (Thomas & Capecchi 1990). Wnt signalling also patterns the posterior

CNS. In *Xenopus,* ectodermal explants overexpressing either *Wnt8* or *Wnt3* mRNA were fused with albino animal caps which acted as a 'Wnt acceptor'. Without the presence of *Noggin* no neural marker gene expression was observed, and so Wnts are not sufficient for neural induction. However a double *in situ* against the hindbrain marker *Krox20* and the midbrain marker *En2* showed that these genes were induced in the acceptor explants and maintained their correct antero-posterior patterning – in other words a result which would be expected if both genes' expression required a Wnt concentration gradient (Kiecker & Niehrs 2001).

Similar to FGF signalling, Wnt signalling also promotes proliferation of neural progenitors in the posterior 'stem zone' (Figure 1.5). Overactivation of Wnt signalling induced by lithium chloride treatment on chick embryos caused a reduction in the primary neural marker *NeuroD*, which is essential for the differentiation of neural cells (Olivera-Martinez & Storey 2007).

1.7.4.3 Cooperation between Wnt and FGF signalling

Ectopic *Wnt3a* expression in neuralised animal caps was found to repress the anterior neural markers *Hesx1* and *Otx2* whilst causing an upregulation of the midbrain and hindbrain markers *En2* and *Krox20*. dnFGFR1 alone could not repress *Hesx1* and *Otx2,* and Wnt3a could not repress *Hesx1* and *Otx2* when co-expressing dnFGFR1, unlike *Wnt3a*-injected controls. This suggests that the ability of Wnt to inhibit anterior neural genes is dependent on active FGF signalling (McGrew et al. 1997). An example of this was shown in the chick, where FGF8 was found to be essential for maintaining the expression of *Wnt8c*, which like FGFs, inhibited neuronal differentiation when overexpressed (Olivera-Martinez & Storey 2007).

Although in some cases Wnt signalling is dependent on FGF signalling, both signalling pathways cooperate in some aspects of neural development. Even with normal levels of FGF signalling, expression of dominant negative Wnt8a (dnWnt8a) in chick embryos caused loss of midbrain and hindbrain markers (Kiecker & Niehrs 2001; McGrew et al. 1997). Secondly, Wnts and FGFs cooperate to activate *Cdx* genes. Overexpression of *Frzb* – an antagonist of Wnt1, 3a and 8, and dnFGFR1 in animal caps has an additive effect on the inhibition of *Cdx4*. However, although it was shown that MAPK signalling was imperative for FGF's actions to activate *Cdx4*, Frzb does not downregulate dpERK and so Wnt must activate *Cdx4* via MAPK independent means (Keenan et al. 2006).

Therefore, in both neural induction and in patterning, Wnt signalling is required in conjunction with FGF signalling to specify and pattern the posterior CNS and repress anterior fates.

1.8 Anterior neural patterning with FGFs

1.8.1 FGF signalling in the anterior prospective CNS

As well as inducing and patterning the posterior CNS, FGF signalling is active in the telencephalon and around the midbrain hindbrain boundary (MHB). This is most easily visualised by looking at the distribution of dpERK by whole-mount immunostaining which shows bursts of active FGF activity in the future MHB regions and in the extreme anterior of the neural plate which borders the non-neural ectoderm, known as the anterior neural border (ANB) (Figure 1.6A). Although in the forebrain FGF signalling does not take centre stage, in both the ANB and the MHB FGF8 displays organiser activity and acts as a morphogen to pattern the prospective anterior neural plate.

1.8.2 FGF signalling at the Isthmic Organiser (IsO)

The Isthmus is a constriction located at the midbrain-hindbrain boundary (MHB). To its anterior is the mesencephalon which will eventually give rise to the tectum. To its posterior is the hindbrain, composed of rhombomeres 1-7 (Figure 1.6). Rhombomere 1, the closest structure posterior to the MHB, gives rise to the cerebellum (Sato et al. 2004).

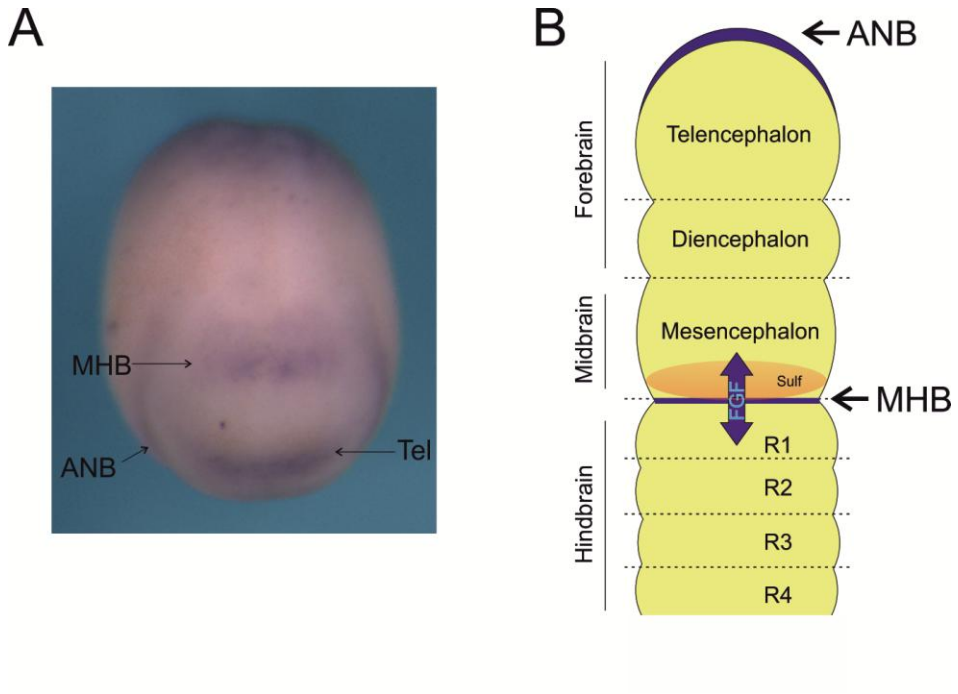

Figure 1.6 – FGF signalling in the forebrain
Figure 1.5A is a dorsal view of a *Xenopus laevis* embryo at neurula stage 17 immunostained with an antibody against diphospho-ERK (ERK). The anterior is facing. DpERK is present in the anterior neural border (ANB), telencephalon (Tel), and midbrain-hindbrain boundary (MHB), as well as in the posterior of the embryo. Figure1.5B is a schematic diagram of the developing brain. Areas of FGF signalling are in blue – around the telencephalon, and at the MHB. The forebrain is divided into the telencephalon and diencephalon. The hindbrain is composed of rhombomeres (R1-4 of 7 shown here). FGF8 emanating out of the IsO in the MHB patterns the rhombomeres and the mesencephalon. It is though that Sulf activity in the mesencephalon provides an asymmetric gradient of FGF8 either side of the MHB, conveying extra positional information to cells.

The Isthmus has been well documented to have an organiser function, and is known as the Isthmic Organiser (IsO). Signals emanating from the IsO pattern surrounding tissues in a dose-dependent manner. This was first shown in chick embryos by grafting the MHB to the posterior forebrain. This produced an ectopic midbrain that was a mirror image to the existing midbrain (Martinez et al. 1991). Further work in the chick found that implantation of an FGF8-soaked bead next to the diencephalon caused surrounding tissue to mimic the more posterior area around the IsO, and become mesencephalic or cerebellar in character (Martinez et al. 1999; Crossley et al. 1996). Therefore, FGF8 was proposed to act as a morphogen secreted out of the Isthmic Organiser (IsO) which is required for correct patterning of the surrounding developing brain tissue.

FGF8 knockout mice and FGF8 knockdown frogs fail to gastrulate, and so the loss of midbrain and cerebellum could be not due to just signalling defects in the IsO. To circumvent this, Chi et al. (2003) made a conditional FGF8 hypomorphic mouse,

where mutant FGF8 was expressed only in the prospective brain. As a result, hypomorphs displayed deletions of mesencephalon/hindbrain derivatives as well as loss of *Wnt1*, *Gbx2* and *FGF17/18* expression in the IsO region (Chi et al. 2003). Conversely, mis-expression of FGF8b by electroporation *in ovo* posteriorised the developing mesencephalon so it differentiated into the cerebellum instead (Sato, Araki, & Nakamura, 2001). Therefore, FGF8 is required for correct midbrain and hindbrain development as well as other genes co-expressed in the region.

Work in other labs around the same time identified a cross-repressive relationship between the transcription factors Otx2 and Gbx2 as being required for correct placement of the MHB, with FGF8 expression at the interface (Broccoli et al. 1999). *Otx2* is expressed in the anterior neural tube and its caudal boundary stops sharply with the MHB/IsO. Ectopic expression of *Otx2* by knocking it into the *En1* locus caused a reduction in size of the cerebellum. This also caused a posterior shift in *Fgf8* expression and the posterior marker *Gbx2*, showing the caudal limit of Otx2 is important for positioning the Isthmic organiser (Broccoli et al. 1999). *Fgf8* in turn also has an influence on *Otx2* expression, as ectopic FGF8 via electroporation repressed *Otx2* and induced *Gbx2* more caudally than normal in the mesencephalon and caudal diencephalon. Therefore, FGF8 exhibits organiser activity in the IsO, and although Otx2 and Gbx2 are required for its positioning, FGF8 has an important role in patterning the IsO and promoting a cerebellar fate. This is clearly illustrated in the *ace* zebrafish mutant, which has a mutation in its *FGF8* gene which renders it non-functional – these fish lack a cerebellum, telencephalic midline structures and the IsO (Reifers et al. 1998; Shanmugalingam et al. 2000).

More recent experiments showed that tissues surrounding the IsO respond to FGF activity in a graded manner – at a low level FGF activity specifies the mesencephalon and a much higher level is needed to specify rhombomere 1 (Basson et al. 2008). Genes close to the IsO have a higher threshold for FGF activation, such as *EphA*, than those in more anterior midbrain such as the *EphA* receptor (Chen et al. 2009). However, there is an ongoing question of how is a cell to know based upon its proximity to the IsO whether it is anterior or posterior to the MHB. This could be because of asymmetrical placement and activities of FGF signalling modulators either side of the IsO. The gradient of *FGF8* across the IsO requires the presence of HSPGs (Chen et al. 2009; Pye et al. 2000). Sulf1 and Sulf2 are sulphatases which remove 6-O-Sulfate groups and destabilise the

tripartite FGF complex, thus inhibiting FGF signalling. There is a stripe of *Sulf2* in the posterior mesencephalon, which would therefore dampen the FGF8 signal anterior to the IsO compared to the same distance posterior of the IsO (Winterbottom & Pownall 2009). Therefore at the highest doses of FGF8, only rhombomere1 will be specified and the slight inhibition of FGF signalling by *Sulf2* anteriorly will result in formation of posterior midbrain. The negative regulator of MAPK signalling, *Sprouty2* is also present around the MHB. When *Sprouty2* is electroporated into rhombomere1, it rostralises the rhombomere into the mesencephalon, supporting the idea of a slightly lower FGF signal being required to form mesencephalon (Suzuki-Hirano et al. 2005).

1.8.3 FGF signalling at the ANB

In zebrafish and frog embryos, the ANB is first visible at late gastrula as a smile-shaped structure located at the interface between the anterior-most region of the neural plate, and the adjacent non-neural ectoderm (Figure 1.6A). The anterior neural ectoderm used to be thought to play a passive role during neural development, however this changed when Houart et al., (1998) ablated populations of these anterior ectodermal cells in zebrafish embryos. This ablation firstly caused damage to the prechordal plate – the precursor to the neural plate – as its marker *goosecoid* was lost. In later development ablation caused a high level of apoptosis in anterior neural regions. Closer examination of gene expression as a result of ablation of the ANB revealed that anterior dorsal forebrain markers *Emx* and *Dlx2* were absent, whereas the diencephalic *Sonic hedgehog* (*Shh*) expression domain was expanded. This suggested that the ANB was in fact critical for initial forebrain patterning and for the survival cells contributing to the telencephalon (Houart et al. 1998).

Earlier research in the rat identified a forkhead transcription factor FoxG1 (also known as BF-1) that was restricted to the rostral neural tube and later in development, the telencephalon (Tao & Lai 1992). *FoxG1*-null mouse mutants died at birth with severe reduction in forebrain structures caused by a lack of proliferation in telencephalon progenitor cells (Xuan et al. 1995). To study the regulation of *FoxG1*, Shimamura & Rubenstein (1997) cultured neural plates dissected from mouse embryos, with or without ANB cells attached. In explants cultured without the ANB, *FoxG1* expression was not activated, unlike explants retaining ANB cells. This suggested that factors secreted from the ANB are required for *FoxG1*

expression. *FGF8* expressed in the anterior forebrain proved to be such a factor, as in neural plate explants without the ANB, the placement of an FGF8-soaked bead underneath the anterior of the neural plate potently activated *FoxG1* expression (Shimamura & Rubenstein 1997).

As the loss of the ANB caused expression of *Shh* in the diencephalon, effectively posteriorising the developing brain, it was hypothesised that as in the IsO FGF signalling in the ANB acts as a morphogen to pattern the surrounding neural structures (Eagleson & Dempewolf 2002). Indeed, ectopic FGF8 expression caused by placing an FGF-soaked bead implanted into the ANB in *Xenopus* embryos caused posteriorisation of *FoxG1* expression (Eagleson & Dempewolf 2002). As well as activating *FoxG1*, *Fgf8* was also shown to be activated by FoxG1 itself so appears to be part of a positive feedback loop required for early forebrain specification (Eagleson & Dempewolf 2002). *FoxG1*-/- mice showed a decrease in rostral expression of FGF8, which with an increase in BMP signalling caused premature differentiation of neurons, depleting the progenitor pool and thus limiting the growth of the telencephalon, therefore intact signalling between FGF8 and FoxG1 is imperative for correct temporal and spatial development of the forebrain (Martynoga et al. 2005). This is also seen in zebrafish, FGF8-mutant fish display defects in commissural axon pathfinding and telencephalon patterning (Shanmugalingam et al. 2000). It was argued that the reason these animals still developed remnants of the telencephalon was that either FGF signalling was not sufficient for *FoxG1* activation and forebrain development, or functional compensation was occurring by other FGFs (Paek et al. 2009). Therefore Paek et al., (2009) abolished FGF activity in the telencephalon by raising conditional triple-knockout FGFR1, FGFR2 and FGFR3 mice (FGFR4 is not expressed in the ANB). These embryos completely lacked the telencephalon and as well as not expressing *FoxG1*, also did not express other telencephalic markers such as *Dlx2* and *Emx1* (Paek et al. 2009). This shows that FGF expression in the ANB is absolutely required for FoxG1 activation and maintenance, and to pattern the telencephalon.

Another way FGF signalling contributes to anterior neural development is through regulation of the GPCR lysophosphatidic acid receptor 6 (LPAR6), which has been identified as being positively regulated by FGFs (Branney et al. 2009; Geach et al. 2014). Knockdown of *Lpar6* and its upstream LPA-synthesising enzyme *Enpp2* in *Xenopus* neurula embryos caused a loss of telencephalic markers *FoxG1* and *Emx1*, whereas midbrain and hindbrain markers were unaffected. Lpar6 morphants

displayed anterior forebrain truncations that were worsened when FGF signalling was inhibited with SU5402. During this PhD, I had the opportunity to contribute towards Geach et al. (2014), and showed by ISH and immunostaining that as well as being FGF targets, knockdown of *Lpar6* and *Enpp2* caused a severe reduction of *Fgf8* expression and dpERK levels in the ANB and MHB. This suggested that as well as being induced by FGF signalling, *Enpp2* and *Lpar6* also affect FGF signalling through FGF8, and this relationship between FGFs and Lpar6 is required for correct forebrain patterning and development (Geach et al. 2014). The paper is included in Appendix 8.2.

As well as FGFs, *Sonic Hedgehog* also plays an important role in ventral telencephalon development. *Shh* is also known to be required for *FoxG1* expression and ventral telencephalic genes (Hébert & Fishell 2008). This is because FGF negatively regulates Gli3, the negative regulator of the Shh pathway. It is this repression that would otherwise prevent FoxG1 from being activated (Rash & Grove 2007). Shh works upstream of FGF as in the murine Shh-/- mutant there is no FGF expression in the telencephalon and because levels of Gli3 rise, ventral cell types are lost (reviewed in Hébert & Fishell 2008). Therefore, the effects of FGF signalling upon telencephalon could be said to be primarily due to its regulation by Shh. However, *Shh* also depends on FGF signalling to form the ventral telencephalon.

1.8.4 Conclusions

Therefore, as well as being important for posterior neural specification and patterning, FGF signalling also has a patterning role in more anterior regions of the CNS - the rhombomeres, MHB and ANB - by acting as a morphogen. Although insufficient by itself to specify the anterior of the embryo, crosstalk with other pathways, such as Wnt, RA and Shh ensures proper development of the forebrain. The repressive influence from posterior FGF upon more anterior *Hox* genes as well as the requirement for FGF signalling to actively pattern areas around the MHB and ANB points to complicated relationship between FGF and other signalling events to specify the full neural program.

1.9 Summary

FGF signalling is required for many processes during embryonic development, but this project will focus on its role in neural development. FGF signalling has previously been shown to be required for neural induction and patterning in addition to BMP inhibition. FGF signalling is known mainly for specifying the posterior CNS, but roles for FGF signalling in the anterior CNS are also emerging. Although the effect of FGF signalling upon activating *Hox* genes and eventually posterior neural tissue has been investigated, the proximal FGF targets that contribute towards neural development and other related processes have not been thoroughly investigated before. Furthermore, it is still not clear how signalling activated by individual FGFRs influence neural development. Therefore this project aims to investigate FGF signalling during neural development through use of inducible FGFRs (iFGFRs) derived from FGFR1-4. Changes to the *Xenopus* transcriptome as a result of FGF induction during neural development will be investigated, and proximal FGF targets found as a result characterised further.

1.10 Core Aims of this project

The main hypothesis for this investigation was that activation of iFGFRs during a period of early neural specification would affect expression of genes involved in the development and specification of the CNS. It was also hypothesised that there would be differences in signalling outputs between the different iFGFRs. The core aims of this project that would test these hypotheses were:

1. To characterise and optimise the use of inducible FGF receptors (iFGFRs) as a means of temporarily and spatially controlling FGF signalling during neural development in *Xenopus* embryos.
2. To investigate the effects of iFGFR activation upon the *Xenopus* transcriptome during neural development by a) analysing a previous microarray dataset and b) performing an RNA seq experiment to find proximal neural targets.
3. To identify proximal neural FGF targets and characterise them further through knockdown and/or overexpression.

2 Materials and Methods

2.1 Embryological Methods

2.1.1 In Vitro Fertilisation of *Xenopus tropicalis* embryos

Xenopus tropicalis females were primed by subcutaneous injection of 10 units of Human Chorionic Gonadotrophin [HCG; Chorulon: Intervet] 24-72 hours prior to the required onset of laying. On the day of laying, females were injected with 100 units of HCG and placed in a darkened 27°C incubator for three hours. Eggs were transferred to Leibovitz's L-15 [Gibco] + 10% foetal calf serum [Invitrogen]-coated 55mm dishes [VWR international] fertilised with crushed male *Xenopus tropicalis* testes suspended in 1ml L-15 + 10% heat treated foetal calf serum. Half an hour after fertilisation embryos were dejellied by placing them in a solution of 3% L-cysteine [Sigma] in MRS/9 (Modified Ringers solution) and washing in MRS/9 (Ubbels et al. 1983). Before and during microinjection eggs were cultured in 3% Ficoll solution [Sigma] in MRS/9 pH 7.8. Before the onset of gastrulation embryos were transferred to MRS/20 and cultured in 1% agarose-coated 55mm dishes. Embryos were staged according to Nieuwkoop and Faber.

2.1.2 In Vitro Fertilisation of *Xenopus laevis* embryos

Xenopus laevis females were primed by subcutaneous injection of 50 units of HCG 24 hours- 2 weeks before laying. 14 hours before laying, females were injected with between 180-250 units of HCG to induce egg laying, and placed in a darkened incubator at 20°C overnight. Eggs were fertilised with crushed male *Xenopus laevis* testes suspended in water. Half an hour after fertilisation embryos were dejellied by placing them in a solution of 2.5% cysteine hydrochloride monohydrate [Sigma] in water, pH 7.8. Embryos were cultured in Normal Amphibian Medium (NAM/10) (Slack & Forman 1980). Before and during microinjection eggs were cultured in 5% Ficoll solution in NAM/3. Before the onset of gastrulation embryos were transferred to NAM/10. Embryos were staged according to Nieuwkoop and Faber.

2.1.3 Microinjection

Xenopus embryos were microinjected using a Harvard Apparatus PLI-100 gas injector. To target mRNA to the whole embryo, mRNA was injected into one or both blastomeres in the animal hemisphere at the 1-2 cell stage. To target mRNA to neural tissue, mRNA was injected into one or both dorsal animal blastomeres at the 8-cell stage. For morpholino injections, morpholinos [Genetools] were warmed to 65°C for 10 minutes before use, centrifuged for 2 minutes at 13000 rpm and kept at room temperature during microinjection. *Xenopus laevis e*mbryos were injected with a total of 4.2-9.6nl mRNA/morpholino per cell and *Xenopus tropicalis* embryos were injected with a total of 2.3-4.2nl mRNA/morpholino per cell at appropriate concentrations.

2.1.4 Injection of iFGFR mRNA and receptor induction with AP20187

Unless otherwise stated, embryos were injected with 20pg iFGFR mRNA at the 2-cell stage. For whole embryo experiments, *Xenopus laevis* embryos were cultured until stage 10.5 and placed in a 1µM solution of AP20187 [Clontech] in NAM/10 until neural specification stages. For targeted injections, embryos were coinjected into both dorsal animal blastomeres at the 8-cell stage with 10pg iFGFR1 and GFP if required, and treated with AP20187 as before. For animal cap experiments, embryos were co-injected with 20 pg iFGFR and 50pg Noggin mRNA into the animal pole at the 1-2 cell stage. Embryos were cultured until Stage 8 before transferring to a solution of NAM/2 and dissecting out ectodermal explants. Animal caps were cultured in NAM/2 until stage 10.5 and transferred to a 1µM solution of AP20187 in NAM/2 for 3 hours. Embryos were snap frozen or fixed at the required stage.

2.1.5 Imaging and manipulation

Embryos were imaged using a Fluorescent Leica MZFLIII microscope and SPOT Advance v4.0.9 software Diagnostic Instruments Inc. Images were optimised using Adobe Photoshop CS3. Figures were made using CorelDRAW Graphics Suite x6.

2.2 Cellular and Molecular Biological Methods

2.2.1 Agarose gel electrophoresis

6x loading buffer (New England Biolabs) was added to samples to be run on an agarose gel. 0.8-2% agarose [Melfords Biolaboratories Inc.] in TAE was heated to make a molten gel and set in gel moulds. Samples were loaded on gels alongside 5µl Log_2 DNA ladder (New England Biolabs). Gels were placed in an electrophoresis tank and run at 180V.

2.2.2 Quantification of nucleic acids

DNA/RNA was quantified using the Nanodrop 2000 or Nanodrop 8000 [Thermo Scientific]. This also enabled the 260/280 and 260/230 absorption ratios to be found to assess nucleic acid purity.

2.2.3 Transformation of plasmids

1µl plasmid DNA was added to 50µl DH5α competent cells [Invitrogen] and kept on ice for 30 minutes. Table 2.1 shows plasmids used for making sense RNA for microinjection with the restriction enzyme and polymerase required to make sense mRNA.

Table 2.1. Plasmids used for microinjection in this project

Construct	Vector	Enzyme to linearise	Promoter for Sense
iFGFR1 VT+	CS2+	NotI	SP6
iFGFR1 VT-	CS2+	NotI	SP6
iFGFR2	CS2+	NotI	SP6
iFGFR3	CS2+	NotI	SP6
iFGFR4	CS2+	NotI	SP6
Cas9	CS2+	NotI	SP6
dnFGFR1	Sp64t	EcoRI	SP6
Nuclear GFP	CS2+	NotI	SP6
Nek6	CS2+	NotI	SP6
Nek6 TALEN Left	CS2+	NotI	SP6
Nek6 TALEN Right	CS2+	NotI	SP6
Noggin	Sp64t	EcoRI	SP6

Samples were heatshocked at 42°C for 90 seconds and placed back on ice for 2 minutes. 800µl Luria Broth (LB) warmed to 37°C was added to the heatshocked

sample and the sample agitated for 1 hour at 37°C. 1/10 of this was plated onto LB/agar plates containing 100µg/ml ampicillin (SLS) and then the remaining sample spun down at 7.2 rpm. Most of the supernatant was removed and the total cell pellet plated onto LB/agar with ampicillin plates. Colonies were left to grow on plates overnight at 37°C.

2.2.4 Minipreps

Colonies from transformations were added to 5ml LB with 100µg/ml Ampicillin and agitated at 37°C overnight. Cultures were pelleted at 8000rpm at room temperature and purified with the Qiagen Miniprep Spin Kit. Minipreps were stored at -20°C.

2.2.5 Cloning strategies

2.2.5.1 Genes cloned for this project

Table 2.2 shows the PCR primers used to amplify the coding DNA sequence (CDS) of a gene which was then T-cloned and linearised to make an antisense probe for *in situ* hybridisation

Table 2.2 PCR primers and conditions for each gene cloned for *In situ* hybridisation

Gene	Forward Primer 5'→3'	Reverse Primer 5'→3'	Insert Size (bases)	Vector	Linearised with	Promoter for antisense
Dynll1	ATTTATTTCTACC TGGGTCAGGTA	TCAGCACAACAG GTTTTCAGTCCT	206	pGEM	XhoI	T7
Dynll2	GAGAGAGAATTC ACCATGGCTGAC AGAAAGGCTGTTA T	CTCTCCTCGAGTT ATAAAGCATTTAC ATTTT	549	pGEM	ApaI	SP6
FoxA4 partial CDS	GATGTTTCCACAG TAACAACAAGC	AGAGTCCAATAG GAGCCTTTACCT	455	pGEM	NsiI	T7
FoxN4	AGAAGAGAATTCA CCATGGTAGACA GTGACATCTCTGC TATAA	TCTTCTCTCGAGT TAAAGCAAAGCAA TAGGCTTGGT	1521	pGEM	NcoI	SP6
Hmx3	AGAAGAGAATTCA CCATGGAGAGAT ACCTGAGCAGCT CAGAGA	TCTCTCCTCGAGT CACAACAAACATT TATTTAACAA	1363	pGEM	SphI	SP6
Lefty	GAGAGAGAATTC ACCATGGGTGTC ACTACCAAATCTT T	TCTCTCCTCGAGT CATATGATAGCGA TATTGTCCA	1104	pGEM	ApaI	SP6
Nek6 5' UTR	CCGGGACCTAGC GAGGACAACTCT	GCCCTCGTGCTG GTATTCCTGCCC	450	pGEM	SpeI	T7
Rax	ATGCACCTGCAC AGCCCTTCCCTG	TTACCAAGGCTTG CCAATAAACTG	969	pGEM	NsiI	T7

2.2.5.2 PCR amplification of fragments to be cloned

Xenopus laevis cDNA was used with the primers in Table 2.2 to amplify the region of interest. The PCR reaction consisted of 50µl 2x PCR mastermix [Fermentas], 2µl Forwards and Reverse Primer [Sigma], 5µl cDNA and 35µl H_2O:

PCR was then conducted following these conditions:

Initial melting	95°C	5 minutes
35 cycles of …	95°C	30s
	55°C*	30s
	72°C	60s/kb
Final extension	72°C	10 minutes

*This temperature changed depending on the lower Tm value provided by Sigma.

The PCR product was loaded on a 0.8% agarose gel and run at 120V for 1 hour. The band was extracted from the gel and purified using a Qiagen Gel Extraction kit.

2.2.5.3 T-cloning

1µl purified PCR products were mixed with 2.5µl 2x ligation buffer, 0.5µl pGEM vector, 0.5µl H_2O and 0.5µl T4 ligase and left at room temperature for 1 hour. They were then transformed into DH5α cells as in Section 2.2.3.

2.2.5.4 PCR screening of colonies

Colony PCR was undertaken to determine how many DH5α colonies contained pGEM with incorporated inserts. Colonies were dispersed using 2µl molecular grade H_2O. 1µl was added to a PCR reaction and 1µl streaked onto a LB/agar + Ampicillin plate. 10µl 2x PCR master mix, 1µl SP6 primer [Sigma], 1µl T7 [Sigma], 2µl colony dispersed in H_2O and 5µl H_2O was mixed per reaction.

The PCR conditions were as follows:

Initial melting	95°C	5 minutes
30 cycles of …	95°C	30s
	60°C*	30s
	72°C	60s/kb
Final extension	72°C	10 minutes

The reaction was run on an agarose gel to confirm that a product had been inserted into the vector. Colonies on the patch plate corresponding to those that had taken up the insert were cultured in LB broth overnight and miniprepped as in Section 2.2.4.

2.2.5.5 Subcloning *Nek6* into CS2

Full length *Xenopus tropicalis Nek6* was obtained from Source Bioscience in the pExpress vector. The *Nek6* gene was excised by cutting the plasmid with EcoRI as described. Simultaneously, 2µg CS2 vector was also linearised using EcoRI. CS2 was also dephosphorylated to reduce religation by adding 1µl Calf Intestinal alkaline phosphatase (CiP) [New England Biolabs] directly to the linearization reaction and heat inactivated at 65°C for 40 minutes. The fragments were run on a gel and the correct sized bands were excised and purified as mentioned in Section 2.2.5.2. The linearised vector and excised gene were mixed in a 1:3 molar ratio and ligated using T4 ligase. Transformation and purification of the ligated product was performed as already described. Purified CS2+ plasmids containing Nek6 were sequenced in the Technology Facility with the Applied Biosystems 3130XL sequencer to determine the orientation and identity of the insert. Correctly subcloned *Nek6* was processed for mRNA synthesis as described in Section 2.2.7.

2.2.5.6 Sequencing of plasmid DNA

Unless otherwise stated, plasmid DNA was sequenced on an Applied Biosystems 3130XL Sanger sequencing machine in York Technology Facility.

2.2.6 Linearising plasmid DNA

Per reaction, 1-5µg plasmid, 10µl 10x Surecut Buffer [Roche], 5µl Restriction Enzyme and H_2O to 100µl was mixed. The reaction was incubated at 37°C for 90 minutes. Table 2.3 shows plasmids in addition to those in Table 2.1 and Table 2.2 from lab stocks that were linearised to make *in situ* probes.

To check the plasmid was cut to completion, 10µl was run on a 1% agarose gel. To clean up the digest, an equal volume of phenol:chloroform [Sigma] was added, vortexed and centrifuged for 5 minutes at 13000 rpm. The aqueous phase was added to 1/10 volume sodium acetate [Sigma] and 2V 100% Ethanol [Fisher] and precipitated at -20°C for 1 hour.

Table 2.3. Plasmids from lab stocks linearised for *in situ* probes

Gene	Vector	Linearised with:	Promoter for Antisense	Source
Cdx4	CS2+	EcoRI	T3	(Illes et al. 2009)
En2	pBluescript KS+	XbaI	T3	Isaacs Lab
HoxA7	pGEM	BamHI	SP6	Isaacs Lab
Krox20	pGEM4	EcoRI	T7	Isaacs Lab
MyoD	Cs2+	BamHI	SP6	(Harvey 1991)
Sox3	Bluescript SK+	EcoRI	T7	Grainger Lab
Sox17	CS107	EcoRI	T7	Tgas004n06
N-tubulin	pBluescriptII KS+	BAMHI	T3	Papalopulu lab
Xbra	pSP64T	ClaI	T7	(Conlon et al. 1996)

The precipitate was pelleted in a 4°C centrifuge at 13000 rpm for 20 minutes. The pellet was washed with 70% ethanol, vacuum dried and resuspended in 50µl H_2O.

2.2.7 *In vitro* transcription of mRNA for microinjection

Reactions were set up at room temperature as follows using Fisher Megascript kits. Per reaction, 4.5µl H_2O, 2µl 50mM ATP, 2µl 50mM CTP, 2µl 50mM UTP, 2µl 5mM GTP, 2.5µl 40mM mGTP cap [Fisher Scientific], 2µl 10x transcription buffer and 2µl enzyme were mixed. GTP was added at a lower concentration to increase the likelihood of mGTP cap being incorporated. Reactions were incubated at 37°C for at least 4 hours. DNase1 [Promega] was added to destroy the template and the reaction incubated for 20 minutes at 37°C. An equal volume of phenol:chloroform was added, the reaction vortexed, centrifuged at 13000 rpm for 5 minutes and the aqueous phase transferred to a new tube. An equal volume of chloroform was added, the reaction vortexed, centrifuged at 13000 rpm for 5 minutes and the aqueous phase transferred to a new tube. An equal volume of isopropanol was added and the reaction left to precipitate at -20°C for 30 minutes. The reaction was centrifuged for 20 minutes at 13000rpm, 4°C. The pellet was washed with 70% ice cold ethanol and dried before resuspending in 20µl H_2O. The concentration of mRNA was quantified using the nanodrop and mRNA divided into 2µl aliquots at a concentration of 200ng/µl.

2.2.8 Transcription of DiG-labelled RNA for *in situ* hybridisation

Per reaction, 15µl 5x Transcription Buffer [NEB], 2.5µl 10x DiG dNTP mix [Invitrogen], 5µl Dithiothreitol (DTT) [Invitrogen], 2µl RNasin [Promega], 4µl DNA polymerase [Promega], 2µl DNA template and 44µl H_2O were mixed.

The reaction was incubated at 37°C for 4 hours. 1µl of DNase1 was added and the reaction incubated for 20 minutes at 37°C. 37.5µl H_2O, 75 µl 3M ammonium acetate [Sigma], 1.5 µl Glycoblue [Ambion] and 468µl 100% ethanol were added to precipitate DiG-RNA and the reaction incubated on dry ice for 1 hour. Reactions were centrifuged at 13000 rpm at 4°C for 20 minutes. The pellet was washed with 70% Ethanol and dessicated before resuspension in 30 µl H_2O. The presence of probe was checked on an agarose gel.

On some probes, particularly those longer than 800bp, their ability to effectively penetrate tissues was improved by hydrolysis. An equal volume of 80mM $NaHCO_3$ [Sigma] plus 60mM Na_2CO_3 [Sigma] was added to RNA probes resuspended in H_2O. The amount of time samples were left to hydrolyse at 60°C was determined by the formula:

$$\frac{starting\ length\ (kb) - desired\ length\ (kb)}{0.11(start\ length\ \times desired\ length)}$$

1/9 volume 3M sodium acetate was added with 2 volumes of 100% ethanol and left to precipitate at -80°C for 10 minutes before centrifugation at 13000 for 15 minutes at 4°C. The pellet was washed with 95% ethanol, and the pellet desiccated and resuspended in H_2O. Probes were stored at -80°C until required.

2.2.9 *In situ* hybridisation

Embryos were previously fixed at the appropriate stage in MEMFA (10% MEM salts [1M MOPS [Sigma], 20mM EGTA [Fisher Scientific], 10mM $MgSO_4$ [Fisher Scientific] in dH_2O], 10% formalin [10% Formaldehyde [Sigma] in dH_2O] for one hour and transferred to 100% methanol. Embryos were rehydrated in progressively weaker solutions of methanol in Phospho-buffered Saline (PBS) plus 1% Tween-20 [Fisher Scientific] (PBST) and then permeabilised with Proteinase K [Roche] at 10µg/ml (*Xenopus laevis*) or 6 µg/ml (*Xenopus tropicalis*) for roughly 1 minute per stage and the reaction quenched with 0.1M Triethanolamine pH 7.8 [Sigma] and 1% acetic anhydride [Sigma]. After washing in PBST embryos were re-fixed in 10%

formalin in PBST. After washing in PBST embryos were equilibriated in 1ml PBST with a 250µl hybridisation buffer (50% Formamide [Applied Biosystems], 5x SSC [Promega], 100µg/ml Heparin [Sigma], 1x Denhardt's solution [VWR International], 0.1% Tween 20, 0.1% CHAPS [Sigma] and 10mM EDTA [Sigma]). Embryos were then blocked in hybridisation buffer containing 1mg/ml total yeast RNA sodium salts [ICN Biomedical] at 60°C for 2 hours. The *in situ* probe was brought to 80°C for 3 minutes and then added to hybridisation buffer at 60°C containing 1mg/ml total yeast RNA. This probe solution replaced the hybridisation buffer and embryos were incubated at 60°C overnight. After washing in hybridisation buffer embryos were washed three times in 2X SSC with 0.1% Tween-20 at 60°C. If required, embryos were treated with 2µl RNaseA [VWR international] in 2x SSC plus 0.1% Tween 20 at 37°C for 30 minutes. Embryos were then washed three times in 0.2X SSC in 0.1% Tween 20 at 60°C. Embryos were moved to RT and washed with maleic acid buffer (100mM Maleic Acid [Sigma], 150mM NaCl and 0.1% Tween) (MABT) for 2x 15 minutes before being blocked in 2% BMB [Roche] + 2% heat-treated lamb serum [Fisher Scientific] in MAB for 2 hours. This was replaced with fresh solution containing 1/2000 dilution of affinity purified sheep anti-digoxygenin antibody coupled to AP [Roche] and samples left at 4°C overnight. The antibody was removed by washing with MABT and then the pH was equilibriated for BM purple by washing in alkaline phosphatase buffer (100mM NaCl, 100mM Tris [Invitrogen], 50mM $MgCl_2$ [Sigma] in dH_2O) and then replacing with BM purple. Once staining had developed by the required amount, embryos were washed in PBST, fixed overnight in 10% formalin and bleached in 5% H_2O_2 in PBST.

2.2.10 Extraction of total RNA

5 *Xenopus laevis* embryos, 10 *Xenopus tropicalis* embryos or 15 animal cap explants were homogenised in 1ml Trizol [Invitrogen]. All centrifugation steps were carried out at 13000 rpm at 4°C unless otherwise stated. Samples were left at RT for 5 minutes then centrifuged for 10 minutes at 13000rpm at 4°C. To the supernatant, 200µl chloroform was added, the sample vortexed and left at room temperature for 5 minutes. The samples were centrifuged for 10 minutes at 13000rpm, 4°C and the aqueous RNA phase added to a new tube. An equal volume of chloroform [Sigma] was added and the previous step repeated. The aqueous phase from this was added to 500µl isopropanol [VWR International] and left to precipitate at -20°C for 30 minutes. The precipitate was pelleted by centrifugation at 13000 rpm for 15 minutes and washed washed with ice-cold 70%

ethanol. The pellet was resuspended in 50µl H_2O and 60 µl of a 9/10 LiCl [Sigma]: 1/10 EDTA mix and precipitated at -80°C overnight. Samples were then centrifuged for 40 minutes at 13000rpm, and the pellet washed twice with ice cold 70% ethanol. RNA was dried and resuspended in 20µl water. RNA was quantified using the Nanodrop 2000.

2.2.11 cDNA first strand synthesis

1µg of RNA was mixed with 1µl OligodT 12-18 primer [Invitrogen], 1µl 10mM dNTPs [Invitrogen] and H_2O to a total volume of 13µl.

This was incubated at 65°C for 5 minutes to denature and secondary RNA structures. After cooling on ice for 2 minutes 4µl First strand buffer [Invitrogen] and 2µl DTT [Invitrogen] were added per reaction and incubated at 42°C for 2 minutes. 1µl Supercript II reverse transcriptase [Invitrogen] was then added to each reaction and placed at 42°C for one hour and then 70°C for 15 minutes to terminate the reaction. cDNA was stored at -20°C until required.

2.2.11.1 *L8* PCR

To ensure cDNA could be amplified, a PCR was performed for the housekeeping gene *L8*. Per reaction, 10µl 2x PCR master mix, 1µl 10µM L8 Forwards primer [Sigma], 1µl 10µM L8 Reverse primer [Sigma], 1µl cDNA and 7µl H_2O were mixed. The conditions for PCR were as in Section 2.2.5.4:

Success of the PCR was determined by running the product out on a 1% agarose gel.

2.2.12 Western blots

5 *Xenopus laevis* embryos, 10 *Xenopus tropicalis* embryos or 10+ animal cap explants previously snap frozen and stored at -80°C were homogenised in 50µl Phosphosafe [Novogen-Merk]. Samples were spun at 13000 rpm, 4°C for 20 minutes and the supernatant added to a fresh tube with 2x sample buffer. Samples were heated at 95°C for 10 minutes to denature protein. Samples were then run on a 12% polyacrylamide gel at 120V alongside a protein ladder [Thermo Scientific] and then transferred onto an Immobilon Millipore membrane [Fisher Scientific] at 100V for 1 hour. The membrane was blocked in a solution of 5% Marvel Milk in PBS for 1 hour, and incubated overnight at 4°C in primary antibody (see Table 2.4).

The membrane was washed in PBS and the incubated overnight in secondary antibody (see Table 2.4). Protein bands were visualised by adding BM Chemiluminescence Western Blotting Substrate (POD) [Roche] to the membrane and exposing it to ECL Hyperfilm [Amersham] and developed using an Xograph machine. If required, membranes were stripped by incubating the membrane in stripping buffer (for 100ml, 0.3g DTT [Melford Biolaboratories Ltd], 2ml Tris pH 6.8, 250µl 10% SDS in dH_2O) at 55°C for 15 minutes, washing in PBS, reblocking in 5% Marvel milk powder in PBS, and treating with antibodies as before. The concentrations of all antibodies used are shown below in Table 2.4.

Table 2.4 Dilutions of all antibodies used

Primary	Dilution	Secondary	Dilution
dpERK	1 in 4000	anti mouse	1 in 4000
FLAG	1 in 5000	anti rabbit light chain	1 in 40000
GAPDH	1 in 5000	anti mouse	1 in 5000
HA	1 in 2000	anti mouse	1 in 4000
pSmad1/5/8	1 in 1000	anti rabbit	1 in 2000
tERK	1 in 500000	anti rabbit	1 in 8000

2.2.13 Immunostaining for dpERK

Embryos to be immunostained were fixed at the appropriate stage in MEMFA for one hour and transferred to 100% Methanol [Fisher Scientific]. Embryos were rehydrated in progressively more dilute solutions of Methanol in PBS. A potassium dichromate ($K_2Cr_2O_7$) solution in 5% acetic acid (for 250ml, 7.35g $K_2Cr_2O_7$ [Sigma] and 12.5ml Acetic acid [Sigma]) was added to embryos for 40 minutes. After washing in PBS, embryos were permeablised and bleached for 45 minutes in 5% H_2O_2 [Sigma] in PBS. After again washing in PBS, embryos were blocked once in BBT (1% BSA [Invitrogen], 0.1% Triton X-100 [SLS] in PBS) for 2x 1 hour and then in BBT + 5% horse serum [VectorLab] for a further hour. Embryos were incubated overnight at 4°C in 1/10000 dilution of anti dpERK antibody [raised in mouse, Sigma]. The embryos were then washed 4x 1 hour in BBT, blocked in BBT + 5% horse serum and this replaced with BBT+5% horse serum containing horse anti-mouse igG-AP conjugated secondary antibody [VectorLab] overnight at 4°C, at a concentration of 1/1000. Embryos were washed in BBT for one hour and then PBS for 4 hours. dpERK localisation was visualised upon the addition of BM purple (Roche). When the colour had developed to the desired level, embryos were fixed and stored in 10% formalin in PBS.

2.3 RT-qPCR

2.3.1 Primers used

Primers for RT-qPCR were designed using the Primer3plus online tool. Primers were selected that had a 60°C Tm, amplified between 80 and 120 bp of cDNA and did not have a high propensity to form primer dimers or bind to other genes. Primers are listed in Table 2.5.

Table 2.5 – RT-qPCR primers

Gene	Forwards 5'→3'	Reverse 5'→3'
ATP6V03	TGCAAACTCTCTGACGCAAA	AGCCAGCAGCTAGACCACTC
Chmp1	AGAAAGTGTCTGCTGTCATGGA	GGGGTGGTTAGTGTCATTGC
Cited2	GCAAACAGCCCAACAGAGTAA	GGAAGAAAGGTTCTGTGTCCA
Cyclin1B	ACTTCCTCAGACGGGCTTC	GAAGGCTTGATGTGGACCAT
Dynll1	TGCTACTCAGGCACTGGAGA	AATTCCTTCCCACAATGCAA
Dynll2	TAATGCACTGATGGCTGAAG	CCAGGCAACTAAACAGAAGTCA
Egr1	GGAGGGAGCTGAGCAATTC	CTGGTTGGCATAGCTGGATT
FoxA4	ACCTCAACTGTGGACCCCTA	GGCCCTGGTAAGCCATTACT
FoxN4	TGATGCCCTTGATCCAAGCA	GGCACCTAATGTGTCCAGACT
H3F3A	ACTGGAGGGGTGAAGAAACC	TGCGAATCAGAAGCTCAGTG
Hesx1	AGACAAGAAGATGGATGTGGCT	GGGATTTGCCAAAAGGTGCC
Hmx3	CCGGGCTGGTGGTATTCTTA	CAGACACTGGAGATGTGGGG
Ift172	CTGCAAAAGCATGGAAAAGAG	GTAATTGAGCCGCCGTAAAC
Krt12	GCAGCCTTCAGAGTTTGGAA	CCATATCGGCCATCTGTTTC
Lefty	AAGAGATCACTGCCCAGCTT	GGACTCCATTCCAAAAACCA
Lmbrd2	TGTGGGCACTCTGTTAGCC	GGTGCAGGAGTCACAGCAT
Med9	GGATGAAGCAGTCGAAGAGG	AGCTCGTTCAGCTCCTGGTA
MyoD	AACTGCTCCGATGGCATGAT	TGGGCTGTCACTGTAGAAGC
Nek6	CCTGTTTTCCCTGTGTCAGAA	CTTTGGTCTGGGTCTGGGTA
Oct-60	TGCCATCTCCAGTAGAGCAG	TGGCAAACTCTTCCATCTCC
ODC	AAAGCTTGTTCTACGCATAGCAACT	AGGGTGGCACCAAATTTCAC
Poc5	TTCCAGAGTGTTCAGCAACG	GAGAACGCTTCCAAACCTGA
Ras-dva	ACTTGGTGCCTACTGCTTGG	TCTCATCCACCAGTGCTTCTG
Rax	GAGATTCATCCCCAACAGGA	CACTCGCTTGAGGTCTTTCC
Slc12a3	TGAAGGGACCAGAAAAAGCA	AAGTGGAGGTTTGCCACAGT
Snx10	TCGACAAAAGCTTCAGAGCA	TCTTGCAATCCACGGACAC
Sprouty2	GGTGGTTGCAGACCGAATA	TTTCCACAATCCTCACACATTA
Tuba1a	GTGAGACAGGAGCTGGGAAG	GAGTTGCTCAGGGTGGAAAA
Xbra	TACGGTTCTGCTGGACTTTG	GGAACCCATTCTCCATTCAC
Zeb2	TCCATGCTTCTTGTCCCTTT	ATGGACTCGGCTCTGTGAAT
Zfp36L1	TATCTCTTTCGCCCCATGTC	CTGGAACTGCTCAGGTAGCC

The RT-qPCR mastermix was, per reaction, 12.5µl Power SYBR™ mastermix [Life Technologies], 2µl Primers, 5.5µl H_2O and 5µl cDNA. Three technical replicates were loaded onto a 96 well plate and run on an Applied Biosystems 7300 PCR machine and results analysed using Applied Biosystems 7300 series software.

2.3.2 Primer Optimisation

Before use in a Relative Expression assay, primers were optimised by performing Absolute quantification qPCR using standard serial 1/10 dilutions of cDNA, thus creating a standard curve, to ensure primers were efficient and had a linear dynamic range. Thermal cycling conditions were as follows:

Stage	Temperature	Time
1	50°C	2 mins
2	95°C	10 mins
3. 40 cycles of..	95°C	15s
	60°C	1 min
4. Dissociation stage	95°C	15s
	60°C	20s
	95°C	15s

Primers were discarded that gave an R^2 value of less than 0.98 or had unevenly spaced Ct values between cDNA dilutions. A dissociation curve was also conducted and primers that formed non-specific products and dimers discarded. Water controls for each primer set were also analysed to ensure absence of any amplified product.

2.3.3 Relative quantification qPCR

After optimisation, relative quantification RT-qPCR was performed. Thermal cycling conditions were as follows:

Stage	Temperature	Time
1	50°C	2 mins
2	95°C	10 mins
3. 40 cycles of..	95°C	15s
	60°C	1 min

Ct values were normalised against those of the housekeeping gene *ODC* for each condition. The Ct threshold was chosen automatically by the software. Average Rq values for each gene and condition were compared using Applied Biosystems software to find the relative expression fold change between control and test samples. Results were exported to an Excel.csv file for further analysis.

2.3.3.1 Graphical representation and statistical analyses of RT-qPCR results

Column graphs for RT-qPCR data were made in Microsoft Excel 2007. Error bars were added following calculation of Standard Error from the mean. Where appropriate (at least three biological replicates performed), a student's 2 tailed T test was performed using SPSS software to compare the mean Ct values for each technical replicate. Data were shown to be normal, but P-values accounting for the equality of variances not assumed chosen due to the low number of values tested.

2.4 Microarray methodology

The following were carried out by other members of the Isaacs lab:

2.4.1 Sample preparation

Xenopus laevis embryos were injected with 20pg of iFGFR1, iFGFR2, iFGFR3 or iFGFR4 mRNA at the 2-cell stage, and cultured until the onset of gastrulation. 1.25µm AP20187 was added to culture medium and embryos cultured throughout gastrulation until stage 13 at 22°C. 10 embryos per condition (induced and uninduced per receptor) were processed for total RNA isolation as previously described. The quality of RNA was tested using an Agilent 2100 Bioanalyzer.

2.4.2 Preparation of cRNA and chip hybridisation

The Affymetrix GeneChip one-cycle target labelling kit [Affymetrix] was used according to manufacturer's instructions, to process 2mg total RNA to cRNA. Resultant biotinylated cRNA was fragmented to 35-200bp lengths at 94°C in fragmentation buffer [Affymetrix]. The biotin-labelled fragments were hybridised to GeneChipH Xenopus laevis Genome Array for 16h at 45°C. The arrays were washed, stained and scanned using the Affymetrix Model 450 Fluidics station and Affymetrix Model 3000 scanner.

2.4.3 Microarray data processing

Processing of the raw microarray data was performed using Affymetrix GCOS 1.2 software. Probe cell intensities were calculated and summarised for the respective probe sets using the MAS5 algorithm.

Data were then imported into BRB ArrayTools software. Spot filters had a threshold minimum value of the spot intensity was below 5. The array was normalised using the median over the entire array. Genes with more than 50% data missing/filtered out were excluded.

Subsequent data analyses were performed by myself:

Genes were excluded which had <1.5-fold expression change upon iFGFR induction. Scatterplots were generated using the 'Phenotypes Averages' tool. Gene lists were generated by comparing iFGFR uninduced to iFGFR induced expression values for each receptor. Target gene annotation was performed using existing Affymetrix Gene array annotation and BLAST searching of target sequences using Genbank databases.

2.5 RNA-seq

2.5.1 Experiment setup

Xenopus laevis embryos were co-injected with 50pg *Noggin* and 20pg *iFGFR1* or *iFGFR4* mRNA at the 2 cell stage and cultured to stage 8. Animal cap explants were taken and cultured in NAM/2 overnight at 12°C. At stage 10.5, injected animal caps were induced with AP20187 for three hours at 22°C and then snap frozen.

2.5.1.1 Quality control of experiment

Whole stage matched controls were also induced at stage 10.5 and collected three hours later for western blot analysis for dpERK and pSmad1/5/8. Some sibling embryos only injected with 50pg *Noggin* were raised to tailbud to ensure a ventralisation phenotype as in Smith & Harland, (1992), and iFGFR-injected siblings raised to check a typical FGF-overexpression phenotype resulted. Western blot analysis was also performed on sibling embryos to confirm upregulation of dpERK in induced samples.

2.5.2 Extraction of total RNA

As described in Section 2.2.9, RNA was extracted from 20 neuralised animal cap explants. RNA integrity was measured by Lesley Gilbert on a Bioanalyser in the Technology Facility. Samples were sent on dry ice to the University of Liverpool Centre for Genomic Research (CGR) and processed further for RNA-seq.

2.5.3 Processing of samples for RNA-seq by the CGR, University Liverpool

Samples were treated with Ribo-Zero rRNA Removal Kit [Illumina]. Samples were then fragmented using light restriction enzymes to lengths of 100-150 bp. A PhiX spike-in control was used for all samples. Samples were sequenced on an Illumina HiSeq 2500. ~110 million paired reads were obtained for iFGFR1 Uninduced, ~80 million for iFGFR1 Induced, ~90 million for iFGFR4 Uninduced, and ~85 million reads iFGFR4 Induced.

The mean read length for all samples before trimming was 100bp. The raw Fastq files were then trimmed for the presence of Illumina adapter sequences using Cutadapt version 1.2.1, with option –O 3, so that 3' end of any reads matching the adapter sequence for >3bp were trimmed. Reads were further trimmed using Sickle version 1.200 with a minimum window score of 20. Reads shorter than 10bp after trimming were also removed. The mean read lengths after trimming were 82-96bp for all samples.

2.5.4 Data Processing by Toby Hodges

Initial analysis of raw data was performed by Toby Hodges from York Technology facility.

The reference transcripts used for mapping are contained in XENLA_2013may.longest_cdna_annot.fa.gz, obtained from the May 2013 ('Mayball') release from http://daudin.icmb.utexas.edu/pub/annot/. Transcripts were indexed ready for mapping using BWA-MEM (http://bio-bwa.sourceforge.net/) (Li & Durbin 2009). Reads were downloaded from CGR Liverpool and mapped against the reference transcript sequencing by BWA-MEM using the following script:

```
bwa mem -M -t20 <referenceSeqs.fasta> <sample_read1.fastq.gz>
<sample_read2.fastq.gz> | samtools view -Sb - \
 > <sample_XENLAmay2013_MEM.bam>
```

The –M flag was used to mark secondary alignments. The transcript collection was of low quality in places, and so a cautious approach for counting mapped reads was employed. The BAM alignment produced from was further filtered as below, and secondary alignments and unpaired reads filtered out.

```
samtools sort <sample_XENLAmay2013_MEM.bam>
<sample_XENLAmay2013_MEM_sorted>
samtools view -bF256 <sample_XENLAmay2013_MEM_sorted.bam> | samtools
view -bf2 - \
 > <sample_XENLAmay2013_MEM_sorted_mappedPairs.bam>
```

Counts of reads per fragment mapping to each transcript were obtained by using SAMtools idxstats software (http://samtools.sourceforge.net/) (Li et al. 2009). Reads were normalised to FPKM values using the python script FPKMcalculator.py, and fold-change differences between iFGFR uninduced and induced samples filtered and returned using the python script FPKMfoldChange.py.

2.5.5 Further Data Processing

Subsequent threshold adjustment and genelist compiling as well as further data analysis was performed by myself in Microsoft Excel. Venn Diagrams were constructed using a tool on the University of Gent's Bioinformatics Evolutionary Genomics website (http://bioinformatics.psb.ugent.be/webtools/Venn/). Scatterplots were plotted using SPSS. Ontological analyses were performed using Network2Canvas (http://www.maayanlab.net/N2C/) (Tan et al. 2013), and PANTHER (http://pantherdb.org/) (Mi et al. 2013).

2.6 CRISPR and TALEN-related protocols

2.6.1 Design of Nek6 TALEN

The target region of the Nek6 TALEN was in the first coding exon of the *Xenopus tropicalis* gene. The CS2+ TALEN plasmids were made by Jared Cartwright in the Technology Facility. The Left TALEN was composed of 19 bases, separated from the Right TALEN by a 16 base spacer region. For immunodetection, a Flag and HA tag were added to the Left and Right TALENs respectively. Plasmids were linearised with NotI enzyme and mRNA synthesised with SP6 as described in Section 2.2.7.

2.6.1.1 Microinjection of TALENs

1ng Left and 1ng Right TALENs were coinjected into *Xenopus laevis* or *Xenopus tropicalis* at the 1 cell stage.

2.6.2 Design of CRISPRs

2.6.2.1 Design and synthesis of template

A target sequence to incorporate into a guide strand was designed using the online tool E-Crisp (Heigwer et al. 2014). The target site was picked in a coding exon of the *Xenopus tropicalis* gene as close to the 5' start site of the gene as possible satisfying the restraint of containing the sequence 5'-G-n_{19}-nGG-3'. Guide strand templates are made with replicating overlapping primers by PCR. An oligonucleotide fragment that acts as a 5' primer was designed incorporating the custom sequence guide stand for each CRISPR:
TAATACGACTCACTATA*Gnnnnnnnnnnnnnnnnnn*GTTTTAGAGCTAGAAATAGC AAG. The T7 promoter is in bold and the sgRNA target in italics as in (Nakayama et al. 2013). The rest of the primer is complimentary to the common 3' primer: AAAAGCACCGACTCGGTGCCACTTTTTCAAGTTGATAACGGACTAGCCTTATTT TAACTTGCTATTTCTAGCTCTAAAAC which contains a recognition motif for Cas9.

5' Primers used are detailed in Table 2.6 below:

Table 2.6 – sgRNA 5' primer sequences

Gene	5' guide strand sequence
Cited2	TAATACGACTCACTATAG*TCAGTTGAGCCCCTTGATT*GTTTTAGAGCTAGAAATAGCAAG
Snx10	TAATACGACTCACTATAG*TTTTCTCTTCCTCTTCCGC*GTTTTAGAGCTAGAAATAGCAAG
Zswim4	TAATACGACTCACTATAG*CCCTCGGTTAAAGGGAACC*GTTTTAGAGCTAGAAATAGCAAG

The PCR reaction to make sgRNA template was composed of 10µl 5x High Fidelity buffer [New England Biolabs], 1µl 10mM dNTPs, 5µl 10µM sgRNA primer [Sigma], 5µl 10µM common reverse primer [Sigma], 0.5µl Phusion High Fidelity polymerase [New England Biolabs] and 21µl H_2O.

PCR conditions were as follows:

Initial melting	98°C	30s
30 cycles of …	98°C	10s
	60°C	30s
	72°C	15s
Final extension	72°C	10 minutes

Templates were stored at -20°C.

2.6.2.2 Synthesis of guide strand mRNA

Components from the T7 Megashortscript kit [Invitrogen] were composed of 1µl 10x Reaction buffer, 1µl 75mM ATP solution, 1µl 75mM GTP solution, 1µl 75mM GTP solution, 1µl 75mM UTP solution, 2µl Template, 1µl T7 enzyme and 2µl H_2O per reaction. Reactions were incubated for 4 hours at 37°C:

DNase treatment and a phenol chloroform cleanup was performed as previously described as in Section 2.2.7. Wild type Cas9 template was used to synthesise mRNA as previously described. mRNA was stored at -80°C.

2.6.2.3 Microinjection of CRISPR mRNA

600pg CRISPR sgRNA was co-injected with 2.2ng of *Cas9* mRNA into *Xenopus tropicalis* embryos at the 1 cell stage.

2.6.3 Extraction of genomic DNA from CRISPR/TALEN-injected embryos

Embryos injected with a CRISPR or TALEN were grown to at least stage 30 and transferred individually to PCR tubes. Lysis buffer was prepared containing 1M Tris pH 7.5, 5M NaCl, 0.5M EDTA, 10% SDS in dH_2O and filter sterilised. 250mg/ml Proteinase K and 5% w/v Chelex 100 resin [BioRad] were added to lysis buffer just before use, and 100µl of this added to embryos. Using a PCR machine, embryos were heated to 55°C for 1 hour and then 95°C for 15 minutes. Samples were then centrifuged at RT at 13000 rpm for 10 minutes and stored at -20°C.

2.6.4 PCR amplification and T-cloning of target region

Primers were chosen to span a <600bp region of genomic DNA around the TALEN/CRISPR target site. The PCR reaction mix was composed of 15µl 2x PCR master mix, 1µl 10µM Forwards Primer, 1µl 10µM Reverse primer 0.5µl gDNA and 12.5µl H_2O.

The PCR fragment was run on an agarose gel, the band cut out and the DNA extracted using a Qiagen PCR clean up kit. The purified product was then transformed into DH5α cells, and then a number of colonies per embryo picked, T-cloned, screened and purified and as described in Section 2.2.3- 2.2.5.

2.6.5 Sequencing of CRISPR/TALEN target region amplicons

Purified pGEM plasmids containing amplified CRISPR/TALEN target regions were mixed with pGEM M13 Forwards primer (ACGACGTTGTAAAACGAC) [Sigma] and sent to GATC Biotech AG. Results were analysed using Seqman software [DNASTAR].

3 Microarray-based analysis of FGF targets in whole embryos

3.1 Introduction

3.1.1 Inducible FGFRs (iFGFRs)

Receptor tyrosine kinases (RTKs), which include FGFRs, rely on ligand-induced dimerisation of inactive receptor monomers to activate downstream signalling (reviewed in Pownall & Isaacs 2010). This property of FGFRs has been exploited in conjunction with dimerisation agents to allow synthesis of inducible FGF receptors. The agents are based upon the 1:1 interaction between FKBP12 and its ligand FK506, also known as Tacrolimus. FK506 is a natural immunosuppressant used for treatment of organ transplant patients (Tanaka et al. 1987). FKBP12 molecules do not normally form dimers, however the fusion of two FK506 compounds provides a surface for dimerisation of two molecules of FKBP12 (Spencer et al. 1993). To minimise the interaction of FK506 with endogenous FKBPs, a synthetic variant – AP20187 – was synthesised which only binds to a variant of FKBP12 with a F36V mutation (FKBPv) (Clackson et al. 1998; Yang et al. 2000). FKBPv domains can be fused to genes of interest such as RTKs, and the addition of AP20187 used to induce dimerisation and activation of the protein when required. An inducible form of FGFR1, iFGFR1 was first used by Welm and colleagues to stimulate mammary tumour progression in a murine model (Welm et al. 2002). A schematic diagram of its structure is shown in Figure 3.1.

The iFGFR1 construct consists of the kinase domain of FGFR1 (amino acids 365-822) fused at the C-terminus to a myristoylation sequence, which targets it to the cell membrane. The N-terminus of the kinase domain is fused to an FKBPv domain. An HA tag is fused to the other end of the FKBPv domain to enable immunodetection of the translated iFGFR protein. Plasmids encoding the inactive iFGFR monomers can be transfected into cell culture, or mRNA injected into

Xenopus embryos at cleavage stages. When required, AP20187 is added directly to *Xenopus* culture medium and diffuses through the vitelline membrane into the embryo. This brings the kinase domains of the inactive monomers into close enough proximity to cause transphosphorylation of tyrosine residues, thus activating the receptor and downstream signalling. The iFGFR does not have an extracellular domain. Therefore induction of the iFGFR is not FGF ligand-dependent.

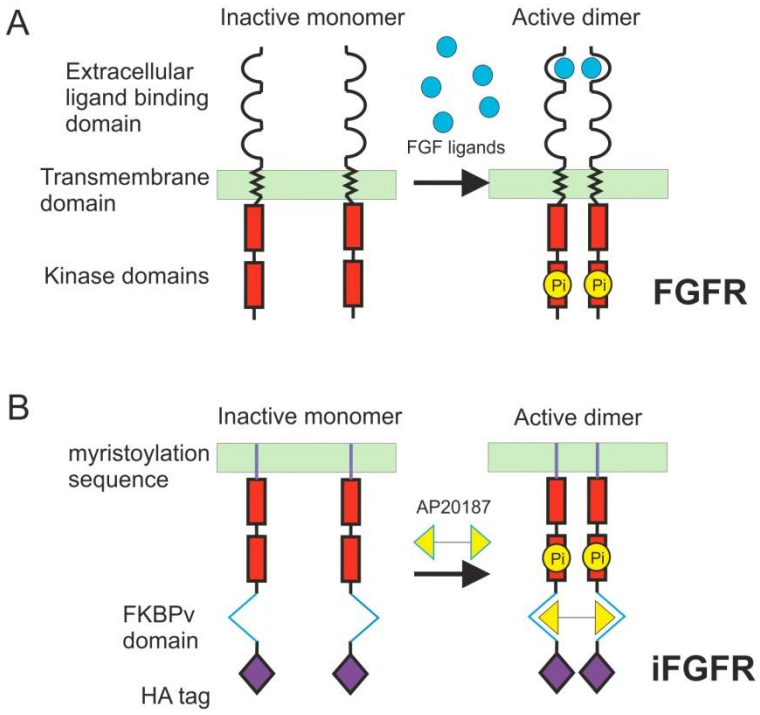

Figure 3.1 Schematic diagram of iFGFRs compared to endogenous FGFRs
A) is a schematic diagram of a wild type FGFR. FGF ligands bind to extracellular Ig-like domains. Receptor monomers are drawn into close proximity, and transphosphorylation of the kinase domains (red) activate downstream FGF signalling pathways. B) shows an iFGFR tethered to the cell membrane by a myristoylation domain. AP20187 added to culture medium binds to the FKBPv domain, bringing the kinase domains as in A). The HA tag tethered to the FKBPv domain enables immunodetection of the construct.

A further advantage of this system in *Xenopus* is that by using fate maps of the early cleavage stage embryos, specific tissues can be targeted with iFGFRs (Moody 1987). For example, by injecting iFGFRs into the two dorsal animal blastomeres at the 8-cell stage, iFGFRs can be confined only to prospective neural tissues.

iFGFR1 was first used in *Xenopus* by this lab. iFGFR1 was shown to robustly activate the MAPK pathway, as well as induce expression of known FGF target genes *Cdx4* and *HoxA7* in neural tissue past the stage where it would be normally competent to respond to FGF signalling (Pownall et al. 2003). As well as iFGFR1,

iFGFRs based upon the intracellular domains of FGFR2, FGFR3 and FGFR4 – as well as another isoform of iFGFR1 lacking a valine and threonine in the transmembrane region (iFGFR1 VT-) – have also been constructed. These were used for an investigative microarray experiment to assess FGF activity during gastrulation.

3.1.2 A microarray experiment using iFGFRs

Previously, other members the lab performed a single run of a microarray using iFGFR1, iFGFR2, iFGFR3 and iFGFR4. The aim of this experiment was to investigate how constitutive FGF induction, from the onset of gastrulation to the beginning of neuralation, affected the global *Xenopus* transcriptome.

A core aim of this project was to identify proximal FGF neural targets by RNA-seq. As the embryos used in this microarray screen express iFGFRs throughout the embryo and the induction period is long, FGF targets found are not necessarily proximal neural targets. Nevertheless data from this experiment are useful experiment in their own right to investigate the effects upon the *Xenopus* transcriptome of global FGF induction during the post-mesodermal period of development. Furthermore, findings from this data could form a foundation for further experiments.

3.1.3 Aims of this chapter

- To identify sets of genes upregulated or downregulated by each iFGFR.
- To assess overlaps of these genelists to gain an insight into the differences in signalling output between different FGFRs.
- To validate the dataset by confirming upregulation of known FGF targets found in the microarray. This will also provide a means of obtaining positive controls for application to optimising a more complicated RNA-seq experiment.

3.2 Results

3.2.1 Experimental methodology

The injection conditions used were as in Pownall et al., (2003). 20pg of each iFGFR mRNA was injected bilaterally into *Xenopus laevis* embryos at the 2-cell stage and

cultured until stage 10. Whole embryos were then treated with 1.25µM AP20187 between stage 10 and 13 – about 5 hours at 22°C. A single experiment was then processed for microarray. Embryos injected with each receptor and treated with AP20187 were compared to injected, but untreated control embryos.

3.2.2 iFGFRs1-4 affect the expression of many genes

The microarray dataset was analysed using BRB Arraytools. Firstly, raw $\log_2$ gene expression values of induced embryos injected with iFGFRs were compared to uninduced control embryos and the ratios displayed in the scatterplots in Figure 3.2A. Most genes fall along y=x (marked in yellow) as they are not affected by changes in FGF expression. Those points falling to the left of the green line correspond to genes showing a >1.5-fold upregulation and those to the right of the red line correspond to genes showing a >1.5-fold downregulation following iFGFR activation. The scatterplots show all four receptors activate many genes. iFGFR1 and 2 points lie over a wider area compared to iFGFR3 and 4, showing that iFGFR1 and 2 have a stronger effect upon gene expression in terms of number and also expression fold change at this point in development.

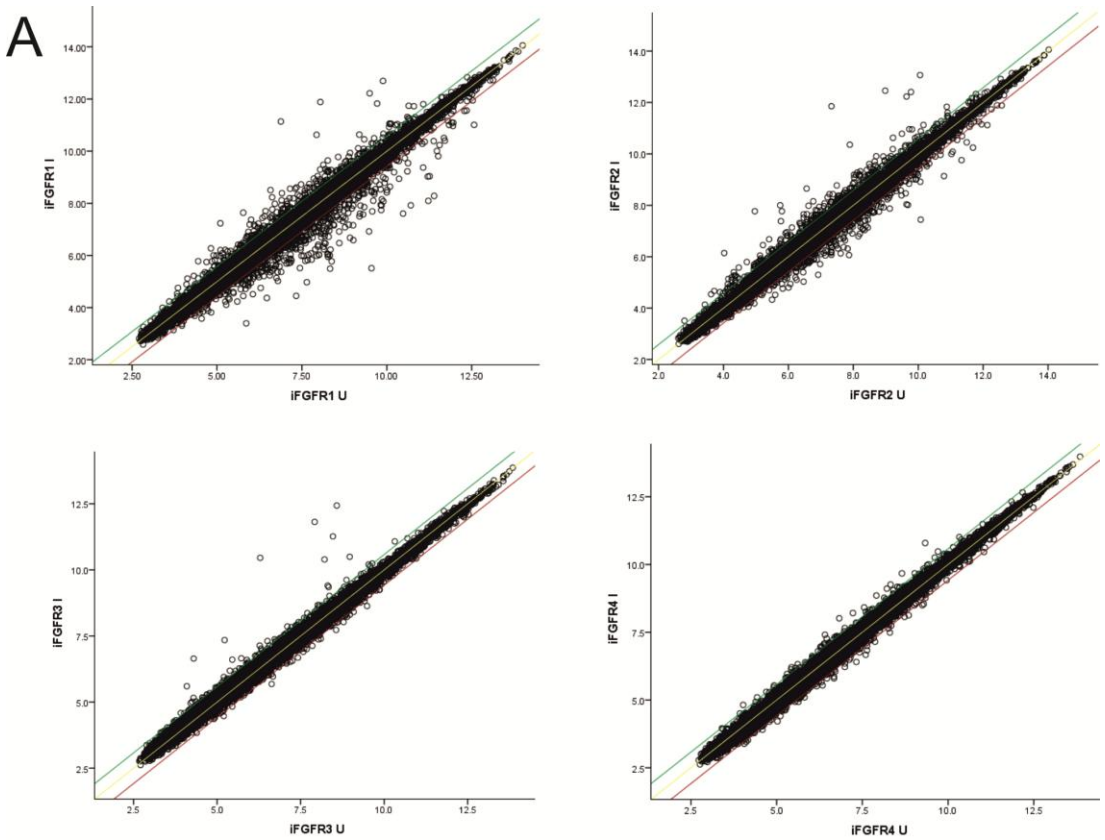

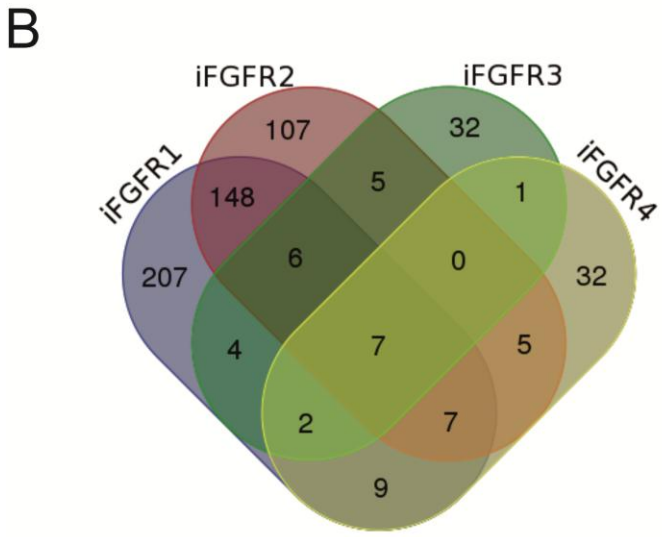

Figure 3.2 Microarray data analysis
A) shows scatterplots for each FGFR tested in the microarray. The log_2 expression value for each gene is plotted as a ratio between whole embryos injected with iFGFR and induced with AP20187 (iFGFR I) between stages 10 and 13 and untreated controls (iFGFR U). Most points lie across y=x, coloured yellow. Points to the left of the green line represent genes upregulated >1.5-fold by iFGFR and points to the right of the red line represent >1.5-fold downregulated genes. B shows genes with expression fold changes over 1.5x sorted by receptor into a Venn diagram.

Table 3.1 Genes commonly regulated by iFGFRs as found by microarray

Overlapping Categories	Number of genes	Genes						
iFGFR1 iFGFR2 iFGFR3 iFGFR4	8	*cnfn*	*capn8*	*fam115a*	*xepsin*	*Unknown*	*MGC115642*	*irg1 TA-2*
iFGFR1 iFGFR2 iFGFR3	6	*plscr1*	*MGC68910*	*junb*	*otog*	*sbk1*	*foxa4*	
iFGFR1 iFGFR2 iFGFR4	7	*cd81*	*wnt3a*	*kremen2*	*slc3a2*	*LOC100127277*	*G protein receptor*	*ubp1*
iFGFR1 iFGFR3 iFGFR4	2	*Rexp44 mRNA*	*Cico01 mRNA*					
iFGFR1 iFGFR2	148	*lefty*	*syt1*	*pitx2*	*tfap2a*	*pdgfa*	*nipal4*	*vill*
		kcnc3	*elf1*	*rab27a*	*lmo2*	*MGC53311*	*gdf3*	*LOC398134*
		fut1	*MGC85058*	*sat1*	*foxi1*	*b3gnt1*	*fam3d*	*rab25*
		mst1	*dnajb14*	*hal.1*	*ehd4*	*gata3*	*hoxa10*	*itln1*
		tob1	*wnt8a*	*hoxc6*	*amd1*	*gprc5c*	*c4orf31*	*LOC443682*
		agr3	*slc1a5*	*foxd4l1.1*	*U8 snoRNA*	*cmahp*	*sulfotransferase*	*MGC80993*
		hoxc10	*stard4*	*tmem45b*	*tpbg*	*eppk1*	*gbx2.2*	*t*
		ido1	*aldh1l1*	*tcf12*	*rax*	*atp1b2*	*nuak2*	*gata2*
		LOC496380	*LOC397753*	*arl5b*	*fa2h*	*eps8l1*	*pfkfb3*	*menf.1*
		xk81a1	*rasl11b*	*cldn4L2*	*agr2*	*LOC398232*	*pitx1*	*mpc2*
		ventx2.2	*LOC100158288*	*znf750*	*hoxa7*	*gdpd1*	*slc19a3*	*ccno*
		MGC68521	*tfap2b*	*grhl3*	*hexokinase -2*	*pou2f1*	*prr5*	*MGC68655*
		esrra	*hoxd3*	*liph*	*MGC78986*	*tmem169*	*kit*	*ca2*
		fezf2	*LOC100037100*	*tspan1*	*LOC100037144*	*kiaa1324l*	*mmp14*	*glo1*
		dynll1	*LOC100158277*	*hesx1*	*hoxa3*	*sgsm3*	*sytl2*	*traf4b*
		cdx4	*MGC82269*	*MGC52875*	*ventx3.2*	*bcat1*	*dusp6*	*cfd*
		dvl3	*LOC494641*	*capn9*	*EIG121L*	*hoxc8*	*MGC80142*	*fzd4*
		loc398404	*anxa9*	*Ras dva*	*egr1*	*MGC81684*	*foxd5b*	*gmpr2*
		LOC443659	*anxa2*	*six3*	*tmcc1*	*LOC100337617*	*crx*	*LOC495248*
		nek6	*wnt11b*	*fam3a*	*LOC100487499*	*MGC131003*	*kitlg*	*cdx1*
		slc25a24	*spry2*	*ca12*	*zfp729*	*LOC398437*	*grhl1*	*mtus1*
iFGFR1 iFGFR3	4	*sox13*	*TA-2*	*LOC503673*	*gdf1*			
iFGFR1 iFGFR4	9	*atp12a*	*MGC53823*	*mmp3*	*foxn4*	*lgals9*	*Cd81*	*sytl1*
		tnnc2	*cml*	*des.1*				
iFGFR2 iFGFR3	5	*ptafr*	*MGC82544*	*MGC52622*	*socs3*	*txn*		
iFGFR2 iFGFR4	5	*laptm4a*	*krt16*	*eps8l3*	*rasd1*	*paqr5*		
iFGFR3 iFGFR4	1	*muc19-like*						

To assess the overlap of genes affected by each receptor and to gain an insight into how FGF signalling output varies between the four receptors, genes more than 1.5-fold up or downregulated by each receptor were compiled into lists. Full genelists separated into up-and downregulated genes are in Supplementary Tables 1-8. Affymetrix Probe IDs for each gene were entered into a Venn Diagram maker from the University of Gent. The resultant Venn Diagram is shown in Figure 3.2B, and genes in overlapping regions displayed in Table 3.1. A breakdown of all overlapping and non-overlapping genes can be found in Supplementary Table 9. Only 8 genes are affected by all four receptors. Two of these, *irg* and *TA-2* can be disregarded as they are likely to be stress-response genes; they are found upregulated by dnFGFR1/4a in Branney et al., (2009). iFGFR1 and iFGFR2 share a relatively high number (148) genes in common compared to iFGFR3 and iFGFR4, which only share 1 gene in common. Furthermore, there are only 9 genes that are common between iFGFR1 and iFGFR4. These include the forkhead box transcription factor *FoxN4,* and *cd81* which encodes a tetraspanin integral membrane protein (Maecker et al. 1997). These are repressed by both receptors. *Tnnc2* which encodes *troponin C* (skeletal muscle) is differentially regulated by iFGFR1 and iFGFR4 (Takayama et al. 2008; Vassylyev et al. 1998). Overall however, these data show that iFGFRs have very different signalling outputs and can therefore provide an insight into how different FGFRs individually regulate development.

3.2.2.1 Genelists

Supplementary Tables 1-8 show the genes affected by each receptor, ranked by expression fold change. Using BRB Arraytool's confidence filtering thresholds and a requirement for genes to show a gene expression change of at least 1.5x, 151 genes were upregulated and 293 genes downregulated by iFGFR1, 160 genes upregulated and 161 genes downregulated by iFGFR2, 39 genes upregulated and 20 downregulated by iFGFR3 and 36 genes upregulated and 33 downregulated by iFGFR4.

Many genes listed in the genelists are already known to be FGF targets. Firstly, members of the MAPK pathway are found in the upregulated genelists as expected, as induced iFGFR1 and iFGFR2 upregulate the MAPK modulators *Dusp6* and *Sprouty2* (reviewed in Pownall & Isaacs 2010) (Table 3.2) . Ras GTPase is a critical link between RTKs such as FGFRs and the rest of the MAPK pathway (McKay & Morrison 2007). All four receptors upregulate Ras-related genes.

Rasl11b, which is not currently known as an FGF target but is involved in TGFβ signalling, is upregulated by iFGFR1 and iFGFR2 induction as is *RasD1,* member of the Ras superfamily involved in MAPK signalling (Pézeron et al. 2008; Liu et al. 2014). iFGFR3 upregulated *Ras* and *Rassf6,* an oncogene which binds activated Ras (Allen et al. 2007). Lastly, iFGFR4 upregulated *RasD1*.

FGFs induce the expression of *Cdx* genes which in turn activate posteriorly expressed 5' *Hox* to pattern the posterior neural tube. Indeed, iFGFR1 and 2 both upregulated *Cdx1* and *4*, and combined upregulated *HoxA3, A7, A10, B7, C10* and *D3* more than 1.5-fold. Other neural genes affected included the rostrally-expressed transcription factors *Dlx2* and *3* as well as forkhead transcription factor *FoxD5* known to regulate neural ectodermal fate and neural differentiation (Luo et al. 2007; Yan et al. 2009).

Members of other signalling pathways were also affected by induced iFGFRs, particularly the Wnt signalling pathway which is known to cooperate with FGF to pattern posterior tissue (reviewed in Garnett et al. 2012). Genes found known to be affected by alternative signalling pathways are shown in Table 3.2. *Wnt3a*, *8a*, *5b*, *11b* were upregulated by iFGFR1 activation and negative Wnt regulators *Kremen* and *Prickle1* upregulated by iFGFR2 activation. iFGFR4 did not activate as many Wnt signalling components compared to iFGFR1 and iFGFR2, but did upregulate *Wnt3a* and *Kremen*. iFGFR1 and iFGFR2 also downregulated the expression of Frizzled receptor *Fzd4* and Wnt effector *Dvl3*. iFGFR1 downregulated the expression of *Ctnnb1,* also known as β-catenin. Other Wnt signalling genes affected were *Cdh1* and *Cdh2, Sfrp2* and *Pcdh10,* all downregulated by iFGFR1, Only iFGFR3 did not affect the Wnt pathway. The Sonic hedgehog (Shh) pathway was also represented as iFGFR2 upregulated *Shh* itself, as well as *Btrc*, and downregulated *Smo.* iFGFR1 upregulated the Shh receptor *Ptch2.* The cellular RA pathway binding protein *Crabp2* was upregulated by iFGFR1, but RA receptors RXR and *retinoic acid receptor responder1* (*Rarres1)* were downregulated by iFGFR2. TGFβ-related genes included Junb, which with iFGFR1 and iFGFR2, was the only gene in this list upregulated by iFGFR3. iFGFR3 downregulated the TGFβ-related factor *Gdf1*.

Table 3.2 Components of other signalling pathways regulated by iFGFRs

Pathway	Gene	Summary/Reference	iFGFR
FGF	*RASL11B*	Small GTPase	iFGFR1, iFGFR2
	SPRY2	MAPK antagonist	iFGFR1, iFGFR2
	DUSP6	MAPK phosphatase	iFGFR1, iFGFR2

	RASD1	Small GTPase	iFGFR2, iFGFR4
	RAS-DVA	Small GTPase	iFGFR1, iFGFR2
	RASSF10	Small GTPase	iFGFR1
	RAS	MAPK small GTPase	iFGFR3
	RASFF6	Small GTPase	iFGFR3
WNT	*WNT3A*	Wnt ligand	iFGFR1, iFGFR2, iFGFR4
	KREMEN2	Wnt antagonist receptor	iFGFR1, iFGFR2, iFGFR4
	WNT11B	Wnt ligand	iFGFR1, iFGFR2
	WNT8A	Wnt ligand	iFGFR1, iFGFR2
	XBRA	Transcription factor (Vonica & Gumbiner 2002)	iFGFR1, iFGFR2
	DVL3	Wnt signal transduction	iFGFR1, iFGFR2
	FZD4	Wnt receptor	iFGFR1, iFGFR2
	WNT5A	Wnt ligand	iFGFR1
	WNT5B	Wnt ligand	iFGFR1
	CDH1	Cadherin, negative Wnt regulator (Colli et al. 2013)	iFGFR1
	CDH2	Cadherin, negative Wnt regulator (Revollo et al. 2015)	iFGFR1
	SFRP2	Frz-related protein (Ladher et al. 2000)	iFGFR1
	PCDH10	Protocadherin (Zhao et al. 2014)	iFGFR1
	CTNNB1	Wnt signal transduction	iFGFR1
	PRICKLE1	Wnt antagonist receptor	iFGFR1
	WNT3	Wnt ligand	iFGFR2
	BTRC	Ubiqutin protein ligase (Su et al. 2008)	iFGFR2
	FZD7	Wnt receptor	iFGFR2
TGFβ	*JUNB*	Transcriptional activator (Busnadiego et al. 2013)	iFGFR1, iFGFR2, iFGFR3
	LEFTY	Nodal effector	iFGFR1, iFGFR2
	GDF3	TGFβ-related growth factor	iFGFR1, iFGFR2
	RASL11b	GTPase	iFGFR1, iFGFR2
	GDF1	TGFβ-related growth factor	iFGFR1, iFGFR3
	BMP7.2	BMP ligand	iFGFR1
	JUND	Transcriptional activator (Lee et al. 2012)	iFGFR2
Sonic Hedgehog	*PTCH2*	Shh receptor	iFGFR1
	BTRC	Ubiqutin protein ligase (Su et al. 2008)	iFGFR2
	SHH	Shh ligand	iFGFR2
	SMO	Shh signal transduction	iFGFR2
RA	*GPRC5C*	G protein receptor (Robbins et al. 2000)	iFGFR1, iFGFR2
	CRABP2	RA-binding protein	iFGFR1
	RXRB	RA receptor	iFGFR2
	RARRES1	RA receptor responder	iFGFR2

Colours refer to Upregulated by iFGFR and Downregulated by iFGFR. Gene functions were found using Xenbase – if the pathway-related function was not listed under gene function, literature searches were conducted and references are shown.

Therefore, all four of the iFGFRs affect the expression of genes active in the other major signal transduction pathways during this period of development. Of the genes listed in Table 3.2, iFGFR1 and iFGFR2 affect the majority, either on their own or in combination with each other. iFGFR3 and iFGFR4 may have roles in regulation of the TGFβ and Wnt signalling pathways respectively, and iFGFR2 affected the most genes in the Shh and RA pathways.

Groups of genes involved in certain developmental processes were also represented in the genelists. Among downregulated genes were those involved with eye development. The eye markers and transcription factors *Rax* and *Pax6* was downregulated by iFGFR1 and 2. Genes involved in Left/Right development were also represented. Nodal interactants *Lefty* and *Pitx1* and *2*, essential for breaking left/right symmetry are upregulated and downregulated by both iFGFR1 and 2 respectively. Other genes involved in Nodal/TGFβ signalling are *FoxI1* and *Menf.1* downregulated by iFGFR1 and iFGFR2 (Kumano & Smith 2002; Zhang & Klymkowsky 2007). *Traf4*, a zinc finger protein with signalling transduction through both Nodal and BMP pathways, was positively regulated by iFGFR2 (Kalkan et al. 2009) . In keeping with FGF's role in inhibiting BMP signalling in the neuroectoderm which would otherwise specify epidermis, epidermal genes such as the transcription factor *Grhl1, 2* and *3* expressed in non-neural ectoderm, and ANB and epidermal marker keratin, are downregulated by iFGFR1 and iFGFR2 and interestingly, upregulated by iFGFR4.

Interesting novel putative FGF targets genes include Dynein light chain 1 *Dynll1* and Never in mitosis kinase *Nek6* upregulated by both iFGFR1 and iFGFR2. Nek6, as part of a complex with Nek7 and Nek9 has been shown be activated through binding of Dynll1 (Regué et al. 2011). One of the largest changes to gene expression by iFGFR1 and iFGFR2 was that of *Tspan1,* an integral membrane protein. A link between *Tspan1* and FGF signalling has not been yet made, but *Tspan1* has been shown to be negatively regulated by BMP signalling and required for primary neurogenesis (Yamamoto et al. 2007).

These data show that in addition to FGF being involved in neural induction and patterning, it also influences the activity of other signalling pathways and developmental processes.

3.2.3 iFGFRs reproducibly upregulate known FGF targets in whole embryos and in a neural context

Some genes in the dataset were picked to be investigated further by RT-qPCR. This was done partially to validate the microarray dataset. Another reason was to ascertain if iFGFRs could reproducibly affect gene expression as only one repeat of the microarray experiment was performed. An aim was to ascertain whether the experimental conditions could be refined to target iFGFRs to the CNS to affect gene expression. Finally, they would provide a number of positive controls for the RNA-seq experiment. *Egr1, Sprouty2* and *Leftyb* were chosen to validate the microarray dataset as they have known connections to FGF signalling.

Early growth response 1 (*Egr1)* is a zinc finger transcription factor previously shown in an enriched cDNA library screen to be a target of the FGF target *Xbra* as well being a direct FGF target in gastrula-staged embryos (Saka et al. 2000; Branney et al. 2009). It was upregulated 3.81-fold by iFGFR1. *Sprouty2* is a well known negative regulator of the MAPK pathway and was upregulated 1.91-fold by iFGFR1 (Hanafusa et al. 2002; Sivak et al. 2005). The Left/Right determination factor *Leftyb,* upregulated 2.41-fold by iFGFR1, is part of the Nodal signalling cascade which is responsible for breaking left/right symmetry in the early embryo. The murine *Lefty1* and *2* genes seem to correspond to *Leftyb* and *a* in *Xenopus laevis* after comparing sequences, and these give a virtually identical protein product (data not shown). There is a single *Lefty* gene in *Xenopus tropicalis.* Therefore *Leftyb* will be hereafter referred to as *Lefty.*

3.2.3.1 RT-qPCR confirms *Egr1* and *Sprouty2* are positively regulated by iFGFR1 in whole embryos

Using the same experimental conditions as those used in the microarray-based analysis, RT-qPCR was performed to confirm the upregulation of *Egr1* and *Sprouty2*. In addition to inducing embryos injected with 20pg iFGFR1 from stage 10.5 to 13, some embryos were also induced until stages 15 and 17 to investigate whether the effects on downstream gene expression caused by iFGFR1 change over time. To provide a complementary experiment, embryos injected with 1ng dnFGFR1 were also collected and subjected to RT-qPCR at the same time points. This dosage of dnFGFR1 caused similar gastrulation defects and anteriorisation of *Xenopus laevis* embryos as those described in Amaya et al. (1991) and a decrease in dpERK levels by western blot analysis (data not shown). RT-qPCR results are shown in Figure 3.3. Expression levels for all RT-qPCR results were normalised to

the housekeeping gene *ornithine decarboxylase* (*ODC*). For iFGFR experiments fold-expression changes are displayed relative to uninduced controls and for dnFGFR1-injected embryos, uninjected controls.

Figure 3.3A shows that at all time points tested, induced iFGFR1 caused upregulation of both *Egr1* and *Sprouty2*, however this ceased to be significant for the longest induction period, from stage 10.5 to 17. The mean fold expression changes for the stage 10.5 to 13-induced embryos were 3-fold for *Sprouty2* and 3.61-fold for *Egr1.* This is slightly higher than the values found in the microarray. A corresponding significant reduction in levels of *Sprouty2* and *Egr1* was seen in dnFGFR1-expressing embryos. This was significant at all stages, suggesting that dnFGFR1's effects on FGF targets are longer lasting than those of iFGFR1. There was no appreciable difference in gene levels between uninjected and uninduced iFGFR1-injected embryos.

3.2.3.2 *Egr1, Sprouty2* and *Lefty* are upregulated by iFGFR1 in neuralised ectodermal explants

As these results confirmed those found in the microarray, RT-qPCR was conducted upon neuralised animal cap explants injected with iFGFR1 to see whether iFGFR1 could influence the expression of *Egr1, Sprouty2* and *Lefty* in a neural context. Embryos were co-injected with 20pg iFGFR1 and 50pg *Noggin* mRNA at the 2-cell stage and explants dissected at late blastula stage 8. An induction time period of 3 hours at 22°C from stage 10.5 was chosen, as *Xenopus* Refseq and RNase protection analysis data suggest this is the time period taken for targets of FGF signalling such as *MyoD* and *HoxA7* to be activated after immediate early targets of FGF such as *Xbra* and *Cdx4* (Keenan et al. 2006; Tan et al. 2013). Expression of *Noggin* mRNA only or *iFGFR1+Noggin* alone did not affect the expression of the three genes. Co-injected induced explants showed significant upregulation of *Lefty, Sprouty* and *Egr1*. To see if these responses were the same when iFGFR1 was induced at a later stage, the experiment was repeated but explants treated with AP20187 at stage 12 – late gastrula. This resulted in an even greater upregulation of all three genes relative to uninduced explants (Figure 3.3B,ii). Therefore, as well as replicating the findings in the microarray, iFGFR1 upregulates *Egr1, Sprouty2* and *Lefty* in a neuralised explants, suggesting these genes are also neural FGF targets. The difference in expression changes between early and later periods of iFGFR1 induction for *Lefty*, *Sprouty2* and *Egr1* suggests the response of genes to iFGFRs may change over time.

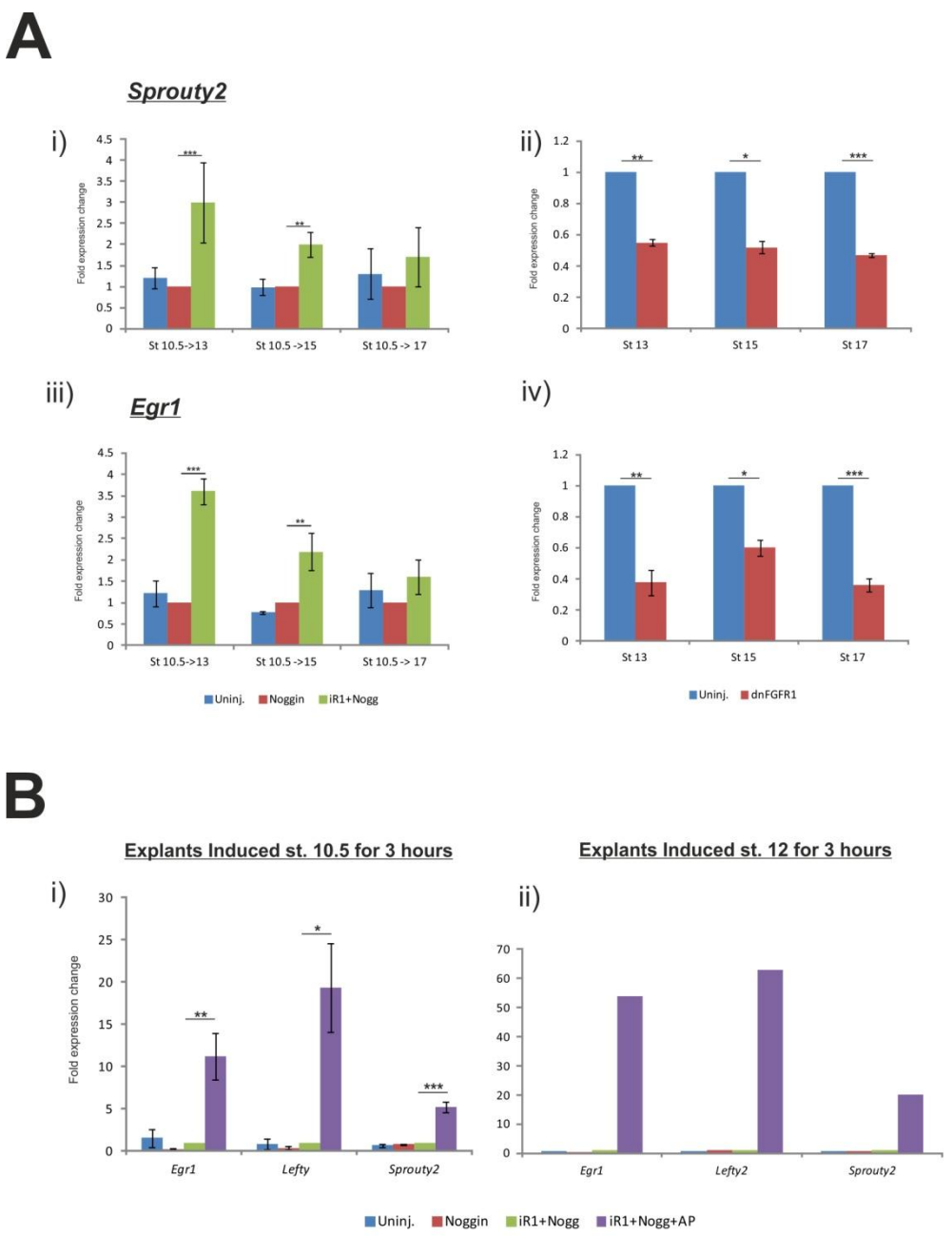

Figure 3.3 RT-qPCR for Lefty, Sprouty2 and Egr1
A)Shows RT-qPCR results for the genes *Sprouty2* (i and ii) and *Egr1* (iii and iv). i) and iii) show embryos injected with 20pg iFGFR1 and treated with AP20187 between stages 10.5 and 13, 15 or 17. ii) and iv) are from embryos injected with 1ng dnFGFR1 and collected at stage 13, 15 or 17. Error bars represent SE from three biological replicates. Asterisks represent statistical significance of normalised Ct values below p=0.05. Ct values were normalised against those of the housekeeping gene *ODC* and fold expression changes normalised against uninduced iFGFR1-injected embryos, which have a fold change of 1.

B)Shows RT-qPCR results for genes *Sprouty2, Egr1 and Lefty* in neuralised animal cap explants. Explants were injected with 50pg Noggin and 20pg iFGFR1 and treated with AP20187 from i) stage 10.5 for three hours or ii) stage 12 for 3 hours. i) Error bars represent SE from three biological replicates. Asterisks represent statistical significance of normalised Ct values below p=0.05. ii) Shows mean expression fold change from technical replicates. Ct values were normalised against those of the housekeeping gene *ODC* and fold expression changes normalised against co-injected uninduced explants which have a fold change of 1.

3.2.3.3 iFGFR1 expands the expression domains of *Cdx4* and *HoxA7*

The known FGF targets *Cdx4* and *HoxA7* were also found in the microarray to be positively regulated by iFGFR1. 10pg iFGFR1 was injected bilaterally into *Xenopus laevis* embryos into the two dorsal animal blastomeres at the 8-cell stage. Embryos were cultured until stage 10.5 and treated with AP20187 for 3 hours at 22°C. They were processed for ISH using antisense DiG-tagged probes against *Cdx4* and *HoxA7*. *Cdx4* is expressed in a ring around the closing blastopore, strongest ventrally. Figure 3.4 shows that iFGFR1 induction in prospective neural tissue expands the *Cdx4* domain both dorsally above the closing blastopore (Figure 3.4 B, compare with A, arrowed), and anteriorly (Figure 3.4B', compared to A, line). *HoxA7* expression is present as a crescent ventrally underneath the closing blastopore and is extended dorsally in some iFGFR1 induced embryos as shown by the dotted lines in (Figure 3.4D compared to C).

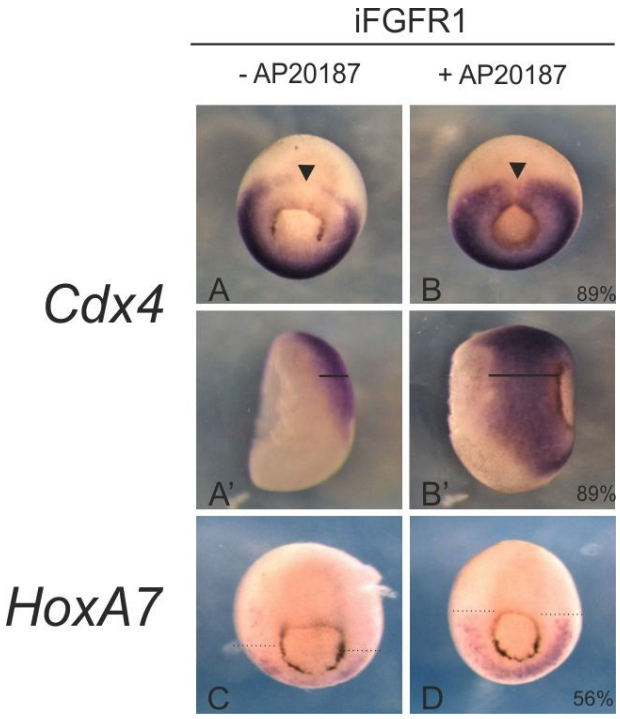

Figure 3.4. iFGFR1 targeted to prospective neural tissue expands the expression domains of *Cdx4* and *HoxA7*.
Embryos were injected bilaterally with 10pg iGFR1 into two dorsal animal blastomeres at the 8-cell stage and processed for ISH. B shows an expansion of the *Cdx4* (N=9) expression domain dorsally as shown by the arrow to compare to the control in A. A' and B' are side views of A and B. The anterior expansion of the *Cdx4* expression domain is shown by a black line. D shows the *HoxA7* (N=9) expression domain expanded dorsally relative to C, the control. Percentages show embryos resembling the representative image.

Therefore, as well as predictably affecting expression levels of known iFGFR1-upreglated genes found in microarray by RT-qPCR, the expression domains of

other FGF target genes *Cdx4* and *HoxA7* were expanded when iFGFR1 was induced in the prospective CNS.

3.3 Discussion

3.3.1 A microarray screen shows iFGFRs profoundly affect the *Xenopus* transcriptome

A dataset from a preliminary microarray performed by previous lab members was analysed which investigated transcriptomic changes that occurred as a result of iFGFR1, iFGFR2, iFGFR3 or iFGFR4 induction in whole embryos throughout gastrulation. iFGFR1 and 2 affected the levels of many genes ≥1.5-fold, whereas iFGFR3 and iFGFR4 generally affected fewer genes to a lesser extent. iFGFR1 and iFGFR2 signalling outputs were the most similar to each other, suggesting that at during this point in development the output of these receptors is fairly similar relative to the other receptors. However, 220 genes were still unique to the iFGFR1 genelist and 96 genes unique to the iFGFR2 genelist suggesting that these receptors must nevertheless have unique roles in development. iFGFR3 and 4 commonly regulate comparatively very few genes with the other receptors and each other. This suggests that at this point in development, FGFRs1-4 indeed have different signalling outputs, and so iFGFRs are therefore a useful tool for assessing differences in FGFR signalling outputs. This finding was not found in Branney et al, (2009) who used dnFGFR1 and dnFGFR4a to investigate the FGF-dependent transcriptome during blastula stages – in this paper the two receptors had an almost identical expression profile. The authors postulated that this may be due to promiscuous heterodimerisation of dnFGFR causing non-specific receptor effects upon gene expression (Ueno et al. 1992; Branney et al. 2009). Therefore, to study individual FGFR signalling outputs, iFGFRs are a better tool to use than dnFGFRs. It would be interesting to use iFGFRs at earlier stages to see how they compared and contrasted with those of Branney et al. (2009).

3.3.2 There is crosstalk between FGF signalling and other pathways

Many genes in the genelists have known links to FGF signalling, or are members of pathways that interact with FGFs. MAPK effectors such as DUSPs and Ras family members were well represented in the data, as were *Cdx* and *Hox* genes which are

well documented targets of FGF signalling in patterning the posterior neural tube (reviewed in Montavon & Soshnikova 2014).

3.3.2.1 Wnt and RA signalling

A significant number (19) of Wnt signalling pathway components, including Wnt ligands and receptors, were found in iFGFR1,2 and iFGFR4 genelists. FGF and Wnt signalling pathways are known to cooperate closely during neural development in the patterning of the posterior neural tube, in part by regulating *Cdx* gene expression (Keenan et al. 2006; Shimizu et al. 2006). Furthermore, Wnt signalling has been reported to be active in the transition zone between opposing FGF and RA gradients during posterior neural patterning and neuron differentiation. In the chick, FGF signalling promotes *Wnt8c* expression which is maintained even as cells leave the posterior influence of FGF signalling. Wnt8c was then found to act similar to FGFs by inhibiting neuronal differentiation, although unlike FGF signalling this does not seem to be through repression of retinoid signalling (Olivera-Martinez & Storey 2007). *Crabp2*, which encodes a retinoic acid binding protein, found here upregulated by iFGFR1 was previously found to be a target of Wnt signalling as well as RA, and so was hypothesised to work at the interface of RA and Wnt signalling during antero-posterior embryonic patterning in *Xenopus* (Janssens et al. 2010). *Crabp2* could therefore be an important point of regulation during development and patterning of the posterior CNS where RA, Wnt and FGF signals meet. The RA receptor *RxrB* and *Rarres,* a RA receptor responder were both downregulated by iFGFR2, indicating a possible role of FGFR2 in negative regulation of the retinoid signalling.

3.3.2.2 Sonic Hedgehog signalling

Shh was upregulated by iFGFR2, as was its receptor *Ptch2* by iFGFR1. Its negative regulator *Smo* was downregulated by iFGFR2. Shh signalling is required for forebrain development as Shh activates *FoxG1* expression (Hébert & Fishell 2008). FGF signalling encourages this event as it negatively regulates *Gli3*, the negative regulator of the Shh pathway (Rash & Grove 2007). Shh is also required for dorso-ventral patterning in the neural tube, where FGF signalling acts to maintain cells in an immature state by repressing neuronal differentiation in general, as well as Shh-activated class 1 and 2 proteins oppose dorso-ventral patterning (Diez del Corral et al. 2002; Diez del Corral et al. 2003; Briscoe & Novitch 2008). Therefore there is a precedent for crosstalk between FGF and hedgehog signalling during neural development.

3.3.2.3 Nodal Left/Right asymmetry cascade

There are also many genes represented that are involved in processes other than neural induction and patterning, such as those involved in left/right asymmetry. *Lefty, Pitx1* and *Pitx2* are all members of the Nodal signalling cascade, which breaks left/right symmetry early in development.

The breaking of left/right asymmetry in early embryonic development is an essential event for correct organ placement. Aberrations in this process can cause bilateral symmetry, isomerism – duplicated left/right sided identity – random organ placement (heterotaxia) or *situs inversus totalis*, where the whole L/R axis is inverted (Ramsdell & Yost 1998). Polarised cilia are required to provide a left-wards flow across the posterior-most roof of the archenteron –the gastrocoel roof plate (GRP) – in *Xenopus,* Kuppfer's vesicle (KV) in zebrafish, and the node in mammals to break left/right symmetry (Schweickert et al. 2007; Nonaka et al. 1998). It is thought that this flow either carries vesicles containing morphogens to the left-hand side of the embryo or sensory cilia also in the node/GRP sense fluid movement and convert this into an asymmetric calcium signal (Okada et al. 2005; McGrath et al. 2003; Nonaka et al. 1998). Leftwards flow connects to changes in gene expression by causing the Nodal inhibitor *Coco* to be downregulated in the left lateral plate mesoderm only, which lifts repression of the TGFβ family member Nodal signalling asymmetrically (Schweickert et al. 2010). Nodal activates a cascade of gene expression in part by activating another TGFβ-related gene *Lefty*, which restricts Nodal protein to the left lateral plate mesoderm where the Nodal effector Pitx1 is also expressed (Ramsdell & Yost 1998). Manipulation of *Lefty*, *Pitx1/2* or *Nodal* cause laterality defects in *Xenopus,* such as left cardiac isomerism, reversed gut looping and heterotaxia (Schweickert et al. 2012).

FGF signalling is linked to both cilia development and regulation of the nodal cascade (Basu & Brueckner 2009). Zebrafish *FGF8* mutants (also known as *ace* mutants) have been reported to have fewer or shorter cilia in the GRP relative to wild-type embryos, impairing leftward flow which consequently caused defects in gut looping (Hong & Dawid 2009; Neugebauer et al. 2009). Other studies in the fish showed 30% of *ace* mutants lacked the KV. As a result embryos developed laterality defects, particularly in the heart. The brains of these fish were also found to contain laterality defects, as *Pitx2c* expression which is normally on the left-hand side of the diencephalon only, was either absent or expressed bilaterally in the majority of *ace* embryos (Albertson & Yelick 2005). *FGF8*-mutant mouse embryos

have laterality defects such as random or absent heart looping and right pulmonary isomerism/*situs inversus* of lungs, reminiscent of *Lefty*-deficient embryos. In these embryos *Lefty2* expression was also not detected suggesting *Lefty* expression requires FGF signalling (Meyers & Martin 1999). In the chick, application of a *Lefty2*-soaked bead to the right hand side of the node caused a loss of *FGF8* expression, suggesting *Lefty2* represses FGF signalling (Rodríguez Esteban et al. 1999). A direct link between FGF8 and *Lefty* downstream has not to my knowledge been established, however in the zebrafish, morpholinos against the FGF targets *Ier2* and *Fibp1* in the zebrafish had randomized expression of *Lefty* (Hong & Dawid 2009).

Lefty, Pitx1 and *Pitx2* were found by this microarray to be upregulated by iFGFR1 and/or iFGFR2, suggesting that FGF signalling regulates left/right asymmetry through mediation of several genes in the Nodal cascade. Other genes also implicated in Nodal/TGFβ signalling found in the microarray-based screen include *Foxi1* and *Menf.1,* downregulated by iFGFR1 and iFGFR2. Although a connection between *FoxI1* with FGF has been reported, as *FoxI1* morphants prevented FGF-mediated mesoderm induction, no link to laterality defects have as yet been reported (Suri et al. 2005). Menf.1 has previously been shown to be activated by Nodal signalling and negatively regulated by FGF activity in induction of ventral mesoderm, however again, no link to left/right asymmetry or laterality defects have been reported (Kumano & Smith 2002).

3.3.3 iFGFRs affect downstream gene expression – validation of a preliminary microarray dataset

Some known FGF targets were picked from the microarray in order to see if iFGFRs could reproducibly achieve the same level of effect by RT-qPCR and ISH and also to validate the microarray. Conditions of the microarray were replicated to investigate *Egr1* and *Sprouty2* by RT-qPCR, and also over a longer iFGFR1 induction period.

3.3.3.1 RT-qPCR shows that *Egr1, Sprouty2* and *Lefty* are FGF targets in whole embryos and in neuralised explants

Early growth response 1 (*Egr1)* is a zinc finger transcription factor previously shown in an enriched cDNA library screen to be a target of the FGF target *Xbra*, imperative for mesoderm induction and maintenance (Saka et al. 2000). Furthermore, it was found in a microarray screen by Branney et al, (2009) to be positively regulated by

FGF in gastrula stage *Xenopus* embryos (Branney et al. 2009). ISH in *Xenopus* embryos showed *Egr1* to be expressed in the mesoderm (Saka et al. 2000). However, outside of early developmental biology, Egr1 has been implicated in neural plasticity and memory through its regulation of neuronal apoptosis (Pignatelli et al. 2003). Therefore there is a precedent for it having a role in neural as well as mesodermal development.

Sprouty2 is a MAPK antagonist and required for correct morphogenesis during *Xenopus* gastrulation (Sivak et al. 2005). However there is also evidence to suggest that it is has a role in neural development. In the chick, *Sprouty2* transcripts are detected in the midbrain and hindbrain regions, as well as specifically in the isthmus and rhombomere 1(Chambers & Mason 2000). In the IsO *Sprouty2* expression overlaps with, and is induced by, *FGF8*. Expression of a dominant-negative form of *Sprouty2* in the chick resulted in an expansion of the *FGF8* expression domain and an anterior shift in the posterior border of the tectum (Suzuki-Hirano et al. 2005). Independent of *FGF8*, *Sprouty2* inhibits neuronal differentiation and survival in a negative feedback loop with another growth factor BDNF in primary cultures of immature neurons (Gross et al. 2007). Also, viral vector-mediated disruption of endogenous *Sprouty2* using dnSpry2 in the dorsal hippocampus of adult rats stimulated neurogenesis. These rats also showed behavioural differences to control littermates as they were more resilient to stress, whereas those overexpressing wild type *Spouty2* displayed more anxiety when startled by white noise (Dow et al. 2015). It may therefore useful to confirm *Egr1* and *Sprouty2* as being neural FGF targets to give an insight into how aberrances in cell signalling in these pathologies originate.

RT-qPCR results reproduced those found by microarray for *Sprouty2* and *Egr1*. These genes were conversely affected by dnFGFR1 and this repression was significant for all time periods tested. The iFGFR1 upregulation response was not significant over the longest induction period from stage 10.5 to late neurula stage 17. Perhaps other FGFRs signalling normally can compensate for constitutively-active iFGFR1 signalling, whereas the blanket FGFR repression by dnFGFR1 prevents this. A greater insight into this result could be provided by using other dnFGFRs such as dnFGFR4a, as well as more induction lengths for iFGFR1 to see if there is a cut-off point for the influence of iFGFRs on *Egr1* and *Sprouty2*, as well as other genes' expression levels.

Lefty, upregulated by iFGFR1 and 2 in the microarray screen was chosen in conjunction with *Egr1* and *Sprouty2* to investigate iFGFR1 upregulation in neuralised animal cap explants. In neuralised animal cap explants, *Lefty, Egr1* and *Sprouty2* were robustly upregulated to a much greater extent relative to whole embryos by iFGFR1 in neuralised animal cap explants. When induced from stage 12 for 3 hours, the extent of the upregulation was even more pronounced. It would therefore be interesting to investigate and compare the transcriptome when FGF signalling is activated during a later period of neural specification. These results suggest that not only are the microarray results reproducible, but those that appear to be neural FGF targets based upon present literature are strongly affected in the context of neuralised animal cap explants. This is encouraging as a foundation for investigating the whole *Xenopus* transcriptome in a neural context.

3.3.3.2 iFGFRs cause ectopic expression of FGF targets *HoxA7* and *Cdx4*

Some of the microarray results were also validated through ISH with known FGF targets *HoxA7* and *Cdx4*. FGF induction expanded the expression domains of all three of these genes. iFGFR1 expressed throughout the *Xenopus* embryo has already been shown to expand the expression domains of *Cdx4* and *HoxA7* by ISH in whole embryos in Pownall et al. (2003). Figure 3.4 shows that when injections of iFGFR1 were targeted to prospective neural tissue, an expansion of *Cdx4* and *HoxA7* is still seen, albeit to a lesser extent than the whole-embryo induction shown in Pownall et al., (2003). Thus, iFGFRs can be used to investigate gene expression in a neural context through targeting iFGFRs to the CNS as well as by using neuralised animal cap explants.

3.3.4 Caveats to the microarray data

Although the experimental conditions for this microarray certainly produced profound effects on downstream gene expression, the methodology was not optimised beforehand for iFGFR2-4, and based upon conditions used for iFGFR1 in Pownall et al. (2003). It was also not reported in Pownall et al., (2003) whether the optimal drug concentration was used to maximise MAPK activation. It was also not reported if iFGFR induction of the MAPK pathway remained constant during neural induction stages to ensure continual activation of FGF signalling. Furthermore, it was unknown how quickly AP20187 was able to diffuse into the embryo to produce a detectable increase in dpERK levels. This is not so important in this experimental context where iFGFRs were activated over a long period of time, but it would be

beneficial to know if activating the iFGFRs for a short window of time from a defined stage – for example, if it took one hour for MAPK signalling to increase from drug application, the drug may have to be added pre-emptively to ensure uniform iFGFR1 dimerisation over the whole induction period.

Only one biological repeat of the experiment was undertaken. Ideally at least three biological replicates would have been performed in order to perform statistical analyses. This is not imperative for the initial aims of the analyses performed here; to provide an initial insight into iFGFR effects upon the transcriptome and to provide positive controls for further experiments to study FGF signalling in the CNS. However, these data were interesting in their own right, as putative novel FGF targets such as *Tspan1* and *Hmx3* were revealed and so to take these findings forward and to complement the RNA seq data, additional biological repeats would be advantageous. They may eliminate false positives in the data – especially for those genes falling on the expression-change thresholds of ≥1.5 fold-expression change such as *FoxN4* which did not meet significance for fold change by RT-qPCR and may be more likely to be false-positives and upregulated/downregulated by chance (discussed in Chapter 6).

3.3.5 Future work

3.3.5.1 Areas of interest in the microarray dataset to investigate further

Compared to iFGFR1 and iFGFR2, iFGFR3 did not affect the expression of as many genes in the microarray experiment. Although iFGFR3 affected the expression of *Junb* and *Gdf1,* effectors of TGFβ signalling, Xenbase searches of most of the genes in the iFGFR3 genelists did not find many that were linked to FGF signalling or neural development. Searching the genelist for GO terms on PANTHER revealed the majority of genes were linked to metabolic processes (data not shown) FGFR3 may function in other cellular processes during neural specification or may be important for later aspects of neural development, as in tailbud embryos it is present in the brain (Lea et al. 2009). However, it will not be investigated further in this project. More detailed analyses of FGFR3's targets at this, and other points in development, and how its effects differ from other receptors would be interesting in its own right to investigate at a later date.

iFGFR1 (VT-) was not included in the microarray-based screen, but iFGFR1 VT- was synthesised along with the other receptors. A comparison between iFGFR1 VT+ and VT- would be interesting to see how signalling differed, if at all, between

these iFGFR1 subtypes, or whether genes are differentially regulated by these two receptors.

3.3.5.2 Investigation of iFGFR signalling in *Xenopus* neural development

For this microarray-based screen, iFGFRs were expressed throughout the embryo and the iFGFR induction length was long enough for secondary or even tertiary targets of FGF signalling to be activated. In order to investigate proximal FGF neural targets, iFGFRs would have to be targeted to the CNS, neuralised explants used or the CNS isolated from the rest of the embryo. The former two options have been shown in this work to be viable approaches to affect downstream neural FGF targets.

3.3.6 Summary

This chapter has shown through the analysis of a microarray dataset that constitutive activation of the FGF signalling pathway using iFGFRs has a strong effect upon the *Xenopus* transcriptome. The low overlap between genes affected by each iFGFR suggests that each FGFR has a unique role in *Xenopus* development. Validation of known FGF targets showed that iFGFR1 reproducibly affects gene expression both in whole embryos and in a neural context.

4 Optimisation of iFGFR injection and induction

4.1 Introduction

4.1.1 Investigating FGF function using Overexpression of Mutant FGF receptors

Reverse genetics are commonly used in biology to investigate the function of a gene or signalling pathway, by inhibition or overexpression of the gene of interest, and observation of the changes in development that result at the physiological and molecular levels. In *Xenopus,* mRNA coding for the gene of interest or mutant constructs can be microinjected into embryos at cleavage stages to study effects of overexpression, or inhibition of genes.

4.1.1.1 Dominant negative FGFRs (dnFGFRs)

There are many components to FGF signalling pathways downstream from the 4 main receptor types, and so repression of any one ligand, receptor, or receptor-interacting protein is unlikely to result in effective signalling inhibition. However mutant versions of the receptors which act as constitutively active or dominant-negative receptors have been used successfully in *Xenopus* to study FGF signalling. Dominant negative FGFRs such as dnFGFR1 and dnFGFR4a lack cytoplasmic kinase domains. DnFGFRs expressed in *Xenopus* embryos dimerise with wild type FGFRs when translated. Without kinase domains, dnFGFR:FGFR heterodimers cannot cross-phosphorylate each other and thus cannot function to mediate signal transduction (Amaya et al. 1991; Hongo et al. 1999).

dnFGFR1 and dnFGFR4 have been used in a number of studies in *Xenopus* and completely block the activation of dpERK in the early stages of development (Christen & Slack 1999). They also have been used to show that FGF is required for mesoderm induction through a positive feedback loop between FGF4 and *Xbra*, the formation of mesodermal tissues such as muscle, correct posterior development, and morphogenetic movements during gastrulation (Enrique Amaya

et al. 1991; Amaya et al. 1993; Isaacs et al. 1994). DnFGFR1 and 4 have also been used in a microarray screen by Branney et al., (2009) to investigate how FGF signalling affects the *Xenopus* transcriptome during mesoderm formation. In this, and previous studies, dnFGFR4a was shown to have more drastic effects than dnFGFR1, perhaps pointing towards differential roles for the two receptors for neural development (Hardcastle et al. 2000; Branney et al. 2009; Hongo et al. 1999). However, as there was considerable overlap between many of the genes affected by the two dnFGFRs in Branney et al, (2009), it could suggest that FGFR1 and FGFR4 signalling outputs are very similar. This result may be due to a lack of dnFGFR specificity however, as dnFGFR1 has also been shown to inhibit FGFR2 and 3 as well as FGFR1. It is likely that this is due to the promiscuous binding of dnFGFR1 to other FGF receptors (Ueno et al. 1992).

4.1.1.2 Constitutive activation of FGF signalling

Injection of mRNA coding for individual FGF ligands has been used previously to investigate the effects upon development of general over-activation of FGF signalling in *Xenopus*. This of course only gives the effects of a subset of FGF signalling events, as many ligand and receptor combinations take place to fine tune FGF signalling during development. There are also synthetic constitutively-active forms of FGFRs available. Ligand-independent synthetic forms of FGFRs have been used to study FGFR function during development. An early type of constitutively-active FGFR is comprised of intracellular domains of FGFR1 or FGFR4 fused to the *Drosophila* mutant *torso* protein, which is permanently dimerised. These constitutively-active receptors were used to show that FGFR1 but not FGFR4 activity converts naïve ectodermal explant cells into mesoderm with activation of the MAPK pathway (Umbhauer et al. 2000). Constitutively-active forms of each FGFR are now available that have been individually expressed in zebrafish embryos to investigate ligand:receptor affinities and the effects each receptor has upon development. It was found that all four caFGFRs caused dorsalisation, brain caudalisation and secondary axis formation (Ota et al. 2009). Constitutively-active FGFR1 and FGFR1 VT- have also been made by fusing the intracellular kinase domains to the Fc region of human antibody molecule IgG1; this permanently dimerises with other Fc molecules via a disulphide bond, rendering the FGFR constitutively active. These receptors showed that the VT- motif of FGFR1-3 is required for interaction with FRS2 (Burgar et al. 2002).

4.1.2 Inducible methods of affecting FGF signalling

To investigate FGF signalling during neural development, the use of dnFGFRs or caFGFRs are problematic as they are translated and act to repress FGF signalling from early stages. Changes caused by disruption of FGF signalling during neural specification stages could be masked by earlier defects of mesoderm formation and gastrulation. Therefore inducible systems that allow timed disruption of FGF signalling are more suitable to investigate FGF signalling in a neural context.

4.1.2.1 Transgenesis

The use of transgenic frogs expressing dnFGFR1 has previously been reported. Kroll & Amaya (1996), studied post-mesodermal FGF signalling by injecting oocytes with sperm containing a dnFGFR1 plasmid under control of the simian cytomegalovirus promoter. Unlike dnFGFR1 mRNA injected embryos, transgenic embryos expressed dnFGFR1 in a non-mosaic manner only from late blastula stages (Kroll & Amaya 1996). This caused severe posterior truncations and a loss of early *HoxA7* and *HoxB9* expression (Pownall et al. 1998). Again, as this uses dnFGFRs, the problem with receptor specificity still exists. Furthermore, use of this method to induce dnFGFRs from later developmental stages would depend on finding suitable regulatory elements to drive expression during the required time period (Pownall et al. 2003).

4.1.2.2 Hormonal methods

One potential way of achieving inducible changes to protein levels is to fuse a protein of interest to a ligand-binding domain of the glucocorticoid receptor. This has been used by Kolm & Sive (1995) to study the master regulator of muscle development, *MyoD* in *Xenopus laevis*. mRNA coding for the gene-of-interest fusion protein is injected, translated and kept in an inactive form until application of glucocorticoid hormone into culture medium. This releases the protein of interest enabling it to activate gene expression in addition to the endogenous protein (Kolm & Sive 1995). Unfortunately, this approach could not be used on secreted proteins such as FGFs as glucocorticoid receptor is a nuclear hormone receptor that acts as a transcription factor.

4.1.2.3 Pharmacological methods

Another approach to manipulate FGF signalling is the use of pharmacological agents such as SU5402 and BCI. SU5402 is an ATP-competitive inhibitor of the tyrosine kinase activity of FGFR1 and can be added to *Xenopus* culture medium

where it diffuses into the embryo (Mohammadi et al. 1997). Thus, it is an inducible method of FGF pathway inhibition and if added from late blastula stage 9 onwards, the negative effects of FGF repression upon gastrulation can be circumvented. An example of this is its use as part of a microarray screen to investigate the effect upon the *Xenopus* transcriptome of inhibiting FGF signalling during a short window from stage 10.5 to 11.5 (Chung et al. 2004). A major drawback of SU5402 however is that it is not specific to just FGFR1 and also inhibits FGFR3 as well as VEGFR and PDGFR signalling (Sun et al. 1999). Similar reagents are not available that are specific to the other FGFRs. Therefore SU5402 is unsuitable for investigating the individual roles of FGFRs. BCI is another pharmacological agent which can be added to culture medium to activate FGF signalling when required. It inhibits the dual-specificity phosphatase 6 (Dusp6), thereby alleviating its repressive effects on the MAPK pathway when added to culture medium (Molina et al. 2009). Again, although suitable for looking at a global increase in FGF signalling output, the use of BCI would not enable study of individual FGFRs' contribution to development.

4.1.3 iFGFRs allow receptor-specific FGF activation in a spatial and temporally controlled manner

iFGFRs provide a way to induce FGF signalling during discrete windows during *Xenopus* development. By using *Xenopus* fate maps, iFGFRs can be targeted to prospective neural tissues also giving spatial control of FGF activation. Thus, iFGFRs have advantages over caFGFRs or pharmacological methods in terms of temporal and spatial control over FGF signalling. The availability of different versions of iFGFRs corresponding to FGFR1-4 enables investigation into the different signalling properties of each receptor during neural development. Therefore by using inducible forms of FGFR1-4, a truer separation of iFGFR subtype and effect upon the transcriptome during discrete periods of *Xenopus* development can be achieved.

4.1.4 Aims of this chapter

The main aim of this study is to identify proximal gene targets of FGF signalling during *Xenopus* neural development using drug inducible FGF receptors. Before embarking this objective, it was necessary to optimise the use of iFGFRs and this is the subject of this chapter. The aims of this chapter are therefore:

- To optimise the injection and activation of iFGFRs in *Xenopus* embryonic development.

- To investigate the effects of iFGFRs on FGF signalling and *Xenopus* development.

4.2 Results

4.2.1 iFGFRs are stably expressed in the developing *Xenopus* embryo

In order to find FGF signalling targets during *Xenopus* neural specification and development, it must be confirmed that iFGFRs proteins translated from injected mRNA are present before, and during neurulation.

In a previous study, 20pg iFGFR1 mRNA was shown to produce effective amounts of inducible protein (Pownall et al. 2003). *Xenopus laevis* embryos were therefore injected bilaterally with 20pg of iFGFR1. The embryos were collected for western blot analysis at a number of stages from early blastula to the end of neuralation. Figure 4.1 is a western blot probed for the HA tag present in the N-terminus of iFGFR1.

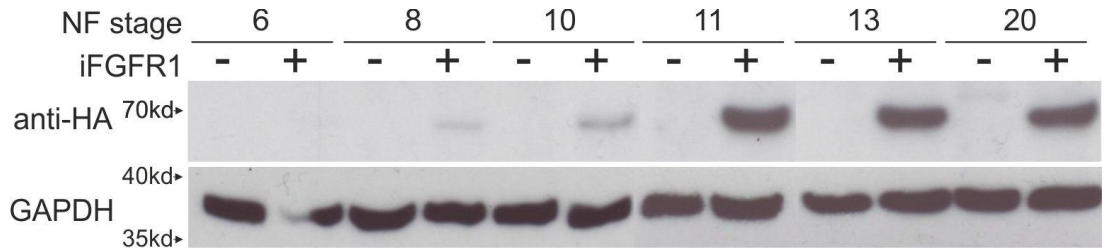

Figure 4.1 – iFGFRs are stably expressed from early stages
Western blot showing the level of HA epitope tag in embryos injected with 20pg iFGFR1 increasing, and being maintained, from blastula stages (NF st.6) to post-neurulation (st. 20). The predicted size of iFGFR1 is ~72Kd. GAPDH was used for a loading control, and is ~37Kd.

The presence of epitope-tagged iFGFR protein is first detectable at mid-blastula stage 8 and increases in abundance throughout gastrulation before plataeuing and remaining constant until at least late neurula stage 20. Therefore for the periods of development which this study focuses on – gastrula to neurula – iFGFRs are translated and present in the embryo at a stable level.

4.2.2 Optimisation of AP20187 dosage required to elicit an FGF-activation response

The concentration of AP20187 required to robustly induce FGF signalling whilst not being toxic to the embryo was investigated. In Pownall et al, (2002) 1.2µM of AP20187 was routinely used, however it was not determined whether concentrations below this would still produce the same level FGF signal activation, or if a higher concentration is optimal without causing non-specific effects. A convenient assay for FGF pathway activity is by immunodetection of the active diphosphorylated form of the MAPK effector ERK, dpERK. 20pg of iFGFR1 was injected bilaterally into *Xenopus* embryos at the 2-cell stage and AP20187 added for two hours from stage 8 by which time iFGFR1 is immunodetectable (Figure 4.1). The embryos were processed for western blot analysis. Figure 4.2 shows that at a concentration of 1µM, approximately equivalent to the concentration used in Pownall et al, (2002), a strong induction of dpERK was observed relative to sibling controls which were injected with iFGFR1 but not treated with AP20187.

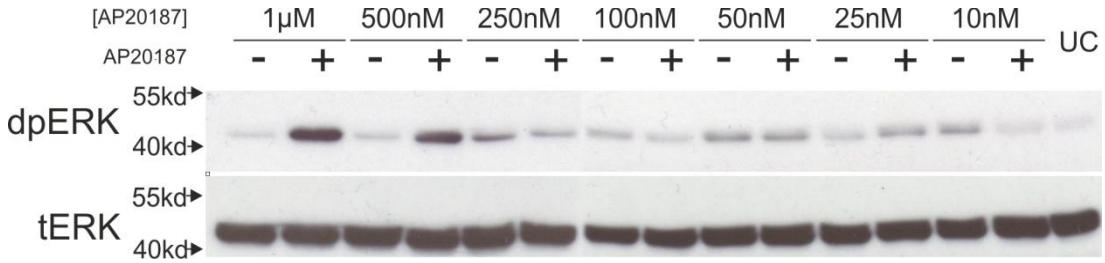

Figure 4.2. 1µM of AP20187 is the optimal dosage of AP20187 to activate the MAPK pathway.
Western blot showing levels of dpERK in embryos expressing iFGFR1 and treated with varying dosages of AP20187 from stage 8 for 2 hours relative to untreated sibling controls. Total ERK (tERK) was used as a loading control. The predicted weight of ERK is 43 Kd.

The strength of this induction weakens considerably when the dosage of AP20187 is reduced from 1µM, suggesting that in order to activate FGF signalling to replicate results in Pownall et al (2002), 1µM of drug should be used at least.

To determine if AP20187 is toxic to embryos at amounts greater than 1µM, and/or developmental defects more severe, embryos were injected with 20pg of iFGFR1 and cultured to stage 10.5. AP20187 was added to both the culture medium of embryos injected with iFGFR1 and also uninjected sibling embryos at a range of concentrations. Embryos were cultured to tailbud stages before fixing for imaging.

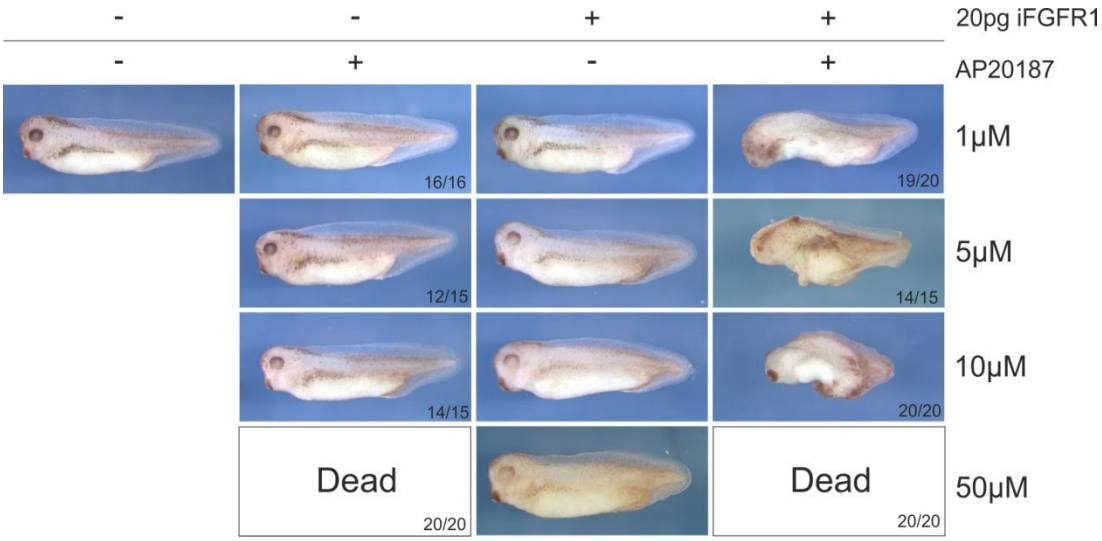

Figure 4.3. AP20187 can be added to embryos at doses up to 10μM without negatively impacting development.
Uninjected embryos or siblings injected with 20pg iFGFR1 were exposed to AP20187 from stage 10.5. Numbers on treated embryos indicate embryos resembling the representative image.

Figure 4.3 shows that for all concentrations of up to 10μM, induced iFGFR1 causes gross morphological defects. The severity of defects do not seem to increase as the concentration of AP20187 increases to 10μM suggesting that it is not necessary to add more than 1μM of AP20187 to achieve the same morphological effects. Secondly, at concentrations of up to 10μM, uninjected embryos develop normally. However, increasing the concentration of AP20187 to 50μM killed 100% of both uninjected and iFGFR1-expressing embryos. As this is fifty times the amount required to elicit a strong dpERK response, toxicity of AP20187 will not be a cause for concern in this investigation.

4.2.3 AP20187 rapidly diffuses into the embryo

As the start and endpoint of induction times with AP20187 need to be tightly controlled it needed to be determined how rapidly AP20187 can diffuse into the embryo and cause a rise in dpERK levels. If this is too slow, AP20187 would have to be added pre-emptively to affect stage-dependent gene expression.

Xenopus laevis embryos were injected bilaterally with 20pg iFGFR1 and cultured to late blastula stage 8 before adding 1μM AP20187 to the culture medium. Embryos were then cultured for different periods of time at 22°C. Figure 4.4 shows that after only 15 minutes exposure to AP20187, a there is a small increase in dpERK in iFGFR1 'induced' embryos relative to 'uninduced' and uninjected sibling controls.

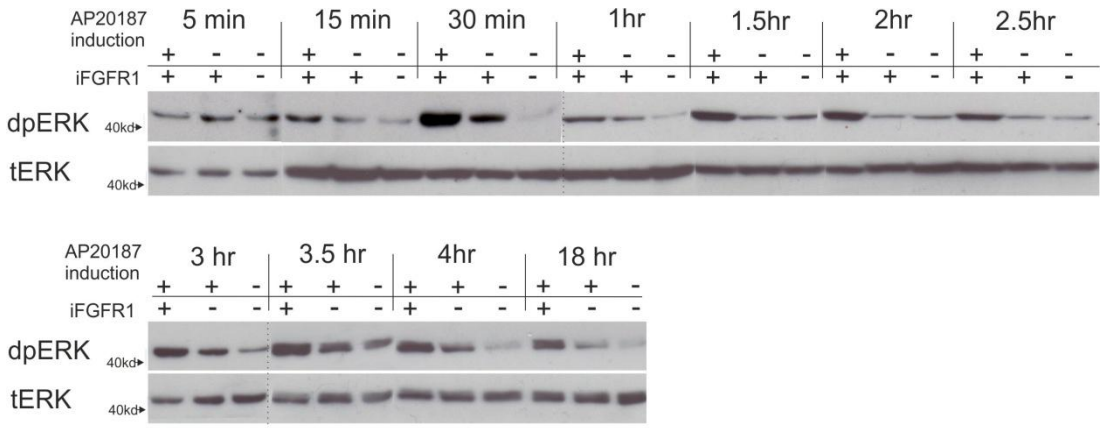

Figure 4.4. The MAPK pathway is activated within 15 minutes upon the addition of 1μM AP20187
Xenopus laevis embryos were injected with 20pg iFGFR1 and cultured to stage 8 before adding 1μM AP20187 to the culture medium. Embryos were cultured at 22°C and collected at various timepoints, and processed for a western blot against dpERK. tERK was used as a loading control. Dotted lines demarcate different experimental repeats.

iFGFR induction can therefore be timed from the addition of AP20187. A dpERK upregulation is still evident after 18 hours, showing that the dimerised iFGFR and/or AP20187 must be stable and continue to activate dpERK until tailbud stages.

4.2.4 iFGFR induction causes severe defects in development

Next, the ability of iFGFR1 (VT-), iFGFR2, iFGFR3 and iFGFRF4 to activate the MAPK signalling pathway and affect development was investigated.

20pg of either iFGFR1, iFGFR1 (VT-), iFGFR2, iFGFR3 or iFGFR4 were injected bilaterally into *Xenopus laevis* embryos at the 2-cell stage and AP20187 added at stage 10.5. Embryos were cultured to tailbud stages and fixed for imaging. Figure 4.5 shows that uninjected embryos and embryos untreated with AP20187 develop normally. Induction of iFGFR1 and iFGFR2 caused the most severe defects, with loss of anterior structures at the expense of an expanded posterior domain, which was also deformed. Thus the embryo could be said to be 'posteriorised', a term used previously to describe posterior domain enlargements upon FGF over-activity in Pownall et al., (2003) and Kudoh et al. (2002). Embryos also failed to elongate relative to controls. Interestingly, the iFGFR1 (VT-) isoform did not have as severe a phenotype as iFGFR1, although embryos exhibited facial defects including incomplete eye development. Embryos expressing iFGFR3 had an expanded cement gland and generally under-developed head. There was often oedema ventrally around the developing head and guts. iFGFR4 also produced milder defects compared to iFGFR1 and iFGFR2, but still had appreciably under-

developed eyes and head with a failure to elongate. In some instances, the neural tube failed to close anteriorly.

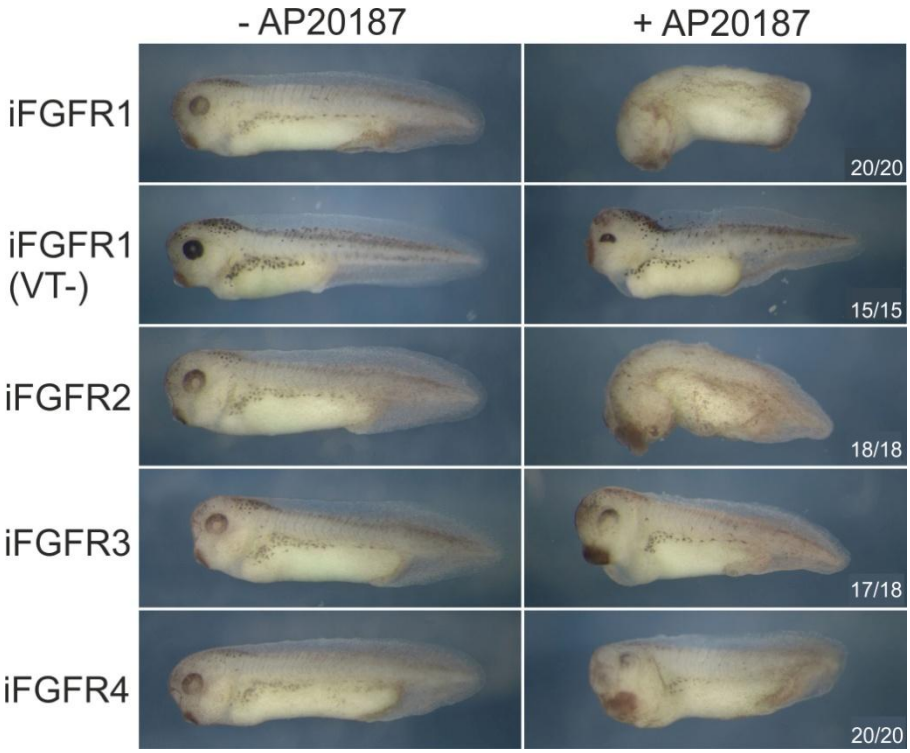

Figure 4.5. Effect upon phenotype after induction of iFGFRs
Xenopus laevis embryos were injected with 20pg iFGFR mRNA and cultured to stage 10.5. AP20187 was then added and embryos cultured until tailbud stages. Numbers indicate embryos resembling the representative image. All iFGFRs cause elongation defects and problems with anterior development, although to different extents.

Therefore, iFGFRs posteriorise the embryos as expected, but also that each iFGFR has different effects on development, suggesting FGFRs have different developmental roles.

Ectodermal explants taken at blastula stages and treated with FGF2 undergo convergent extension from gastrula stages whereas untreated counterparts remain spherical (Slack et al. 1987). In order to investigate the effects of activating iFGFR1, iFGFR1 (VT-) iFGFR2, iFGFR3 and iFGFR4 on animal cap explants, 20pg of each iFGFR was injected into bilaterally the animal pole of *Xenopus laevis* embryos at the 2-cell stage. Explants were dissected at stage 8 and transferred to culture medium containing AP20187. When stage-matched controls reached late neurula stages, animal caps were fixed for imaging.

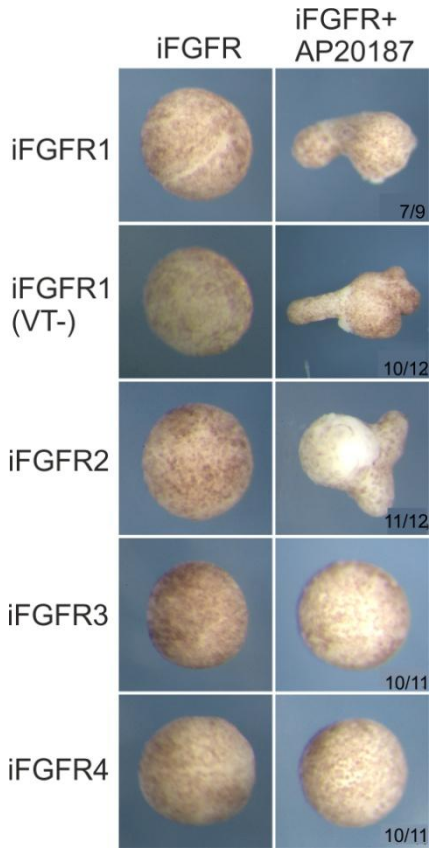

Figure 4.6. Activation of iFGFR1 VT+/- and iFGFR2 causes convergent extension of animal caps.
20pg iFGFR mRNA was injected bilaterally into *Xenopus laevis* embryos at the 2-cell stage. Ectodermal explants were taken from embryos at stage 8 and cultured until late neurula. Numbers of animal caps resembling the representative image are shown. N=9-12 caps per condition.

Figure 4.6 shows that animal caps expressing both isoforms of iFGFR1, and iFGFR2 elongated in the majority of cases. iFGFR3 and iFGFR4 however, remained spherical and resembled untreated controls suggesting that mesodermal tissues that are responsible for elongation in the embryo are not specified in induced iFGFR3/4-injected embryos.

4.2.5 iFGFRs activate the MAPK pathway to varying extents

4.2.5.1 iFGFR-injected explants exhibit increased MAPK activation

It was important to check that the phenotypes seen in Figure 4.5 and Figure 4.6 correlate with activation of the MAPK pathway for all iFGFRs. 20pg iFGFR mRNA was injected bilaterally into *Xenopus laevis* embryos at the 2-cell stage. Ectodermal explants were taken at stage 8. Explants are commonly used in *Xenopus* experiments as their cells are still pluripotent and can be forced down different differentiation pathways, as they have not been exposed to signalling events

elsewhere in the embryo. Thus they provide an isolated system in which to study signalling away from other signalling pathways in the embryo which could interfere with FGF activity. Explants were added to culture medium containing AP20187 for 2 hours and processed for western blot analysis.

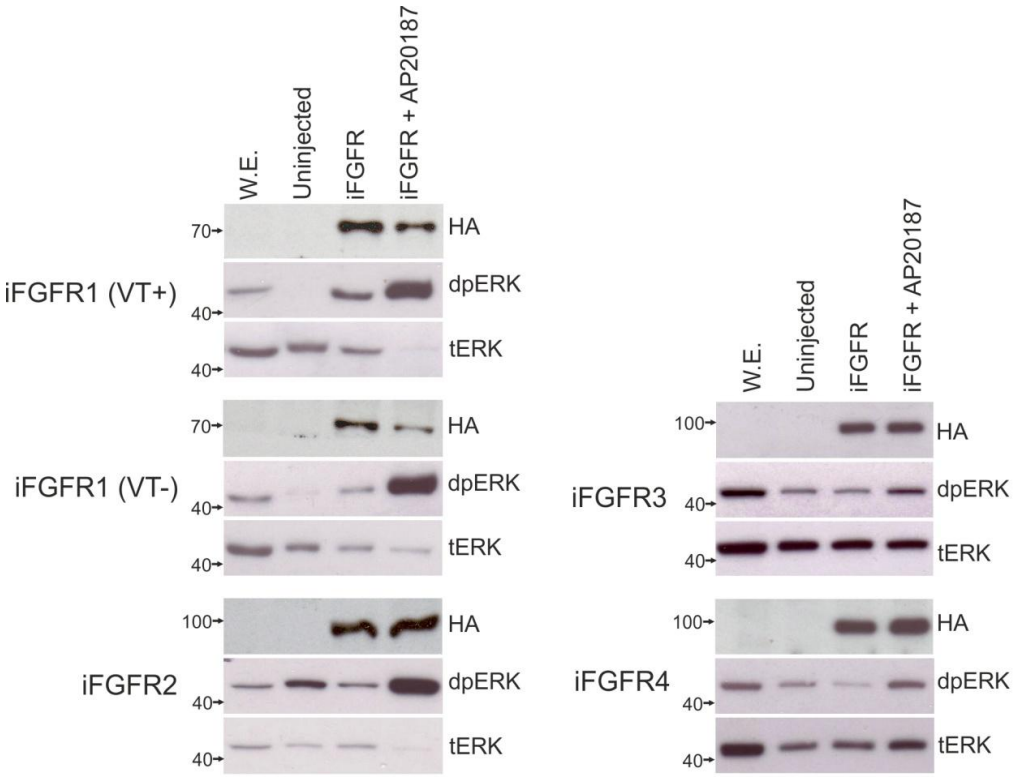

Figure 4.7 iFGFRs increase dpERK levels
20pg iFGFRs were injected bilaterally into *Xenopus laevis* embryos at 2-cell stage. Ectodermal explants were taken at stage 8, cultured in the presence of AP20187 for 2 hours, and collected for western blot analysis. Untreated or uninjected explants as well as whole stage-matched controls (W.E.) were also analysed. Western membranes were probed with either anti-HA to detect the presence of iFGFR, or dpERK. tERK was used as a loading control. The iFGFRs' weight is expected to be between 70 and 100Kd.

Figure 4.7 shows that compared to untreated or uninjected controls, explants expressing one of the five iFGFRs and induced with AP20187 exhibit increased levels of dpERK. This is much more pronounced in iFGFR1, iFGFR1 (VT-) and iFGFR2-injected embryos compared to iFGFR3 and iFGFR4. As levels of HA in iFGFR3/4-injected embryos are comparable to the other receptors, it can be concluded that their weaker response is not due to a lesser amount of iFGFR translated.

4.2.5.2 iFGFRs cause ectopic MAPK pathway activation

Next, the effects on the spatial distribution of active dpERK were investigated in embryos by immunostaining whole embryos with an antibody against dpERK.

Xenopus laevis embryos were injected unilaterally into the animal pole at the 2-cell stage with 10pg iFGFR. Embryos were cultured until stage 10, which is when endogenous dpERK is present in a vegetal ring around where the blastopore will develop (Figure 4.8), and processed for immunostaining against dpERK.

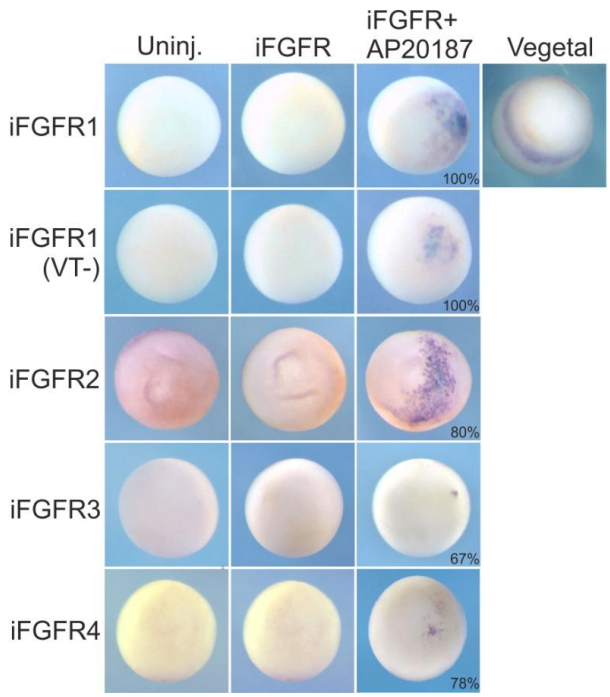

Figure 4.8 iFGFRs cause ectopic dpERK
Embryos were unilaterally injected with 10pg iFGFRs and exposed to AP20187 from stage 8 to stage 10. Animal views of embryos are shown with a vegetal view of endogenous dpERK at stage 10 as a comparison. Ectopic dpERK can be seen in AP20187-treated embryos on the right injected hemisphere only. Percentages show AP20187-treated embryos resembling the representative image. N values - iFGFR1 VT+ (17/17), iFGFRVT- (15/15), iFGFR2 (12/15), iFGFR3 (6/9), iFGFR4 (7/9).

Figure 4.8 shows that all iFGFRs can induce ectopic dpERK on the animal pole of injected embryos as shown by blue staining on the injected right hemisphere. Uninduced and uninjected embryos did not show ectopic staining. Again, the level and extent of dpERK activation is less in iFGFR3 and iFGFR4-injected embryos compared to the other iFGFRs.

4.2.6 Using iFGFRs to activate FGF signalling in the developing CNS

The principal aim of this investigation was to study the effects of activating FGF signalling in neural tissue, which can be achieved for example by targeted injections using fate maps, or using neuralised explants. At the 8-cell stage, only the two animal dorsal blastomeres contribute to neural development (Moody 1987).

Therefore iFGFRs injected and induced in only these blastomeres would activate FGF signalling only in prospective neural tissue, giving spatial as well as temporal control of FGF signalling. Another method commonly used to simulate conditions in the developing CNS is to use neuralised ectodermal explants. At late blastula when explants are dissected from the animal pole, their cells are still pluripotent. They can therefore be pushed into a neural fate by co-injecting 50pg of the BMP antagonist *Noggin* with iFGFRs into the animal pole (Schulte-Merker & Smith 1995; Smith & Harland 1992; Yamagishi & Okamoto 2010).

4.2.6.1 Targeting iFGFRs to prospective neural tissue

iFGFR1 and iFGFR4 were chosen to observe the effects of FGF signalling upon *Xenopus* phenotype when expressed solely in the developing CNS. This is because induction of iFGFR1 and 4 cause different convergent extension behaviours and signalling properties in this work, and when constitutively active in developing *Xenopus* embryos (Umbhauer et al. 2000). To observe the effect of iFGFR1 and iFGFR4 expression solely in the developing CNS, 20pg of either receptor was injected bilaterally into the 8-cell stage *Xenopus laevis* embryos. Embryos were treated with AP20187 from stage 10.5 and fixed at stage 40 for imaging.

Figure 4.9 shows that activating iFGFRs in prospective neural tissues does not have as severe an effect as when iFGFRs are expressed globally. However both induced receptors caused defects in eye development which for each receptor fell into two categories. For iFGFR1-induced embryos, retina pigmentation was fainter or the whole eye smaller, lacking a defined retina and lens. For iFGFR4-induced embryos, the most visibly-affected embryos had eyes missing pigment in parts of the retina and/or lens. A smaller number had thinner retinas.

Following this, immunostaining against dpERK with embryos injected with iFGFR1 at the 8-cell stage was performed to see if iFGFRs could ectopically activate FGF signalling in the developing neural plate. Embryos were induced for various lengths of time from stage 10.5 to see if the strength of MAPK activation remained constant, as in Figure 4.4. The amount of injected iFGFR1 was halved to 10pg. This was because in the smaller dorsal animal blastomeres spontaneous dimerisation of iFGFR1 occurred in previous experimental repeats using 20pg, leading to ectopic dpERK staining in uninduced control embryos (data not shown). GFP was co-injected as a visual check that injections were targeted to the neural plate (data not shown).

Figure 4.9 – targeting iFGFRs to prospective neural tissues affects phenotype
20pg iFGFR1 (N=18) or 20pg iFGFR4 (N=23) were injected bilaterally into dorsal animal blastomeres at 8-cell stage and treated with AP20187 at stage 10.5. Embryos were fixed at stage 40. Induced iFGFR1-injected embryos either had fainter retina pigment (left) or had more severe eye defects (right). IFGFR4-injected embryos had either thinner lenses (left) or missing pigment in the retina/lens (right). Numbers on AP20187-treated embryos refer to numbers of AP20187-treated embryos resembling the representative image.

Figure 4.10 shows after 1 or 2 hours exposure to AP20187, there is a strong ectopic dpERK response in the posterior dorsal region of the embryo. Unexpectedly, given the stability and continued upregulation of dpERK in whole embryos after an 18 hour induction (Figure 4.5) this dpERK response was not maintained after 4 hours treatment with AP20187.

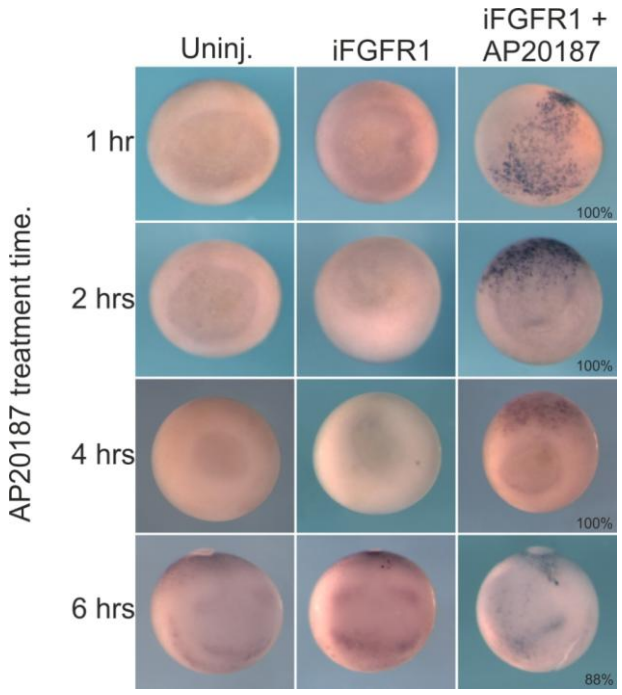

Figure 4.10 – targeting iFGFR1 and treating with AP20187 for different periods of time
10pg iFGFR1 was injected bilaterally into prospective neural blastomeres at the 8 cell stage. Embryos were cultured at stage 10.5 and treated with AP20187 for 1 (N=10), 2 (N=7), 4 (N=9) or 6 (N=8) hours. dpERK protein is stained blue. Endogenous dpERK is present ventrally in earlier stages (only animal view shown) and in later stages is present in the posterior, midbrain hindbrain boundary and apical ectodermal ridge as in 6 hr controls. Percentages in induced embryos show embryos exhibiting ectopic dpERK.

After this period dpERK staining was fainter, more diffuse and not concentrated at the developing neural plate. This may be caused by compensation of signalling events in the rest of the embryo not expressing iFGFR1. Partly on this basis, and because *Xenopus tropicalis* RNA-seq and RNase protection analysis data suggests that roughly three hours is the time taken for FGF signalling targets such as *Cdx4* to be activated after onset of FGF activity, a three hour induction time was picked for future experiments to ensure activation of proximal targets, but not any subsequent negative regulators (Tan et al. 2013; Keenan et al. 2006).

4.2.6.2 Using neuralised animal cap explants to simulate FGF signalling in neural tissues

A common way of mimicking neural conditions in an isolated system is by using neuralised ectodermal explants. To ascertain that the MAPK pathway is induced above normal levels in neuralised animal cap explants by iFGFR1 similar to when only iFGFR1 is activated, 50pg of *Noggin* mRNA was co-injected with 20pg iFGFR1 bilaterally at the 2-cell stage in *Xenopus laevis* embryos. Explants were taken at mid-blastula stage 8, cultured until whole stage-matched controls reached early gastrula stage 10.5 and then treated with AP20187 until stage 15. Explants were then processed for western blot analysis against dpERK and the BMP effectors pSmad1/5 and 8.

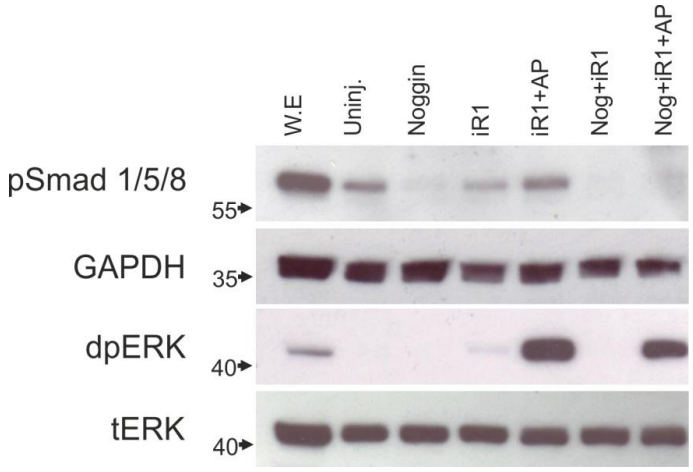

Figure 4.11 – MAPK activation in iFGFR1-injected neuralised animal caps
Embryos were injected with 50pg*Noggin,* iFGFR1 or both *Noggin* and iFGFR1 and treated with AP20187 from stage 10.5 to 15. Western blots were performed with samples either being probed with pSmad 1/5/8 antibody, or dpERK antibody. Loading controls were GAPDH and tERK respectively. pSmad 1/5/8 has a predicted weight of 58Kd.

Figure 4.11 shows that *Noggin* inhibited the BMP pathway, thus neuralising the explants. As shown by reduced levels of pSmad1/5/8 in *Noggin*-injected embryos.

dpERK is strongly induced at the same level in explants expressing solely iFGFR1 or iFGFR1+*Noggin*. This shows that FGF signalling can be activated robustly in neuralised animal cap explants.

4.2.7 Conclusions

Data in this chapter have shown that iFGFRs are translated early in development, are induced rapidly in response to addition of AP20187 to culture medium and are stable for the duration of gastrulation and neurulation. All five iFGFRs tested activated the MAPK pathway when induced, however not to the same extents. There were also differences in morphological phenotypes and convergent extension phenotypes in ectodermal explants. Lastly, iFGFRs have been shown to activate FGF signalling when targeted to the CNS, or expressed in neuralised ectodermal explants. This provides a good foundation upon which to plan an RNA-seq experiment to investigate FGF signalling during neural development.

4.3 Discussion

This chapter has shown that iFGFRs are stably expressed in *Xenopus* embryos, and can be activated in whole embryos as well as neuralised animal caps to activate MAPK signalling. Induction of FGF signalling through all iFGFRs tested affected normal *Xenopus* development, with phenotypes reminiscent of FGF over-expression phenotypes in whole embryos and explants.

4.3.1 Signalling by iFGFRs cause gross morphological defects

The five different iFGFRs had varying effects on *Xenopus* embryo phenotype when induced from early gastrula to tailbud. iFGFR1 and iFGFR2 produced the most severe phenotypes, with a complete loss of anterior structures and also posterior defects. These posterior defects were not as severe as those caused by activating iFGFRs from stage 8, which disrupted gastrulation (Pownall et al. 2003). These phenotypes resemble those seen in *Xenopus laevis* embryos microinjected with *FGF3* and *FGF4* mRNA at cleavage stages as well as expressing FGF4 from a plasmid – in this case posterior defects were shown to be accompanied by an anterior expansion of *Cdx4, HoxA7* and *HoxB9* expression domains (Lombardo et al. 1998; Isaacs et al. 1994; Pownall et al. 1996). These severe defects were also found after iFGFR1 induction by Pownall et al (2003). The eye defects found in

embryos with activated iFGFR1 and iFGFR4 in prospective neural structures were also found by Lombardo et al, (1998), who placed an FGF4-soaked bead next to the developing eye. Embryos displayed a loss of eye pigment resembling those in which was found to be due to a loss of differentiation of pigmented epithelial cells (Lombardo et al. 1998).

Analysis of developmental defects of embryos over-activating other individual FGFRs is sparse in the literature. Ota et al. (2009) injected constitutively-active FGFRs 1-4, (caFGFRs) into zebrafish embryos, as well as the VT- equivalent of FGFR2 (FGFR2 VT-). In this study, the most severe phenotypes occurred with the expression of caFGFR1 and caFGFR2, similar to the results in Figure 1.6, with injected embryos displaying a complete loss of anterior tissue and eyes. caFGFR2 VT- also displayed anterior truncations, but these were not as severe as those from caFGFR2, which also follows findings in Figure 1.6 for iFGFR1 and iFGFR1 VT-. The presence of these defects in iFGFR1 VT- embryos however, contrast with the findings of Paterno et al, who overexpressed the VT- isoform of FGFR1 in *Xenopus* embryos and saw no difference in tadpole phenotype (Paterno et al. 2000). These defects may be due to the fact that Paterno and colleagues overexpressed a ligand-dependent receptor which may become inactive at some points during development due to lack of specific ligands (Paterno et al. 2000). caFGFR3 and caFGFR4-expressing zebrafish embryos displayed distinct phenotypes with only slightly smaller heads and defective eyes compared to controls, which the authors proposed as being due to the lower signalling potential of caFGFR3 and caFGFR4 than the other caFGFRs, instead of producing distinct effects (Ota et al. 2009).

The convergent extension behaviour observed in ectodermal explants due to FGF over-expression has also been well documented. Explants either treated with FGF2, FGF3 or FGF4 protein, or mRNA coding for these FGFs also displayed convergent extension of animal caps to a similar degree to caps expressing iFGFR1, iFGFR1 (VT-) and iFGFR2 in Figure 1.7 (Isaacs et al. 1994; Lamb & Harland 1995; Lombardo et al. 1998; J. M. Slack et al. 1987). Overexpression of a constitutively active FGFR2 also caused convergent extension of explants (Neilson & Friesel 1995). The result of FGFR3 overexpression has not been reported, but injection of iFGFR4 into neuralised explants similarly failed to elicit as great a convergent extension response as those expressing iFGFR1 or *Noggin* alone (Yamagishi & Okamoto 2010).

These experiments therefore agree with research in the literature into the effects of over-activating the FGF signalling pathway during neural development. They also provide insight into the different effects each FGFR subtype brings to development.

4.3.2 iFGFRs activate the MAPK pathway, but to different extents

Western blot analyses on ectodermal explants expressing iFGFRs, as well as immunostaining with whole embryos showed that dpERK is upregulated and expressed ectopically after receptor induction (Figures 1.8 and 1.9). As with the findings with phenotype, the dpERK response was most potent in iFGFR1, iFGFR1 (VT-) and iFGFR2-expressing embryos. Previous work analysing FGFR2 VT- transfected with human BaF3 cells found them to be unable to activate the MAPK signalling pathway, based upon the lack of detectable phosphorylated ERK2. (Twigg & Burns 1998). Furthermore, Burgar et al. (2002) found that in 293T cells, transfected FGFR1 VT- could not interact with FRS2, a key component of the MAPK and PKC pathway. This contrasts with findings here showing iFGFR1 VT- expressing embryos and explants repeatedly displayed dpERK upregulation at similar levels to iFGFR1 VT+. This may reflect differences between wild type FGFR1 VT- and iFGFR1 VT-, or could be a cell type specific effect or found only *in vitro* as other interacting partners are present *in vivo* to activate MAPK. Further work in different cell types and model organisms would be needed to get a better insight into these discrepancies.

iFGFR3 and iFGFR4-expressing embryos also activated the MAPK pathway, but to a lesser extent and over a smaller area. An explanation for this is that only cells closest to the injection site inherited the highest amounts of iFGFR3/4 mRNA and protein which would activate an amount of dpERK detectable by immunostaining. The weaker effect FGFR4 has on the MAPK pathway relative to iFGFR1 has been previously documented. One explanation for this is that FGFR4 kinase domain has an inherently weaker autophosphorylation potential and therefore activates downstream signalling proportionally less compared to FGFR1 (Yamagishi & Okamoto 2010). Yamigishi and colleagues overexpressed FGFR4 in *Xenopus*, thereby increasing the likelihood that FGFR4 would receive FGF ligands over FGFR1. Interestingly, a posterior shift in anterior neural markers reminiscent of when FGFR1 is inhibited was observed, indicating a weaker net FGFR signalling output (Yamagishi & Okamoto 2010). Therefore, the authors concluded that

competition between FGFRs for ligands, with FGFR4 being a 'weak FGFR1', is responsible for regulating neural development.

Other research disagrees with this finding, and concludes that these signalling differences are mainly due to cellular context. Although some studies found the phosphorylation level of FGFR4 to be weaker than that of FGFR1 in PC12 cells, other studies in *Xenopus laevis* animal caps found that phosphorylation of the two receptors was indistinguishable (Raffioni et al. 1999; Umbhauer et al. 2000). In these explants, FGFR4 was unable to activate the MAPK effector *Ras*, supporting the relative lack of dpERK activation in Figure 1.8 and 1.9. However, FGFR4 did activate PLCγ, thereby activating *Wnt1* and the midbrain marker *En2* (Umbhauer et al. 2000). Therefore the authors postulated the differences in pathways activated by the two receptors provided the difference in signalling properties, rather than quantitative differences in receptor phosphorylation potential (Umbhauer et al. 2000). On this basis it would be interesting to perform western blot analysis using antibodies against the other branches of FGF signalling such as PLCγ or Akt for iFGFR3 and 4-induced embryos.

The data obtained from the microarray in the previous chapter seem to agree with this latter view of different FGFRs having unique signalling outputs – as if iFGFR4 and 3 are indeed just 'weaker' versions of iFGFR1 and iFGFR2, one would expect the microarray genelists to be very similar to each other, with iFGFR3 and iFGFR4 lists activating the same genes as iFGFR1/2 but to a lesser extent. As discussed in the last chapter, very little overlap of genes between the different receptor lists was evident, indicating that in this context, different iFGFRs had distinct developmental roles and effects upon the *Xenopus* transcriptome and FGF targets.

4.3.3 Challenges to the use of iFGFRs

It would be very hard to account for all FGF ligand/receptor variants and combinations to give a comprehensive view of the effects of ectopic FGF activation during *Xenopus* neural development. As iFGFRs are a ligand-independent system without an alternatively-spliced extracellular domain, along with HSPG interactions that are responsible for the fine-tuning of signalling output, iFGFRs may be considered a simplification of FGF-mediated signalling events during neural induction. Another potential concern with the use of iFGFRs is that the kinase domains of the iFGFRs may not introduce enough variability to reproduce the induction of a given receptor, as they do not account for regulation by FGF ligands

or receptor splicing. However, this simplification from the use of iFGFRs allows focus on finding novel targets of each receptor, and this receptor variability is adequate enough to meet the aims of the project. Indeed, the preliminary microarray dataset discussed in the last chapter showed there to be a low degree of overlap between genes activated or repressed by the four receptors tested, suggesting that iFGFRs 1-4 are varied enough to produce unique signalling outputs. Also, it is unknown whether iFGFRs are targeted solely to the plasma membrane and not to other compartments in the cell such as the nucleus, which FGFR1 has been reported to translocate to, which could be another point of difference from wild type FGFRs (Stachowiak et al. 2003). There therefore will inevitably be differences between iFGFRs and wild type receptors, but for the scope of this project, these two chapters taken together have shown that iFGFRs produce differing and measureable effects upon the *Xenopus* transcriptome and development.

4.3.4 Further work

4.3.4.1 Using neuralised animal cap explants to study FGF signalling in neural development

The ability of iFGFR1 to activate downstream neural gene targets and the MAPK pathway shown to be robust using neuralised animal caps. These results could not be replicated using whole embryos where iFGFR1 injections were targeted to the prospective CNS (data not shown). This was probably due to activity in the rest of the embryo not expressing iFGFRs, such as activity of other signalling pathways, regulating and minimising the effects of iFGFR1 induced in only a small proportion of the total embryo. Therefore neuralised animal cap explants are the superior method to investigate specifically FGF signalling in neural development. Another approach would be to dissect out prospective neural tissue at neural specification stages and conduct RNA-seq upon neural plate tissue. However, this would be tricky due to the dissection of the correct cells at early neurula stages and the fact that these would need to be collected soon after dissection. This is a problem because as a response to wounding, the embryo upregulates dpERK for a few hours. With the neuralised explant protocol in this study, the time between taking the caps and inducing them is overnight, allowing them to heal and the dpERK response to subside (Christen & Slack 1999). Nevertheless, this dissection of neural plate methodology has been used successfully in RNA seq screen in *Xenopus tropicalis* seeking to identify targets of the eyefield marker *Rax* (Fish et al. 2014).

4.3.4.2 Length of iFGFR induction

In order to investigate proximal gene expression the induction time period must be kept fairly short as developmental events are rapid in *Xenopus.* After longer periods, multiple rounds of gene transcription may occur. Furthermore, secondary targets may crosstalk with other signalling pathways or auto-regulate and obfuscate the primary FGF targets. This may have been the case with the loss of ectopic dpERK after a 4 hour induction with AP20187, although RT-qPCR experiments to see if, as well as *Sprouty2*, other negative FGF regulators are also upregulated would be needed to support this. This choice is also supported by *Xenopus* Refseq data, and the time taken for *Cdx4* to be induced in explants after FGF4 treatment in RNase Protection Assays. These data suggest 3 hours is roughly the time period taken for targets of FGF signalling to be activated (Tan et al. 2013; Keenan et al. 2006).

4.3.5 Summary

This chapter has outlined how the microinjection and induction of iFGFRs causes an increase in FGF signalling and affects *Xenopus* development. Taken with the previous chapter, iFGFRs have an effect on downstream gene expression in both whole embryos and in neuralised explants. iFGFR injection has been optimised in order to pave the way to an RNA-seq experiment to investigate FGF signalling in neural development. iFGFR1 and iFGFR4, since they have been shown to have very different behaviours, will be used in the context of neuralised ectodermal explants and this will be described further in the next chapter.

5 Investigating the effect of iFGFR signalling by RNA-seq

5.1 Introduction

5.1.1 Investigating transcriptomes

Investigating the regulation of gene expression and gene networks is fundamental in linking genotypes to phenotypes (Marguerat & Bähler 2010). Manipulation of signalling pathways gives us clues as to how they are regulated and the consequences upon development or pathologies when they are abnormally regulated. Developmental processes are often regulated by a small number of 'master regulators' such as BMPs, Wnts and FGFs. Understanding the global targets of these pathways and how the interact in a developmental context gives insight into the many subsidiary processes they feed into.

5.1.2 Methods of investigating the *Xenopus* transcriptome

Microarrays were the predominant technology for transcriptome analysis up until the start of the last decade. Microarrays however, have a number of shortcomings, one of which is a high level of background and reduced specificity due to cross-hybridisation. Furthermore, compared to sequencing based approaches, microarrays have a lower dynamic range -100-200-fold compared to 5 orders of magnitude (Wang et al. 2009). This means that very small or large changes in gene expression are difficult to detect. Compared to RNA-seq, microarrays are inferior at distinguishing different splice-variants of a gene as many different isoforms will bind to one representative oligo probe. Lastly, unless expensive tiling arrays are used, there is a reliance on existing knowledge of the genome – if a DNA sequence is not present on the chip for hybridisation, or is not yet annotated, it will not be detected (Marguerat & Bähler 2010; Wang et al. 2009). In *Xenopus laevis*, this is becoming progressively less of a problem after the recent sequencing and annotation of the genome (Karpinka et al. 2014).

These problems can be partially overcome by investigating transcription using sequence-based means such as RNA-seq and Serial Analysis of Gene Expression (SAGE). SAGE uses 14-20bp sequence tags from the 3' ends of genes to measure and identify gene expression levels (reviewed in Harbers & Carninci, 2005). The 5' variant of SAGE is called cap analysis of gene expression – CAGE. SAGE and CAGE have the advantage over microarrays of being able to detect different transcription start sites and different promoter usages. It also provides a digital readout of gene expression levels, useful for in-depth gene regulation studies. However, because only gene termini are counted, splicing events and SNPs are not usually detected. Lastly, SAGE and CAGE are based on Sanger sequencing technology, making them relatively expensive (Wang et al. 2009).

5.1.3 Next generation RNA sequencing using Illumina Technology

RNA-seq is a high-throughput sequencing approach and since the first published experiments in 2008 has dramatically increased in popularity. More cost-effective than microarrays and cDNA/EST sequencing described above, it can also identify SNPs, novel splice events, non-coding RNA and unknown regions depending on the depth of sequencing. Unlike microarrays, there is not a reliance on genomic sequence with RNA-seq, although for the purposes of this project it is easier if a well annotated genome is available (Wang et al. 2009). Comparisons between Illumina sequencing data and array data shows the results are reproducible across these platforms, with RNA-seq allowing easier detection of low-expressed genes, novel spliced variants and novel transcripts (Marioni et al. 2008). Illumina technology was chosen for use in this experiment by the Technology Facility based upon the sequencing depth it could achieve relative to the in-house Ion Torrent PGM sequencer.

5.1.3.1 RNA-seq methodologies

A schematic workflow diagram of typical RNA-seq using Illumina technology is shown in Figure 5.1 and is reviewed in Nagalakshmi et al. (2010). Firstly, mRNA is isolated from the total RNA extraction, by either rRNA depletion or mRNA enrichment to prevent the high proportion of ribosomal RNA skewing results. The mRNA is reverse transcribed into cDNA and then broken into approximately 100bp fragments by digestion with DNase 1. The cDNA library is prepared by ligating adaptors onto both ends of the double-stranded fragments enabling pooling of samples together. Quantification is performed at this step to ensure that the library

reflects natural conditions as much as possible. The cDNA is added to a flow cell populated by oligos that bind the adaptors on the termini of cDNA fragments. The fragments are extended, and bind to an adjacent surface oligo forming a bridge. This enables double stranded replication and amplification of the cDNA, known as solid phase bridge amplification. Reverse strands are cleaved and discarded. This amplification step results in more than 40 million clusters, each containing around 1000 clonal copies of the original template molecule (Morozova & Marra 2008).

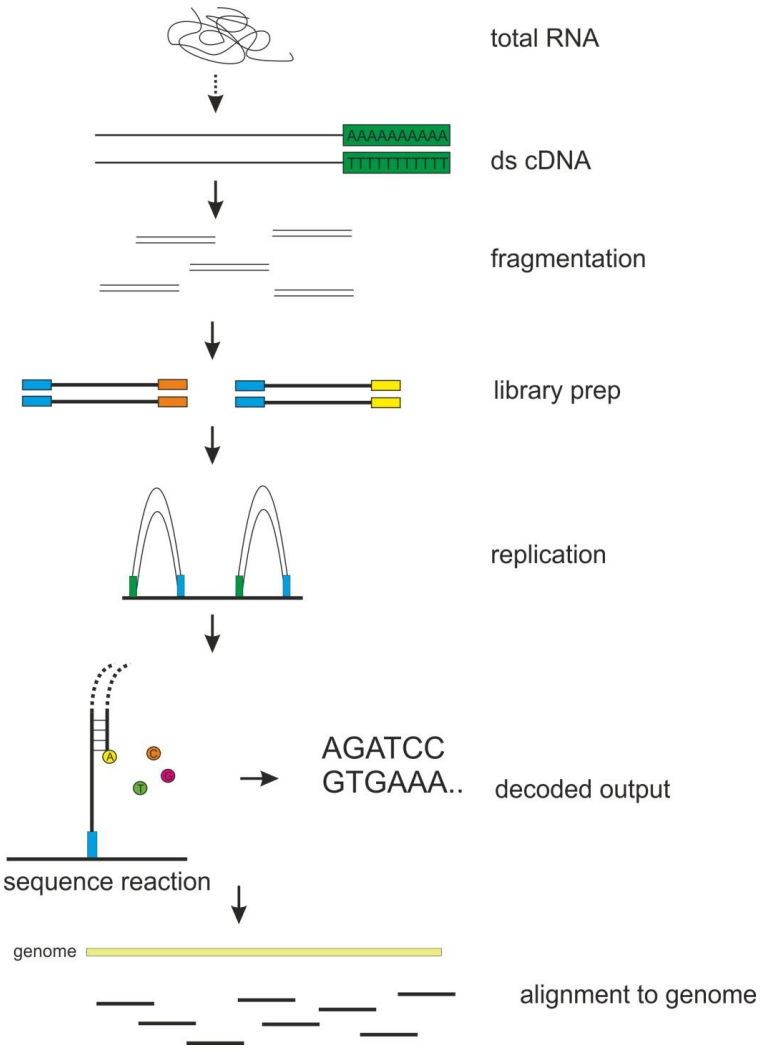

Figure 5.1 – RNA seq workflow
Total RNA is extracted from cells or tissue. It is reverse transcribed into cDNA and fragmented into roughly 100bp fragments. After quantification, adaptors are fused to each end of the fragments to prepare a library. The samples are pooled together and their adaptors bound to oligos fused to an Illumina flow cell surface. After amplification, sequencing primers are added. Light emitted when bases are incorporated allows the sequence of the fragments to be identified. The sequences are then aligned to the genome.

The ends of the fragments are capped to eliminate overhangs, and then sequencing primers are added. All four bases, each fused to a different coloured fluorophore, are introduced to the flow cell. When each is incorporated to the oligo template, a

laser excites the fluorophore and the base's colour is recorded. The fluorophore is cleared, and the next base can then bind. Therefore the raw sequencing output is image records of light emitted by every parallel sequencing reaction across the whole chip. The images are then processed to get numerical values for each base – this is an assignment of 'base call quality' (Nagalakshmi et al. 2010). Fragments containing too many low-quality base calls are discarded.

After sequencing, the pooled samples are isolated once more. The forwards and reverse sequences are paired. This is important, as if the paired reads are much more than 100bp apart, this points to non-specific binding so is a point for quality control. The sequences are then aligned to the genome and reads per gene converted to Fragments Per Kilobase Of Exon Per Million Fragments Mapped (FPKM), a commonly used unit for RNA-seq. Therefore, both the gene sequence and the abundance in each sample can be calculated. A base resolution profile of each gene is formed.

5.1.4 Aims of this Chapter

- To undertake an RNA-seq based analysis aimed at identifying genes regulated by FGF signalling during neural development
- To organise the data into genelists and gain an overview by literature searches and ontological analyses after initial processing by the University of York Technology Facility.
- To validate the RNA-seq data by RT-qPCR.

5.2 Results

5.2.1 Experimental Methodology

The aim of this study was to investigate the role of FGF signalling in a neural context, as well as the differences in signalling output between the different FGFRs. Ideally, all five iFGFRs would be investigated, but in order to maximise the depth of sequencing with the resources available, it was decided to investigate the effects of induction of iFGFR1 and iFGFR4 in a single RNA-seq run. These two receptors were chosen as they are known to have different signalling properties, and overexpression of constitutively active/dominant negative receptors of both result in

abnormal neural development in the fish and frog (Hongo et al. 1999; Ota et al. 2009). Secondly, the initial iFGFR microarray-based analysis suggested that iFGFR1 and iFGFR4 affected very different genes, so would give a wider picture of the role of FGF signalling in neural development (see Figure 3.2). For this reason iFGFR2 was not chosen as the microarray showed it to have a relatively similar profile to iFGFR1 and so its use may not find represent the full range of FGFR effects. Although interesting for a future investigation, iFGFR1 VT- was not used for the same reason. iFGFR3 in the microarray did not seem to affect many neural genes or conventional FGF targets, and so although interesting, it is less of a priority to investigate than iFGFR4. Therefore 4 samples were prepared – iFGFR1+Noggin uninduced control, iFGFR1+Noggin induced, iFGFR4+Noggin uninduced control and iFGFR4+Noggin induced.

As shown in the previous chapter, western blot and RT-qPCR analyses on neuralised ectodermal explants showed robust activation of dpERK and known FGF targets, showing them to be a good system to study neural development. Use of these explants rather than whole embryos enabled investigation of iFGFR induction solely in a neural context, away from the interference of signalling processes occurring elsewhere in the embryo. 50pg of *Noggin* was co-injected bilaterally into the animal pole of *Xenopus laevis* embryos at the 2-cell stage with 20pg of either iFGFR1 or iFGFR4 mRNA (Figure 5.2). The embryos were cultured until stage 8, and ectodermal explants taken. These were cultured until stage-matched sibling embryos reached stage 10.5. Half of these explants were then cultured with AP20187 to activate FGF signalling for 3 hours at 22°C. Explants were then processed for total RNA extraction. At least 1µg of RNA per sample was required for Illumina RNA seq, and so 20 explants per condition were collected.

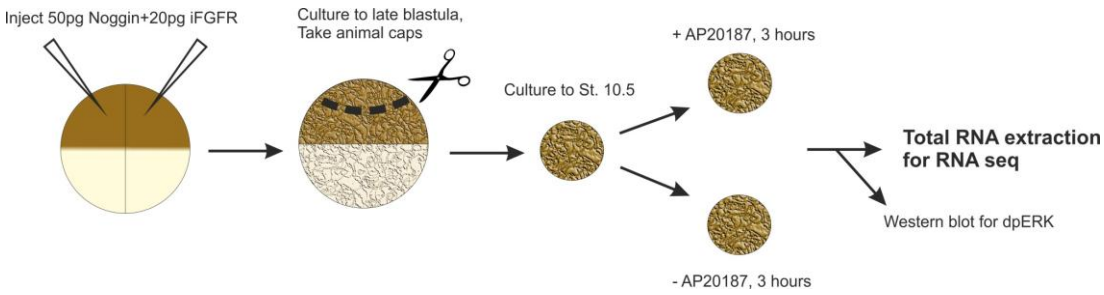

Figure 5.2 RNA-seq sample preparation methodology
Schematic diagram of RNA-seq sample preparation protocol. *Xenopus laevis* embryos were coinjected with 20pg FGFR1 or 4 and 50pg Noggin at the 2-cell stage, neuralised caps taken, and cultured to stage 10.5. FGF signalling was induced for three hours and then caps snap frozen. RNA extraction was then performed and western blot analysis on sibling caps undertaken to ensure upregulation of dpERK.

As a quality control check of iFGFR induction and neuralisation, sibling whole embryos were cultured further and displayed typical Noggin and FGF-overexpression phenotypes (data not shown).

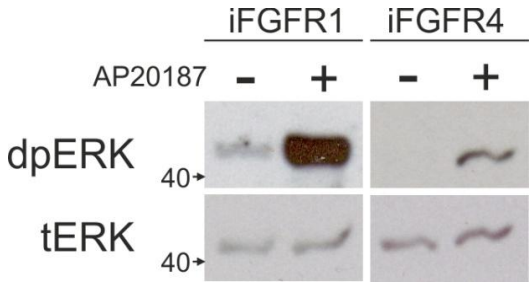

Figure 5.3 Western blot check for RNA-seq samples
10 neuralised animal caps treated with AP20187 from stage 10.5 for 3 hours were processed for western blot analysis for dpERK. tERK was used as a loading control. dpERK was successfully induced compared to untreated controls.

A western blot for dpERK – shown in Figure 5.3 - was also conducted and showed activation of the MAPK pathway was at a comparable level to previous experiments in neuralised explants as seen in Chapter 4. Therefore further quality control of collected total RNA was undertaken.

The quality of the extracted RNA was measured in the University of York Technology Facility with an Agilent 2100 Bioanalyzer. Figure 5.4 shows a representative trace. For RNA-seq, total RNA was required to have an RNA integrity number (RIN) of at least 7. Figure 5.4 shows a representative trace of a sample passing these requirements, with a RIN of 7.9. Absorption is on the y-axis against nucleic acid length on the x-axis. The largest absorption peaks correspond to the ribosomal subunits, and smaller sized fragments to their left corresponding to mRNA. This is also observed on the virtual gel on the right.

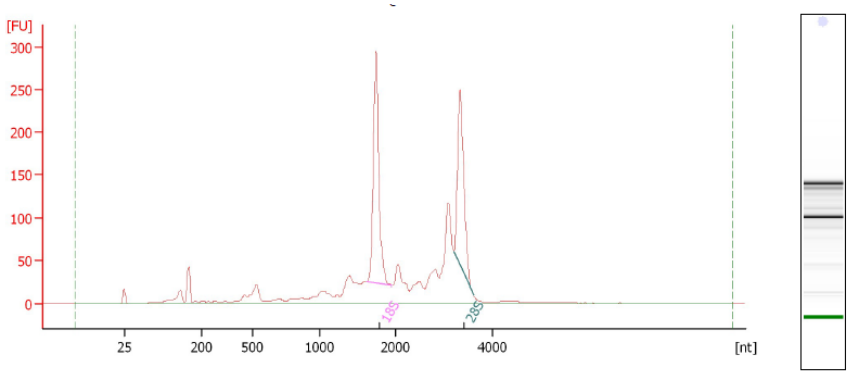

Figure 5.4 Representative total RNA spectra and virtual gel
The above shows a representative bioanalyzer output spectra of a total RNA sample with a

virtual gel image. This sample had a RIN of 7.9. The x-axis refers to RNA fragment size, and absorbance is on the Y axis. The major peaks and bands are ribosomal subunits. Minor peaks and lower weight bands show mRNA. Nt on x axis = nucleotide length, FU on y axis = fluorescent units.

5.2.2 Processing and running of samples

The workflow of the RNA-seq experiment and the contributions by myself, the Centre for Genomic research at the University of Liverpool, and Toby Hodges of the University of York technology facility is shown in Figure 5.5. Further detail is given in the Methods section.

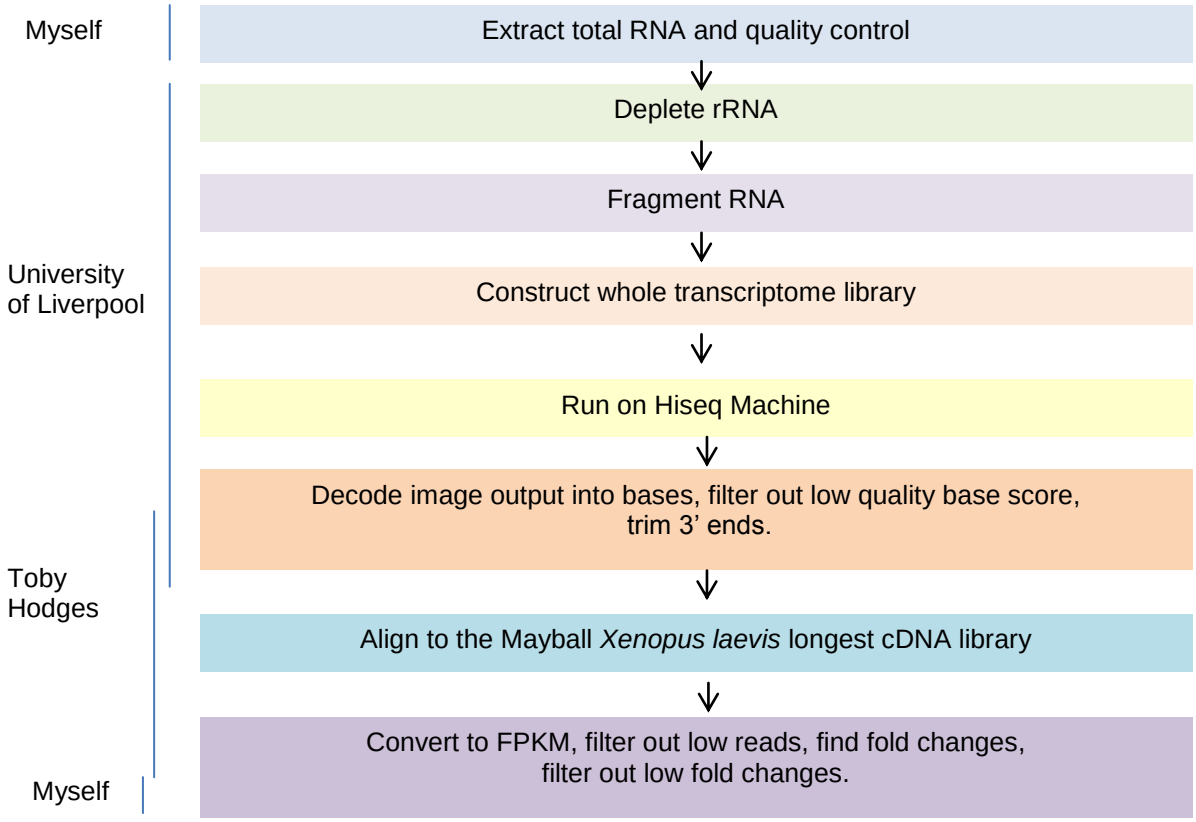

Figure 5.5. Workflow undertaken for RNA-seq.
Lines on the left hand side of the flow diagram indicate the contribution from myself, Toby Hodges from the York Biology Technology Facility and the University of Liverpool Centre for Genomics Research.

After total mRNA was sent to the University of Liverpool, it was processed as described in the Chapter introduction and Methods. Samples were sequenced on the Hiseq 2500 machine and between ~80 and ~120 million reads were obtained for each sample – far higher than initially predicted. Fragments were sequenced from both ends in order to obtain paired reads.

The raw RNA-seq output was processed by Toby Hodges of the University of York Technology Facility, as outlined in the Methods section. The trimmed reads were then aligned using BWA-MEM (Li & Durbin 2009) software to the *Xenopus laevis* Mayball repository of longest cDNAs, collated by the Marcotte lab (accessible at http://daudin.icmb.utexas.edu/). This repository was used as although the *Xenopus laevis* genome has been sequenced, its level of annotation was not sufficient for this study. Counts of reads per fragment mapping to each transcript were obtained by using SAMtools software (Li et al. 2009). Reads per fragment were normalised against the length of the transcript to prevent biases towards longer genes to obtain FPKM values. From this, FPKM values for induced samples could be compared against uninduced samples for each receptor to find the expression fold change for each gene after iFGFR induction.

5.2.3 Scatterplots show many genes are affected by induction of iFGFR1 and iFGFR4

Raw FPKM values for each gene were tabulated and genes with values of 0 FPKM in either or both uninduced control and induced fields eliminated. To obtain an overview of the data, induced $\log_2$ FPKM values were plotted against uninduced $\log_2$ values for each receptor, shown in Figure 5.6. Predictably, most points align along y=x indicating no fold expression change as a result of FGF induction. However, many data points for both receptors lie outside of the lines y=x±1, indicating that they have a 2-fold or greater expression level change. This indicates that many genes were affected by induction of FGF signalling over the course of this experiment. The uninduced samples, as they are expressing the inactive iFGFRs, would not be expected to differ much in terms of gene expression levels. This is seen when plotting iFGFR1 and 4 uninduced values against each other, as far fewer points lie outside the lines y=x±1. However, towards the bottom left of the plot where FPKM values are lower, there is a greater amount of noise indicating the need to interpret the expression changes of these genes with caution.

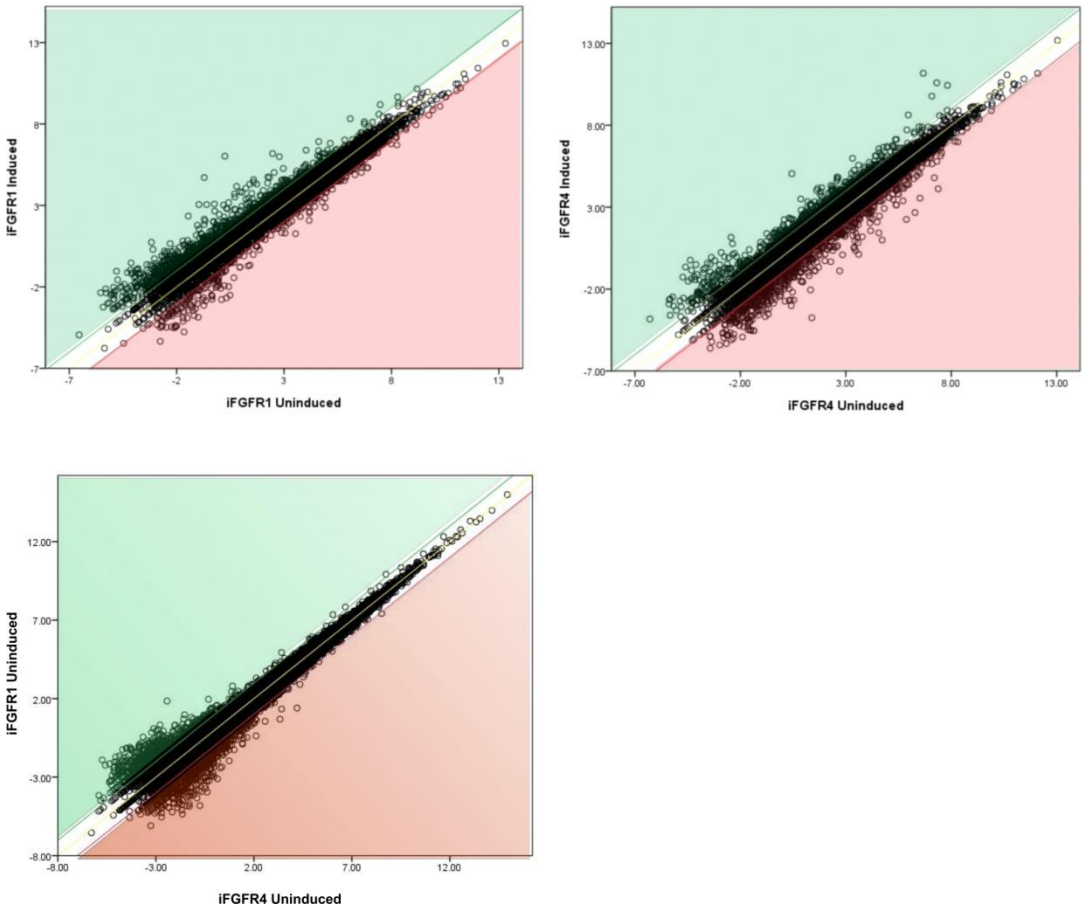

Figure 5.6. Scatterplots to show ratio of uninduced to induced log_2 FPKM for iFGFR1 and iFGFR4 iFGFR1 and iFGFR4 uninduced values were also plotted against each other (bottom). Those points in the green area (to the left of y=x+1) are >2-fold upregulated by FGF induction, and those in red are (to the left of y=x-1) >2-fold downregulated. The yellow line is y=x.

Towards the bottom left of the scatterplots are genes with low read counts that may be false positives in induced vs. uninduced scatterplots - for instance, they may display a 5-fold change in expression but their FPKM change from only 0.01 to 0.05, which is unlikely to be biologically relevant. As only one run of this experiment was performed, genes not meeting fairly stringent FPKM thresholds or certain fold changes must be filtered out to minimise noise and false positives in the data.

5.2.4 Initial filtering of the dataset and compilation of genelists.

The filtering conditions suggested by the Technology Facility were implemented upon the dataset. The first condition was that one or both of the uninduced or induced samples for each gene had to have an FPKM of ≥ 30. Secondly, only genes that exhibited an expression change of ≥ 2-fold were included. Genes were then sorted into either up or down-regulated genes for each receptor and ordered by the magnitude of expression change. The genelists are displayed in Supplementary

Tables 10-13 and include gene symbols, their source entry from the Mayball longest cDNA library, and the region of *Xenopus laevis* genome to which the entry aligns.

These genelists show that many genes were affected by FGF induction enough to pass these filtering thresholds. Among the top iFGFR1-upregulated genes in the RNA-seq data are *FoxA4, Lefty FoxD5/FoxD4L1.1* and *Tspan1,* all of which were found in the microarray analysis described in Chapter 3 to degrees summarised in Table 5.1. *Lefty* and *Sprouty2* were also upregulated in this experiment by 8 and 19.6-fold respectively, although the FPKM of *Sprouty2* was not included in genelists as its induced FPKM was 23.9, slightly under the threshold of 30. *Hesx1* was similarly downregulated by 3.2 and 7.8-fold by iFGFR1 and iFGFR4 respectively.

Table 5.1 Comparison of highly-affected genes

Gene	Receptor	Expression fold change		
		Microarray	RNA-seq	RT-qPCR (if performed)
Tspan1	iFGFR1	6.47	4.1	-
Egr1	iFGFR1	3.81	25.9*	11.19
Lefty	iFGFR1	2.41	19.6	19.3
Sprouty2	iFGFR1	1.91	8*	5.24
Cdx4	iFGFR1	1.67	FPKM <1	-
FoxD5/FoxD4L1.1	iFGFR1	1.62	5.18	-
FoxA4	iFGFR1	1.56	166.51	-
T/Xbra	iFGFR1	1.55	FPKM <1	-
Hmx3	iFGFR4	-1.63	FPKM <1	-
FoxN4	iFGFR4	-1.67	FPKM <2	-5
Hesx1	iFGFR1	-2.18	-3.23	-3.56

*Genes were between 20-30 FPKM and just under filtering thresholds to be included in Genelists.

Hmx3 and *FoxN4,* found by microarray and in neuralised animal caps to be downregulated by iFGFR4, were not found by RNA-seq to be affected by iFGFR induction and their FPKMs were extremely low – 'induced' values were 1.7 for *Hmx3* and 1.9 for *FoxN4*. *Egr1,* previously found upregulated by iFGFR1 by RT-qPCR and the microarray also did not pass filtering conditions due to low read counts (18.5 FPKM). Therefore inevitably due to filtering conditions, some known targets of FGF may be excluded from the genelists above. The mesodermal genes *Cdx4* and *Xbra* (listed as *T*) were both upregulated in whole embryos in the microarray screen. They would not be expected to be present in neuralised caps, and indeed their read levels were extremely low in the RNA-seq data. This was also true of the mesodermal *MyoD1,* which was not affected by iFGFR1 or 4 in the RNA-seq screen and was expressed at extremely low levels with an FPKM of <1. This confirms that

these neuralised explants are indeed representative of neural tissue. However there are also genes, such as *Hba1* encoding *haemoglobin* found upregulated by RNA-seq that are very unlikely to be truly upregulated by FGF induction in a neural context. Therefore the thresholds picked although rigorous probably do not eliminate all 'noise' and will inevitably exclude true low-read FGF targets.

5.2.5 iFGFR1 and iFGFR4 affect the expression of different genes

The preliminary microarray results suggested that iFGFR1 and iFGFR4 modulated the expression of different genes. To investigate the extent of redundancy or otherwise between the different receptors during early neural specification the filtered genelists were compared to observe the extent of overlap between genes activated or repressed by each receptor in a Venn Diagram - Figure 5.7.

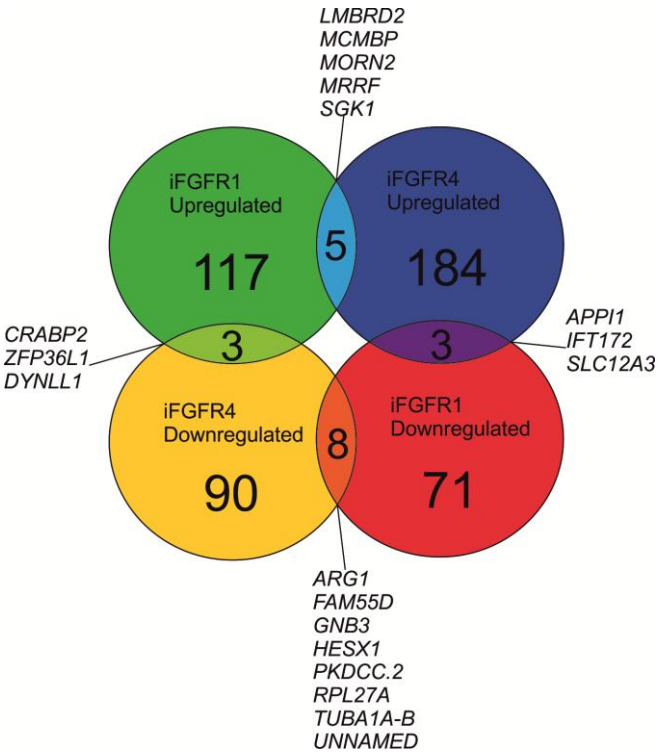

Figure 5.7 – Venn Diagram of iFGFR1 and iFGFR4 signalling targets
Genes taken from the genelists in Supplementary tables 10-13 were compared. Genes lying in overlapping regions are listed.

117 genes were found upregulated and 71 genes found downregulated by iFGFR1, and 184 genes upregulated and 90 genes downregulated by iFGFR4 induction. Figure 5.7 shows that only a relatively small number of genes were commonly upregulated or downregulated by iFGFR1 and iFGFR4. Interestingly, *Crabp2,*

Zfp36l1, Dynll1, Appl1, Ift172 and *Slc12a3* were differentially regulated by the two receptors, suggesting although in the main iFGFR1 and iFGFR4 function independently, there may be a degree of cooperation and competition between them.

5.2.6 Comparison of RNA-seq genelists with other datasets

To assess the similarity between these RNA-seq data and the iFGFR microarray described in Chapter 3, the Venn Diagram tool was used to identify genes these datasets had in common. In addition to this, two other datasets were compared to the RNA-seq and the microarray screens, from Branney et al, (2009) and Chung et al, (2004). The results are shown in Table 5.2.

Table 5.2 – Overlap of RNA-seq data to other datasets

Dataset	Compared to…	Number of genes	Overlapping genes			
RNA-seq	iFGFR Microarray	38	*Agr2*	*Eif1*	*Krt12*	*Rax*
			Arl5	*FoxA4*	*Loc398207*	*Snai1*
			Arg	*FoxD4L1.1*	*Nr6A1*	*Sox13*
			Ccnb1	*Gnb3*	*Nuak2*	*Spry1*
			Crabp2	*Hesx1*	*Patch2*	*Tmem169*
			Crx	*Insm1*	*Pkfb3*	*Tspan1*
			DnajB14	*Irg1*	*Pnp*	*Wnt11b*
			Dusp5	*KIAA124-L*	*Prickle*	*Xepsin*
			Dynll1	*Kit*	*Ptafr*	
			Eppk1	*Lefty*	*Slc312a3*	
	Branney et al 2009	16	*Admp*	*Frz*	*Noggin*	*Sp5l*
			Dusp5	*Hes*	*Oct.1*	*Sprouty1*
			FoxA4	*Hesx1*	*Pnp*	*Tspan1*
			FoxD4L1.1	*Lin28*	*Prickle*	*Zeb2*
	Chung et al 2004	4	*Arl5*	*Dusp1*	*FoxB1*	*Zfp36L1*
iFGFR Microarray	Branney et al 2009	17	*Cdx1*	*FoxD5*	*Lin28a*	*Spry1*
			Cdx4	*Gsc*	*Meso05*	*Spry2*
			Egr1	*Hesx1*	*Nog*	*Wnt5*
			FoxA4	*Irg*	*Prickle*	*Wnt8*
						Xmc
	Chung et al 2004	5	*Arl5*	*Cdx4*	*Gata4*	*Gdf3*
						Mst1

The microarray dataset, as mentioned previously, represents whole embryos with iFGFRs activated over a greater period of time compared to the RNA-seq experiment, and so is not strictly looking at proximal neural targets. However 38 genes found in the microarray were also found more than 2-fold affected by iFGFR1 or iFGFR4 in this dataset, lending more support for these genes being FGF targets.

In addition there are other genes from the same families if not the exact same gene found in both datasets– for example other *Dusps*, *Wnts*, *Hes*, and *Fox* genes.

In 2009, Branney et al. investigated the FGF-dependent transcriptome with the use of dnFGFRs shortly after the onset of mid-blastula transition in *Xenopus tropicalis*. dnFGFR1 or dnFGFR4-expressing embryos were cultured until stage 10.5 and processed for microarray analysis. 67 genes were found to be positively regulated and 16 genes negatively regulated by FGF signalling (Branney et al. 2009). 16 genes found by Branney and colleagues appear in this RNA-seq dataset. *Hesx1* and *Hes1* were found similarly downregulated, whereas *Fox4l1.1*, *FoxA4*, *Pnp*, *Dusp5*, *Admp*, *Noggin*, *Frz1*, *Sp5l*, *Sprouty1* and *Prickle1* were found similarly positively regulated by FGFR signalling. *Egr1* and *Sprouty2* did not pass thresholds for RNA-seq but was found upregulated by Branney et al too. However, *Otx2*, *Zeb2* and *Lin28A* were found positively regulated by FGF signalling by Branney et al but listed as negatively regulated by iFGFR4 in this investigation. Furthermore, some mesodermal genes, for instance *Xbra* found 19x upregulated by Branney et al., are not changed in this study, reinforcing this RNA-seq data as being representative of neural as opposed to mesodermal development, although a similar number of genes were found shared between Branney et al., and the microarray data.

Another microarray study investigating FGF signalling targets used SU5402 to inhibit FGF signalling in whole *Xenopus laevis* embryos between stages 10.5 and 11.5. 38 genes were found to be positively regulated by FGF signalling and 5 genes negatively regulated by FGF signalling (Chung et al. 2004). Due to the age of Chung et al., 11 genes were classed as unidentified proteins and their accession numbers are still only recognised as an unidentified 'transcribed locus' or have been retired on NCBI. Upon closer inspection a further 15 genes listed in general terms such as 'reverse transcriptase' still have no entry on Unigene and Xenbase, and the identities of these genes are still unknown. Of the remaining genes, after conversion into modern gene symbols 4 were found in common with the RNA-seq dataset – *Arl5, FoxB1, Dusp1* and *Zfp36l1* – and 5 in common with the iFGFR1/4 microarray – *Arl5, Mst1, Gdf3, Cdx4* and *Gata4.* This suggests that these genes are important for FGF signalling during development in general rather than in a solely neural context.

These comparisons with other datasets show that as well as novel putative FGF targets, the RNA-seq experiment has replicated some of the findings made by other

research groups, which lends weight to these overlapping genes being FGF targets in a neural context.

5.2.7 Many genes identified by RNA-seq have roles in neural development and/or FGF signalling

An extensive literature search was conducted on genes up- and downregulated by iFGFR1 and iFGFR4. The aim of this search was to gain an insight into how many genes in the dataset were already known to have roles in neural development and/or have known links to FGF signalling.

Firstly, genes were searched for on Xenbase. On Xenbase, each gene entry normally includes its function if known, and a community-submitted ISH image of gene expression, although the amount of information available about each gene is variable. When basic information was unavailable, other model organism databases were searched such as eMAGE (mouse) and ZFIN (zebrafish) for expression data. Genes which appeared from this preliminary search to be expressed in the developing CNS, were involved in neural development, or were listed as being involved in other FGF-related processes such as ciliogenesis or the cell cycle were investigated more extensively using Pubmed. This more extensive literature search revealed many of these genes to indeed have known links to neural development and patterning, as well as often being involved in FGF signalling. The results of this search are tabulated in Table 5.3-4.

The majority of the upregulated genes investigated were already known to be expressed in the CNS. Several genes or their family members were found affected by iFGFRs in the microarray screen. Furthermore, many genes have published links to FGF signalling either directly or indirectly, and in some cases other genes in the dataset (in **bold**). Genes identified in the microarray screen using iFGFRs discussed in Chapter 3 were often members of other major signalling pathways including TGF, Wnt, Shh, and RA and targets of these pathways were also represented in this RNA-seq data. Furthermore, patterns emerged such as genes involved in ciliogenesis, left/right asymmetry and eye development - processes of which FGF signalling is known to be required for.

This lends support for this dataset being representative of neural genes, and many findings are in keeping with what is already known about FGF signalling and targets.

Table 5.3 – Selection of genes upregulated by iFGFR1

Gene	Fold Change	Role	In microarray?	Expression	Summary	References
ADMP	5.7	TGFβ growth factor	No	Dorsal midline	ADMP is a member of the BMP pathway which has ventralising activity. Required for correct anterior-posterior neural patterning. Represses FGF signalling in *Ciona*.	(Ohta & Satou 2013; Reversade & De Robertis 2005)
ATP6V0C	2.8	H+ v-ATPase subunit	No	Brain neural tube, neurons	Also known as Ductin. Implicated in early laterality through its association with Rab11, and pharmacological inhibition causes heterotaxia in *Xenopus,* zebrafish and chick. Possible link to ***Snx10*** in regulating ciliogenesis. Involved in control of neuronal excitability.	(Adams et al. 2006; Vandenberg et al. 2013; Chung et al. 2010)
BCL9	2.2	Transcription co-activator	No	unknown	Implicated in lens and body axis development. BCL9 is part of a complex which, with canonical Wnt signalling, activate FGF18 and 20	(Katoh & Katoh 2006; Kennedy et al. 2010)
BTG2	4.5	Anti-proliferation factor	No	Notochord, somitic mesoderm	Inhibition causes anterior head defects and downregulation of neural markers such as *EN2* and ***Otx2*** and ***Rax***. Interacts with ***Ccnb1*** and ***Not-b*** and required for notochord differentiation	(Sugimoto et al. 2007; Ryu et al. 2004)
CRABP2	2.1	Retinoic acid binding protein	Yes	CNS	Involved in retinoid signalling. Represses 3' Hox genes. RA and FGF pattern the antero posterior neural axis	(Lloret-Vilaspasa et al. 2010)
CREBBP	2.1	Creb binding protein	Creb3	CNS (mouse)	Listed on Xenbase as interacting with BMPs, Chordin, Smads, NeuroD, Wnts, ***Cited2***, ***Zeb2*** and FGF8. It is known to be controlled by FGFR1 signalling to stimulate cell differentiation	(Fang et al. 2005)
DUSP1	2.1	MAPK phosphatase	Dusp6	Telencephalon (mouse)	MAPK phosphatase, also found upregulated by FGFR1 in a previous microarray screen.	(Branney et al. 2009)
DUSP5	10.6	MAPK phosphatase	DUSP6	Anterior CNS, branchial arches	MAPK phosphatase also found upregulated by FGFR1 in a previous microarray screen.	(Branney et al. 2009)
DYNLL1	2.3	Microtubule motor component and scaffolding	Yes	Cilia, neural tube	Differentially regulated by the two receptors in this screen. Light chain component of motor protein dynein, but found to bind to a wide range of complexes as a scaffolding protein. Interacts with Nek6 (found in	(Rapali et al. 2011; Regué et al. 2011; Kim et al. 2011;

		protein			microarray) through binding to Nek9 and is required for ciliogenesis. Also an effector of ***Nde1*.**	Goggolidou et al. 2014)
FOXA4	116.5	Transcription factor	Yes	Notochord, Spemann's organiser	Also known as Pintallavis. *FoxA4* is a notochord marker which restricts anterior neural development, including the expression of **Hesx1** and is required for maintenance of the CNS.	(Murgan et al. 2014; Martynova et al. 2004)
FOXB1	6.0	Transcription factor	no	CNS	FGF is required for *FoxB1*-suppression of anterior neural structures. *FoxB1* also promotes neural induction	(Takebayashi-Suzuki et al. 2011)
FOXD4L1.2	7.3	Transcription factor	Yes	Posterior CNS	Also known as FoxD5A. Early neural gene regulated by FGF and BMP signalling. Regulates a number of neural transcription factors to regulate transition from immature neural ectoderm to neural progenitors.	(Marchal et al. 2009; Neilson et al. 2012)
HES1	2.9	Transcription factor	Hes5.2/6	Neural plate border	**Notch** effector. Essential for neural crest proliferation downstream of FGFs with **Hes2**. Interacts with Neurogenin. With **Rax** and Notch, Hes1 promotes glial cell formation at the expense of neuronal fates in the rat.	(Furukawa et al. 2000; Nichane et al. 2008)
ID3	3.3	Transcription factor	No	Neural plate	A known FGF target. It's interaction with ***HES1*** is essential for neural crest formation. It is able to disrupts a Stat3-FGFR4 complex formation in neural crest development	(Nichane et al. 2010; Nichane et al. 2008)
IKZF2	15.5	Zinc finger	No	CNS (mouse), neurons	Also known as Helios. Required for lateral ganglion eminence and striatal neuron development.	(Martín-Ibáñez et al. 2012)
IRX1	2.3	Transcription factor	No	Dorsal midline, primary neurons	Also known as Iroquois. Required for neural patterning, MHB formation, and required for FGF8 expression in the Isthmic organiser.	(Glavic et al. 2002)
LEFTY	19.6	Left/right asymmetry	Yes	CNS, head, paraxial mesoderm	FGFs may interact directly with *Lefty* and interacts indirectly through *Fibp1* and *Ier2* to mediate left/right patterning. Both *Lefty* and FGFs are required for correct breaking of left/right asymmetry.	(Rodríguez Esteban et al. 1999; Hong & Dawid 2009)
MXI1	2.6	Transcription factor	No	Brain	*Mxi1* is essential for neurogenesis and positively regulated by the pan -neural marker *Sox3* and negatively by ***Notch***. Overexpression of *Mxi1* inhibits the primary neuron marker *N-tubulin*	(Klisch et al. 2006)

NOT-B	8.1	Transcription factor	No	Notochord	Required for notochord development and can be suppressed by SU5402.	(Chung et al. 2004)
NOTCH3	2.1	Signal transduction	No	Neural ectoderm, somites	FGF known to interact with Notch pathway	(Harada et al. 1999; Mitsiadis et al. 2010; Faux et al. 2001)
OCT-25	3.3	Transcription factor	No	Dorsal midline	*Oct25* is a known neuralising factor known to upregulate ***FoxB1***.	(Kole et al. 2014; Takebayashi-Suzuki et al. 2011)
POU3F4	2.8	Transcription factor	POU2F2,2F3	neural plate, brain	A noggin-inducible gene, with neuralising activity. Other interactants listed on Xenbase are *Cdx2*, *4* and posterior *Hox* genes. It is controlled by RA and FGF signalling.	(Robert-Moreno et al. 2010)
POU4F2	52.2	transcription factor	No	CNS	Involved in retinal ganglion cell differentiation. Interacts with other **Pou** family members	(Li et al. 2014)
PRICKLE1	2.8	Wnt negative regulator	Yes	Posterior CNS, somites	FGF are known to interact with Wnts to pattern CNS	See General Intro
PTCH2	2.5	Hedgehog receptor	Yes	CNS, somites	FGF and Hedgehog signalling interact in other developmental contexts such as the limb, the anterior neural border, neocortical patterning and neural tube patterning.	(Bénazet & Zeller 2009; Kessaris et al. 2004; Briscoe & Novitch 2008)
SMURF2	2.0	Ubiquitin protein ligase	No	Neural plate	A Member of the TGFβ signalling family, *Smurf2* binds to inhibitory Smads to mark them for degradation.	(Inoue & Imamura 2008)
SP5L	4.3	Transcription factor	No	Posterior CNS	A known FGF target involved with antero-posterior patterning. Found in a microarray to be downstream of ***FoxD4L1.2***.	(Sun et al. 2006; Zhao et al. 2003)
SPROUTY1	8.0	MAPK negative regulator	Yes	Branchial arches, MHB, tailbud	Negative regulator of MAPK pathway	See general introduction
TSPAN1	4.1	Tetraspanin membrane protein	Yes	Posterior CNS, cement and hatching gland	Integral membrane protein negatively regulated by BMPs also required for gastrulation movements and neural differentiation.	(Yamamoto et al. 2007)

WNT11B	14.1	Wnt signalling ligand	Yes	CNS	FGFs are known to interact with Wnts to pattern the CNS	See General Intro
YY1	2.1	Transcription factor	No	Anterior neural tube	Regulates expression of the neural crest marker *Slug*. Interacts with ***Ruvbl2*** and involved in anterior posterior patterning.	(Morgan et al. 2004; Kwon & Chung 2003)
ZFP36L1	2.0	Zinc finger protein	No	Pronephros, otic vesicle, brain	Shown to be downstream of ERK and required to control lipoprotein receptor mRNA stability	(Adachi et al. 2014)

Table 5.4 – Selected genes upregulated by iFGFR4

Gene	Fold change	Role	In microarray?	Expression	Summary	References
CCNB1	3.1	Cell cycle regulator	Yes	Global	Phosphorylated by MAPK.	(Walsh et al. 2003)
CDC6	2.6	Cell cycle	No	Global	Cdc6 is involved in the cell cycle, like FGFs, and is downregulated by FGF in chondrocytes; repressive complexes on the Cdc6 promoter increases upon FGF treatment.	(Kolupaeva & Basilico 2012)
CITED2	2.9	Transcriptional regulator	No	CNS (mouse)	Required for breaking left/right asymmetry and part of the nodal signalling cascade. Overexpression induces anterior genes such as ***Otx2*** but represses the posterior *HoxB9* and the eyefield marker ***Rax***.	(Lopes Floro et al. 2011; Bamforth et al. 2004; Yoon et al. 2011)
DUSP22	2.6	Dual-specificity phosphatase 22	DUSP6	Posterior CNS	**Dusp1**, **Dusp5** and **Dusp6** also mentioned in this dataset and microarray.	
FGFR1OP2	2.2	FGFR1 oncogene partner	No	Thymus (mouse)	Novel gene fused to FGFR1 in 8p11 myeloproliferative syndrome, causing its deregulation.	(Grand et al. 2004)
FOPNL	2.2	**FGFR1OP** n terminal-like	No	Unknown	Involved in ciliogenesis, a centrosome protein	(Lee & Stearns 2013)
FRS3	4.6	Docking protein	No	Anterior CNS, somites	FGF Receptor substrate also required for lens placode development.	(Kim et al. 2015)
GREM1	2.4	BMP antagonist	No	CNS, somites	Found downregulated in zebrafish *fgf8* mutants.	(Nicoli et al. 2005)

HES2	2.8	Transcription factor	Hes members in microarray	Forebrain, hindbrain, retina	**Notch** effector. Interacts with ***Id3*** downstream of FGF to specify neural crest progenitors. ***Hes1*** is also an interactant. *Hes2* is expressed in the retina and increases glial cell production by repressing neurogenesis.	(Nichane et al. 2008; Sölter et al. 2006)
HN1	2.1	Human notch paralogue	No	CNS	FGF signalling known to regulate Notch pathway	(Faux et al. 2001; Akai et al. 2005; Mitsiadis et al. 2010)
IFT172	6.5	Ciliogenesis	No	Unknown	Ift172 regulates FGF8 in MHB development. Positively regulated by ***Mxi1***. When upstream regulator ATMIN is depleted, *Ift172* and ***Dynll1*** are both downregulated.	(Gorivodsky et al. 2009; Ko et al. 2013)
INSM1	2.3	Transcription factor	No	CNS, PNS, pancreas	Depletion of *Insm1* caused upregulation of FGFR4 in cells, and Insm1 also regulates *Neurogenin3.*	(Osipovich et al. 2014)
ITPKC	2.1	1D-myo-inositol-triphosphate 3-kinase A	No	Unknown	Part of the inositol triphosphate pathway, a branch of FGF signalling	
KLF2	3.4	Zinc finger	klf17	CNS	Repression of FGF signalling reduces KLF2 levels *in vitro*	(Lanner et al. 2010)
MARK4	24.3	Ciliogenesis	Yes	Unknown	Promotes axoneme extension during ciliogenesis, a process FGF is involved with	(Kuhns et al. 2013)
NDE1	2.1	Scaffolding protein	No	CNS	Inhibits ciliogenesis which affects cell cycle re-entry. Deficiencies cause left-right patterning defects. MAPK modulation by the Nde1- Lis1-Brap complex patterns the mammalian CNS. Influences ***Dynll1*** expression.	(Kim et al. 2011; Lanctot et al. 2013)
NEDD9	4.3	Adaptor protein	NEDD4-like	Unknown	Retinoic-acid inducible protein. Regulates neural crest cell migration.	(Aquino et al. 2009)
NOGGIN	2.2	BMP antagonist	No	CNS	Well-documented FGF interaction	(Branney et al. 2009; Fletcher & Harland 2008)
OCT60	3.1	Transcription factor	No	Neural plate	Also known as Pou5F3.3. Linked to FGF through its target *Spalt-like 4*, which activates *Oct60*.	(Young et al. 2014)
POC5	2.1	Centriolar protein	No	Spinal cord, retina, dorsal root	Required for the formation of full-length centrioles but in mouse is localised to the CNS.	(Azimzadeh et al. 2009)

				ganglion (mouse)		
RAB21	2.3	Small GTPase	RAB4 and RAB27	Global	Member of Ras superfamily.	
RASSF3	2.7	Ras-associating protein	Yes	Global	MAPK effector	
RND3	2.0	GTP binding protein	No	Brain, somites	Required for somitogenesis, and knockdown of *FGF8* causes a posterior shift in *Rnd3* expression	(Goda et al. 2009)
SNX10	2.6	Sorting Nexin	No	Unknown	A regulator of ciliogenesis and required for correct left/right patterning. Possible functional link to ***Atp6V0C***.	(Chen et al. 2012)
TAPT1	2.2	Transmembrane protein	No	Global (mouse)	Tapt1 is a downstream effector of *HoxC8* and when mutated causes homeotic transformations	(Howell et al. 2007)
VANGL2	3.3	Non canonical Wnt signalling protein	VANGL1	Somites, notochord	Interacts with FGF signalling through cadherin and has a role in left/right asymmetry. Also listed as interacting with *Cdx4*, ***FoxA4***, *Wnts*, *Shh*, *HoxD1*, *Xbra*, and *Nodal* on Xenbase.	(Nagaoka et al. 2014; Vandenberg et al. 2013)

Table 5.5 – Selected genes downregulated by iFGFR1

Gene	Fold change	Role	In microarray?	Expression	Summary	References
APPL1	-2.6	Signal transduction	No	Anterior CNS	An APPL1/Akt signalling complex regulates dendritic spine and synapse formation in hippocampal neurons.	(Majumdar et al. 2011)
CIRBP	-2.0	Cytoplasmic RNA binding protein	No	CNS, pronephros	In *Xenopus*, compared to controls *Cirpb* morphants have a slower cell migration rate, inhibit eFGF and activin-induced animal cap elongation and have defects in brain development	(Peng et al. 2006)
HES3.1	-2.4	Transcriptional repressor	Hes family members also in microarray	anterior CNS	Hes1 and Hes3 regulate maintenance of the isthmic organizer and development of the mid/hindbrain. Loss of FGF activity or Hes1/Hes3 function results in premature differentiation of ventricular zone progenitor cells.	(Hirata et al. 2001)
HESX1	-3.2	Transcription Factor	Yes	Anterior CNS	*Hesx1* controls neural differentiation and patterning of the anterior CNS. Represses ***Ras-dva***, Activates ***Otx2*** and anterior *FGF8*. It is repressed by Hmx3	(Ermakova et al. 1999; Tereshina et al. 2014;

					(microarray). **FoxA4** is essential for defining its posterior limits.	Ermakova et al. 2007; Martynova et al. 2004)
IFT172	-3.0	Ciliogenesis	No	Unknown	*Ift172* regulates FGF8 in MHB development. Positively regulated by ***Mxi1***. When upstream regulator Atmin is depleted, *Ift172* and ***Dynll1*** are both downregulated.	(Gorivodsky et al. 2009; Ko et al. 2013)
KRT12	-5.3	Keratin	Yes	Epidermis	Neural induction represses epidermal genes such as keratin	(Delaune et al. 2005)
MDK	-2.2	Growth factor	No	CNS	Midkine/MDK is a growth factor with neurotrophic and neurite outgrowth activities and known to be positively regulated by RA. Found in microarrays similarly affected by changes in RA levels with ***Dusp6***, ***Cdx4***, ***Cited2***, and ***Otx2***.	(Hayata et al. 2009; Arima et al. 2005)
PIN4	-2.0	Parvulin-like peptidyl-prolyl cis-trans isomerase	No	Unknown	NIMA-interacting. Closely-related Pin1-mediated activation of *Runx2* is needed for FGF2's role in osteoblast differentiation, as well as interaction with *Nek6.*	(Chen et al. 2006)
PITPNB	-2.8	Phosphatidylinositol transfer protein	No	Thymus primordium (mice)	Part of phosphatidylinositol cascade	
PTMA-A	-2.7	Ubiquitin ligase	No	CNS	Involved in cell proliferation and differentiation.	(Donizetti et al. 2008)
RUVBL2	-2.3	DNA helicase	No	CNS	Interacts with ***Yy1***. It regulates transcription through multiple chromatin remodelling complexes. Essential for cilia motility in zebrafish.	(López-Perrote et al. 2014; Zhao et al. 2013)
SNAI1	-2.8	Transcriptional repressor	Yes	CNS	Required for neural crest development. Loss of FGFR1 causes loss of *Snai1* expression in mice	(Ciruna & Rossant 2001)
TUBA1A-B	-2.2	alpha tubulin	No	epidermis	Neural induction represses epidermal genes	

Table 5.6 – Selected genes downregulated by iFGFR4

Gene	Fold change	Role	In microarray?	Expression	Summary	References
CCND1	-2.6	Cell cycle	No	CNS	Wnt target through *Frz* (microarray) based on the ***Bcl9*** complex. Upregulated by FGF2 *in vitro*.	(Katoh & Katoh 2006; Lai et al. 2011)
CRABP2	-9.6	Retinoic acid binding protein	Yes	CNS	Represses 3' Hox genes. RA and FGF pattern the antero posterior neural axis.	(Lloret-Vilaspasa et al. 2010)
CRX-A/B	-2.0/-2.1	Transcription Factor	Yes	Anterior CNS	Implicated in eye development, interacts with ***Rax***, and increased in *FoxN4* (microarray) mutants. Mesodermal *Crx* is depleted when FGF is inhibited.	(Giudetti et al. 2014; Vignali et al. 2000; Xiang & Li 2013; Fletcher & Harland 2008)
CYP26A1	-5.9	RA hydroxylase	No	CNS	FGF activates *Cyp26A1,* an enzyme that triggers RA degradation. It sharpens the RA gradient during patterning of the midbrain/hindbrain regions.	(Rhinn & Dollé 2012; Shiotsugu et al. 2004)
DYNLL1	-2.5	Scaffolding protein	Yes	Cilia, neural tube	Differentially regulated by the two receptors in this screen. Light chain component of motor protein dynein, but found to bind to a wide range of complexes as a scaffolding protein. Interacts with Nek6 (found in microarray) through binding to Nek9 and is required for ciliogenesis. Also an effector of ***Nde1*.**	(Rapali et al. 2011; Regué et al. 2011; Kim et al. 2011; Goggolidou et al. 2014)
GNB3	-3.1	G protein b subunit	Yes	MHB, retina	Involved in eye development, *Gnb3* is expressed by Islet1-positive cone ON-bipolar cells and by cone photoreceptors.	(Ritchey et al. 2010)
HESX1	-7.8	Transcription Factor	Yes	Anterior CNS	*Hesx1* controls neural differentiation and patterning of the anterior CNS Represses ***Ras-dva***, inhibits ***Otx2*** and *FGF8*.	(Ermakova et al. 1999; Ermakova et al. 2007; Tereshina et al. 2014)
KRT5.7	-3.4	keratin	Other keratins present	Epidermis	Neural induction inhibits epidermal genes such as keratin	(Delaune et al. 2005)

LIN28A	-3.0	RNA processing	No	Dorsal blastopore lip	Found in previous microarray screen for FGF targets. Required for germ layer specification in *Xenopus*. A loss stops cells responding normally to FGF	(Branney et al. 2009; Faas et al. 2013)
NR6A1	-4.7	Transcription Factor	Yes	CNS	Also found in screen for RAR target. Downregulates ***Oct4***. A knockout phenotype failed to close the neural tube and had ectopic tail and deformed heads.	(Barreto et al. 2003)
OTX2	-2.9	Transcription Factor	No	Anterior CNS	Anterior neural marker repressed and activated by FGF8 at various times during neural development. Affects the expression of ***Btg2***. In positive loop with ***Ras-dva*** and FGF8. Inhibited by ***Hesx1*** and *Cdx4*.	(Liu et al. 2003; Tereshina et al. 2014; Isaacs et al. 1998; Ermakova et al. 2007)
RAX	-2.6	Transcription Factor	Yes	Retina	An eyefield marker, expression downregulated as neuralation proceeds. Reduced when FGF target *Lpar6* is knocked down.	(Giudetti et al. 2014; Geach et al. 2014)
ROR2	-3.5	Kinase	No	Branchial arches, posterior CNS	Interacts with Wnt5. Ror2 receptor mediates **Wnt11** ligand signalling and affects convergence and extension movements in zebrafish.	(Oishi et al. 2003; Bai et al. 2014)
SHISA2	-2.1	ER protein	No	Somites; branchial arches	Shisa2 promotes the maturation of somitic precursors and is required for somitogenesis. Wnt and FGFs rescue Shisa2 MO defects. Shisa2 promotes head formation through the inhibition of the caudalising factors, Wnt and FGF	(Nagano et al. 2006; Yamamoto et al. 2005)
SHROOM3	-2.8	Actin regulating protein	No	CNS	Important for morphogenesis during gastrulation and neuralation. *Shroom3* induces apical constriction and is required for hingepoint formation during neural tube closure. Overexpression of ***Vangl2*** inhibits its apical restriction.	(Ossipova et al. 2015)
TUBA1A	-2.0	Alpha tubulin	No	Epidermis	Neural induction represses epidermal genes	
ZEB2	-18.1	Transcription factor	No	CNS	FGFs activate *Zeb2* through *Churchill*, which is required for Zeb's expression in neural plate. Transcriptional repression during neural induction and inhibits *Bmp4*. It is required for neural induction and depletion causes loss of *N-tubulin*.	(Nitta et al. 2004; van Grunsven et al. 2007)

Therefore even though only one biological experiment was undertaken instead of a replicated study, the links between the genes in the data, the documented activity of many of these genes in the CNS and in connection to FGF signalling and each other strengthens the likelihood of this dataset being a true reflection of FGF overactivation in a neural context.

5.2.8 Ontological Analyses

Ontological analyses were performed to find further functional patterns in putative FGF targets during neural development by searching for common gene ontology 'GO' terms. A range of online programs were tried to achieve this, among them DAVID and GOrilla, using the genelists above containing genes with an FPKM of ≥30 FPKM and fold change of ≥2. Unfortunately, due to these tools not being optimised for *Xenopus*, only 17% of genes from already small genelists were included in the output so no meaningful results were obtained.

Therefore to increase the size of the dataset for easier statistical enrichment analyses, the filtering conditions of the dataset were relaxed slightly - genes from the original unfiltered dataset were picked out that had an FPKM of at least 20 for either or both uninduced and induced samples, and an expression fold change of ≥1.5. Also, the A and B pseudoalleles unique to the tetraploid *laevis* were merged into just one form to increase the likelihood they would be recognised by other databases.

The PANTHER (Protein ANalysis THrough Evolutionary Relationships) Classification System was then tried with these new conditions with better results. The PANTHER website which has several options for analysing genelists and performing enrichment analyses based on a background genelist dataset (the whole organism genelist). The aspect of PANTHER used in this study compare gene symbols in the input (one of the four genelists) against a *Xenopus* background list, and performed statistical tests to determine if a GO term, protein or pathway component was enriched or depleted based upon an expected value predicted from a dataset of a certain size (Table 5.7 and Table 5.8).

5.2.8.1 Clustering genes by GO term

Although not of interest to this study, all four of these genelists are enriched highly significantly for metabolic genes, showing that FGFs have a role in regulation of metabolism as well as neural development. Cell cycle genes are also enriched in all

four genelists, although it is most significant in the iFGFR1 downregulated and iFGFR4 upregulated genelists, where the P-values were 6.73E-6 and 2.44E-6 respectively. An interesting point of difference between the receptor genelists are the terms involving development. The iFGFR1 upregulated genelist was significantly enriched for the term 'developmental process' and 'ectoderm development' whereas the iFGFR1 downregulated genelist was depleted for the terms 'mesoderm development', 'system development' and 'developmental process'. This confirms that FGF signalling is involved in many developmental processes, in keeping with known roles of FGF. However, the 'iFGFR4 upregulated' GO term output had more in common with 'iFGFR1 downregulated' output in this respect. Nervous system, ectodermal, muscle, heart, skeletal system and system-developmental processes were all present at less than the expected value. It is not surprising that heart, muscle and skeletal developmental processes are not enriched in a neuralised animal cap, but the net downregulation of the nervous and ectodermal development across the whole datasets is interesting, seeing as this experiment is within neuralised explants system. Plenty of known neural targets were picked for the literature analysis in the iFGFR4 upregulated dataset, so it is undeniable that iFGFR4 has an important role in neural development and other aspects of development at this time, but maybe across the whole dataset there are less of these genes present than the expected value and iFGFR4 is more heavily involved in other processes. Common to both downregulated genelists, genes implicated in RNA processing, splicing and translation are enriched. Ribosomal metabolism is also enriched – although this needs to be interpreted with caution as the rRNA depletion methods used enrich total RNA for mRNA to use in RNA-seq may leave variable residual amounts of ribosomal transcripts in the samples.

According to these analyses components of cell cycle regulation and metabolism are both positively and negatively influenced by FGF signalling. Therefore, although there is little overlap between genes appearing in iFGFR1 and iFGFR4 genelists, the receptors cooperate to regulate some processes. Some processes such as RNA processing are negatively regulated by both receptors during *Xenopus* neural development. Developmental processes may be differentially regulated by iFGFR1 and iFGFR4, suggesting there are also fundamental differences between the long-term outputs of each receptor.

Table 5.7 iFGFR1 GO Term Enrichment

iFGFR1 Upregulated

Go terms	Enriched/ depleted	P-value
nucleobase-containing compound metabolic process	+	3.07E-07
metabolic process	+	4.02E-07
transcription from RNA polymerase II promoter	+	7.43E-07
transcription, DNA-dependent	+	8.89E-07
RNA metabolic process	+	1.70E-06
regulation of nucleobase-containing compound metabolic process	+	3.85E-06
primary metabolic process	+	5.03E-06
regulation of transcription from RNA polymerase II promoter	+	1.61E-05
regulation of biological process	+	1.01E-04
cellular process	+	1.23E-04
cell cycle	+	2.81E-04
Unclassified	-	1.04E-03
locomotion	+	2.87E-03
biological regulation	+	3.37E-03
regulation of phosphate metabolic process	+	4.11E-03
cellular component movement	+	4.68E-03
chromatin organization	+	7.25E-03
biosynthetic process	+	7.31E-03
mRNA polyadenylation	+	1.35E-02
cell growth	+	1.51E-02
mRNA 3'-end processing	+	1.60E-02
phosphate-containing compound metabolic process	+	1.63E-02
developmental process	+	2.32E-02
cell-cell signaling	-	2.58E-02
RNA splicing	+	2.68E-02
RNA splicing, via transesterification reactions	+	2.68E-02
organelle organization	+	2.74E-02
growth	+	2.88E-02
mRNA splicing, via spliceosome	+	2.93E-02
multicellular organismal process	+	3.02E-02
single-multicellular organism process	+	3.02E-02
cellular component organization	+	4.22E-02
ectoderm development	+	4.45E-02
cation transport	-	4.74E-02
cellular component organization or biogenesis	+	4.90E-02
neurotransmitter secretion	-	5.28E-02

iFGFR1 Downregulated

Go term	Enriched/ Depleted	P-value
RNA splicing	+	1.23E-18
RNA splicing, via transesterification reactions	+	1.23E-18
mRNA splicing, via spliceosome	+	6.11E-18
mRNA processing	+	1.11E-16
translation	+	6.34E-15
primary metabolic process	+	1.67E-12
nucleobase-containing compound metabolic process	+	2.01E-12
metabolic process	+	5.70E-12
DNA replication	+	2.72E-09
rRNA metabolic process	+	7.87E-09
RNA metabolic process	+	1.76E-08
protein metabolic process	+	3.20E-07
DNA metabolic process	+	4.60E-07
organelle organization	+	2.22E-06
chromatin organization	+	3.96E-06
immune system process	-	4.53E-06
cell cycle	+	6.73E-06
mRNA polyadenylation	+	1.69E-05
cell adhesion	-	1.74E-05
biological adhesion	-	1.74E-05
mRNA 3'-end processing	+	2.30E-05
response to stimulus	-	1.51E-04
Unclassified	-	1.93E-04
ion transport	-	2.18E-04
cell-cell signaling	-	3.98E-04
immune response	-	4.37E-04
cell communication	-	6.24E-04
protein folding	+	6.71E-04
cellular component organization or biogenesis	+	6.88E-04
cation transport	-	6.92E-04
oxidative phosphorylation	+	7.05E-04
regulation of translation	+	1.41E-03
cell-cell adhesion	-	2.08E-03
lipid metabolic process	-	4.74E-03
cellular component organization	+	5.44E-03
synaptic transmission	-	6.38E-03
cellular defense response	-	9.01E-03
mesoderm development	-	9.11E-03
phosphate-containing compound metabolic process	-	1.30E-02
cellular component biogenesis	+	1.30E-02
carbohydrate metabolic process	-	1.45E-02
protein complex biogenesis	+	1.60E-02
protein complex assembly	+	1.60E-02
system development	-	1.94E-02
reproduction	-	2.01E-02
cytokinesis	+	2.70E-02
mitochondrion organization	+	2.71E-02
mitochondrial transport	+	2.71E-02
mitosis	+	2.81E-02
macrophage activation	-	2.99E-02
developmental process	-	3.15E-02
localization	-	3.46E-02
response to external stimulus	-	3.51E-02
gamete generation	-	4.31E-02
transport	-	4.85E-02

Table 5.8 iFGFR4 GO terms Enrichment

iFGFR4 Upregulated

GO term	Enriched/ Depleted	P value
metabolic process	+	8.52E-08
cell cycle	+	2.44E-06
mitosis	+	3.66E-06
cell-cell adhesion	-	4.99E-05
DNA metabolic process	+	1.50E-04
regulation of catalytic activity	+	1.69E-04
skeletal system development	-	1.95E-04
regulation of molecular function	+	2.72E-04
mesoderm development	-	3.22E-04
cellular protein modification process	+	3.77E-04
system process	-	3.77E-04
regulation of transcription from RNA polymerase II promoter	-	4.65E-04
system development	-	5.98E-04
nervous system development	-	6.36E-04
multicellular organismal process	-	1.00E-03
single-multicellular organism process	-	1.00E-03
muscle organ development	-	1.16E-03
cell adhesion	-	1.21E-03
biological adhesion	-	1.21E-03
ectoderm development	-	1.82E-03
regulation of phosphate metabolic process	+	1.92E-03
neurological system process	-	2.30E-03
angiogenesis	-	2.74E-03
protein transport	+	2.94E-03
intracellular protein transport	+	3.40E-03
primary metabolic process	+	3.55E-03
protein localization	+	3.74E-03
RNA catabolic process	+	4.47E-03
phosphate-containing compound metabolic process	+	4.68E-03
response to external stimulus	-	5.77E-03
asymmetric protein localization	+	6.41E-03
vesicle-mediated transport	+	6.74E-03
synaptic transmission	-	6.80E-03
localization	+	6.93E-03
DNA replication	+	7.39E-03
protein phosphorylation	+	9.67E-03
transcription from RNA polymerase II promoter	-	9.72E-03
protein metabolic process	+	9.73E-03
glycolysis	+	9.81E-03
cytokinesis	+	1.01E-02
visual perception	-	1.05E-02
cell-cell signaling	-	1.22E-02
transcription, DNA-dependent	-	1.26E-02
protein targeting	+	1.45E-02
heart development	-	1.48E-02
catabolic process	+	1.62E-02
regulation of nucleobase-containing compound metabolic process	-	1.65E-02
muscle contraction	-	1.81E-02
chromosome segregation	+	1.82E-02
transport	+	1.83E-02
RNA localization	+	2.00E-02
cellular process	+	2.15E-02
tRNA metabolic process	+	2.16E-02
blood coagulation	-	2.47E-02

iFGFR4 Downregulated

GO terms	Enriched/ Depleted	P-value
RNA metabolic process	+	4.42E-10
nucleobase-containing compound metabolic process	+	1.04E-09
mRNA splicing, via spliceosome	+	5.38E-09
mRNA processing	+	1.21E-07
RNA splicing	+	5.52E-07
RNA splicing, via transesterification reactions	+	5.52E-07
primary metabolic process	+	9.20E-07
metabolic process	+	2.15E-06
translation	+	9.05E-06
Unclassified	-	1.10E-05
DNA replication	+	9.72E-05
rRNA metabolic process	+	1.04E-04
transcription from RNA polymerase II promoter	+	1.91E-04
transcription, DNA-dependent	+	2.17E-04
DNA metabolic process	+	5.86E-04
pattern specification process	+	8.73E-04
regulation of transcription from RNA polymerase II promoter	+	1.43E-03
mRNA polyadenylation	+	2.00E-03
regulation of nucleobase-containing compound metabolic process	+	2.35E-03
mRNA 3'-end processing	+	2.48E-03
regulation of biological process	+	2.61E-03
segment specification	+	3.57E-03
cellular defense response	-	3.88E-03
biological regulation	+	6.18E-03
organelle organization	+	6.47E-03
cell-cell signaling	-	7.46E-03
protein ADP-ribosylation	+	9.17E-03
cell cycle	+	1.01E-02
spermatogenesis	+	1.55E-02
macrophage activation	-	1.60E-02
biosynthetic process	+	1.74E-02
synaptic transmission	-	1.81E-02
protein metabolic process	+	1.92E-02
immune system process	-	2.19E-02
complement activation	+	2.51E-02
reproduction	+	3.21E-02
cellular component organization	+	3.21E-02
nervous system development	+	3.22E-02
chromatin organization	+	3.23E-02
sulfur compound metabolic process	+	3.30E-02
nitrogen compound metabolic process	+	3.38E-02
B cell mediated immunity	-	3.53E-02
cellular component organization or biogenesis	+	3.62E-02
induction of apoptosis	-	3.84E-02
protein phosphorylation	-	4.59E-02
cell communication	-	4.60E-02

5.2.8.2 PANTHER Protein Analysis

Statistical enrichment analysis was repeated on the same genelist to pick out classes of protein associated signalling by iFGFR1 and iFGFR4 (Table 5.9). As with GO term analysis findings, ribosomal proteins were enriched in both downregulated lists, as were cell:cell adhesion related proteins. An interesting point of difference between the two receptors was the terms involving transcription factors. The iFGFR1 upregulated lists were enriched for the terms ‘transcription factor’, ‘homeobox transcription factor’, ‘helix-loop-helix transcription factor’, ‘KRAB

box transcription factor', 'basic leucine zipper transcription factor' and 'helix-turn-helix transcription factor'. The iFGFR1 downregulated list was enriched for 'HMG box transcription factor' but depleted for 'zinc finger transcription factor' and 'KRAB-box transcription factor. As with the GO terms pertaining to developmental processes, this pattern was reversed with iFGFR4 genelists with the upregulated genelist being significantly depleted for these terms and the downregulated genelist enriched for 'transcription factor'. Similar to GO terms suggesting transcriptional and translational-related genes are enriched in both downregulated genelists, downregulated genelists for both receptors were similarly significantly enriched with transcription, translation and RNA processing-related protein terms, although the significance of this is unclear. Lastly, defence immunology-related proteins were present at significantly less than the expected value in the upregulated lists for both receptors, suggesting that stress-response genes were not activated in large amounts in response to FGF induction.

5.2.8.3 PANTHER pathways

The preliminary microarray dataset contained a lot of genes involved in other developmental signalling pathways, particularly Wnts of which FGF signalling is known to cooperate with in the patterning of posterior neural tissue (McGrew et al. 1997; Kudoh et al. 2002; Dyer et al. 2014). Do iFGFR1 and iFGFR4 also modulate the expression of other signalling pathways in neural development? To answer this question, PANTHER pathway enrichment analysis was undertaken using the same genelists as for previous PANTHER studies, and the genes involved in each pathway listed (Table 5.10). Indeed, the iFGFR1 upregulated genelist was significantly enriched for FGF, Wnt, PI3K and Notch pathway components indicating a wide range of crosstalk between FGFR1 and these pathways. The iFGFR4 output was very different, and few non-metabolic pathways were found significantly enriched.

Table 5.9 PANTHER Protein Class Enrichment

iFGFR1 Upregulated

PANTHER Protein Class	Enriched/ Depleted	P-Value
nucleic acid binding	+	9.02E-08
transcription factor	+	3.64E-06
DNA binding protein	+	2.01E-04
transferase	+	3.32E-04
acetyltransferase	+	1.16E-03
Unclassified	-	1.76E-03
G-protein coupled receptor	-	9.24E-03
DNA glycosylase	+	1.07E-02
methyltransferase	+	1.24E-02
KRAB box transcription factor	-	1.26E-02
ribonucleoprotein	+	1.28E-02
mRNA polyadenylation factor	+	1.30E-02
basic helix-loop-helix transcription factor	+	1.54E-02
defense/immunity protein	-	2.29E-02
kinase	+	2.35E-02
homeobox transcription factor	+	2.60E-02
helix-turn-helix transcription factor	+	2.60E-02
mRNA splicing factor	+	2.62E-02
basic leucine zipper transcription factor	+	3.20E-02
CREB transcription factor	+	3.20E-02
cation transporter	-	3.26E-02
transmembrane receptor	+	3.64E-02
nuclease	+	3.71E-02
endodeoxyribonuclease	+	3.87E-02
non-receptor serine/threonine protein	+	3.92E-02
cell adhesion molecule	-	4.83E-02

iFGFR1 Downregulated

PANTHER Protein Class	Enriched/ Depleted	P-value
RNA binding protein	+	1.89E-37
nucleic acid binding	+	1.83E-30
ribosomal protein	+	9.82E-23
mRNA splicing factor	+	1.12E-18
mRNA processing factor	+	6.01E-17
ribonucleoprotein	+	5.45E-10
chromatin/chromatin-binding	+	4.53E-06
mRNA polyadenylation factor	+	1.56E-05
DNA binding protein	+	5.54E-05
receptor	-	8.29E-05
phosphatase inhibitor	+	8.70E-05
HMG box transcription factor	+	1.77E-04
zinc finger transcription factor	-	2.35E-04
DNA-directed RNA polymerase	+	3.26E-04
chaperone	+	4.14E-04
translation initiation factor	+	4.16E-04
cell adhesion molecule	-	7.09E-04
transporter	-	9.37E-04
phosphatase modulator	+	1.85E-03
Unclassified	-	2.15E-03
translation factor	+	2.72E-03
nucleotidyltransferase	+	3.24E-03
extracellular matrix protein	-	3.41E-03
histone	+	5.32E-03
KRAB box transcription factor	-	6.79E-03
defense/immunity protein	-	7.44E-03
ion channel	-	1.68E-02
helicase	+	3.31E-02
cytokine receptor	-	3.42E-02
serine protease	-	3.42E-02
nuclease	+	3.57E-02

iFGFR4 Upregulated

PANTHER Protein Class	Enriched/ Depleted	P-value
defense/immunity protein	-	1.13E-07
enzyme modulator	+	2.03E-06
receptor	-	5.12E-06
transferase	+	1.84E-05
kinase modulator	+	2.01E-05
cytokine receptor	-	1.04E-04
G-protein modulator	+	2.23E-04
kinase activator	+	3.51E-04
kinase	+	3.63E-04
G-protein coupled receptor	-	3.69E-04
cell adhesion molecule	-	1.01E-03
kinase inhibitor	+	1.76E-03
protein kinase	+	2.30E-03
immunoglobulin receptor superfamily	-	2.67E-03
transcription factor	-	3.12E-03
non-receptor serine/threonine protein kinase	+	4.37E-03
RNA binding protein	+	4.62E-03
G-protein	+	6.84E-03
mutase	+	7.56E-03
KRAB box transcription factor	-	7.60E-03
isomerase	+	1.08E-02
phosphatase	+	1.41E-02
extracellular matrix protein	-	1.45E-02
tyrosine protein kinase receptor	+	1.91E-02
non-motor microtubule binding protein	+	2.02E-02
homeobox transcription factor	-	2.07E-02
helix-turn-helix transcription factor	-	2.07E-02
structural protein	-	2.12E-02
zinc finger transcription factor	-	2.19E-02
DNA strand-pairing protein	+	2.26E-02
anion channel	+	2.93E-02
oxidoreductase	+	3.44E-02
small GTPase	+	3.65E-02
DNA helicase	+	3.70E-02
immunoglobulin superfamily cell adhesion molecule	-	3.99E-02
metalloprotease	-	4.26E-02
non-motor actin binding protein	-	4.47E-02
esterase	+	4.92E-02

iFGFR4 Downregulated

PANTHER Protein Class	Enriched/ Depleted	P-value
nucleic acid binding	+	7.55E-15
RNA binding protein	+	4.82E-13
ribosomal protein	+	3.46E-10
ribonucleoprotein	+	3.77E-08
mRNA splicing factor	+	5.25E-07
mRNA processing factor	+	4.04E-06
DNA binding protein	+	2.01E-05
Unclassified	-	1.20E-04
transcription factor	+	2.73E-04
chromatin/chromatin-binding protein	+	4.65E-04
mRNA polyadenylation factor	+	1.89E-03
DNA topoisomerase	+	3.43E-03
nuclear hormone receptor	+	5.20E-03
cytokine receptor	-	1.87E-02
HMG box transcription factor	+	2.27E-02
complement component	+	2.94E-02
intermediate filament	+	3.18E-02
DNA-directed RNA polymerase	+	3.19E-02
DNA ligase	+	4.18E-02

Table 5.10 PANTHER Pathway Enrichment

iFGFR1 Upregulated

Pathway	Enriched/ Depleted	P Value	Genes Involved (fold changes)
Gonadotropin releasing hormone receptor pathway	+	2.70E-04	DGKZ (1.5); TCF7L1 (1.6); EP300 (1.8); GNAS (1.5); FOS (14.9); GNAQ (1.5); MAPK5 (1.6); POU2F1 (1.9); ID3 (2.6); NCOA3 (1.6); RAC1 (1.7); ARHGAP32 (2.3)
Notch signaling pathway	+	4.35E-04	NOTCH1 (1.6); MAML1 (1.7); CIR1 (1.9); HES4 (1.7); HES1 (2.9)
Heterotrimeric G-protein signaling pathway-Gq alpha and Go alpha mediated pathway	+	2.07E-03	RAP1GAP (1.6); GNAQ (1.5); RHOB (1.8); PLCB3 (1.8); RGS12 (1.8); ARHGEF1 (1.6); GRK6 (1.6)
Endothelin signaling pathway	+	8.07E-03	GNAS (1.5); GNAQ (1.5); PLCB3 (1.8); PTGS2 (2.3)
p53 pathway	+	8.92E-03	MTA2 (1.5); EP300 (1.8); PIK3C2A (1.9); TNFRSF14 (1.6); PTEN (1.6)
Cytoskeletal regulation by Rho GTPase	+	9.37E-03	ROCK2 (1.5); RHOB (1.8); VASP (1.6); ARHGEF1 (1.6); RAC1 (1.7)
Angiogenesis	+	9.98E-03	NOTCH1 (1.7); CRKL (1.7); NRAS (1.6); FOS (14.9); RHOB (1.8); PDGFB (2.8); PIK3C2A (1.9)
EGF receptor signaling pathway	+	1.28E-02	NRAS (1.6); SPRY1 (5.0); NF1 (1.6); SPRY2 (7.1); PIK3C2A (1.9); RAC1 (1.7)
Axon guidance mediated by netrin	+	1.62E-02	VASP (1.6); PIK3C2A (1.9); RAC1 (1.7)
Wnt signaling pathway	+	1.82E-02	LRP6 (1.8); TCF7L1 (1.6); PCDH1 (1.9); EP300 (1.8); BCL9 (2.2); GNAQ (1.5); ARID1A (2.5); PLCB3 (1.8); PCDH10 (1.6); DACT1 (1.7)
Integrin signalling pathway	+	2.00E-02	CRKL (1.7); NRAS (1.6); RHOB (1.8); VASP (1.6); PIK3C2A (1.9); RAC1 (1.7)
Angiotensin II-stimulated signaling through G proteins and beta-arrestin	+	2.02E-02	GNAQ (1.5); PLCB3 (1.8); GRK6 (1.6)
Insulin/IGF pathway-protein kinase B signaling cascade	+	2.02E-02	TSC1 (1.5); PIK3C2A (1.9); PTEN (1.6)
FGF signaling pathway	+	3.40E-02	NRAS (1.6); SPRY1 (5.0); SPRY2 (7.1); PIK3C2A (1.9); RAC1 (1.7)
Axon guidance mediated by semaphorins	+	3.53E-02	ARHGEF1 (1.6); RAC1 (1.7)
PI3 kinase pathway	+	3.70E-02	NRAS (1.6); GNAQ (1.5); PTEN (1.6)
Xanthine and guanine salvage pathway	+	4.52E-02	PNP (3.4)

iFGFR1 Downregulated

Pathway	Enriched/ Depleted	P-value	Genes involved (fold change)
General transcription by RNA polymerase I	+	8.54E-04	POLR2K (0.59); POLR1D (0.55); RPA2 (0.52)
Parkinson disease	+	2.27E-02	PSMB1 (0.58); HSPA8 (0.63); PSMA2 (0.60); PSMD13 (0.65)
DNA replication	+	3.72E-02	HIST2H3A (0.50); RPA2 (0.52)

iFGFR4 Upregulated

Pathway	Enriched/Depleted	P-value	Genes Involved (Fold change)
Circadian clock system	+	3.43E-03	CSNK1E (2.2); CRY1 (2.3); PER3 (1.7)
Cadherin signaling pathway	-	6.51E-03	no representation
Parkinson disease	+	9.47E-03	UCHL1 (1.9); ADRBK2 (2.0); TOR2A (1.6); CSNK1E (2.2): UBE2J2 (1.9); CCNE2 (1.5); CSNK1G2 (1.6); CSNK1G3 (1.8)
Tyrosine biosynthesis	+	3.23E-02	GOT2 (2.0)
Glycolysis	+	3.27E-02	GAPDH (1.8); ALDOC (2.1); PGK1 (1.9)
TCA cycle	+	4.33E-02	ACO2 (2.1); FH (1.6)

iFGFR4 Downregulated

Pathway	Enriched/ Depleted	P-value	Genes Involved (fold change)
Cell cycle	+	3.52E-03	PSMD14 (0.4); CINP (0.54),
FAS signaling pathway	+	1.02E-02	PARP3 (0.34); PARP1 (0.42);
p53 pathway feedback	+	3.02E-02	RBL1 (0.52); CCNG1 (0.61);
Transcription regulation by bZIP transcription factor	+	3.19E-02	GTF2B (0.66); POLR2H (0.28); CREB1 (0.61)
BMP_signaling_pathway-drosophila	+	4.18E-02	SMAD4 (0.53)
Xanthine and guanine salvage pathway	+	4.18E-02	PNP (0.57)
Activinbetasignaling_path	+	4.18E-02	SMAD4 (0.53)
DNA replication	+	4.99E-02	TOP2A (0.66); TOP2B (0.56)

5.2.8.4 Kinase enrichment analysis using Network2Canvas

Kinase enrichment analysis using Network2Canvas was performed to complement the PANTHER pathway analysis, as kinases are often components of cell signalling pathways. Network2canvas is a way of visualising networks within datasets. Commonly interacting genes form a 'node', and these nodes are visualised in Network2Canvas on a toroidal grid, with the brightness of the nodes proportional to the strength of connection to its neighbouring nodes.

Thus, in Network2Canvas kinase enrichment analysis (KEA), nodes are built around kinases. Not all kinases are in the genelists, but if a significant number of intersecting genes in the genelists interact with it, it will be listed as a node. This is observed with Nek6, found upregulated by iFGFR1 in the preliminary microarray and RNA-seq by iFGFR1 but not included in RNA-seq genelists due to low read

counts. In Table 5.11 Nek6 is listed as forming an interactant node with SGK1, SMAD4, SMURF2 and NUP98. Information about other nodes was found by looking up their genecard reference on the NCBI database. Other nodes from iFGFR1 listed are the cell cycle-related CDK1, CDK2 and FRK as well as the Pi3K/Akt related kinases AKT1 and MTOR. MAPK1 is listed as well as MAPKAPK2 and MAPK14, so therefore the FGF pathway effectors are well represented in the dataset.

Table 5.11 Kinase enrichment for iFGFR1-upregulated genes

Node Name	P-Value	Associations	Intersecting Genes
CDK2	2.37E-04	Cell Cycle	*AFF1;AKT1S1;ARID1A;BCL9;BRD3;CCNA1;CDC27;CREBBP;EP300;FNBP4;ID3;MYBL2;POLR2A;PPM1B;RAP1GAP;RPS3;SF1;SMAD4;SOX11;TSC1;UBE2E3;ZNF217;SGK1;C1ORF198;FOXK2;MLL2;MTA2;NUFIP2;NUMA1;NUP153;NUP98;PBRM1;POU2F1;WHSC2*
AKT1	8.42E-04	FGF-AKT	*AKT1S1;EP300;FLNA;PLXNA1;PTEN;RAC1;TSC1;YAP1;THRA;CREBBP;KHSRP;PFKFB3;RPS3;SMAD4;SH3BP4;TTC3;ZFP36L1;CDC25B*
MTOR	1.59E-03	FGF- AKT	*AKT1S1;SGK1;UBR4;CDC42BPB;FLNA;FOXK2;NUMA1;POLR2A;RC3H1*
NEK6	1.88E-03	NIMA-related kinase	*SGK1;SMAD4;SMURF2;NUP98*
GSK3B	3.53E-03	WNT	*AFF1;ARID1A;BCL9;BRD3;CDC25B;CDC27;CNOT4;CRKL;FLNA;FNBP4;IER3;LRP6;MYBL2;NOTCH1;PCDH1;POGZ;POLR2A;PTEN;RAP1GAP;RPS3;SF1;SMAD4;SON;SOX11;SPEN;UBE2E3;WHSC2;ZNF217;SGK1;MLL2*
CDK1	1.07E-02	Cell cycle	*AKT1S1;C13ORF15;CCNA1;CDC25B;CDC27;CNOT4;CRKL;DUSP1;FLNA;GADD45G;MLL4;MYBL2;PCDH1;PIK3C2A;POGZ;POLR2A;POU2F1;RAP1GAP;SON;SPEN;TSC1;WHSC2;FOXK2;MLL2;NUMA1;NUP98;PI4KB*
MAPK1	1.37E-02	FGF-MAPK	*CNOT4;DUSP1;DUSP5;IER3;MYBL2;POLR2A;RPS3;SMAD4;TGIF1;WHSC2;SGK1;CREBBP;SF1;BTG2;EP300;NUP153;WASF2*
FRK	1.60E-02	Cell cycle	*RAC1;PTEN*
MAPK14	2.08E-02	FGF-MAPK	*AKT1S1;BCL9;CDC25B;CDC27;DUSP1;FLNA;FNBP4;IER3;KHSRP;MYBL2;NUP153;NUP98;POLR2A;SF1;SON;SPEN;TSC1;WHSC2;ZFP36L1;SGK1;BTG2;MLL2*
TRIO	2.09E-02	Serine/threonine kinase	*FLNA;RAC1*
RPS6KA5	3.00E-02	Ribosomal kinase	*ATF1;CREBBP;EP300;ETV1*
MAPKAPK2	3.77E-02	FGF-MAPK	*CDC25B;ETV1;HNRNPA0;ZFP36L1*
PLK4	3.88E-02	Cell cycle	*FAM46C;SMAD4*
CAMK1	4.22E-02	Calcium/calmodulin kinase	*ATF1;EIF4G3;EP300*

The iFGFR4-based analysis in Table 5.12 also contains FGF-related kinases, such as the MAPK components RAF1, BRAF and STK24, the PI3K/AKT pathway kinases –AKT1, PIK3CA and BRSK1 as well as the PKC pathway kinase PRKCA. Cell cycle-related kinases feature numerous times, showing again that iFGFR4 is important for regulating the cell cycle. There are also two nodes involved in AMPK signalling.

Table 5.12. Kinase enrichment for iFGFR4 upregulated genes

Node Name	P-Value	Associations	Intersecting Genes
RAF1	3.64E-04	FGF-MAPK	*CDC25A;CFLAR;GNG4;GRB10;HRAS;MRAS;PPP1CC;PPP2R2B;RAF1;RAP1A;PPP1R12A*
CDK1	1.93E-03	Cell cycle	*C13ORF15;CCNA1;CCNB1;CCNB2;CDC16;CDC20;CDC25A;CEP55;CRKL;DUSP1;DYNC1LI1;GADD45G;GOLGA2;GRB10;HOMEZ;NASP;NDE1;RPA2;STMN1;TLE1;TMPO;WEE1;ACLY;APPL1;BRCA2;CARHSP1;DNMT1;KIF2C;MCM3;ORC1;PDIA3;PKN2;POC5;UNG*
MST4	4.01E-03	Serine/Threonine kinase	*GOLGA2;RAF1;PDCD10*
EPHB6	8.87E-03	Wnt-Ephrin receptor B6	*CBL;CRKL;SAT1*
BRAF	9.71E-03	FGF-MAPK	*HRAS;MRAS;RAF1;RAP1A*
PRKAA1	1.99E-02	AMPK	*RAF1;CSNK1E;CRY1;PFKFB3;PPP1R3C*
TBK1	2.50E-02	NFκB	*ATP5A1;AZI2;GAPDH;HSPA5;LDHB;TUBA3C*
PLK1	2.22E-02	Cell cycle	*BRCA2;CCNB1;CEP55;MCM3;TUBG1;WEE1;CDC16;CDC6*
AKT1	2.37E-02	FGF- AKT	*APPL1;CHUK;GRB10;PKN2;RAF1;TNFSF11;UXS1;CARHSP1;CFLAR;DNMT1;PFKFB3;PIKFYVE;RNF11;WEE1;ZFP36L1;ACLY*
STK25	1.61E-02	Neuronal migration	*GOLGA2;PDCD10*
PRKCI	2.17E-02	FGF-PKC	*CHUK;FRS3;GAPDH;HRAS;MARK4*
BUB1B	1.91E-02	Cell cycle	*BRCA2;CDC16;CDC20*
NUAK1	3.08E-02	AMPK	*HSPA5;MARK4;NUAK2;PPP1R12A*
STK24	2.87E-02	FGF-MAPK	*PDCD10;STK24*
BRSK1	3.61E-02	FGF-PI3K	*WEE1;TUBG1*
PIK3CA	3.81E-02	FGF-PI3K	*APPL1;HRAS;MRAS*
DAPK1	4.76E-02	Cell cycle	*DAPK1;BECN1;MCM3*

Among the two upregulated genelists, within the cell cycle related kinases, spindle and centriole-related kinases Nek6, Bub1B, Plkk are listed, giving a greater insight into FGF's role in the cell cycle function asides from the phosphorylation and regulation of cyclin related proteins.

5.2.9 RNA seq validation by RT-qPCR

Some of the findings of the RNA-seq data were validated by other means in order to assess how successful the experiment was in identifying genuine FGF targets. Several genes from across the dataset were picked that had varied roles and fold changes, as well as some which were shown to be commonly or differentially regulated between the two receptors. RT-qPCR was chosen as a way to validate the findings of RNA-seq. Primers against the genes chosen were optimised, and then three biological replicates of relative expression RT-qPCR performed using neuralised explants treated the same way as for RNA-seq. The results are shown in Figure 5.8.

Figure 5.8 A and A' show genes predicted to be upregulated by iFGFR1. *FoxA4* is extremely positively upregulated by iFGFR1 induction and so is represented on different y-axis to the other iFGFR1 upregulated genes, and this is highly significant. *Atp6V0c*, *Lmbrd22* and *Zfp36l1* are also upregulated as predicted by RNA-seq, although not to the same magnitude. Only *Zfp36l1* is significantly upregulated. Figure 5.8B shows genes predicted by RNA-seq to be downregulated by iFGFR1. The histone component *H3f3a* was actually found by RT-qPCR to be significantly upregulated by iFGFR1, and the transcriptional coactivator *Med9* was also slightly upregulated, although this was not significant. These genes may be dynamically regulated by iFGFR1, or may not be FGF targets at all. *Krt12* however, is significantly downregulated, although to a lesser extent (-2.5x) than in the RNA seq experiment (-5.1x). *Ift172* and *Tuba1A* did not appear to change expression levels upon FGF signal induction by RT-qPCR.

Ccnb1, *Chmp1A*, *Cited2*, *Ift172*, *Lmbrd2*, *Oct60*, *Poc5* and *Snx10* were all listed as being upregulated by iFGFR4 by RNA-seq. All of these genes exhibited a small upregulation, but there was a high degree of inconsistency between replicates for *Ccnb11*, *Lmbrd2* and *Oct60* so the levels of these genes were not significantly altered. *Chmp1a*, *Cited2*, *Ift172*, *Poc5* and *Snx10* all showed small but significant increases in expression after iFGFR4 induction. Again, these increases were not as large as expected given the RNA-seq fold changes. Lastly, *Rax*, *Slc12a3*, *Tuba1a* and *Zeb2* were all listed as being negatively regulated by iFGFR4, and indeed *Rax*, *Slc12a3* and *Zeb2* indeed significantly downregulated. *Tuba1a* was slightly downregulated but this was not significant.

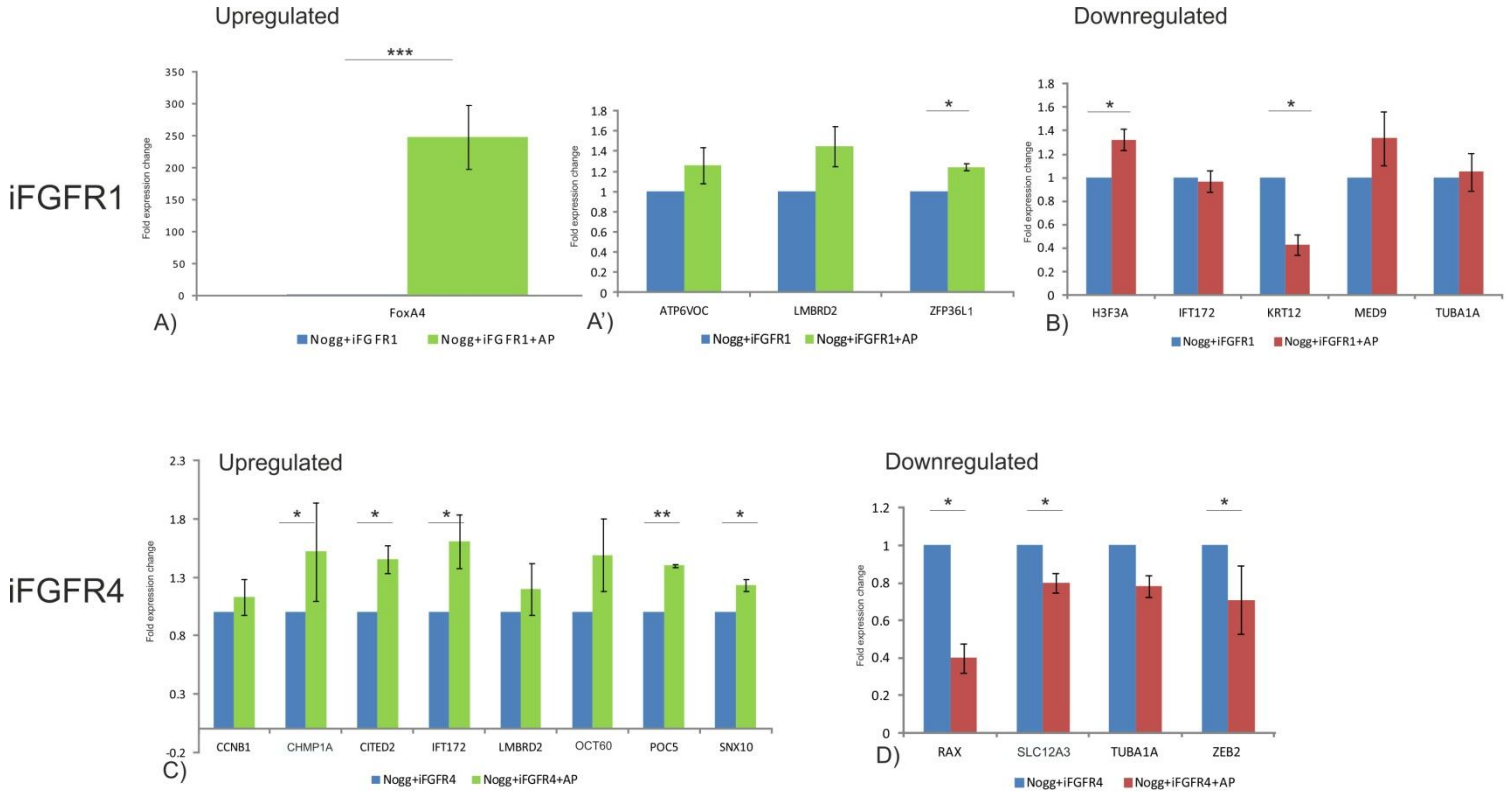

Figure 5.8. Validation of selected RNA-seq genes with RT-qPCR.
Embryos were injected with 20pg iFGFR1 or iFGFR4 as well as 50pg Noggin bilaterally into 2-cell stage *Xenopus laevis* embryos. iFGFRs were induced at 22°C for 3 hours from stage 10.5. Ct values were normalised against those of the housekeeping gene *ODC* and fold expression changes normalised against uninduced iFGFR1/4-injected embryos. Error bars represent SE from three biological replicates. Asterisks represent statistical significance of normalised Ct values below p=0.05 found by 2 sample T-tests. A) and A') show the expression change of genes predicted to be upregulated by iFGFR1. B) shows expression changes of genes predicted to be downregulated by iFGFR1. C) shows the expression change of genes expected to be upregulated by iFGFR4 and D) shows expression changes of genes predicted to be downregulated by iFGFR4.

Lmbrd2 and *Tuba1a* were upregulated or downregulated by both receptors respectively. *Lmbrd2* is slightly upregulated by both receptors although this is not significant. *Tuba1a* on the other hand was unchanged upon iFGFR1 induction and slightly, although not significantly, downregulated by iFGFR4. *Ift172* was chosen to validate in part as it was listed as differentially regulated by iFGFR1 and iFGFR4. These results show that although *Ift172* was significantly upregulated by iFGFR4, it was not downregulated by iFGFR1.

5.3 Discussion

5.3.1 Comparison of Methodology to other Recent *Xenopus* RNA-seq experiments

5.3.1.1 Use of *Xenopus laevis*

To date, most RNA-seq experiments performed with *Xenopus* have utilised *Xenopus tropicalis*. As *Xenopus tropicalis* are diploid as opposed to the polyploid *Xenopus laevis,* its genome has been available for longer making it simpler to perform transcriptomic studies. However, recently the *Xenopus laevis* genome was made available as well as numerous cDNA libraries, collected together by the Marcotte lab. *Xenopus laevis* embryos were used for this study as all experimental optimisation took place in *Xenopus laevis* and due to differences in *Xenopus tropicalis* embryo culture, the experiment was more practical to do routinely in *Xenopus laevis*.

However there are still challenges with the use of *Xenopus laevis*. Firstly, many *Xenopus laevis* genes exist in 'A' and 'B' forms which arose through genome duplication, Kwon. et al (2014), authors of one of the first RNA-seq papers using *Xenopus laevis,* found that only 23-31% of reads mapped to both duplicated genes. To assess the effects of how counting these genes affected final results, the authors counted only the 'a' form, and then only uniquely mapped reads– 68-75% of the data, and finally whichever was the 'best' target. No significant differences in the outcome of analyses was found, and so as comparing isoforms is not a priority for this experiment, it is unlikely to be a cause for concern (Kwon et al. 2014).

Another disadvantage of using *Xenopus laevis* is that there are still gaps in the genome annotation, which affected the choices made by the Technology Facility for choosing programs to analyse the raw RNA-seq data. Tools used to map transcript

sequences onto a reference genome can be categorised as ‘splice aware’ and ‘non splice aware’ mappers. Tophat is an example of a splice-aware mapper where reads are mapped to the reference genome, and any unmapped reads further fragmented and re-aligned to find novel splice sites, a program used by Chiu et al. (2014) and Fish et al. (2014) for their RNA-seq studies in *Xenopus tropicalis*. However because of the poor quality of the *laevis* genome annotation in some regions, a ‘non-splice aware’ called BWA-MEM was chosen, invented by Li & Durbin (2009). This program maps reads against a reference cDNA database – the *Xenopus laevis* Mayball longest cDNA collection in this case – quickly and efficiently as it uses a Burrows-Wheeler transform method taking relatively low computational time compared to similar programs (Li & Durbin 2009).The disadvantage for using this program is that any novel splice sites may not be detected. A very similar algorithm called Bowtie was recommended for use in *laevis* studies (Amin et al. 2014; Kwon et al. 2014) and has also been used for published *Tropicalis* RNA-seq experiments (M. H. Tan et al. 2013; Collart et al. 2014) and as the first priority of this RNA seq experiment is to find detect whole genes, this should not be a great disadvantage.

Other important considerations for RNA-seq experimental design are how reads are sequenced (single end vs. pair end sequencing) and how they are measured, the most common units being FPKM and RPKM – Fragments/Reads per Kilobase of transcript per Million mapped reads. The difference between RPKM and FPKM is subtle. Although in this study, only paired reads were included in mapping, both the reads in a pair might not necessarily be mapped if one is of poorer quality. FPKM counts one alignment per paired read, whereas RPKM counts individual mapped reads - therefore some transcripts could be counted twice and others counted once, skewing the data. In this study paired reads were measured. Although single end sequencing is much quicker to perform, paired end sequencing provides an element of quality control, as pairs should align a known distance apart. Also, by reading paired reads instead of single end reads more information about the fragments can be gathered such as splice variants and SNPs, their genomic positional information, as well as better 3’ end coverage which would be missed using single reads (Fang & Cui 2011). Paired end sequencing has also been used for all recent *Xenopus* RNA-seq papers listed on Xenbase apart from Chiu et al (2014).

The filtering thresholds used in this study are fairly stringent, but may be viewed as slightly arbitrary as some genes known to be affected by iFGFRs did not pass

thresholds, and *vice versa*. Statistical confidence values based upon replicates were used by Tan et al. (2013), Chiu et al. (2014), and Fish et al. (2014) in *Xenopus tropicalis* based RNA-seq and this was the basis of their filtering conditions instead of choosing fold changes. Kwon et al, used a similar 2-fold expression cut-off for their single experimental run of RNA-seq, and so there is a precedent for the methods used here in the literature (Kwon et al. 2014). Therefore, these decisions taken about how to perform and analyse the RNA-seq data are similar to other published methodologies in *Xenopus.*

5.3.1.2 Caveats to the experiment

The main caveat to this methodology was that unfortunately, due to limited time and resources, only one biological run of the RNA seq experiment was completed instead of the minimum of three needed for most statistical analyses. Therefore the data are more likely to contain false positives which could be eliminated with the use of programs such as Cuffdiff that eliminate non-statistically relevant reads.

It was originally planned to perform a pilot RNA experiment to compare the effects of iFGFR1 induction in whole embryos, neuralised animal caps and whole embryos where iFGFR1 had been targeted to the prospective CNS. The methodology returning the most neural targets and most closely matching the fold changes for genes found in the microarray and by RT-qPCR such as *Egr1, Sprouty2* and *Lefty* and other highly regulated genes like *FoxA4* would be used for two more biological repeats using the other iFGFRs. This experiment was performed with the in-house Ion Torrent PGM sequencer. Unfortunately, due to the high level of multiplexing only ~750000 reads were obtained per experimental condition. In comparison, of the *Xenopus* RNA-seq experiments detailed above which reported their read counts, obtained 20-70 million reads per condition (M. H. Tan et al. 2013; Collart et al. 2014). Therefore, genes such as *Egr1*, reproducibly found upregulated by RT-qPCR in whole embryos and animal caps, was not found affected by iFGFR induction in any condition and had very low read counts (<1 FPKM). There were also technical issues, possibly stemming from the use of the wrong adaptors during library preparation meaning only 30% of total transcripts read were mapped. Therefore data from this experiment was not used.

Due to constraints upon time and resources following this, it was decided to outsource samples from a single experiment on an Illumina Hiseq machine to maximise sequencing depth – Illumina RNA-seq has been reported to produce

between 50-200 million reads per lane (Li & Durbin 2009). It was advised that use of the Hi-seq would yield a far higher read count per condition - approximately 45 million reads if multiplexing four samples. As it turned out, a far higher read count/condition was achieved - approximately 75 million reads. It would therefore have been possible to multiplex more biological repeats on the same run.

Biological replicates of the dataset could enable relaxation of the cut-off thresholds applied here which eliminated genes such as *Egr1* and *Nek6* significantly upregulated by iFGFR1 by RT-qPCR and the preliminary microarray. And as can be seen from the validation results by RT-qPCR, there are some genes in the dataset that could not be replicated, and may have been eliminated from the data upon replication. This indicates some noise in the data and underlines the importance of careful validation of the dataset.

5.3.2 Comparison to other datasets looking at FGF-mediated effects upon gene expression in *Xenopus*

5.3.2.1 Yamigishi and Okamoto, 2010

iFGFR1 and iFGFR4 have been used and compared functionally before in *Xenopus* by Yamigishi and colleagues, and their conclusions were that the two wild-type receptors compete for ligands in order to regulate neural development. This was based upon the finding that overexpression of FGFR1 mRNA in *Xenopus* embryos shifted the MHB marker *Pax2* anteriorly*;* whereas FGFR4 mRNA caused a posterior shift similar to when FGF signalling is inhibited, suggesting that when FGFR4 is more prevalent, it is more likely to bind to FGF ligands, and the embryo is anteriorised due to its 'weaker' signalling properties. However, using ligand-independent over-activation of FGF signalling using iFGFR1 and iFGFR4 caused an anterior *Pax2* shift for both receptors. The authors concluded that the elimination of ligands excluded the possibility that differences in downstream signalling caused a differential effect in *Pax2* positioning. Therefore one would expect iFGFR4 to affect the gene expression in the same way as iFGFR1, but to a lesser extent. However, the 'anterior' shift for iFGFR4 was only observed in ~10% of embryos, with ~80% of embryos with unchanged *Pax6* positioning. Therefore, maybe iFGFR4 does not regulate *Pax2*, rather than ligand binding being responsible for all shifting effects. Ligand binding must have some influence upon *Pax2* though, as although iFGFR1 induction and FGFR1 mRNA produced the same proportions of embryos with anteriorised *Pax2*, the same cannot be said when comparing iFGFR4 induction and FGFR4 mRNA. FGFR4 mRNA caused 60% of embryos to exhibit a posterior shift

in *Pax2* expression whereas the majority of iFGFR4 had normal *Pax2* expression. This could be inducible vs. non-inducible effects, but could potentially point to a shortcoming of iFGFRs in being a ligand-independent system (Yamagishi & Okamoto 2010).

5.3.2.2 iFGFR Microarray

Finally, the microarray dataset using iFGFR1 and iFGFR4 discussed in the first experimental chapter was compared with this dataset. This dataset as mentioned previously is in the context of whole embryos over a greater period of time and so is not strictly looking at proximal neural targets. However 35 genes found in the microarray were also found more than 2-fold affected by iFGFR1 or iFGFR4 in this dataset, lending more support for these genes being FGF targets. In addition there are other genes from the same families if not the exact same gene found in both datasets– for example other *Dusps*, *Wnts*, *Hes*, and *Fox* genes.

5.3.2.3 Branney et al, 2009 and Chung et al 2004

These datasets have been described in more detail in the results section. In contrast to the findings of this study, only 5 genes in the Branney dataset exhibited a greater than 2-fold difference in expression change between each receptor. Therefore at this developmental stage, no real differences in signalling output between dnFGFR1 and dnFGFR4 were observed. However, this may be due to the lack of specificity of the dnFGFRs (Ueno et al. 1992). The differences between the RNA-seq findings and Branney et al could suggest that the regulation of FGF signalling targets may change at different stages of development, although further validation would be needed to make this assertion.

Only four genes, after conversion into modern gene symbols, were found in common with the RNA-seq dataset – *Arl5, FoxB1, Dusp1* and *Zfp36l1* – and 5 in common with the iFGFR1/4 microarray – *Arl5, Mst1, Gdf3, Cdx4* and *Gata4.* This is partly due to the ambiguous nature of the genes identified as FGF targets and their Ensembl tags being retired on Unigene. However, the genes in common with RNA-seq and the microarray-based screen suggests that these genes are important for FGF signalling during development in general rather than in a solely neural context.

These comparisons with other datasets show that as well as novel putative FGF targets, the RNA-seq experiment has replicated some of the findings made by other

research groups, which lends weight to these overlapping genes being FGF targets in a neural context .

5.3.3 Themes in the RNA seq data

The extensive literature search found many genes that were already found to be linked to FGF signalling. Examples of commonalities between genes that were interesting are discussed below. They show that as well as neural induction and patterning, FGF signalling is also important for other developmental processes at this time of early neural specification.

5.3.3.1 The Cell Cycle

Ontological analyses and literature searches showed cell cycle-related genes to be present in both iFGFR1 and iFGFR4 genelists and highly significantly enriched. FGF signalling is well known for its roles in the cell cycle and pluripotency – FGFs were named after their mitogenic properties, and FGF signalling favours cell proliferation over differentiation.

A nuclear form of FGFR1, nFGFR1, has been implicated in this process, derived from newly translated FGFR1 released from the pre-golgi membrane and translocated into the nucleus (Terranova et al. 2015). Translocation of FGFR1 through the nuclear membrane and accumulation was first shown *in vivo* in the rat brain and shown to be dependent on the transporter importin-B (Stachowiak et al. 1996; Stachowiak et al. 2003). Within the nucleus nFGFR1 binds to genes on several different chromosomes and so is a general transcriptional regulator and stimulates multiple signalling pathways involved in cell growth and differentiation (Stachowiak et al. 2003). nFGFR1 was later shown to be important for glial growth, dendritic outgrowth in rat neurons and differentiation of neuronal progenitors (reviewed in Stachowiak et al. 2007). This is in contrast to the 'anti-differentiation' role of canonical FGFRs. This may be important to this project as nFGFR1 has been shown to directly target many genes during development, including those involved in neural development. nFGFR1 binds to promoters of pluripotency genes such as *Oct4*, *Klf4* and *Myc*, as well as sites identified as consensus sequences for these pluripotency factors themselves (Terranova et al. 2015). *Oct4* is negatively regulated by the nuclear hormone receptor *Nr6a1*, found in this screen as being downregulated by iFGFR4 (Barreto et al. 2003). As iFGFRs are not transported to the nucleus, the use of these will not provide information about genes affected by FGF signalling in the nucleus. This is important to consider when extrapolating the

effect upon the transcriptome of iFGFR induction to wild-type FGF signalling behaviour, as iFGFRs may not represent the full potential of FGFR signalling events.

Links between FGF signalling and the cell cycle itself have been reported. The degradation of the cyclin dependent kinase Cdkn1b in late G1 phase of the cell cycle activates CDK2-cyclinE and Cdk20-cyclinA complexes that signal cells to enter S phase (Ganoth et al. 2001). Cks1 mediates this degradation of Cdkn1b. In 3T3 cells, FRS2 binds and sequesters Cks1 until FRS2 is phosphorylated by FGFR1, releasing Cks1. Cks1 is then free to bind to the Cdkn1b/Cyclin/Cdk complex and target it for ubiquitin-mediation degradation. This is therefore a way FGF stimulates cell proliferation (Zhang et al. 2004). Another method involves phosphorylation of CyclinB (Ccnb1) by ERK. Entry into mitosis is regulated by the activation of the CyclinB/Cdc2 complexes, the formation of which is catalysed in part by the enzyme Wee1. This is accompanied by a translocation of the complex into the nucleus. Walsh et al, (2003) showed that in *Xenopus* oocytes and egg extracts, the translocation of CyclinB into the nucleus is caused by its phosphorylation by ERK (Walsh et al. 2003). *Cyclin B* (*Ccnb1*) and *Wee1* were found upregulated by iFGFR4 in this screen, however *Wee1* was upregulated 1.8-fold and so did not pass the filtering conditions. In addition, another cyclin, *Ccnd1,* also required for the G1/S transition and upregulated by exposure to FGF2 in murine mesenchymal stem cells which caused inhibition of differentiation, was downregulated by iFGFR4 (Lai et al. 2011). *Cdc6*, part of the pre-replicative complex formed in G1, is essential for the proper initiation of chromosomal replication in the S phase (Kim et al. 2015). It has been reported to be repressed by FGFs in chondrocytes, however in this RNA-seq screen it was upregulated by iFGFR4 (Kolupaeva & Basilico 2012).

Therefore, as iFGFR4 stands out as affecting the majority of the genes mentioned here, it may have a larger role in the cell cycle than the other receptors. Validation by RT-qPCR of more cell cycle genes, as well as use of the other iFGFRs would be useful for investigating this further.

5.3.3.2 Cilia and Left/Right asymmetry related genes

FGF signalling, as discussed in previous chapters, is required for both ciliogenesis and regulation of the nodal cascade, which underpins left/right asymmetry. Of the genes subjected to an in-depth literature search, 11 were found that have published connections to ciliogenesis or left/right asymmetry – two processes which are

closely connected. These include *Lefty, Vangl2, Cited2, Atp6V0C, Ift172*, *Snx10, Dynll1, Mark4, Fopnl, Nde1* and *Ruvbl2*. Targeted deletion of *Ift172* in mouse embryos die prior to birth with neural tube defects, telencephalic truncations and holoprosencephaly, as well as randomization of left/right asymmetry. Mutant embryos possessed cilia with very truncated axonemes that containing no visible microtubules (Gorivodsky et al. 2009). *Ruvbl2* is essential for cilia motility in zebrafish, and mutant embryos contained axonemes with fewer dynein arms. Although this caused ciliary disorganisation and loss of function in ciliated kidney cells, this was not linked to laterality defects (Zhao et al. 2013). RPE-1 cells transfected with siRNA against *Fopnl* or *Mark4* failed to undergo ciliogenesis (Kuhns et al. 2013; Lee & Stearns 2013). In contrast, zebrafish embryos injected with a morpholino against *Nde1* contained longer cilia compared to controls, but as cell division was inhibited in the KV, embryos still exhibited laterality defects (Kim et al. 2011). Injection of a translation blocking morpholino against *Snx10* into zebrafish embryos caused a loss of cilia and laterality defects, and mechanistically interacts with V-ATPases, of which *Atp6V0C,* the proton pump subunit of H+-V-ATPase, is an example (Chen et al. 2012). *Atp6V0C* is also implicated in laterality in its own right, as it is asymmetrically located in the ventral right blastomere at the 4-cell stage, localised to Rab11 (Vandenberg et al. 2013). Expression of a dominant negative Rab11, or pharmacological inhibition of Atp6V0C both cause consistent heterotaxia in *Xenopus* embryos (Vandenberg et al. 2013; Adams et al. 2006). *Xenopus Vangl2* has also been linked to left/right asymmetry as 60% of morphants develop laterality defects (Vandenberg et al. 2013). This is thought to be due to Vangl2's role as part of the planar cell polarity pathway, as it is responsible for the polarity of cilia in the KV of zebrafish (May-Simera et al. 2010). *Cited2*-null mouse embryos die before birth and have a range of heart defects, including abnormal heart looping and left atrial isomerism. As *Nodal, Lefty and Pitx2* were not expressed in the lateral mesoderm in null mutants, this suggested that an aspect of *Cited2* activity was required for correct left right patterning (Weninger et al. 2005; Bamforth et al. 2004).

7 of the 11 genes found were upregulated upon iFGFR4 induction (*Cited2, Snx10, Vangl2, Mark4, Fopnl, Nde* and *Ift172)* suggesting that FGFR4 has an important role in regulating this process as well as FGFR1. iFGFR1 induction upregulated 4 (*Dynll1, Lefty, Atp6V0c) and* downregulated *Ift172* and *Ruvbl2*. Thus *Ift172* was differentially regulated between the two receptors, although validation of *Ift172* by RT-qPCR could not reproduce this downregulation by iFGFR1. FGF is already

known to be required for correct ciliogenesis, but a common view in the literature is that this is due to its positive influence on Wnt signalling, as Wnts regulated the expression of the early ciliogenesis gene *FoxJ1* in zebrafish (Caron et al. 2012). The findings of so many of these genes in this RNA-seq data suggest that proximal putative FGF targets are directly involved in ciliogenesis and left/right patterning.

5.3.3.3 Eye development

A number of genes in the dataset were found to be required for eye development. iFGFR4 was listed as downregulating *Gnb3*, expressed in photoreceptors and involved in eye development, as well as the eyefield marker Rax and its interactant *Crx*, also active in cone cells and implicated in eye development (Ritchey et al. 2010; Giudetti et al. 2014; Vignali et al. 2000). FGFs and FGFRs are known to be expressed in the developing *Xenopus* eye and are required for initiation of the eye developmental program, but not for its maintenance (Atkinson-Leadbeater et al. 2009; Lea et al. 2009). Cross sections of *Xenopus laevis* embryos by Lea et al., (2009) showed that only FGFR3 was strongly expressed in the lens. FGFR1 and 4 expression was concentrated around the lens and FGFR2 only seemed to be expressed in cells on the periphery of the eye. This suggested that the eye requires different combinations of FGFR to develop (Lea et al. 2009).

Transient inhibition of FGF signalling in *Xenopus* by adding the FGFR inhibitor SU5402 at early but not late neural specification stages disrupted the dorso-ventral axis of the developing retina, and caused changes in retinal gene expression (Lupo et al. 2005; Atkinson-Leadbeater et al. 2009). Furthermore, the FGFR effector FRS3 – found upregulated by iFGFR4 in this screen – was found to be expressed in the anterior CNS and eye, with morphants having defects in lens placode formation. Although this could be rescued by wild-type *Frs3*, a mutant *Frs3* lacking the FGFR phosphatase SHP2-binding tyrosine residues could not rescue the morphant phenotype, further implicating FGF signalling pathways as being necessary for correct eye development (Kim et al. 2015). *Pou4F2*, found by this RNA-seq to be upregulated by iFGFR1, is known to be involved in retinal ganglion differentiation (Li et al. 2014). Also upregulated by iFGFR1, *Hes1* has been previously found to push retinal progenitor cells into a Müller glial fate at the expense of neural fate in *Xenopus*, and with *Rax* and *Notch1* promotes Müller gliogenesis in retinal progenitor cells at the expense of neural (Furukawa et al. 2000). Finally *Xenopus Hes2*, found upregulated by iFGFR4 in this screen, is expressed in the retina and other sensory organ progenitor cells. When overexpressed it also causes an upregulation of glial

cells again by the repression of proneural genes including *NeuroD* (Sölter et al. 2006). This suggests therefore that FGFR4 and 1 can act to repress neural genes in order to activate eye development.

5.3.3.4 Anterior CNS

The Nieukwoop activation-transformation model of neural induction postulates that firstly anterior neural tissue is specified, and then caudalising FGF and Wnt signals cause posteriorisation of neural fates (Pownall & Isaacs 2010). FGF is well known in the literature for its role in posterior neural development and patterning because of its role in activating *Cdx* and *Hox* genes. FGFs also have an antagonistic relationship with anterior BMP, and RA pathway genes which promote anterior fates. However, FGF is present in the MHB and the anterior ectodermal border, and is required for telencephalon development and as a morphogen in the Isthmic Organiser (reviewed in Pownall & Isaacs 2010). Reflecting this, a number of putative FGF targets found in this screen are expressed in the anterior CNS and have been previously shown to be required for correct telencephalon and diencephalon development.

The forebrain is specified after Wnt antagonists secreted from the anterior of the developing *Xenopus* embryo caudalise the anterior neural ectoderm (Niehrs & Feld 1999). This anterior decrease in Wnt signalling causes activation of rostral forebrain markers *FoxG1* and *Emx1*. The posterior forebrain marker *Otx2,* found in this screen to be downregulated after iFGFR4 induction, and *Pax6* are thereby repressed in this region, to favour rostral telencephalon development.

Hesx1, also known as *Xanf,* activated by the Wnt antagonist Dkk and found by this microarray and RNA-seq based screen to be negatively regulated by both iFGFR1 and iFGFR4, is a transcription factor expressed in the prospective forebrain from late gastrula stages (Matsuda & Kondoh 2014). Overexpression of *Hesx1* in *Xenopus* expanded the neural plate as shown by ISH for the pan-neural marker NCAM, but suppressed the differentiation of primary neurons (Ermakova et al. 1999). Furthermore, ectopic *Hesx1* caused anteriorisation of the forebrain, as the expression domain of the rostral telencephalic marker *FoxG1* expanded into the diencephalon. The posterior forebrain markers *Otx2* and *Pax6* were repressed, leading to the conclusion that the function of *Hesx1* is to repress posterior forebrain fates and encourage rostral identities (Ermakova et al. 1999). This is supported by later work showing knockdown of *Hesx1* in *Xenopus* using a morpholino caused an

expansion of *Otx2* and *Pax6* anteriorly, as well as ectopic differentiation of retinal pigment in the diencephalon normally only fund in posterior forebrain. Furthermore, expression of *FGF8* in the ANB and *FoxG1* were diminished (Ermakova et al. 2007).

The confinement of *Hesx1* expression to the forebrain was shown to be important by Martynova et al. (2004), who identified a 14bp region in its promoter which when deleted, caused posterior expansion of the *Hesx1* expression domain (Martynova et al. 2004). A yeast one hybrid screen using the region as bait identified *FoxA4* - found in this screen potently upregulated by iFGFR1 - as being responsible with *XVent2* for delineating the posterior limits of *Hesx1*. Therefore, as well as being important for development of the antero-posterior axis and notochord, an early burst of *FoxA4* expression in the organiser region is directly involved in restricting anterior neural development (Murgan et al. 2014). Therefore FGFR1 and 4 signalling has a repressive influence on *Hesx1* expression from the posterior directly shown by these RNA-seq results, and indirectly through iFGFR1's activation of *FoxA4*.

Hesx1 also represses the Ras family member *Ras-Dva* found in the iFGFR microarray discussed in Chapter 3 to be downregulated by iFGFR1 in whole embryos. In the RNA-seq data *Ras-dva* was found to be upregulated 1.8-fold by iFGFR1, (thus not meeting filtering thresholds) but RT-qPCR gave conflicting results (data not shown). *Xenopus* embryos injected with a morpholino against *Ras-Dva* exhibited defects in head development including reduction of forebrain, inhibition of *FoxG1* and *Otx2,* and disruption of *FGF8* expression (Tereshina et al. 2006). Later work by the same group revealed that *Ras-Dva* expression is restricted to non-neural cells in cement and hatching glands, so this may explain why neuralised explants gave conflicting results. *FGF8* secreted by neighbouring cells in this region activated *Ras-Dva*, which in turn induced expression of *Otx2*. *Otx2* was found to then activate Agr-secreted factors including *Agr2*, which was found by this data as being downregulated by iFGFR4 (Tereshina et al. 2014).

Therefore a positive feedback loop involving *FGF8*, *Ras-Dva*, *Otx2* and *Agr2* – which positively affects FGF8 – are found as putative neural FGF targets in the RNA-seq data, with a negative input from *Hesx1.* According to this data, both iFGFR1 and 4 regulate these genes, showing that signalling by both receptors is required for this process.

5.3.4 Gene Ontology analyses identify further themes in the RNA-seq data

The ontological analyses, taken with the patterns that emerged from the dataset discussed above suggest that in some instances, although different genes are activated by each receptor, they often feed into the same processes. For example, GO terms associated with metabolic processes are significantly enriched in all four genelists, as are cell cycle components, particularly with iFGFR4.

Other developmental processes are differentially regulated by iFGFR1 and iFGFR4 during neural development based upon these analyses. PANTHER protein analysis suggested that transcription factors are differentially affected by each receptor. FGFR1 induction positively affected transcription factors, and several classes were found enriched in the upregulated genelist and conversely depleted in genes downregulated by iFGFR1. Genes upregulated by iFGFR4 however were less likely than predicted to be transcription factors. This gives an insight into the 'division of labour' between the receptors.

Another point of receptor output difference were terms pertaining to developmental processes, which were conspicuously enriched in iFGFR1 upregulated/iFGFR4 downregulated genelists and depleted in iFGFR4 upregulated /iFGFR1 downregulated genelists. It is not surprising that heart and skeletal developmental processes are depleted at this stage; however the neurogenesis, ectodermal and mesodermal-related terms which are differentially enriched between the two receptors may be more biologically relevant. Further validation and testing of the genes picked out as being implicated in these processes would be required to confirm this.

Although the PANTHER pathway analysis did not yield as many significant results, the iFGFR1-upregulated genelist was enriched with components from the Notch, Wnt and FGF signalling pathways in line with current knowledge about FGF:Wnt and FGF:Notch pathway interactions (McGrew et al. 1997; Pera et al. 2014; Faux et al. 2001; Akai et al. 2005). Other signalling pathways did not prominently feature in iFGFR4 genelists and so iFGFR4 may not be as involved as iFGFR1 in crosstalk with other pathways. The kinase enrichment analysis provided more information and leant support for FGFR4 signalling down other branches of the FGF signalling pathways involved in Akt and PKC as found in (Umbhauer et al. 2000).

These results and conclusions must be interpreted with caution however, as the dataset filtering thresholds had to be relaxed in order to provide enough numbers for PANTHER to conduct analyses. This inevitably incorporated noise into the data which could obfuscate the outputs. Further RNA-seq biological repeats would help eliminate some of the noise in the data, which would then enable the inclusion thresholds of the RNA to be relaxed, thereby hopefully giving more solid conclusions.

5.3.5 Validation by RT-qPCR does not completely reproduce RNA-seq data

Validation was performed using 17 different genes picked across the dataset. The aim of this was to assess how likely any given gene picked could be independently identified as an FGF signalling target, or if for example, genes below 3-fold were not predictably regulated, the filtering thresholds could be adjusted accordingly to increase the probability that the dataset represented true FGF targets.

The genes assayed were generally up or downregulated predictably based on the dataset but, with the exception of *FoxA4,* none were regulated to the same extent, and only roughly half of these were significant. There was also no real correlation between genes significantly regulated by RT-qPCR and their fold change; *Zeb2* for example was just significantly regulated by iFGFR4 in RT-qPCR experiments, but the most downregulated gene of iFGFR4 found by RNA-seq (-18.1x). However other genes like *Poc5* were more highly significantly affected by RT-qPCR but only upregulated 2.1 fold by iFGFR1 in RNA-seq. Therefore adjustment of the RNA-seq filtering threshold is unlikely to definitively eliminate false positive/negative FGF targets.

There was a high degree of variation between experimental repeats. Although all clutches of *Xenopus* embryos were cultured under the same conditions, their speeds of development varied. Although good consistency of induction times from stage 10.5 was aimed for and embryos kept in the same incubator at 22°C, the onset of stage 10.5 is subjective and even small temperature fluctuations change the rate of embryo development. Secondly some of these genes are likely to be highly dynamically regulated. Cell cycle genes such as *Ccnb1* and transcriptional/translational components such as *H3f3a* and *Med9* are likely to be very dynamically regulated, and RNA-seq findings determined by the stage of the

cell cycle in which cells happen to be. This was borne out by their very different expression fold changes between biological replicates found by RT-qPCR.

In addition to RT-qPCR, *in situ* hybridisation could be employed alongside RT-qPCR to see if gene expression domains are changed as a result of iFGFR1/4 induction. Furthermore, in addition to injecting iFGFRs, dnFGFR1 could be expressed in sibling embryos to see if complementary effects upon gene expression occur, which would improve the argument for them being FGF signalling targets. A number of groups such as Collart et al,. (2014) who investigated the *Xenopus tropicalis* transcriptome during MBT, employed Nanostring technology to validate their data, which can digitally investigate the relative expression of up to 800 genes at once (Collart et al. 2014). With this dataset, validating a larger set of genes would provide a better insight into how reproducibly this data is.

5.3.6 Further work and conclusions

It would be interesting to compare and contrast all iFGFRs in the future, particularly the VT+ and VT- isoforms of iFGFR1 to give a more global insight into the roles of each iFGFR in neural development. Also, comparing the transcriptome after early and late periods of FGF induction would be useful to see how FGFs role in neural development changes over time.

In the RNA-seq genelists there is information that has not been analysed in this study, including the many 'Unknown' hits, and information relating to the 'A' and 'B' forms of each gene, as well as any non-coding mRNAs that may have been sequenced. Further analysis of A and B forms of each gene, which will be more feasible when the *laevis* genome improves, would be interesting to gain insight into gene evolution and function, but is outside the scope of this project. The 'B' form of *Hes2* in *Xenopus laevis* for example, is present at a much higher level in the neural plate than the 'A' form, and the 'A' form is a maternal factor whereas the zygotic 'B' form becomes predominant after MBT, the significance of which is unclear (Murato et al. 2007). In order to analyse the 'unknown' files, the original sequence would have to be found. This proved difficult as the sequence data contributing to the Mayball longest cDNA library is no longer available, and the Mayball search engine only recognises the gene name, and not the read name attached to each gene. Due to time constraints, this was not looked into further although could yield interesting results if investigated at a later date. As there was a high level of sequencing depth in this study, it is possible that miRNAs and ncRNAs are present

in this data. To affirm this would require more in-depth data processing and re-alignment of the sequencing data, and may not yield optimal results as the fragmentation and library preparation protocols were optimised for longer fragments of RNA. The protocol for finding smaller RNAs selects RNA fragments of only ~24 bp and makes libraries of these, which would exclude the longer fragments which were used for library preparation in this study (Harding et al. 2014; Hafner et al. 2008). Nevertheless, it could be possible to see if miRNAs are present in their mature form in the sequenced fragments by aligning them to the *Xenopus tropicalis* collection of known miRNAs on miRBase (www.mirbase.org) to see if there are any miRNAs or other short RNAs present before proceeding further. Lastly, there may be different splice variants of genes present in the data, particularly those that feature in the genelists more than once. A disadvantage of using a non splice-aware read mapper during sequence alignment means that no novel splice junctions will be found, but further investigation into this could give an insight into how FGF signalling might regulate splicing during neural development, and what functional implications this has.

5.3.7 Summary

To my knowledge, an in-depth comparison between different FGF receptor signalling outputs has not been reported before in *Xenopus* to study specifically neural development. The RNA-seq data show that the *Xenopus laevis* transcriptome was strongly affected by induction of iFGFR1 and iFGFR4 during early neural specification stages. The literature search undertaken and the overlap of these findings with other datasets and previous RT-qPCR experiments show that these data are in keeping with previously reported roles of FGF signalling during neural development. Genes involved in related developmental processes such as Left/right asymmetry, anterior neural patterning and eye development are also represented in the dataset, as are putative FGF targets that have not been investigated in any capacity yet. Very few genes were commonly regulated by both receptors, showing that iFGFR1 and iFGFR4 have very different signalling outputs. However, searches in the literature and ontological analyses showed that there are similarities as well as differences between the processes and signalling pathways modulated by each receptor. This suggests a level of cooperation as well as possibly competition between FGFRs in regulating development. The aims of the chapter have been met, although further biological repeats of the RNA-seq would probably improve the confidence of picking FGF targets and downstream analyses.

6 Characterisation of novel FGF targets

6.1 Introduction

6.1.1 Inhibition and characterisation of FGF targets

After analysis and validation of the RNA-seq and microarray datasets, it was decided to investigate a number of potentially interesting novel FGF targets in more detail. ISH was used in some instances to ascertain the expression patterns of these during *Xenopus* development. To gain an insight into FGF target gene function, it was decided to make use of recently introduced gene editing technology to assess the effects of gene knockout upon *Xenopus* development. *Nek6* was investigated through knockout by employing a TALEN. Additionally, the effects of knockout of three putative neural FGF targets found in the RNA-seq dataset– *ZSwim4*, *Snx10* and *Cited2* – were investigated by using the CRISPR/Cas9 system.

6.1.1.1 TALE nucleases - TALENs

TALE nucleases (TALENs) are, like CRISPRs, very recent technologies that make custom knockdowns of genes much simpler and cheaper than morpholinos. TALEs are naturally occurring zinc finger proteins derived from the plant pathogenic bacteria *Xanthomonas.* TALEs contain DNA-binding regions composed of a series of 33-35 amino acid tandem repeat domains that each recognise a single base pair. Each tandem repeat is identical apart from repeat-variable di-residues - RVDs – at positions 12 and 13, which recognise each base (Lei et al. 2012; Gaj et al. 2013). TALE repeats can be recombined to bind a user-defined DNA sequence of interest (Schmid-Burgk et al. 2013). Custom TALEs fused to endonucleases, (TALENs), bind to target sequences and produce double stranded breaks (DSBs) (Miller et al. 2011). These DSBs are improperly repaired through non-homologous end joining (NHEJ), leading to small inserts or deletions (indels) in the DNA sequence. These cause frameshift mutations in the translated protein (Santiago et al. 2008; Ishibashi et al. 2012).

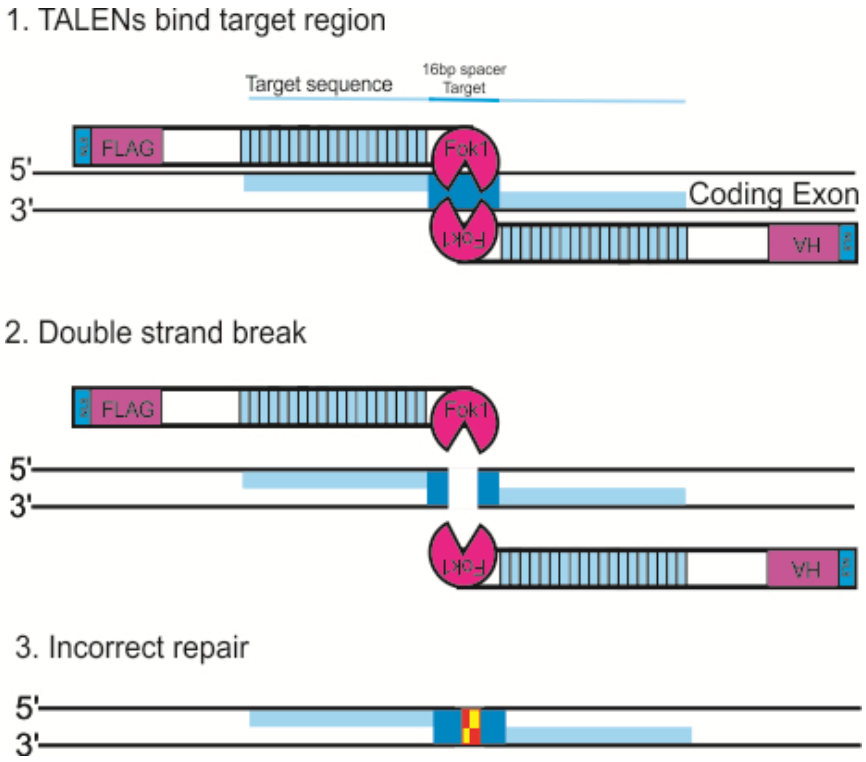

Figure 6.1. TALEN method of action illustrating how they work
Left and Right TALEN mRNAs are injected into *Xenopus* embryos, and when translated bind to the forward and reverse strands either side of the genomic target region, typically within the first coding exons. Both TALENs contain epitope tags and also nuclear localisation signals (NLS). When both bound, the Fok1 nucleases make a double stranded break (DSB) which is improperly repaired. This introduces indels into the sequence, causing frameshift mutations and non-functioning proteins.

Figure 6.1 is a schematic diagram of how TALENs were used in this study. mRNA coding for a 'Left' and 'Right' TALEN were injected into *Xenopus* embryos. Each TALEN half contains a nuclear localisation signal (NLS) and an epitope tag, which in this case was Flag (left) and HA (right). When translated the left and right TALENs bind to the genomic DNA around a target site in the first exon of *Nek6,* with a spacer region of 16bp between them. This region is cleaved by the endonuclease Fok1, fused to the TALE region.

6.1.1.2 CRISPR/ Cas9 genome editing

The (Clustered Regularly Interspaced Short Palindromic Repeats) CRISPR/Cas9 genome editing system has recently increased in popularity due to the relative speed and ease of making targeted gene alterations. In bacteria, the CRISPR system provides immunity against invading foreign DNA by the activation of endonuclease Cas9-directed cleavage (reviewed in Gaj et al. (2013). This can be exploited by designing a guide RNA that is complementary to a portion of a coding exon within a gene of interest. A sequence in preferably the first coding exon is

chosen that starts with a G - to bind T7 polymerase and initiate transcription- and after 19 bases ends with the PAM sequence, NGG, required for Cas9-mediated cleavage. The guide RNA is attached to a 'seed' sequence to which the endonuclease Cas9 binds (Bassett et al. 2013). As with TALENs, this break is repaired by NHEJs, leading to indels. Figure 6.2 shows a schematic diagram of how CRISPRs were designed in this study, following the PCR method of template synthesis by Nakayama et al. (2013).

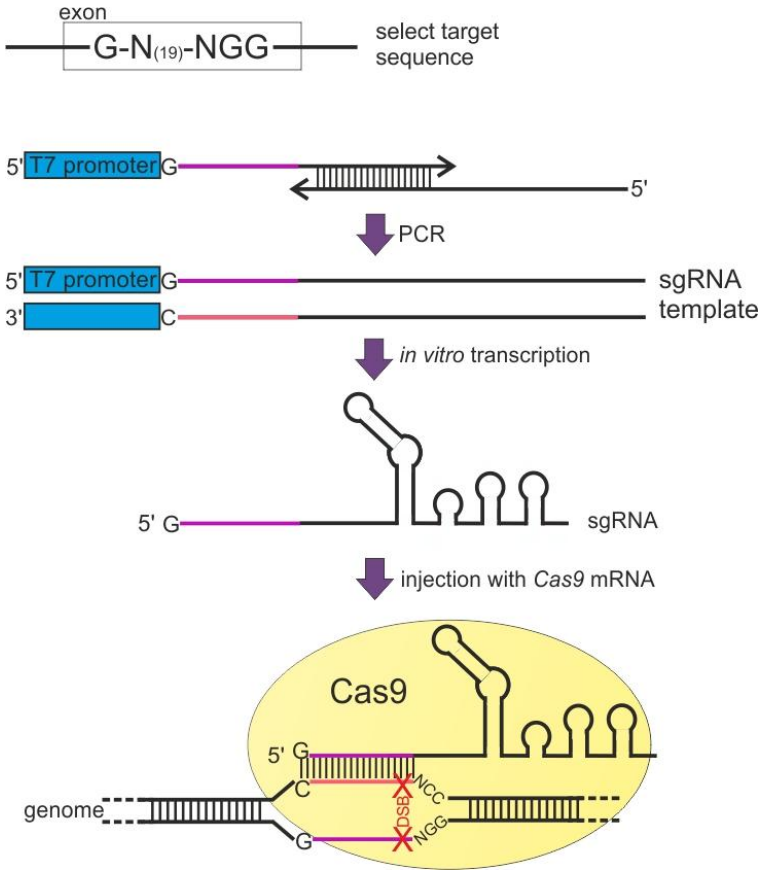

Figure 6.2. CRISPR/Cas 9 method of action
A target site in a gene of interest is picked based on it satisfying the conditions that it starts with a G, and 20 bases later is followed by another GG. This NGG constitutes the Protospacer Adjacent Motif (PAM) sequence, which is required for Cas9-mediated DSBs. Templates for *in vitro* transcription are made by PCR amplification of overlapping primers. The 5' primer contains a T7 polymerase binding motif, the target sequence and a stretch that overlaps with a common 3' primer containing the Cas9 endonuclease binding motif. From this, the single synthetic guide RNA (sgRNA) can be transcribed *in vitro* and co-injected into the *Xenopus* embryo with *Cas9* mRNA. The sgRNA binds to the target sequence, and when translated, Cas9 binds to the sgRNA and introduces a DSB upstream of the PAM sequence. Incorrect repair of the DSB introduces indels into the gene, causing defective protein synthesis.

Overlapping primers - 5' primer containing a T7 promoter, the target sequence and a sequence complementary to that of a common 3' primer containing the Cas9 binding motif – were amplified by PCR to form a template for *in vitro* transcription

containing the guide RNA and seed sequence for Cas9 binding. Using T7 polymerase, a synthetic guide RNA (sgRNA) is synthesised *in vitro*, which when injected into the *Xenopus* embryo, binds to the target sequence. The co-injected Cas9 mRNA when translated binds to the sgRNA and forms a DSB just upstream of the PAM sequence (Nakayama et al. 2013).

6.1.2 Aims of this Chapter

The aims of this chapter were to begin to analyse in detail the expression and function of a number of putative FGF targets identified by the microarray and RNA-seq based screens.

6.2 Results

Investigation of putative FGF targets *Hesx1, FoxN4* and *Hmx3*

As well as the validated FGF targets *Egr1*, *Sprouty2* and *Lefty* found in datasets generated by the microarray-based screen, some putative FGF targets negatively regulated by iFGFR1/iFGFR4 were identified. Literature searches and existing expression data on Xenbase suggested that *Hesx1*, *FoxN4* and *Hmx3* are expressed in the anterior CNS. They were found to be negatively regulated by iFGFR1 and/or iFGFR4. Therefore further investigation of their responses to iFGFR1 and 4 in whole embryos and neuralised explants was performed both to validate previously unanalysed aspects of the microarray dataset and to ascertain whether these genes are targets of FGF signalling in whole embryos and/or in a specifically neural context

Hesx1 and *FoxN4* were downregulated by iFGFR1 in the microarray by 1.65 and 1.67-fold respectively. iFGFR4 induction decreased the expression levels of *FoxN4* 1.58-fold and *Hmx3* 1.63-fold. *Hesx1, Hmx3* and *FoxN4* have been previously shown to be expressed in the anterior nervous system (Martynova et al. 2004; Bayramov et al. 2004; Schuff et al. 2006). *Hesx1* and *Hmx3* have been associated previously with FGF signalling, as both positively regulate FGFs, although it is not known if they are regulated themselves by FGF signalling (Adamska et al. 2001; Tereshina et al. 2014). There is no known link between *FoxN4* and FGFs. As FGF signalling has traditionally been investigated in the context of posterior neural development, the investigation of these anterior genes could shed light on the

repressive role of FGF signalling upon anterior neural development for iFGFR1 and iFGFR4.

6.2.1 Expression of *FoxN4* and *Hmx3,* downregulated by iFGFR4

The expression patterns of *FoxN4* and *Hmx3* were investigated in the *Xenopus* embryo. The CDS of these genes were cloned into pGem to provide a template for the synthesis of antisense DiG-labelled probes for ISH analysis on *Xenopus laevis* at a number of developmental stages. Results are shown in Figure 6.3.

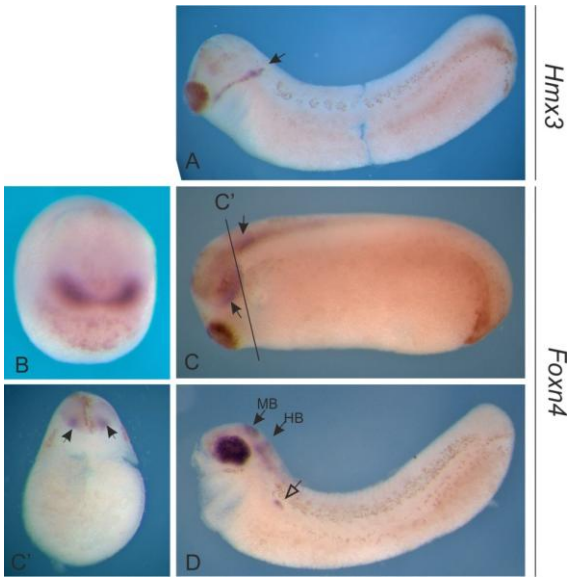

Figure 6.3. The expression of putative iFGFR4 targets *Hmx3* and *FoxN4* in the developing *X. laevis* embryo
A shows expression of *Hmx3* in tailbud stages is present in a dorsal to ventral stripe near the head (arrowed). *Hmx3* was not detectable in earlier-staged embryos. B-D shows *FoxN4* expression. At mid-neurula, it is present in the developing eye fields (B, anterior view). At stage 25 it is present in the developing retina and hindbrain, C, arrowed. C' shows *FoxN4* expression in discrete places in the neural tube when a cross section is cut at the point indicated in C. D is a tailbud embryo (head is damaged) with strong expression in the Midbrain (MB), Hindbrain (HB), pronephros (open arrow) and retina.

At mid-neurula stages, *FoxN4* was present in the developing eye fields (Figure 6.3B). At stage 25 it was expressed in the developing eye and hindbrain (Figure 6.3C). A transverse cross-section of the head of a stage 25 embryos showed *FoxN4* to be located in the domain where V2 neurons will be specified in the neural tube (Dessaud et al. 2008). In tailbud embryos *FoxN4* expression was strong in the midbrain, hindbrain and retina (Figure 6.3D). *Hmx3* was not detectable at earlier stages – indeed available Refseq data shows *Hmx3* is expressed at low levels during neurula stages and increases in abundance to peak relatively late at Stage 33 (M. H. Tan et al. 2013). At tailbud stages, *Hmx3* was present in a stripe

comprising of (from dorsal to ventral) the anterior otic vesicle, the otic ganglion and the anteroventral lateral line placodes, but not visibly in the CNS (Figure 6.3A).

6.2.2 RT-qPCR validates microarray findings for iFGFR1 targets

RT-qPCR was firstly performed using primers against the putative iFGFR1 targets *Hesx1* and *FoxN4* in whole *Xenopus laevis* embryos injected with 20pg iFGFR1 at the 2-cell stage, cultured to stage 10.5, and treated with AP20187 until stage 13 to replicate the conditions of the microarray. Fig Figure 6.4Ai shows both genes to be downregulated compared to controls - *FoxN4* significantly - after iFGFR1 induction by degrees similar to that of the microarray. As a complementary experiment, this experiment was repeated with embryos injected with 1ng dnFGFR1 and collected at stage 13. *Hesx1* and *FoxN4* showed a ~2-fold upregulation in expression, further strengthening their role as FGF targets in whole embryos.

The expression patterns of *FoxN4* and *Hesx1* were then investigated in neuralised animal cap explants induced from stage 10.5 to 13. *Hesx1* was downregulated 3.57-fold by induced *iFGFR1+Noggin*-expressing explants, but interestingly uninjected controls had a very low relative abundance of *Hesx1* compared to *Noggin*-injected explants. Therefore *Noggin* may induce *Hesx1* expression which is in turn repressed in the presence of activated iFGFR1. The opposite was true of *FoxN4* which was downregulated in the presence of *Noggin,* and repressed further in induced co-injected explants. *Hesx1* was found by RNA seq to be downregulated by both iFGFR1 and iFGFR4 so is likely to be a neural FGF target. However, FoxN4 was present at very low abundances and was not affected by iFGFR1 induction in this context.

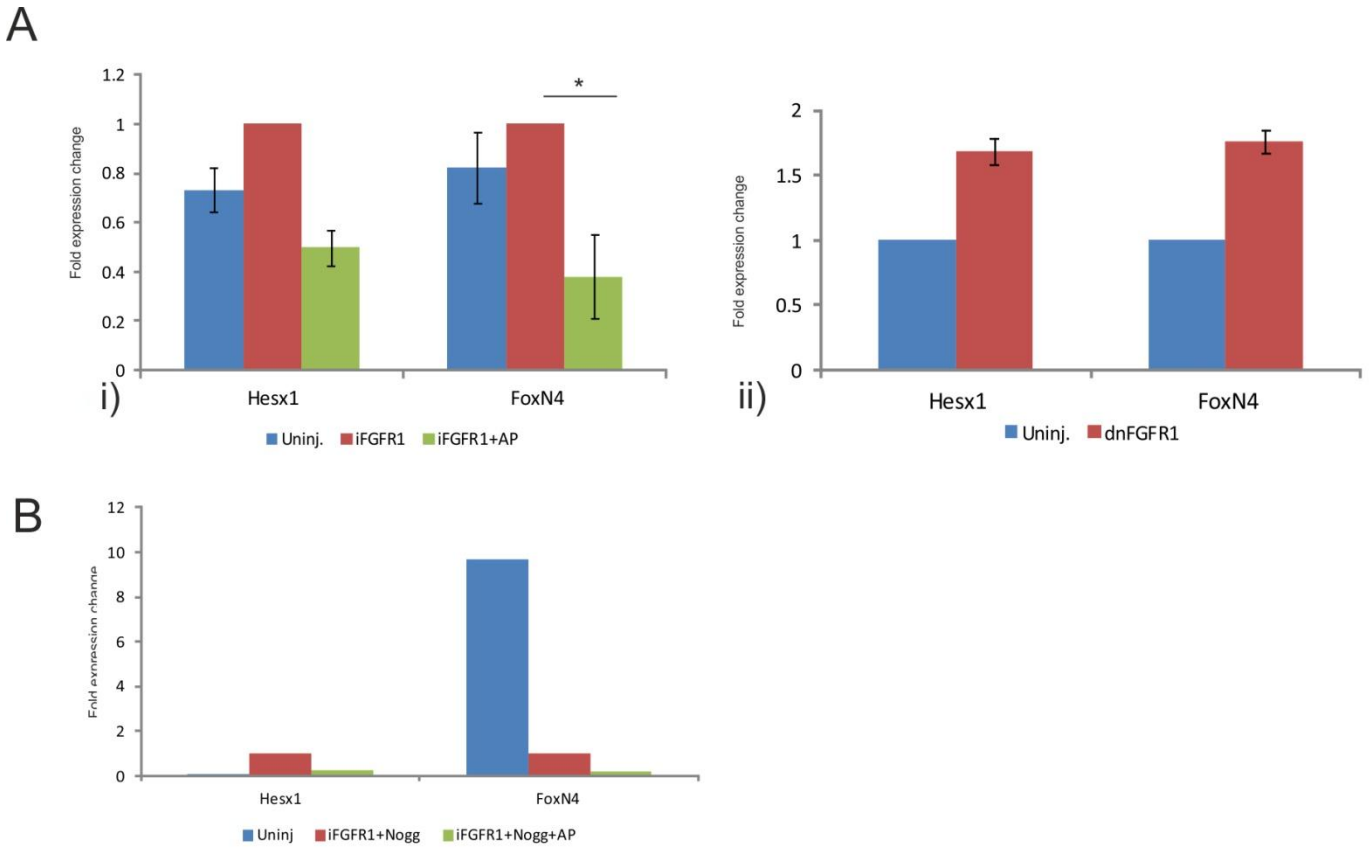

Figure 6.4 RT-qPCR experiments involving genes predicted to be downregulated by the microarray by iFGFR1
Graphs showing RT-qPCR results for the genes *FoxN4* and *Hesx1*. Whole embryos in Ai) were injected with 20pg iFGFR1 and treated with AP20187 between stages 10.5 and 13. Whole embryos in A) ii were injected with dnFGFR1 and collected at stage 13. Explants co-injected with 50pg Noggin were treated the same in B as in Ai). In Ai) error bars represent SE from three biological replicates. Asterisks represent statistical significance of normalised Ct values below p=0.05. In Aii) Error bars represent SE from two biological replicates. B) shows mean fold changes from technical replicates. Ct values were normalised against those of the housekeeping gene *ODC* and fold expression changes normalised against iFGFR1-injected uninduced embryos/explants.

6.2.3 Investigating *FoxN4* and *Hmx3*, putative iFGFR4 targets

RT-qPCR was performed in whole embryos expressing iFGFR4, replicating the conditions of the microarray to validate them as iFGFR4 targets (Figure 6.5). *Hmx3* was significantly downregulated by iFGFR4 induction in whole embryos. *FoxN4* was also downregulated but this was not significant.

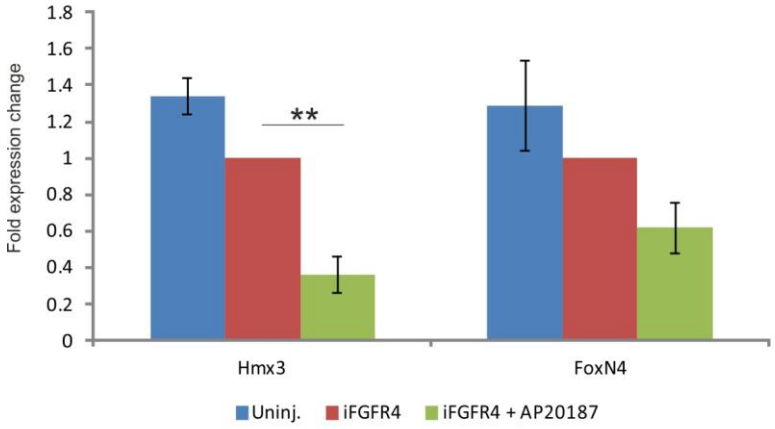

Figure 6.5 – *Hmx3* and *FoxN4* are negatively regulated by iFGFR4
These are results of RT-qPCR for the genes *Hmx3* and *FoxN4.* Embryos were injected with 20pg iFGFR4 and treated with AP20187 between stages 10.5 and 13. Error bars represent SE from three biological replicates. Asterisks represent statistical significance of normalised Ct values below p=0.05. Ct values were normalised against those of the housekeeping gene *ODC* and fold expression changes normalised against uninduced iFGFR1-injected embryos.

6.2.4 RNA-seq confirms *Hesx1* as being a neural FGF target

RNA-seq results showed *Hesx1* to be downregulated by iFGFR1 -3.2-fold, and by iFGFR4 -7.8-fold in neuralised explants. This further confirms *Hesx1* as a target of both iFGFR1 and iFGFR4. The raw RNA-seq readings showed *FoxN4* and *Hmx3* to be present at very low abundances in neuralised animal caps (FPKM <2), and their levels did not change upon either iFGFR1 or iFGFR4 induction, suggesting they may not be FGF targets during neural development. Therefore, the microarray and RT-qPCR show all three genes to be negatively regulated by FGF signalling in whole embryos, and RNA-seq shows *Hesx1* to also be a neural FGF target.

Nek6

6.2.5 NIMA-related Kinase 6 (Nek6)

Nek6, Nek7 and Nek9 are NIMA-related kinases comprising the NIMA complex which is active during mitosis and involved in regulation of the mitotic spindle (Quarmby & Mahjoub 2005). Nek6 was initially chosen to study as it was shown to interact with putative FGF target Dynll1 (See Dynll1 section in Appendix) indirectly through Nek9. Nek6 is a relatively unstudied protein, and the majority of investigations into its functions have taken place in cell culture with its *in vivo* function unexplored. Nek6 also has no previous reported FGF connection. In the preliminary microarray, *Nek6* was upregulated 2.8-fold by iFGFR1 induction and 2.6-fold by iFGFR2 induction. By RNA-seq, Nek6 was upregulated by iFGFR1 5-fold, however low read counts excluded it from genelists.

6.2.6 The expression pattern of *Nek6* in *Xenopus*

Xenbase contains automated ISH images of *Nek6* of variable quality at a few stages of *Xenopus* development. Therefore ISH was undertaken with a wider range of stages in *Xenopus laevis* embryos to investigate *Nek6* expression during development. The sequence of *Xenopus* Nek6 protein shares a 94% similarity to Nek7 and so therefore, to make an ISH probe specific only to *Nek6,* the 3' untranslated region was cloned into pGEM. *Nek6* was first detectable at mid-neurula stages (Figure 6.6A) in the posterior paraxial mesoderm. By stage 24, it was present in the developing somites (Figure 6.6B). In the tailbud stage embryo, *Nek6* expression persisted in the somites, branchial arches and also in the posterior extremities, which overlaps with FGF expression at this time (Lea et al. 2009). Sections along the antero-posterior axis at this stage revealed *Nek6* expression in the notochord, but not the neural tube - Figure 6.6C,C' and C''. *Nek6* did not show a high level of localised expression in neural tissue.

Figure 6.6 Expression of *Nek6*
Xenopus laevis embryos were cultured to a range of stages and processed for ISH against a probe specific to *Nek6*. A) shows *Nek6* is first detectable at mid-neurula stage 15 in the dorsal paraxial mesoderm. B shows a stage 24 embryo with *Nek6* expression in the developing somites (arrowed). C shows a tailbud stage 30 embryo with *Nek6* expression in the branchial arches (Ba) and somites, as well as in the posterior-most tip (open arrow). C' and C'' show cross sections of embryos with *Nek6* in the notochord (Nc arrowed in C) and the surrounding posterior ectoderm in C'' (open arrow).

6.2.7 RT-qPCR shows *Nek6* positively regulated by FGFR1

To ascertain whether the findings of the microarray could be replicated through other means, RT-qPCR was conducted using primers specific to *Nek6.* *Xenopus laevis* embryos were injected bilaterally with 20pg iFGFR1 at the 2-cell stage, and AP20187 added to culture medium at stage 10.5. Embryos were collected at stage 13, and sibling embryos were also collected at stages 15 and 17. A complementary experiment was performed where 1ng dnFGFR1 was injected bilaterally into *Xenopus laevis* embryos at the 2 cell stage and embryos processed for RT-qPCR at the same stages as before. Results from these experiments are shown in Figure 6.7. During all three induction periods, iFGFR1 induction increased the levels of *Nek6*, and this was significant for embryos induced from stage 10.5 to 15 and from stage 10.5 to 17. Figure 6.7B shows that at all three stages, dnFGFR1 significantly

reduced levels of *Nek6.* Therefore *Nek6* is positively regulated by FGF signalling in whole embryos.

Next, RT-qPCR was performed to see if *Nek6* was a target of FGF signalling in neuralised ectodermal explants. In the raw RNA-seq data, *Nek6* was shown to be upregulated by iFGFR1 5.2-fold, however read counts were not high enough to pass filtering thresholds and so it does not appear in the genelists. iFGFR1 and 50pg *Noggin* mRNA were co-injected bilaterally into *Xenopus laevis* embryos. Also, 50pg *Noggin* only was injected into sibling embryos. At stage 8, ectodermal explants were taken and cultured until stage 10.5. AP20187 was added to induce FGF signalling for 3 hours at 22°C. The presence of *Noggin* did not have an effect on *Nek6* expression (Figure 6.7C). However, relative to uninduced neuralised caps, induced iFGFR1 caused a significant 1.7-fold upregulation, suggesting *Nek6* is an FGF target in a neural context as well as in whole embryos, even though it is not detected at high levels by ISH.

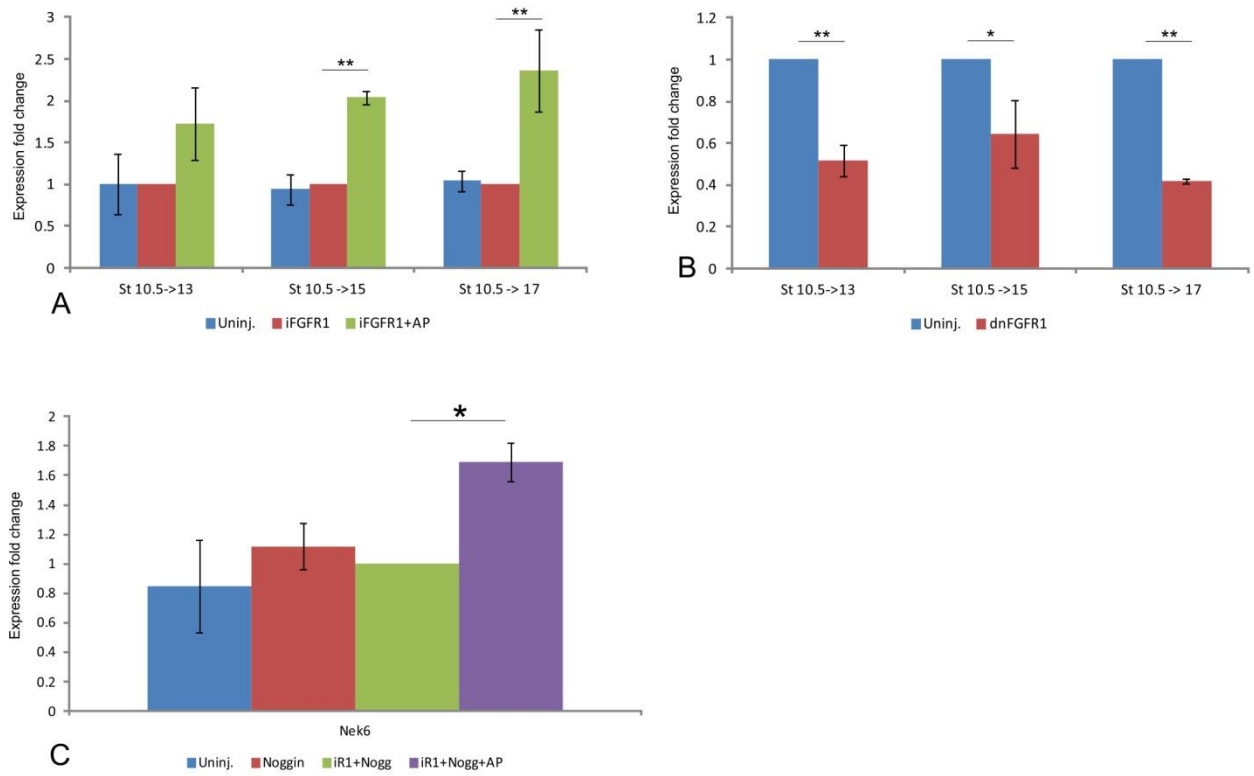

Figure 6.7 RT-qPCR to investigate iFGFR1 induction on *Nek6*
In A, whole *Xenopus laevis* embryos were injected bilaterally with 20pg iFGFR1 and cultured until stage 10.5. AP20187 was then added to culture medium and sibling embryos cultured at 22°C until stage 13, 15 or 17. In B, 1ng dnFGFR1 was injected bilaterally into *Xenopus laevis* embryos and cultured until the same stages as A. In C, 20pg iFGFR1 and 50pg Noggin were coinjected bilaterally into *Xenopus laevis* embryos, ectodermal explants taken at stage 8, and iFGFR1 induced from stage 10.5 for 3 hours. Ct values were normalised against those of the housekeeping gene *ODC* and fold expression changes normalised against iFGFR1-injected uninduced embryos (A and C) or uninjected controls (B and D). Error bars represent SE from the mean of three biological replicates. Asterisks represent statistical significance as measured by performing a two-sample T test on normalised Ct values.

6.2.8 FGFR inhibition causes loss of *Nek6*

To determine if FGF inhibition changed the expression domain of *Nek6, Xenopus laevis* embryos were injected at the 2-cell stage bilaterally with 1ng dnFGFR1 and cultured until stage 15. Samples were then processed for ISH using a *Nek6 in situ* probe.

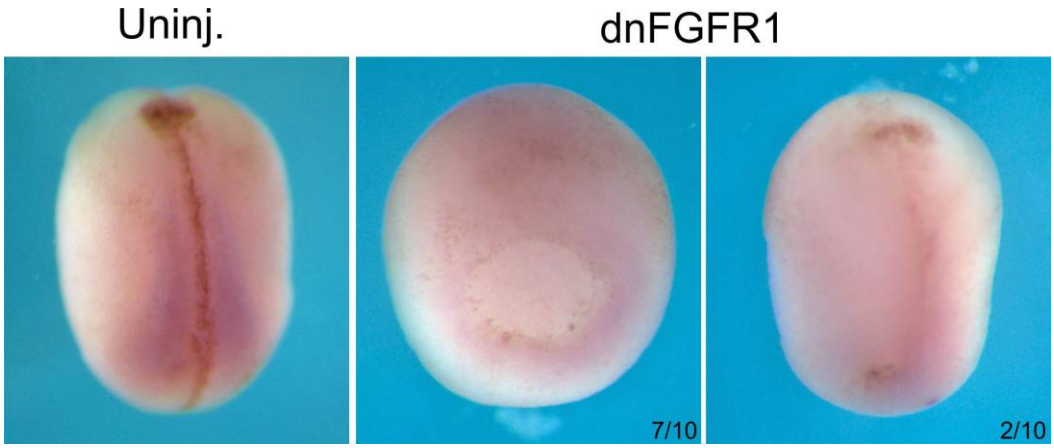

Figure 6.8 Effect of FGF signal manipulation upon *Nek6* expression
Xenopus laevis embryos were bilaterally 1ng dnFGFR1(N=10) and cultured until stage 15. ISH using a probe against *Nek6* CDS was undertaken. Numbers represent embryos resembling the representative images shown.

In uninjected controls, *Nek6* was present in the dorsal paraxial mesoderm and more intensely in the posterior (Figure 6.8). Most sibling embryos injected with1ng dnFGFR1 exhibited a partial loss of *Nek6* expression. This may be due in part to the gastrulation defects seen in many embryos (Figure 6.8, centre), however embryos expressing dnFGFR1 and more successfully completing gastrulation also displayed a loss of *Nek6* expression (Figure 6.8, right).

These ISH and RT-qPCR studies as well as the RNA-seq experiment show that *Nek6* is positively regulated by FGF signalling in whole embryos, and neuralised explants. Therefore, it was decided to investigate the function of *Nek6* further.

6.2.9 Characterisation of *Nek6* function by knockout using a TALEN

6.2.9.1 Nek6 TALEN design

The Nek6 TALEN pair was designed and synthesised by the Technology Facility using the first coding exon of *Nek6* I provided. The first coding exon was chosen as a target site to maximise the chance that a truncated non-functional protein product

would be translated. Figure 6.9 shows the TALEN-binding region in the first *Nek6* exon, with a 16bp spacer region in between where Fok1 endonuclease produces DSBs.

A

Nek6 exon 1

caccagaattcctgtgatgataaccattacatttgtattgtc
ttccagCTGCATCAGAGTGCACATATAAACTGGAATGTTACC
ATGGAAGGACAGCATCGACTAGAAGACCAAAACAGCCCTATG
TGCAAAGTCCAGGGGCAGGAATACCAGCACG...

Left TAL:	NN	NG	NG	NI	HD	HD	NI	NG	NN
NN	NI	NI	NN	NN	NI	HD	NI	NN	HD
Right TAL:		NG	NG	NN	HD	NI	HD	NI	NG
NI	NN	NN	NN	HD	NG	NN	NG	NG	NG

B

Score	Expect	Identities	Gaps	Strand
76.8 bits(41)	2e-11	49/53(92%)	0/53(0%)	Plus/Plus

```
Tropicalis 1   GTTACCATGGAAGGACAGCATCGACTAGAAGACCAAAACAGCCCTATGTGCAA  53
               ||||| ||||| ||||||||||||||||||||||||||||| ||| ||||||||
Laevis 118     GTTACTATGGAGGGACAGCATCGACTAGAAGACCAAAACAACCCAATGTGCAA  170
```

Figure 6.9 Nek6 TALEN design
A)The first coding exon of *Xenopus tropicalis Nek6* was chosen as a TALEN target region. The exon is capitalised. The Left TALEN binds to a 19bp region in red, and the right TALEN binds to the region in blue. The 16bp target spacer region is underlined. The TALEN RVDs are listed below. B)Shows a BLAST alignment of the *Xenopus tropicalis* and *Laevis* left and right TALEN and target sequences

The Left and Right TALENs were synthesised and cloned into pCS2+ by the Technology Facility, and from this templates and synthetic mRNA was synthesised.

6.2.9.2 Optimisation of TALEN injection

Firstly, to determine that both Left and Right TALENs are translated in the *Xenopus* embryo, either 1ng or 2ng *Nek6* TALEN mRNA was injected into *Xenopus laevis* embryos at the 1 cell stage and cultured to early neurula stage 14. They were then processed for western blot analysis using antibodies against the Flag epitope within the Left TALEN and the HA epitope present within the Right TALEN.

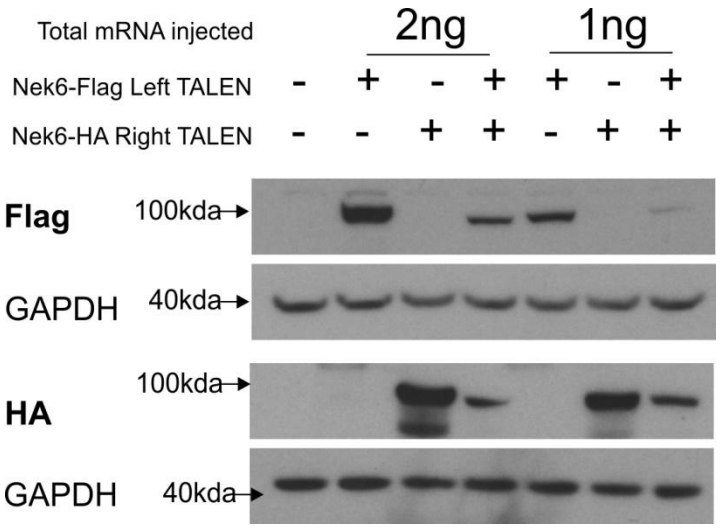

Figure 6.10 Western blot showing Nek6 TALEN mRNA is translated into protein
Xenopus laevis embryos were injected at the 1 cell stage with either 1ng or 2ng of Flag-tagged Left TALEN, HA-tagged Right TALEN, or both. The expected size of each TALEN is 100kDa. GAPDH was used as a loading control.

Figure 6.10 shows that both left and right TALENs are translated into protein at both dosages at detectable levels, both when expressed on their own or when co-injected.

6.2.10 Nek6 TALEN injection causes major developmental defects

2ng of Nek6 TALEN (co-injection of 1ng Left TALEN+1ng Right TALEN) was injected into *Xenopus tropicalis* and *Xenopus laevis* embryos at the 1-cell stage to maximise the likelihood of all daughter cells inheriting Nek6 TALENs. Embryos injected with 2ng Right TALEN only developed as uninjected controls. However those injected with 2ng Left and Right TALEN exhibited gross developmental defects in both species from early stages. Figure 6.11 shows the phenotype of Nek6 TALEN-injected *Xenopus laevis* embryos throughout development. *Xenopus tropicalis* embryos displayed the same phenotype (not shown).

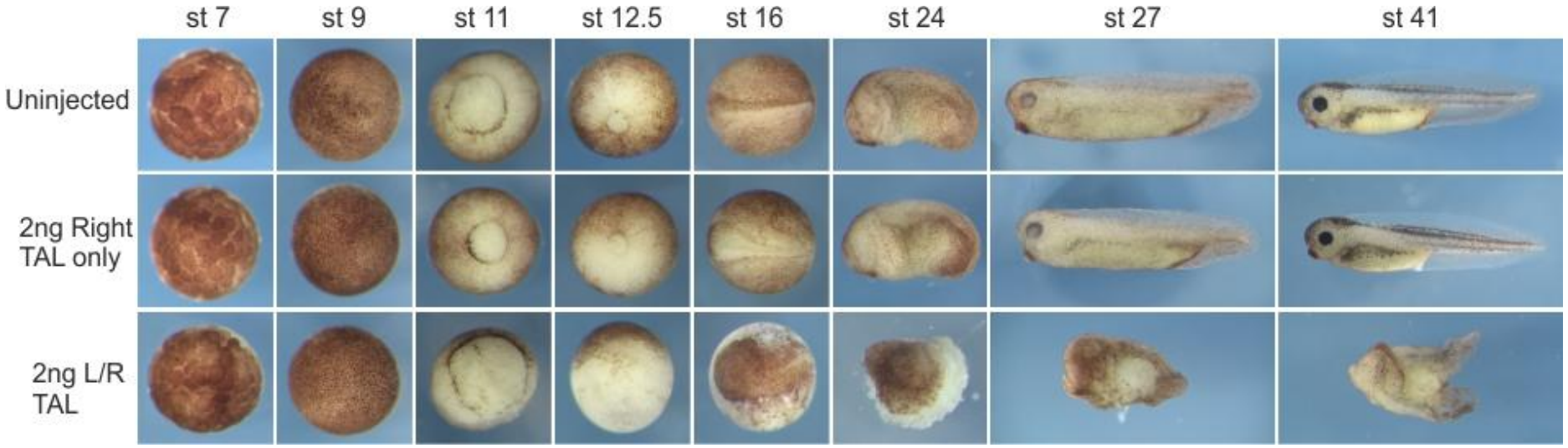

Figure 6.11 Development of the Nek6 TALEN phenotype
2ng Nek6 TALEN – 1ng Left TALEN + 1ng Right TALEN – was injected into *Xenopus laevis* embryos at the 1 cell stage and embryos fixed and imaged at various developmental stages. Embryos injected with only 2ng Right TALEN developed as uninjected controls. TALEN injected embryos developed normally until mid-gastrula, where they failed to complete gastrulation, and then failed to neurulate. As a result, at stage 41, embryos exhibited anterior and posterior truncations, a failure of neural tube closure and a lack of discernible organogenesis. This effect was reproducible and seen in almost all injected embryos.

Embryos injected with both Left and Right TALENS developed as controls until mid-gastrulation (St 11), when the blastopore failed to close. This was succeeded by a failure to neurulate properly (St16 and 24). At early tailbud stages, (St 27), surviving TALEN-injected embryos had not elongated and displayed an open neural tube, with severe posterior and anterior truncations. At stage 40, control embryos displayed typical organogenesis and were able to swim. However TALEN-injected embryos lacked all recognisable organs, head, tails or recognisable antero-posterior/dorso-ventral axes; although the epidermis was fairly well developed as pigment cells formed. Therefore *Nek6* knockout has a profound effect on development.

It was unclear from the ISH experiment whether *Nek6* was expressed in the CNS and thus could conceivably be involved in neural development, although the neuralised animal cap RT-qPCR data do support a role for *Nek6* in neural development. Therefore the Nek6 TALEN was targeted to the CNS by injecting 2ng bilaterally into the two dorsal animal blastomeres of *Xenopus laevis* embryos at the 8-cell stage. A slight phenotype was seen, namely that the eyes of Nek6 TALEN embryos were smaller. This is depicted in Figure 6.12 as a box plot. Both eyes of 17 control embryos injected with just 2ng Right TALEN only, and both eyes of 33 embryos injected with 2ng both TALENs were photographed under the same magnification and their diameter measured in pixels. The differences in eye size were highly significant. Therefore a *Nek6* may influence eye development, supporting a role for *Nek6* in neural development.

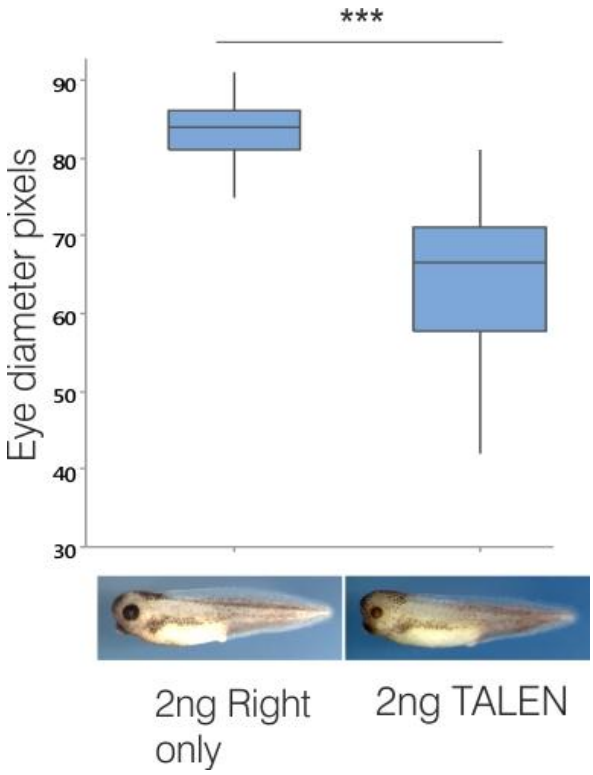

Figure 6.12 – Embryos with Nek6 TALEN targeted to the developing CNS exhibit a reduction in eye size
Xenopus laevis embryos were injected bilaterally at the 8-cell stage with 2ng of Nek6 Left and Right TALEN or just 2ng of the Right TALEN and cultured to stage 40. Each eye on 17 2ng Right TALEN only embryos, and 33 2ng TALEN injected embryos was photographed and the eye diameter measured in pixels along its widest length (y axis). Representative images are shown on the x axis. Asterisks represent statistical significance as determined by a 2 sample T test.

6.2.10.1 Nek6 TALEN injection causes movement defects

In addition to morphological defects, *Nek6* TALEN-injected embryos displayed aberrant movement phenotypes, similar to those of Dynll1 morphants (See Appendix Section 8.1). From tailbud stages, embryos 'coast' around the culture dish by beating epidermal cilia on their trunks in order to circulate oxygen – tailbud embryos did not move around the culture dish, or waft cellular debris away suggesting cilia defects. Nek6 TALEN embryos failed to do this. This lack of 'coasting' movement is shown in Movies 1-3 on the Accompanying Material CD. Uninjected control embryos (Movie 1) and 2ng Right TALEN control embryos (Movie2) coasted normally around the culture dish, however 2ng TALEN-injected embryos did not (Movie 3). Figure 6.13 shows this information in a column chart, using the following criteria to categorise embryos based upon movement: embryos that moved as wild type, embryos that moved at a slower rate than wild type, those that remained stationary but could still waft away cellular debris with beating cilia, and those that remained stationary and could not waft away debris.

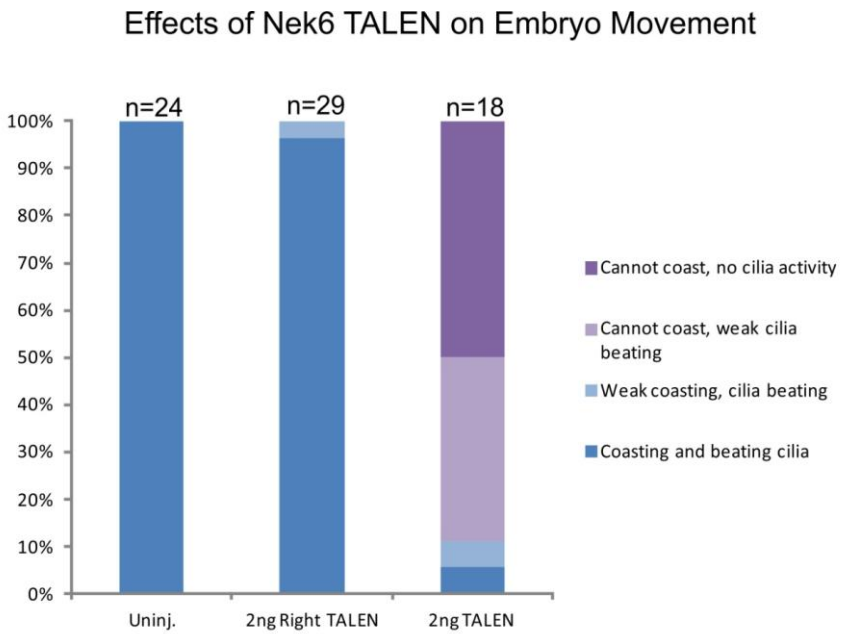

Figure 6.13 Effects of Nek6 TALEN on Embryo movement
Stage 30 *Xenopus laevis* embryos injected with 2ng Nek6 TALEN or 2ng Right TALEN only at the 1 cell stage were scored based upon their ability to coast around the culture dish and whether cellular debris could be wafted away.

Uninjected embryos and those injected with 2ng of Right TALEN moved normally around the culture dish. However, most embryos injected with 2ng TALEN were unable to move around the dish, with around 50% of these unable to waft away debris, which could be due to major defects in epidermal cilia.

6.2.11 Nek6 TALEN causes deletions in genomic *Nek6* sequence

The next aim was to determine that these phenotypes were due to indels in the genomic DNA (gDNA) sequence of the *Nek6*. The TALEN was designed against the *Xenopus tropicalis* Nek6, however the sequence targeted is almost identical to the *Xenopus laevis* Nek6. Both *Xenopus laevis* and *Xenopus tropicalis* embryos were injected with 2ng Nek6 TALEN mRNA and cultured to stage 30. gDNA was extracted from individual embryos and the genomic target region amplified by PCR using primers spanning the target region of the TALEN. In order to observe individual indel events, the PCR products were purified and T-cloned. Individual clones were then cultured and sequenced. Figure 6.14 shows aligned fragments of clones from both species.

A. *Xenopus laevis*

B. *Xenopus tropicalis*

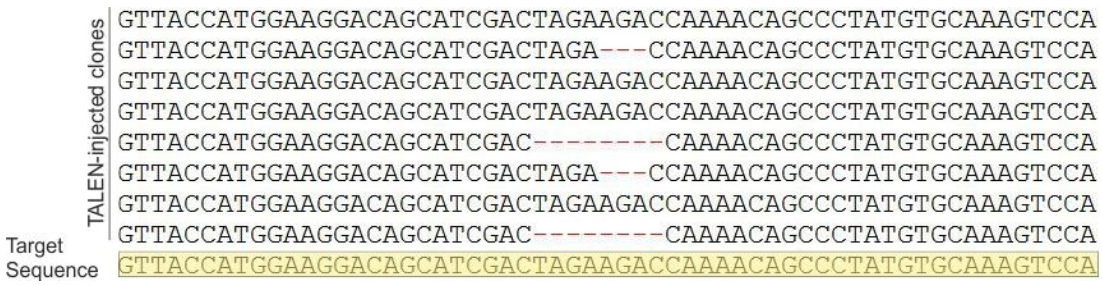

Figure 6.14 Nek6 TALEN causes deletions in the *Xenopus laevis* and *tropicalis* genomes
2ng Nek6 TALEN was injected into *Xenopus laevis/tropicalis* embryos and genomic DNA extracted from individual embryos. The genomic region around the TALEN target region was amplified by PCR, and fragments cloned, transformed and sequenced. The aligned sequences are shown above. In each case, the target sequence is highlighted in yellow with the spacer region in the centre.

In *Xenopus laevis* 7/10 clones sequenced contained deletions, all of which would cause frameshift mutations. In *Xenopus tropicalis,* half of the sequenced clones contained deletions, two of which would definitely cause frameshift mutations. Therefore, the *Nek6* TALEN causes mutations in the genome at a fairly high frequency in the F0 generation.

6.2.12 Effect of *Nek6* knockout upon gene expression

6.2.12.1 *Nek6* knockout negatively affects mesodermal but not endodermal gene expression domains

The next aim of the investigation into Nek6 function was to find out if Nek6 knockout had an effect on endodermal, mesodermal and/or (neur)ectodermal gene expression. Firstly, ISH was performed on *Xenopus laevis* embryos - injected with 2ng TALEN at the 1-cell stage and cultured to mid-gastrula (stage 11) - with probes against the mesodermal genes *Xbra, MyoD,* and *Cdx4*. In addition, the endodermal

marker *Sox17b* was also utilised to see whether *Nek6* knockout affects endoderm development.

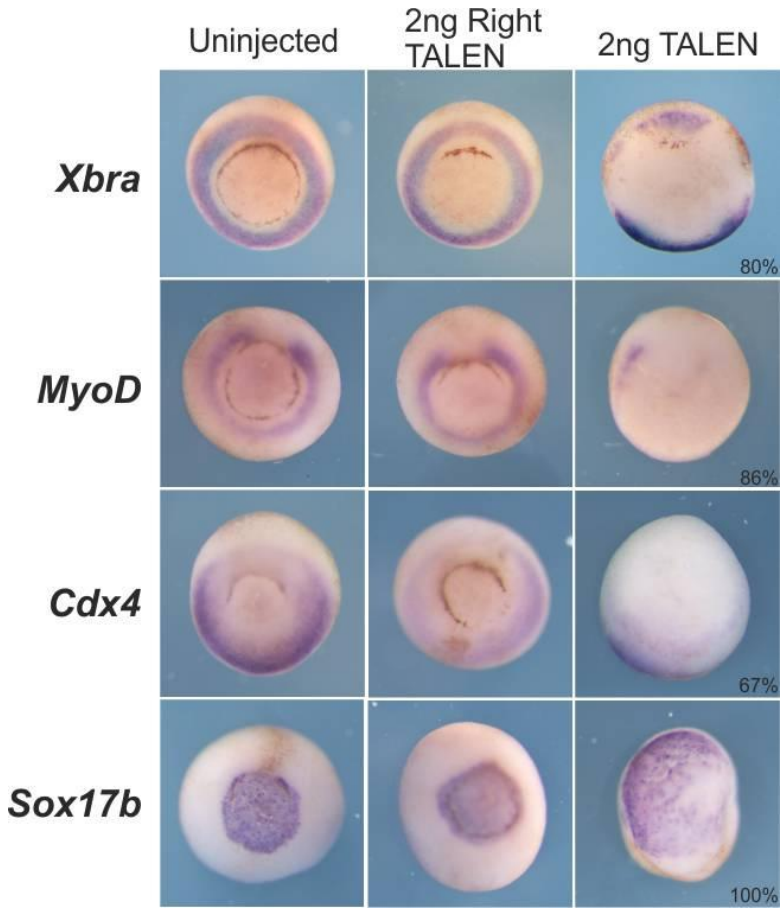

Figure 6.15 Effect of Nek6 knockdown on mesodermal genes
Xenopus laevis embryos were injected with 2ng TALEN at the 4-cell stage and cultured to stage 11, where they were processed for ISH with probes against the mesodermal *Xbra, MyoD* and *Cdx4* as well as the endodermal marker *Sox17b.* Expression of mesodermal genes around the closing blastopore was lost in TALEN-injected embryos; however *Sox17b* expression was not affected. Percentages show numbers of embryos resembling the representative image. *Xbra* n=56, *MyoD* n=35, *Cdx4* n=15 and *Sox17b* n=16.

Mesodermal genes are expressed in a ring around the closing blastopore during gastrula stages. The expression of *Xbra, MyoD* and *Cdx4* were partially, or in some instances completely lost in embryos injected with Nek6 TALEN compared to controls, as shown in Figure 6.15. In some cases – shown by *Xbra* here – this loss of expression was patchy probably due the mosaicism of cells inheriting Nek6 TALEN. Therefore knockout of Nek6 causes a loss of mesodermal gene expression. Conversely, although the expression domain of *Sox17b* is larger because the blastopore failed to close in these embryos, the expression pattern of *Sox17b* did not change. This indicates that loss of Nek6 affects mesodermal, but not endodermal gene expression.

6.2.12.2 *Nek6* knockout also negatively affects expression of neural markers

Next, the effect of *Nek6* knockdown on genes involved in neural development was investigated. ISH probes for the pan-neural marker *Sox3*, the eyefield marker *Rax*, the primary neuron marker *N-tubulin*, the hindbrain marker *Krox20* and the MHB marker *En2* were synthesised. As Nek6 TALEN caused severe gastrulation defects which could mask neural gene expression, *Xenopus laevis* embryos were injected with 2ng Nek6 TALEN into the two dorsal blastomeres at the 4-cell stage to partially circumvent gastrulation defects whilst still targeting the developing CNS, although a high proportion still did not gastrulate. Injected embryos were cultured until mid-neurula stage 15 and processed for ISH.

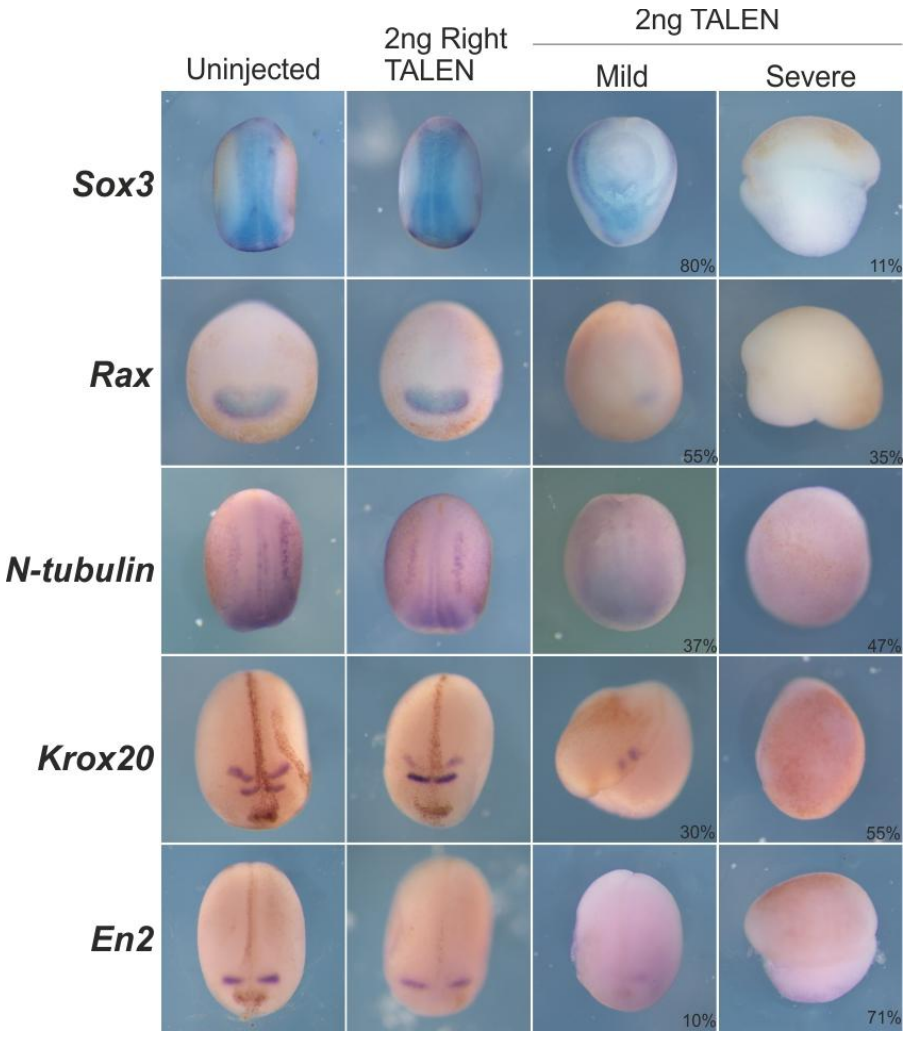

Figure 6.16. Effect of *Nek6* TALEN upon neural genes
Xenopus laevis embryos were injected with 2ng TALEN, and controls were either uninjected or injected with 2ng Right TALEN only. Embryos were cultured until stage 15 and processed for ISH for the pan-neural marker *Sox3* (n=19), eyefield marker *Rax* (n=20), primary neuron marker *N-tubulin* (n=19), hindbrain marker *Krox20* (n=40) and the MHB marker *En2* (n=21). The loss of gene expression was sorted into mild and severe. Percentages show numbers of embryos resembling the images shown.

The effects on the expression of these genes were classed as mild or severe, shown in Figure 6.16, which tended to correlate with how well embryos gastrulated. In wild type and 2ng Right TALEN only-injected controls, *Sox3* expression demarcated the neural plate. In TALEN-injected embryos where gastrulation proceeded fairly normally, *Sox3* expression was patchy and in those where gastrulation failed completely, *Sox3* expression was absent. This suggests that early neural marker genes are negatively affected upon *Nek6* knockout. Nek6 TALEN injected embryos also displayed ill-defined *N-tubulin* expression patterns pattern in some embryos, or a complete loss in others showing Nek6 is required for proper neurogenesis. The neural markers *Krox20* and *En2* were also severely depleted in many TALEN-injected embryos, showing that *Nek6* knockout also affects brain patterning and development. Lastly, the eyefield marker *Rax* was also almost completely lost further supporting a role for Nek6 in eye development. These effects upon gene expression could be due to in part to gastrulation defects, as even though embryos were injected at the 4 cell stage, they did not gastrulate completely – however those that did gastrulate still displayed a loss of gene expression suggesting *Nek6* has a separate effect on neural gene expression separate from its earlier effect upon the mesoderm.

Therefore, as well as disrupting mesodermal gene expression, *Nek6* knockout has a detrimental impact on the expression of key early neural markers, both the pan-neural marker *Sox3*, as well as those specific to the eyes, hindbrain, midbrain and neurons.

6.2.13 The effect of *Nek6* knockout on FGF signalling

6.2.13.1 During neurula stages, knockout of Nek6 increases MAPK signalling

It is unknown if these effects upon mesodermal and neural genes are because they are also downstream targets of Nek6, or whether Nek6 knockout disrupts FGF signalling or other signalling pathways which cause the loss in mesodermal and neural gene expression. Therefore, the effect Nek6 TALEN injection had upon the dpERK levels was tested at a number of stages by western blot analysis with whole embryos injected with 2ng TALEN at 1-cell stage and cultured to stage 11, 14 and 17.

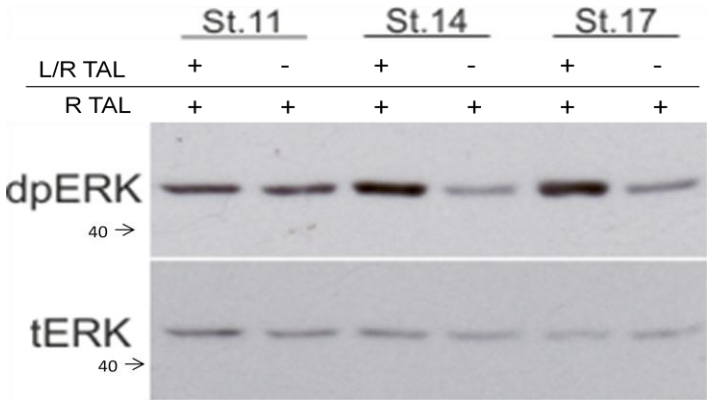

Figure 6.17 Effects of *Nek6* knockout on the MAPK pathway
Xenopus laevis embryos were injected with 2ng Nek6 TALEN and cultured to stage 11, 14 and 17 before being processed for western blot analysis with dpERK antibody. Left and Right TALEN-injected embryos (L/R) contained higher levels of active ERK than embryos injected with the Right TALEN only (R). tERK was used as a loading control.

As shown in Figure 6.17, at stage 11 there was no difference in dpERK levels between TALEN-injected embryos and Right TALEN controls. However, at early and late neurula stage 14 and 17, TALEN-injected embryos contained higher levels of active ERK relative to controls. This suggests that at neurula stages, *Nek6* may normally repress MAPK signalling.

6.2.13.2 Knockout of Nek6 affects the ability of iFGFR1 to induce target genes

To investigate the effects of Nek6 TALEN upon FGF signalling further, a series of RT-qPCR experiments were performed using ectodermal explants. 20pg iFGFR1 and 1ng TALEN were co-injected at the 1 cell stage. Ectodermal explants were taken at stage 8 and explants treated with AP20187 until stage 10.5 to coincide with mesoderm specification. As positive controls, explants injected with only 20pg iFGFR1 were treated in the same way. Relative to uninjected control explants, *Xbra*, *MyoD* and *Sprouty2* were significantly upregulated by iFGFR1 induction as expected (Figure 6.18). *Xbra* and *Sprouty2* were also upregulated significantly when iFGFR1 was co-injected with Nek6 TALEN, however to a lesser extent to when iFGFR1 was expressed alone. For *Xbra,* the differences between these conditions were significant. Therefore, *Nek6* knockout significantly negatively affected the ability of FGF induction by iFGFR1 to upregulate *Xbra*. *MyoD* was upregulated by iFGFR1 and slightly more so in iFGFR1+Nek6 TALEN embryos, but there was no significant difference between *MyoD* levels in these two induced conditions.

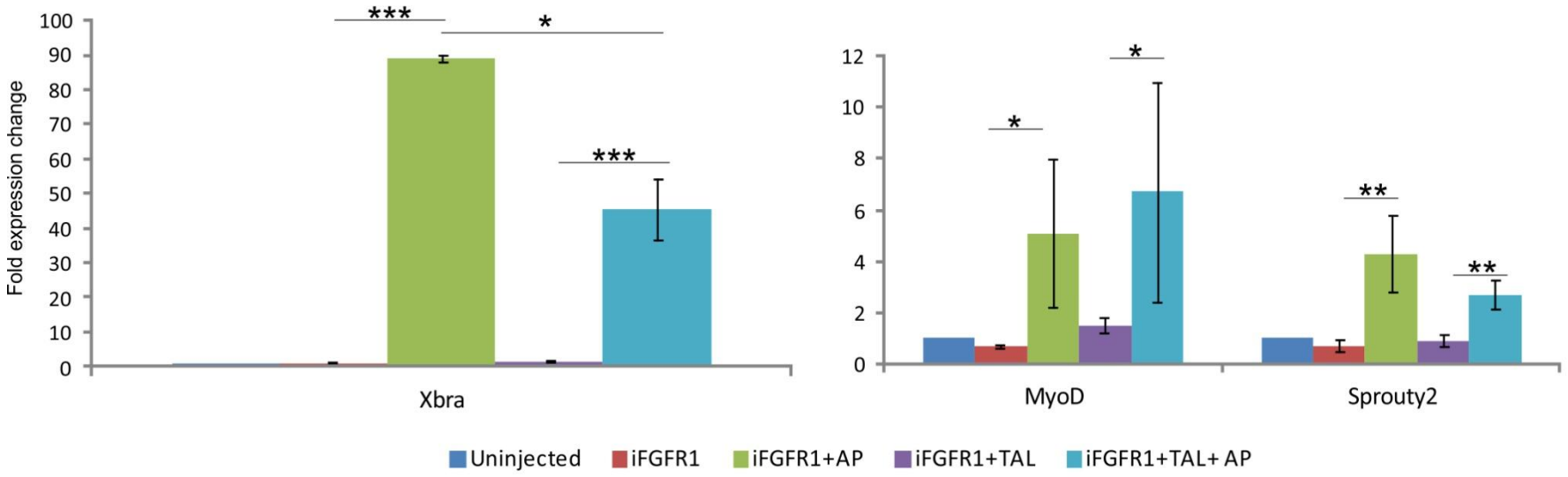

Figure 6.18 Effects of Nek6 knockout on mesodermal gene expression
Xenopus laevis embryos were injected with 20pg iFGFR1, or co-injected with 1ngTALEN + iFGFR1. Ectodermal explants were taken at stage 8, and AP20187 added until stage 10.5. Ct values were normalised against those of the housekeeping gene ODC and fold expression changes normalised against uninjected explants. Error bars represent SE from the mean of three biological replicates. Asterisks represent statistical significance as measured by performing a one-way ANOVA on normalised Ct values. *Xbra* data shown is on a different scale for ease of visualisation.

6.2.14 Overexpression of *Nek6*

6.2.14.1 Injection of *Nek6* mRNA

Full-length *Xenopus tropicalis Nek6* was obtained in a vector from Addgene. It was subcloned into CS2+ and used to make sense mRNA for injection into *Xenopus* embryos. Figure 6.19 shows the phenotype of *Xenopus laevis* embryos injected with increasing amounts of *Nek6* mRNA. At the lowest dose, only a few embryos displayed a noticeable phenotype which was a smaller eye than siblings and controls. This was also seen at a slightly higher frequency in embryos injected with 200pg of Nek6 mRNA. Embryos injected with twice this dose showed more severe phenotypes, with some embryos failing to gastrulate. At the highest dose tested, 800pg, embryos with the most severe defects resembled the knockout phenotype, with severe gastrulation and neurulation defects, as well as anterior and posterior truncations in the majority of embryos. Those that did gastrulate had under-developed eyes and kinks in the tail.

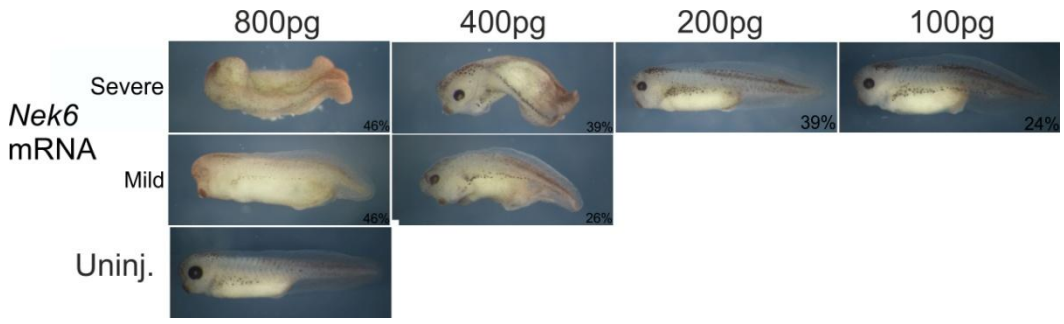

Figure 6.19 Phenotype of *Xenopus* embryos overexpressing Nek6 mRNA
Xenopus laevis embryos were injected with varying amounts of *Nek6* mRNA and cultured to stage 40. Percentages show embryos showing a phenotype. 100pg N=23, 200pg N=20, 400pg N=23, 800pg N=26. 800pg and 400pg injected embryos contained mild and severe phenotypes, as shown.

Therefore, both overexpression and knockout of Nek6 cause similar and severe developmental defects, so its proper regulation must be imperative for correct *Xenopus* development.

6.2.14.2 *Nek6* mRNA partially rescues gastrulation defects caused by *Nek6* TALEN

Although both overexpression and knockout of *Nek6* caused similar phenotypes, *Nek6* mRNA was co-injected with Nek6 TALEN to see if the mRNA could rescue the defects associated with the TALEN embryo. This would also be a means to assess the specificity of the TALEN phenotypical defects. Figure 6.20 shows embryos that injected with *Nek6* mRNA, Nek6 TALEN, or a combination of both. The amount of TALEN injected was kept at 1ng, and increasing amounts of *Nek6* mRNA co-

injected. Representative images are shown for each condition that corresponds to the column graph, made after scoring embryos on their ability to gastrulate.

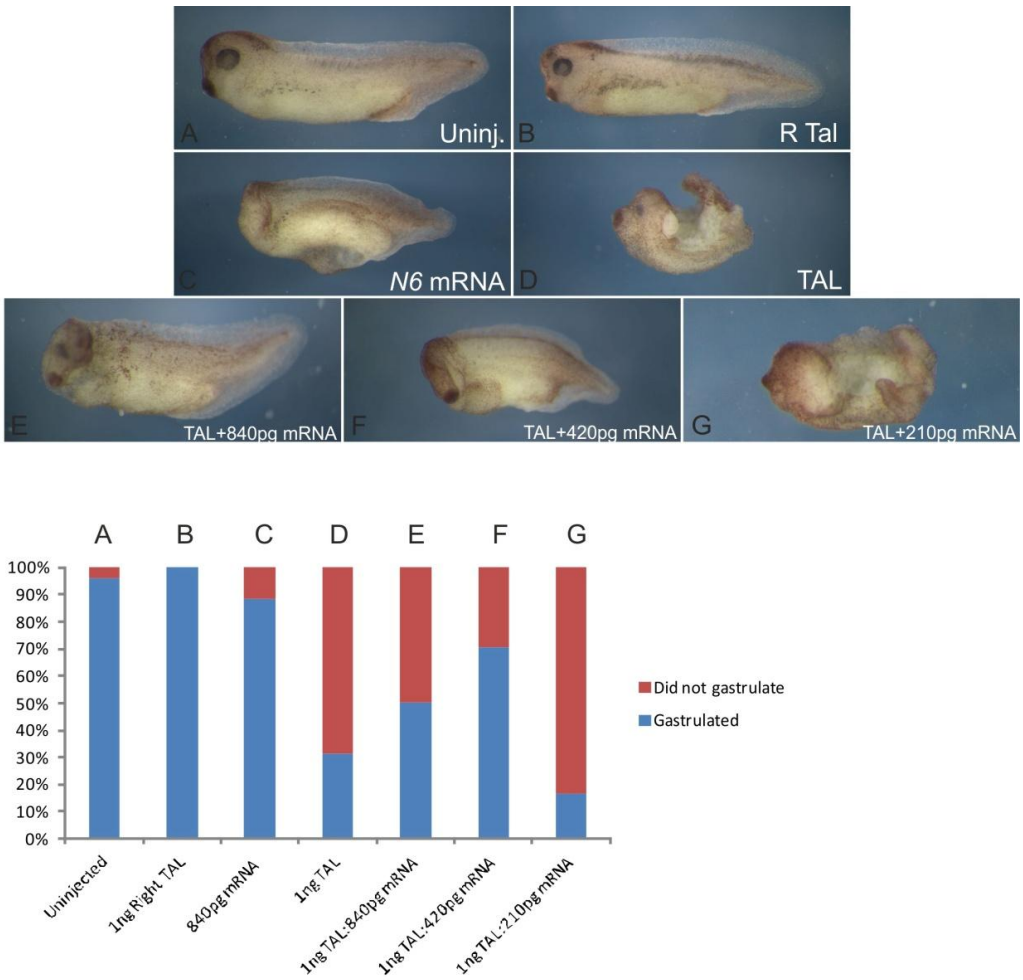

Figure 6.20
Xenopus laevis embryos were injected at the 1 cell stage with B-1ng Right TALEN, C-840pg *Nek6* mRNA, D-1ng TALEN, E – 1ng TALEN+840pg *Nek6* mRNA, F – 1ng TALEN + 420pg *Nek6* mRNA and G – 1ng TALEN + 210pg *Nek6* mRNA. Representative images of each condition are shown above a corresponding column chart detailing percentages of embryos which gastrulated. N values – A=26, B=20, C=17, D=16, E=20, F =17, G=12.

The majority of uninjected control embryos, and control embryos injected with 1ng Right TALEN only gastrulated normally. Only 30% of 1ng TALEN-injected embryos completed gastrulation. Embryos injected with 840pg *Nek6* mRNA mostly gastrulated, but displayed anterior truncations (65%). Co-injection of 1ng TALEN:420pg mRNA resulted in 70% of embryos completing gastrulation, thus partially rescuing the TALEN-only phenotype. This rescue was also seen in 1ng TALEN:840pg mRNA injected embryos, although it was not as penetrant with 50% of embryos completing gastrulation,. Embryos injected with 1ng TALEN and 210pg mRNA actually gastrulated at a lower efficiency than TALEN-injected embryos,

(10% vs 30%), so therefore the best dosage for rescue of gastrulation is 1ng TALEN:420pg mRNA. This does not produce an embryo that resembles the controls, as some anterior and posterior defects are still present, however they tended to be less severe than embryos injected with either Nek6 TALEN or *Nek6* mRNA alone.

6.3 Using CRISPRs to characterise RNA-seq FGF targets

The next aim was to characterise putative novel FGF targets using CRISPR technology. Three genes were picked from the RNA seq dataset to investigate further: *Cited2, Snx10* and *Zswim4*.

As discussed in previous chapters, a theme emerging from the microarray and RNA-seq datasets was that of a role of FGF signalling for ciliogenesis and left/right asymmetry. FGF signalling has previously been implicated in ciliogenesis and the Nodal laterality cascade, partially through the control of Wnt signalling, although its exact role is unclear. Therefore two validated iFGFR4 targets identified by RNA-seq, previously implicated in laterality but not as yet linked with FGF signalling, were chosen to be characterised further. In addition, *ZSwim4* was investigated as it has an unknown function. Therefore knockout of this gene could help illuminate its role as an FGF target during *Xenopus* development.

Cited2 is a transcriptional regulator required for breaking left/right asymmetry and part of the nodal signalling cascade (Bamforth et al. 2004; Lopes Floro et al. 2011). By RNA-seq, it was found upregulated by iFGFR4 induction 2.9-fold, and was also significantly upregulated by iFGFR4 by RT-qPCR. *Sorting Nexin 10* (*Snx10*) is a regulator of ciliogenesis and also required for correct left/right patterning, as zebrafish *Snx10* morphant embryos displayed randomised heart looping (Chen et al. 2012). In this RNA-seq, *Snx10* was found upregulated by iFGFR4 induction 2.6-fold and was also found to be significantly upregulated by iFGFR4 by RT-qPCR. The third gene studied was a zinc finger protein of unknown function, *ZSwim4*, upregulated by iFGFR1 induction 4.1-fold. These genes were not affected by iFGFRs in the microarray-based screen. Knockout of these genes has not been performed in *Xenopus* before or previously linked to FGF signalling to my knowledge, and so their function was investigated using the new CRISPR technology.

6.3.1 Design of CRISPRs

CRISPRs were designed using the E-CRISP software. As in Nakayama et al. (2013), the CRISPR target site had to satisfy the following sequence: 5'-G-n19-nGG-3', where the 5' G is for T7 polymerase binding and initiation of transcription and the 3' nGG is the PAM site. *Cited2* only has one exon, but a suitable site was found in the centre for CRISPR design. The first exon of *Zswim4* was not present in the *Xenopus tropicalis* genome version used by ECrisp, and so the second coding exon was used. As *Snx10* consists of many very small exons, the only suitable site for CRISPR design was in the 5th exon. BLAT against the *Xenopus tropicalis* genome confirmed that these target sequences were specific to the genes of interest.

6.3.2 Optimisation of CRISPR/Cas9 injection conditions using *Tyrosinase*

The *Tyrosinase* CRISPR from Nakayama et al. (2013) was used to optimise the dosage of sgRNA and *Cas9* mRNA for microinjection. *Tyrosinase* is commonly chosen for TALEN and CRISPR studies as it is required for pigment production, so its albino knockout phenotype is easily visualised (Ishibashi et al. 2012). Nakayama et al (2013) used 2.2ng of *Cas9*, so this amount was injected into *Xenopus tropicalis* embryos without ill effect, and increased the degree of embryo albinism. The concentration of sgRNA was then adjusted, and doses below 600pg found not to be toxic to embryos. This optimisation is summarised in Figure 6.21

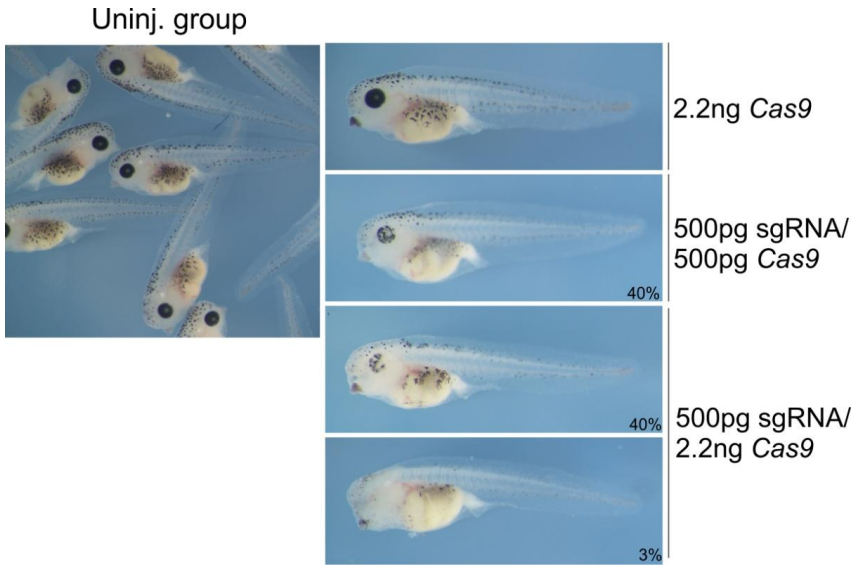

Figure 6.21 Optimising CRISPR/Cas9 injection using Tyrosinase sgRNA
Varying amounts of Tyrosinase sgRNA and *Cas9* were injected into *Xenopus tropicalis* embryos at the 1 cell stage. Embryos were cultured to stage 40. 2.2ng of *Cas9* mRNA could be injected without any detrimental effects to development. 500pg sgRNA/500pg *Cas9* produced a mild mosaic phenotype in some embryos (n=35). By increasing *Cas9* concentration to 2.2ng, a greater degree of albinism was observed in some of the embryos (n=29). Percentages indicate numbers of embryos resembling the representative image.

Therefore, 500-600pg *Zswim4*, *Snx10* and *Cited2* sgRNA was co-injected with 2.2ng *Cas9* mRNA.

6.3.3 ZSwim4 CRISPR causes head abnormalities and cyclopia

600pg Zswim4 CRISPR was co-injected with 2.2ng Cas9 mRNA. This CRISPR had a more penetrant effect than the other CRISPRs tested. Compared to uninjected embryos, dorsal views of injected embryos in Figure 6.22 showed most embryos to have narrower heads, with more severely-affected embryos having smaller and cyclopic eyes, and one even had complete cyclopia. The CRISPR also caused defects in organogenesis and the tail. This suggests that *ZSwim4* may be required for correct facial development.

6.3.4 Sequencing shows that ZSwim4 CRISPR causes indels

To ensure these defects occurred in embryos showing indels in *Zswim4,* embryos injected with *ZSwim4* CRISPR/Cas9 showing a phenotype were collected and gDNA extracted from 9 individual embryos.

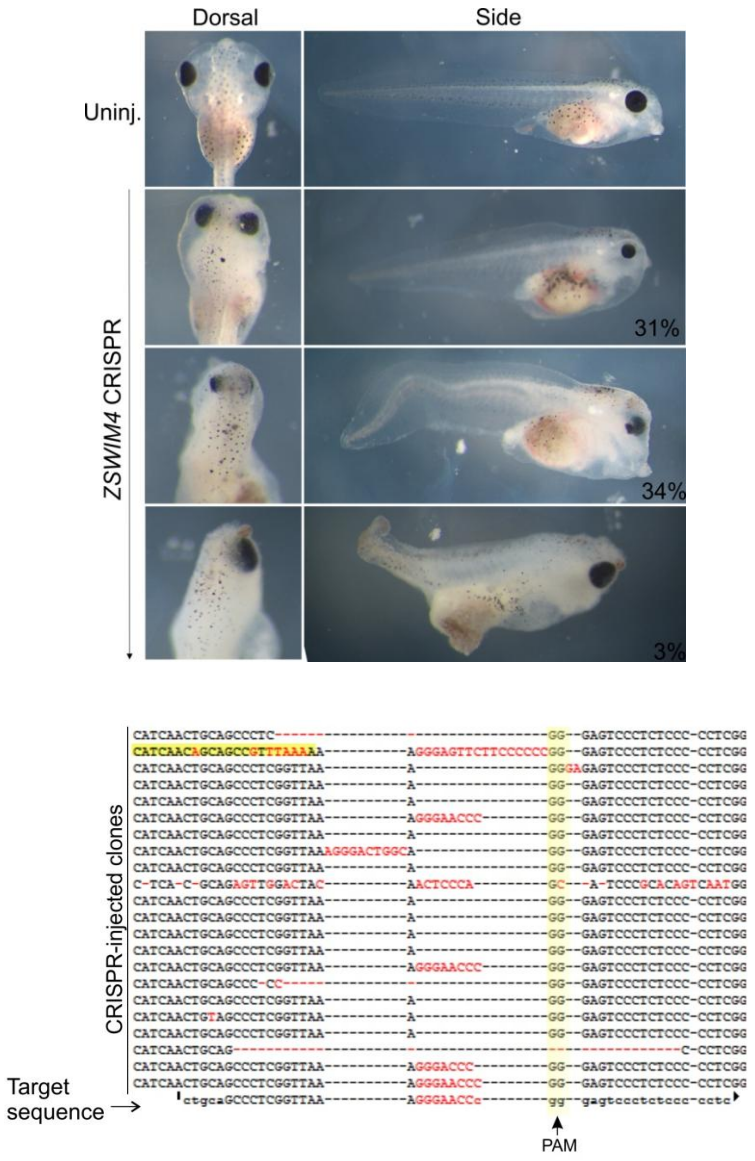

Figure 6.22 Effects of *ZSwim4* CRISPR on *Xenopus* development
600pg *ZSwim4* and 2.2ng Cas9 mRNA were co-injected into *Xenopus tropicalis* embryos at the 1 cell stage. N=31. Two thirds of embryos had narrowing of the head as shown by dorsal views and these varied in severity with some exhibiting cyclopia. 1 embryo had total cyclopia (bottom). Percentages indicate numbers of embryos resembling the representative image. As well as these defects, side views of injected embryos show there were defects in the AP axis. Alignment of the *ZSwim4* genomic CRISPR target regions against sequenced clones *Zswim4*-CRISPR injected embryos is shown below. The PAM is highlighted, around which Cas9 will bind to cause double stranded breaks. Out of 22 clones sequenced, only 3 were unchanged from the original sequence. A large insertion was found in 2 of the sequences (highlighted) and the rest had deletions

Within the target region, the CRISPR is shown in uppercase. All but three of the 22 *Zswim4* clones sequenced contained deletions in the genomic sequence. Two of the clones contained insertions (highlighted). These deletions are large enough to have a profound effect on the protein sequence to render *Zswim4* non functional. PCR was performed using primers to amplify the genomic region around the target sequence. The PCR product was T-cloned and individual clones sequenced.

Alignments of the sequenced clones against the genomic *Xenopus tropicalis* target sequence are shown in Figure 6.22.

6.3.5 Snx10 and Cited2 CRISPRs cause laterality defects

Snx10 has been previously knocked down in zebrafish and shown to cause laterality defects, as has a null murine Cited2 mutant (Lopes Floro et al. 2011; Chen et al. 2012). Therefore *Xenopus tropicalis* embryos injected at the 1 cell stage with 600pg *Snx10* or *Cited2* sgRNA and 2.2ng *Cas9* were cultured to stage 42/43 when the heart and guts are in the process of looping.

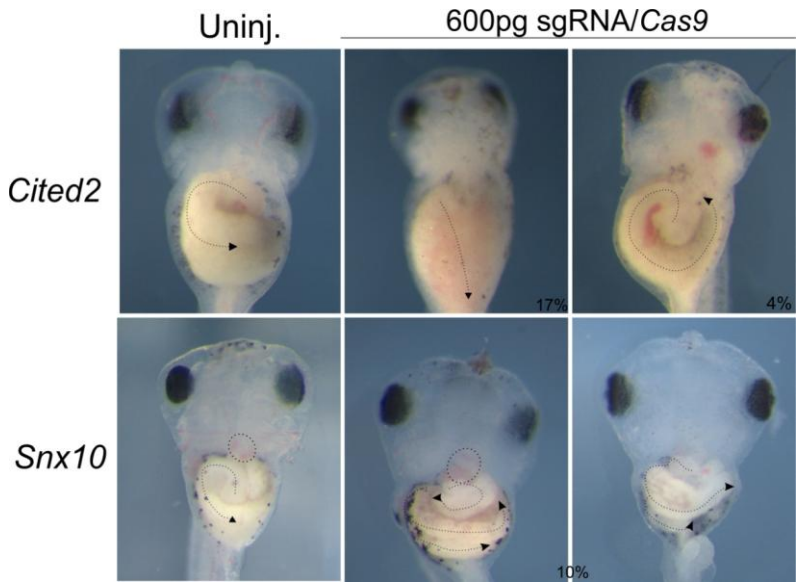

Figure 6.23 Effects of Cited2 and Snx10 knockout by CRISPR on development
600pg Cited2/Snx10 sgRNA was co-injected into *Xenopus tropicalis* embryos at the 1 cell stage and cultured to stage 42 (Cited2, n=54) or stage 43 (Snx10 n=44). Ventral views of CRISPR /Cas9 injected embryos showed a small number of embryos to have laterality defects. *Cited2* CRISPR embryos appeared normal, however a small number had either unlooped guts, or defective looping (compare with uninjected typical gut looping shown by arrow). In *Snx10* CRISPR embryos, a small number had defective gut looping compared to controls (typical gut looping direction shown by arrow). In the central image, the embryo also had *situs inversus* of the developing heart (compare dotted circles showing heart orientation). Percentages indicate embryos resembling the representative image.

A small number of *Cited2* CRISPR-injected embryos displayed either unlooped guts, or erratic gut looping suggesting laterality defects. A small number of *Snx10* CRISPR-injected embryos also displayed laterality defects in gut looping, as well as one case of *situs inversus* of the heart.

6.3.6 Sequencing of *Snx10* CRISPR-injected embryos

Embryos injected with Snx10 CRISPR were processed for sequencing using the same methods as for the Zswim4 CRISPR. Due to time constraints, sequencing for Cited2 CRISPR was not completed. Alignments of the sequenced clones against the genomic *Xenopus tropicalis* Snx10 CRISPR target sequence are shown in Figure 6.24.

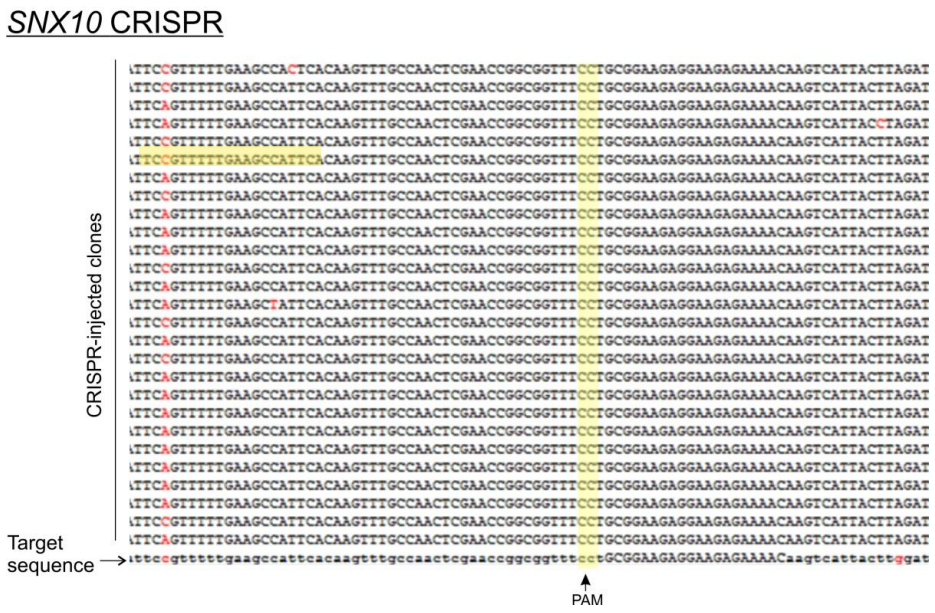

Figure 6.24 *Snx10* CRISPR alignment
Alignments of the *Snx10* genomic CRISPR target region against sequenced clones from *Snx10* CRISPR-injected embryos. The PAM is highlighted, around which Cas9 will bind to cause double stranded breaks. None of the sequenced clones for *Snx10* had a change in the surrounding sequence (PAM is reverse complimented, sgRNA is capitalised).

Unfortunately, of the 27 *Snx10* clones sequenced, none had deletions close to the PAM. A small number of clones had point mutations quite far from the PAM, and all had a C→A substitution. These however do not alter the protein sequence and given their distance from the PAM, could be simply polymorphisms. Therefore, the Snx10 CRISPR may either work at very low efficiency, reflected in the low numbers of phenotypically affected embryos, or the gut mutations be due to chance or off-target effects.

6.3.7 *Dynll1* is not an FGF targeted

Dynein light chain 1 (Dynll1) was investigated because the preliminary microarray showed it to be upregulated 2.6-fold by iFGFR1 and 2.3-fold by iFGFR2. Furthermore, RNA-seq showed *Dynll1* to be 2.3-fold upregulated by iFGFR1 and

2.5-fold downregulated by iFGFR4 and so could be an example of a gene differentially regulated by FGFRs. The function of *Dynll1* was characterised through use of a morpholino, and found to have detrimental effects on organogenesis, and function of epidermal cilia, similar to that of *Nek6* as embryos did not move around the culture dish. However, the findings of the microarray and RNA-seq could not be replicated in whole embryos using iFGFRs or dnFGFRs by RT-qPCR and ISH. The raw RNA-seq data was revisited, as it was hypothesised that maybe only a certain splice form of *Dynll1* was affected by iFGFR induction, as *Dynll1* was listed a number of times in the dataset and not always associated with a >2-fold expression change with either iFGFR. These two 'classes' of *Dynll1* were found to be associated with different sequences. Unfortunately a BLAST search revealed that the sequences of *Dynll1* that were listed as upregulated in both the microarray and RNA-seq were not in fact *Dynll1,* and were instead highly similar to apolipoprotein-C1. As this removed any connection between Dynll1 and FGF signalling, Dynll1 was not investigated further.

6.4 Discussion

6.4.1 *FoxN4, Hmx3* and *Hesx1* are negatively regulated by FGF signalling

In this chapter a number of genes were analysed from the microarray dataset that were novel putative FGF targets down-regulated by iFGFR1 and/or iFGFR4.

Hesx1, also known as *Xanf*, is a homeodomain transcription factor. It is the earliest known repressor present in the anterior neuroectoderm and is essential for the proper development of the telencephalon (Ermakova et al. 1999). These genes have been described in Chapter 3, as they are known to be required for anterior neural development and are involved in a feedback loop required for forebrain patterning and development. *Hesx1* was found downregulated by iFGFR1 and iFGFR4 by microarray, and RNA-seq results supported this finding in neuralised animal caps. This could be another example of FGF promoting posterior neural fates by repressing telencephalic development in part mediated by *Hesx1*. *Hesx1* has been functionally linked to *Ras-dva,* part of a positive feedback loop with *AGRs*, and *Otx2* which activate *FGF8,* disruption of which affects forebrain development.

Ras-dva was found by both microarray to be downregulated by iFGFR1 and iFGFR2, and by RNA-seq to be downregulated by iFGFR1, however RT-qPCR in neuralised explants and the use of dnFGFR1 produced conflicting results (data not shown). Also, knockdown of *Hesx1* in *Xenopus* has been performed previously (Ermakova et al. 2007). Therefore, these genes were not characterised functionally further.

Forkhead domain transcription factor Forkhead box N4, (FoxN4) is expressed in progenitor cells in the developing *Xenopus* and chick retina and brain (Kelly et al. 2007; Boije et al. 2013). *FoxN4* has no previously reported link with FGF signalling but its expression domain overlaps that of FGF8 in the midbrain and hindbrain as well as active dpERK regions (Kelly et al. 2007). *FoxN4* was downregulated by iFGFR4 1.58-fold in the microarray. *FoxN4* was slightly downregulated by iFGFR4 by microarray, but this was not significant upon RT-qPCR validation. However, iFGFR1 induction in whole embryos significantly downregulated *FoxN4* expression so it may be an FGFR1 target. Our preliminary data indicated that *FoxN4* was repressed by *Noggin* and further repressed by iFGFR1 induction. Further experimental repeats would be required to confirm the effect of FGFR induction upon *FoxN4*.

Hmx3, also known as *Nkx5.1,* has a role in regulating lateral line and inner ear development in zebrafish (Feng & Xu 2010). *Hmx3* is expressed in the brain, and previously found to be positively regulated, and to positively regulate FGF signalling through FGFR1 (Adamska et al. 2001). However, in the microarray-based screen *Hmx3* was found downregulated by iFGFR4. A negative regulation by iFGFR4 could therefore point to an example of differential regulation of a gene by FGFRs. Furthermore, in *Xenopus*, Hmx3 represses *Hesx1* (Bayramov et al. 2004). Overexpression as well as inhibition of *Hmx3* caused inhibition of posterior forebrain markers *Otx2*, *Pax6* and *Six3* in the developing *Xenopus laevis* forebrain due to aberrations in the balance between *Hmx3* and *Hesx1*; so *Hmx3* is important for neural development and is a good candidate for FGF regulation (Bayramov et al. 2004). Although not tested by RT-qPCR in neuralised ectodermal explants, RNA-seq did not show *Hmx3* expression to change at all upon iFGFR1 or iFGFR4. Therefore on this basis it cannot be said that *Hmx3* is a neural FGF target, but may be an FGF target in the whole embryo.

6.4.2 *Nek6* is a novel FGF target

The initial microarray, RNA-seq and validation of these data has revealed *Nek6* to be positively regulated by FGF signalling in both whole embryos and neuralised explants. Knockout of *Nek6* using a TALEN causes extreme developmental defects, and in whole embryos a loss of mesoderm and neural markers. In explants, *Nek6* knockout dampens the response of FGF targets to iFGFR1 induction. Therefore, as well as its role in the cell cycle, *Nek6* is also required for *Xenopus* mesodermal and neural development, possibly through regulation of FGF signalling.

6.4.2.1 Current knowledge about Nek6

The 11 identified vertebrate Nek kinases are serine/threonine kinases structurally related to the *Aspergillus nidulans* never in mitosis, gene A (NIMA). In *Aspergillus,* NIMA is essential for progression from G2 to mitosis, and is required for localisation of CyclinB to the nucleus (Wu et al. 1998). Nek6 is 84% similar to Nek7, and these are 80% similar to Nek9. The three Neks comprise the NIMA complex which is active during mitosis and involved in regulation of the mitotic spindle (Quarmby & Mahjoub 2005). Dynll1 is able to bind to Nek9, increasing Nek9's autoactivation potential, whilst inhibiting its ability to form a complex with Nek6 and activate it. However there is no evidence yet that this interaction takes place naturally *in vivo* (Regué et al. 2011).

Research into the localisation of Nek6 using HeLa cell extracts showed it to localise to different microtubule-based structures during mitosis, including mitotic spindles, but not the spindle poles themselves (Fry et al. 2012). HeLa cells expressing a kinase-dead Nek6 had more fragile mitotic spindle microtubules and less focussed spindle poles, which resulted in metaphase growth arrest. On this basis, Nek6 was implicated in microtubule organisation and stability during mitosis (O'Regan & Fry 2009). Furthermore, Nek6 as part of the NIMA complex was also found to control centrosome separation during prophase in HeLa cell extracts (Bertran et al. 2011). Nek9 is activated by phosphorylation in two steps involving the cyclin-dependent kinase Cdk1, and the serine/threonine kinase Plk1. Cdk1, together with CyclinB1, phosphorylates Nek9 at several sites during mitosis, allowing it to interact with and be activated by Plk1 (Bertran et al. 2011; Sdelci et al. 2011). The C-terminus of Nek9 then binds to and phosphorylates and activates Nek6 and Nek7 (Fry et al. 2012).

As Nek6 is essential for cell division *in vitro*, one could hypothesise that it would be globally expressed throughout the *Xenopus* embryo. However, *in situ* results in *Xenopus* suggest that *Nek6* is confined to discrete areas of the embryo in the somitic mesoderm, branchial arches and notochord and stage 40 TALEN-injected embryos are still alive, albeit without any recognisable features. Overexpression of *Nek6* also causes in some cases a failure to gastrulate and head defects (Figure 6.19). *In vivo* studies of Nek6 function are rare, although unpublished work referenced by Bertran et al. (2011) stated that a Nek6-/- null murine mutant was embryonic lethal. Automated ISH images on Xenbase report expression in the brain, although this was not detected here. Earlier work in mouse embryos investigating *Nek6* and *Nek7* expression suggested that *Nek6* was firstly expressed in the trophoblast and in later embryonic stages expressed almost exclusively in the CNS in the ventricular and sub-ventricular zones, whereas *Nek7* was expressed in the thalamus (Feige & Motro 2002).

Given the cell cycle roles mentioned above, it could be predicted that *Xenopus* embryos would not survive at all post MBT, as Nek6 is required for mitotic progression *in vitro* (O'Regan & Fry 2009). However, these *Xenopus* knockout data show embryos survive until at least stage 40 despite being very deformed, therefore *Nek6* must have other roles in mesodermal and neural development.

6.4.2.2 Is Nek6 a neural FGF target?

Collectively, RNA-seq and microarray results, ISH, as well as RT-qPCR show that Nek6 is positively regulated by iFGFR1 induction in whole embryos and neuralised ectodermal explants. However, ISH of *Nek6* showed it to not be detected in the CNS in *Xenopus* in this study, although as mentioned, it has been found in the developing murine CNS and on ISH data on Xenbase (community submitted image) (Feige & Motro 2002). RT-qPCR showed *Nek6* expression to be unaffected by excess *Noggin*, perhaps counting against it being a neural FGF target, however other posterior neural FGF targets such as *HoxB9* are also unaffected by *Noggin* (Roche et al. 2009).

In the raw RNA-seq data, consistently low read counts (increasing from 1-2 FPKM to 5-7 FPKM) meant that *Nek6*, although being upregulated by iFGFR1 induction 5 fold by RNA seq, did not meet filtering thresholds and therefore was not included in genelists. This could mean that it is a purely mesodermal gene, and its low read presence is a result of mesodermal cell 'contamination' from taking too-large

ectodermal explants containing mesodermal cells reacting to FGF induction. Refseq data by Tan et al. (2013) includes quantified levels of *Xenopus tropicalis* genes at all developmental stages. Betweens stages 10 and 12, *Nek6* is expressed at very low levels - ~4 RPKM, similar to the raw RNA seq FPKMs of ~5 found here. As a comparison, *MyoD*, *Cdx4* and *Xbra* are expressed at ~100, ~80 ~290 RPKM respectively (M. H. Tan et al. 2013). In this RNA seq, *Xbra* expression was increased from only 0.2 to 2 FPKM by iFGFR1 induction, MyoD from 2.7 to 6, and Cdx4 from 0.1 to 0.9 – very low read counts compared to Tan and colleagues' results. This shows that known mesodermal genes expressed at a very high level in whole embryos are predictably expressed at very low levels in neuralised ectodermal explants. *Nek6* levels are not similarly reduced. Therefore, it is possible that *Nek6* did not pass filtering conditions because it is naturally expressed at low levels, and not because it's solely a mesodermal gene not normally expressed in a neuralised explant.

Some of the data support a role for Nek6 in the CNS, as knockout of *Nek6* using a TALEN targeted to the CNS reduced eye size, as well as the expression domain of the eyefield marker *Rax*. Furthermore, ISH of embryos injected with Nek6 TALEN into dorsal cells at the 4-cell stage displayed reduced expression of MHB and hindbrain markers *En2* and *Krox20* as well as disrupted expression of the pan-neural marker *Sox3* and primary neuron marker *N-tubulin*. Even though in some cases, gene disruption could have been due to the profound gastrulation defects caused by the TALEN, in injected embryos more able to undergo gastrulation these markers were still partially or totally lost. Therefore, collectively this shows that knocking down *Nek6* may have a role directly or indirectly in neural development as well as the mesoderm.

6.4.2.3 What is *Nek6*'s function in development?

ISH on embryos injected with 2ng TALEN displayed patchy loss of *MyoD, Cdx4* and *Xbra*, suggesting that Nek6 normally has a positive effect on mesoderm development (Figure 6.15). Maybe Nek6 targets and directly influences the expression of mesodermal genes, or Nek6 knockout interferes with the FGF signalling output at this stage, perhaps via an intermediate gene or effects on other pathways, such as those regulated by TGFβ (see later). At stages where mesoderm induction is occurring, western blots showed that dpERK levels were unchanged in Nek6 TALEN-injected embryos. Therefore these effects on mesodermal genes may not be due to changes in MAPK signalling output.

However, embryos collected at early and later neurula contained higher dpERK levels compared to controls. Therefore at neurula stages, the Nek6 TALEN may affect the FGF signalling pathway to influence gene expression.

To see if the presence of Nek6 TALEN affected the normal response of known FGF targets to FGF induction, explants co-injected with *Nek6* TALEN and iFGFR1 were induced during the period of mesodermal gene action and the levels of *Xbra*, *Sprouty2* and *MyoD* investigated. For *Xbra* and *Sprouty2*, the presence of *Nek6* TALEN partially inhibited FGF-induced gene expression (Figure 6.18), and this was significant for *Xbra*. Therefore even though this is not matched by changes in dpERK at these stages, Nek6 knockout seems to dampen FGF signalling (even though TALEN-only injections increased gene expression). This could impair FGF-mediated processes during mesodermal and neural development. Further experiments using different genes at different timepoints would be needed to make this assertion more concrete.

6.4.2.4 Interaction of Nek6 with other signalling pathways

It is probable that Nek6's effects on gene expression are due to it interacting with other pathways as well as FGF. Network2Canvas analyses on iFGFR1 RNA seq data (see last chapter) identified Nek6 as being a kinase node due to its interactions with *Sgk1*;*Smad4*;*Smurf2* and *Nup98*, even though *Nek6* did not itself appear in the filtered dataset. *Sgk1* was upregulated by 5-fold by iFGFR1 and 3.5-fold by iFGFR4 induction by this RNA-seq. In the literature, Sgk1 was identified as being phosphorylated by *Nek6 in vitro* but not in rats *in vivo*, so confirming an *in vivo* interaction in *Xenopus* could be interesting (Lizcano et al. 2002). *Smurf2* (upregulated 2-fold by iFGFR1 induction) is an ubiquitin protein ligase and TGFβ signalling effector. In a high-throughput protein interaction screen to find novel TGFβ targets, an interaction between Nek6 and Smurf2 was found in mammalian cells using LUMIER (luminescence-based mammalian interactome mapping). This technology used bait –Smurf2 – fused to luciferase, which emits light when it binds to FLAG-tagged prey, and its interaction with Nek6-FLAG was significant (Barrios-Rodiles et al. 2005). However, a recent paper by Zuo et al., (2014 in press) could not show through co-immunoprecipitation experiments that Nek6 and Smurf2 co-precipitate in Hep3B cells or *in vivo* using murine antibodies. They did find however that the TGFβ effector Smad4 co-precipitated with Nek6 in these conditions, and a luciferase assay in Hep3b cells with a Smad-reponsive reporter showed that reporter transcription was inhibited in the presence of Nek6, showing Nek6 to have

a negative effect on Smad4. TGFβ/Smad4 downstream target genes such as Dapk1,p27 and p21were also inhibited by Nek6 in this paper. Mechanistically, this negative interaction was shown to work in part because Nek6 sequestered Smad4 it in the cytoplasm (Zuo et al. 2014, in press). To follow this up, RT-qPCR on whole embryos as well as animal caps treated with BMP4 protein, or expressing BMP antagonists/dominant negative Smads could be performed to investigate the effect of Nek6 TALEN on BMP signalling. Given Nek6's interaction with TGFβ, also investigating Nodal targets, such as Lefty, or activating early Nodal signalling with Activin could be useful in understanding Nek6's function in early development.

6.4.3 The use of a TALEN to investigate *Nek6*

The Nek6 TALEN was 70% efficient in producing indels in *Xenopus laevis* and 50% efficient with *Xenopus tropicalis*, although ideally more sequencing of clones from more embryos would have been performed, as was done with Snx10 and ZSwim4 CRISPR.

Ishibashi et al. (2012) were one of the first groups to use TALENs in *Xenopus*. They also used a *tyrosinase* TALEN to show TALENs produced partial or full albinos in 90% of cases in the F0 generation. It was confirmed that these mutations passed to the germ line and were inherited in the F1 generation (Ishibashi et al. 2012). Lei et al. (2012) also investigated the targeting efficiencies of a number of TALENs in *Xenopus tropicalis* and found the highest efficiency to be 90% in the F0 generation in terms of generating indels. On this basis, TALENs were hailed as a cost-effective alternative to morpholinos, and morpholinos also have varying effects as they knock down rather than knock out gene expression, and work temporarily meaning that investigating gene effects later in development is tricky (Lei et al. 2012). In my hands, the TALEN was more effective in *Xenopus laevis* than *tropicalis,* although sequencing more clones would lend more support for this. Lei et al. (2012) and Suzuki et al. (2013) compared TALEN efficiencies between *Xenopus laevis* and *Xenopus tropicalis* with conflicting results, suggesting that it may be the individual TALEN responsible for this variation, rather than the frog species.

Although TALEN mutations are long lasting and produce heritable mutations, Nakajima & Yaoita (2015) showed there to be low efficiencies in gene targeting the first few hours of development while translation of the left and right TALEN pair are taking place at the same time as rapid cell division. The efficiencies of TALENs early after injection are important to ensure early blastula effects of gene knockout

are seen. When investigating knockout of *Nek6* in early stages, or targeting the TALEN at 8-cell to the CNS, it is important that the translation and activation of the TALEN is rapid and it is inherited uniformly amongst daughter cells to ensure that all daughter cells contain working TALEN. Nakajima and colleagues improved the Tyrosinase TALEN by fusing it to a gene called *Deadsouth,* which promotes mRNA translation in the oocyte. This fusion construct was injected into *Xenopus* oocytes, which were stained with a vital dye and implanted into a host female. When the oocytes were fertilised, TALEN expression was already 52% at 3 hours post fertilisation (hpf), rising to 99% at 8 hpf. In contrast, for TALENs injected into embryos at 1-cell the indel efficiencies were 7% 4hpf, rising to 60% at 5.5 hpf and then slowly increased to 79% over 24 hours and maintained at 80%. Therefore this could possibly increase the efficiency of the Nek6 TALEN early on, but it might be represent a more demanding protocol than is practicable to perform routinely in *Xenopus*.

6.4.4 Using CRISPR to characterise FGF targets

Three novel FGF targets – *Snx10*, *ZSwim4* and *Cited2* – were picked from the RNA seq dataset to characterise neural FGF targets. All three of them produced a phenotype, albeit of variable efficiencies, and *Zswim4* efficiently caused indels.

ZSwim4 was found in an RNA-seq experiment to be upregulated in pregnant cow endometrium (Forde et al. 2012). It is not referenced elsewhere in the literature. An automated ISH image on Xenbase shows *ZSwim4* to be expressed in the *Xenopus* CNS (Karpinka et al. 2014). The ZSwim4 CRISPR caused indels at a high efficiency, 19/22 clones tested containing indels in the expected region next to the PAM. The cyclopic narrow head phenotype of CRISPR embryos is reminiscent of embryos treated with the Shh inhibitor cylopamine (Dunn et al. 1995). Therefore ZSwim4 could also have an effect on Shh signalling, and effects upon Shh pathway genes in ZSwim4 knockout embryos by ISH and RT-qPCR could be employed to test this hypothesis. FGF signalling has also been implicated in craniofacial development, as syndromes associated with defective FGF signalling such as Apert Syndrome include cleft palates. Furthermore FGFR2b and FGFR2c-null mice show multiple skeletal and facial abnormalities including premature fusion of the parietal and squamous temporal skull bones (reviewed in Nie et al. (2006). It is Wnt signalling in the ANB, particularly through Lrp6 which mediates FGF signalling in cleft palate formation (Wang et al. 2011).

Sorting nexins such as *Snx10* are characterised by the presence of a phox-homology (PX) domain and they are present in all eukaryotes with 33 members identified in humans. Snx proteins are involved in a range of processes including endocytosis, protein sorting and degradation (Cullen 2008). *In vitro*, overexpression of *Snx10* causes large vacuoles to form in the cytosol, although the functional relevance of this is unclear (Qin et al. 2006). Chen et al designed a translation blocking morpholino against *Snx10* and injected it into zebrafish embryos. Whilst the morphology of the embryos was largely unchanged, the heart exhibited randomized or reduced looping in 30% of embryos, and bilateral or reversed *spaw* expression in the KV, suggesting that Snx10 influences left/right asymmetry. Closer look at the KV revealed that the cilia number, but not length was reduced in morphants (Chen et al. 2012).

Based upon this, a CRISPR-mediated knockout of Snx10 in *Xenopus* would also be expected to cause laterality defects. Although heart looping defects were not seen, there was one observed case of heart *situs inversus* where the heart leant to the left rather than the right (Figure 6.23). Furthermore, a few embryos exhibited randomization of gut looping, another L/R regulated process. However, this was not at the higher frequency found by the morpholino. It would be interesting to see how the expression of nodal-related genes in *Xenopus* change as a response to Snx10/Cited2 CRISPR to further investigate the effects of these genes on early left/right symmetry breaking.

Cited2 (Cbp/p300-interacting transactivator, with Glu/Asp-rich carboxy-terminal domain) is a transcriptional co-activator. *Cited2* has been shown to promote the expression of anterior neural genes, such as *Otx2*, and repress the eyefield marker *Rax* and the posterior neural marker *HoxB9* (Yoon et al. 2011). In mouse embryos, null mutants of *Cited2* have heart defects caused by a perturbation of left/right asymmetry (Lopes Floro et al. 2011). Similar to *Snx10*, *Cited2* has also been implicated in left/right asymmetry. Cited2-null mouse embryos die before birth and have a range of heart defects, including abnormal heart looping and left atrial isomerism. As *Nodal, Lefty and Pitx2* were not expressed in the lateral mesoderm in null mutants, this suggested that an aspect of *Cited2* activity was required for correct left/right patterning (Weninger et al. 2005; Bamforth et al. 2004). More detailed analysis of the mutant showed that although deletion of Cited2 from the lateral plate mesoderm did not affect laterality or *Nodal* expression, Cited2 present adjacent and posterior to the Node is required to bind to the asymmetric enhancer

element of Nodal, to initiate Nodal expression. Furthermore, *Cited2* was also found to potentiate BMP signalling, counteracting the initiation of Nodal expression. Therefore very early in development, *Cited2* is required for the initiation of the Nodal cascade and its regulation via interactions with BMP.

In this CRISPR-potentiated knockdown in *Xenopus*, although at a very low frequency, a number of *Xenopus* embryos here also had laterality defects – although no heart defects were seen, gut looping was disrupted or did not take place. Sequencing the region around the PAM in these embryos would confirm this was due to new indels in *Cited2.* More detailed analyses of Snx10 and Cited2 CRISPR embryos earlier in development by looking at gene expression of Nodal-regulated genes such as *Coco, Lefty* and *Pitx1/2* could add support for Snx10 and Cited2 being required for left/right asymmetry in *Xenopus* (Schweickert et al. 2012).

6.4.4.1 Problems with CRISPR efficiency

The efficiency of the two CRISPRs tested, against *Snx10* and *ZSwim4*, were very different. Guo et al. (2014) compared the efficiency of 10 CRISPRs made in their lab against *Xenopus tropicalis* genes. In this paper they made CRISPRs against 10 genes. 6 of these had 72-100% targeting efficiency, when seen by sequencing clones. ZSwim4 therefore gives comparable rates of efficiency to this. Four CRISPRs made had very low efficiencies, which were rectified by changing the amounts of sgRNA or remaking an alternative sgRNA. Therefore CRISPR efficiencies are variable in *Xenopus*, and designing another sgRNA for *Snx10* and *Cited2* could improve the penetrance of their phenotype. This unfortunately would not be an option for *Snx10*, as the only site compatible with CRISPR design was the one chosen in the 5th exon which in itself is not optimal.

Increasing the efficiency of Cas9 could help increase the frequency of NHEJs. The two *Xenopus tropicalis* CRISPR papers published at time of writing use different forms and dosages of Cas9. Nakayama et al. (2013) compared bacterial Cas9, used in Guo et al. (2014) and a humanised form of Cas9 which is optimised for use in mammalian systems and has been successfully used in the zebrafish and in this study (Chang et al. 2013). The 'human'Cas9 injected at 2.2ng gave a much higher rate of albinism when co-injected with *Tyrosinase* sgRNA than bacterial Cas9. However, the optimal dosage of bacterial Cas9 was found to be just 300pg for Guo and colleagues which gave equivalent efficiencies. Therefore it is unclear which Cas9 form is best to use, although the 2.2ng dosage used for this study was the

maximum practicable to inject into *Xenopus tropicalis* embryos. A drawback to the CRISPR and TALEN system is that it relies on several injected mRNAs injected at 1-cell to be rapidly translated and inherited evenly when cells divide. Injecting the sgRNA with recombinant Cas9 protein could improve the efficiency of CRISPRs and partially get round this problem, which has been done by Gagnon et al, (2014).

6.4.5 *Dynll1* is not an FGF target

Dynein light chain 1 (Dynll1) is a component of the Dynein motor complex and involved in the trafficking of molecules around the cell. In cytoplasmic dynein, two Dynll1 molecules interact with dynein intermediate chain, inducing dimerisation and organisation of the dynein complex (Regué et al. 2011). Dynll1 was investigated because the preliminary microarray showed it to be upregulated 2.6-fold by iFGFR1 and 2.3-fold by iFGFR2. Furthermore, RNA-seq showed *Dynll1* to be 2.3-fold upregulated by iFGFR1 and 2.5-fold downregulated by iFGFR4 and so could be an example of a gene differentially regulated by FGFRs. It is also functionally linked to Nek6 through its interaction with Nek9 (Regué et al. 2011). Based upon this, *Dynll1* was functionally characterised with the use of a Morpholino, and results are in Appendix 8.1. However, 'Dynll1' was found to be misidentified in microarray and RNA-seq due to an errant entry on Unigene, and BLAST searches identified it as *ApoC1*. This explained why these results could not be replicated by RT-qPCR and ISH using primers and morpholinos made against the actual *Dynll1*.

This also happened with *Zfp36L1*, which was identified by RNA-seq as being upregulated by iFGFR1 and this was validated by RT-qPCR. In addition to this, the RNA-seq found induction of iFGFR4 to cause downregulation of *Zfp36L1*. Comparison of the sequence files to ascertain whether this differential regulation of *Zfp36L1* was down to differences in splicing showed that the iFGFR4-associated sequence for *Zfp36L1* was not in fact *Zfp36L1* as BLAST searches did not show alignment to a recognised gene.

This highlights the importance of double-checking sequences of genes of interest before characterising them further, as there are evidently errors in *Xenopus* gene annotation.

6.4.6 Further work and conclusions

In this Chapter Nek6 has been identified as a novel FGFR1 target in *Xenopus.* *Nek6* knockout caused a loss of mesodermal and neuroectodermal genes. During neurula stages, *Nek6* knockout caused an increase in dpERK levels, suggesting a feedback interaction with FGF signalling. Furthermore, *Nek6* knockout impaired the ability of known FGF targets *Xbra* and *Sprouty2* to respond to FGF induction by iFGFR1. Therefore *Nek6* has important developmental roles during *Xenopus* development in addition to its well-documented roles in the cell cycle. Further work to identify interacting pathways and *Nek6* knockout effect on mesodermal and neural gene function could give a better understanding of its role in *Xenopus* development. The aspect of *Nek6* phenotype that would be interesting to investigate further in this study was the movement phenotype which is probably caused by defective cilia. It would be interesting to find out if the knockout causes a loss of cilia, or defects such as shortening which render them unable to beat. This could be done using an antibody against alpha tubulin to visualise cilia and their movement by live fluorescent imaging. It would be optimal to investigate cilia defects in the GRP, but TALENs would have to be targeted to this structure as the severe phenotype would make it difficult to study.

Characterisation of genes found in the RNA-seq dataset through knockout by CRISPR also produced phenotypes in novel FGF target genes *Snx10* and *Cited2* which displayed laterality defects, and *Zswim4* which when knocked out causes defects in head development. The next steps for *Snx10* and *Cited2* would be to try and increase their efficiency, and then see what effect CRISPR mediated knockout of these had on other cilia and nodal related genes. There were other genes implicated in cilia and left right patterning in this study, such as *Atp6V0c* and *Ift172* which would also be interesting to investigate by CRISPR. Lastly there are other examples of genes like *ZSwim4* which are very scarcely mentioned in the literature, such as *Ikzf2* and *Zfp36L1* of which their developmental functions are unknown. Further characterisation of *Zswim4* by investigation of its interaction with other signalling pathways, as well as other unknown targets would give a greater insight into the processes FGF signalling is involved with during neural development.

7 General Discussion

7.1 Summary

The microarray and RNA-seq based screens undertaken during this project showed that activation of iFGFR1-4 affected many genes during periods of early neural development. These datasets showed that each iFGFR had very different signalling outputs, as there was little overlap between the genelists for each gene. Therefore, different FGFRs must function independently and cooperate to specify and pattern the CNS. As well as genes known to be involved in neural development and/or expressed in the developing CNS, genes involved with other signalling pathways, particularly Wnt signalling, as well as genes implicated in other developmental processes such as laterality, cell cycle and anterior CNS development were affected by FGF induction. Some novel FGF targets found as a result of these screens were characterised further. TALEN-mediated knockout of one of these, *Nek6,* affected the expression of several mesodermal and neural markers. In addition, loss of Nek6 appeared to interfere with the ability of iFGFRs to affect gene expression. CRISPR-mediated knockout of putative FGF targets *Cited2* and *Snx10* lent support for these genes in being involved in laterality, and a CRISPR specific to *ZSwim4*, a gene of unknown function, caused cyclopia and defects in the anterior CNS. Therefore, FGFRs have a range of effects that change the transcriptome and eventual phenotype of *Xenopus* embryos when induced.

Taken as a whole, the data also confirms FGF signalling as important for neural induction, patterning of the developing CNS, and also neurogenesis itself. FGFs have long been known to be required for posterior neural development. As well as *Cdx* and *Hox* genes found in the microarray screen, genes such as *FoxA4, FoxB1* and *FoxD4l1.1* that have previously been implicated in posterior neural induction and inhibit genes associated with anterior neural development were found upregulated by iFGFR1 by RNA-seq (Martynova et al. 2004; Takebayashi-Suzuki et al. 2011; Neilson et al. 2012). Interestingly, iFGFR4 induction in neuralised animal caps was shown to negatively affect other anterior CNS genes such as *Otx2, Hesx1, Shisa2* and *Agr2,* which are all part of a positive feedback loop with Fgf8 in

the ANB (Tereshina et al. 2014). This suggests a role for FGFR4 in promoting a posterior neural fate whilst Fgf8 in the IsO and ANB regulates anterior neural development, which would be interesting to investigate further. Another role for iFGFR4 could be in eye development, as a number of genes previously implicated in this process were found by the RNA-seq based screen. *Gnb3, Crx* and *Rax* were all downregulated, and *Frs3* and *Hes2* upregulated by iFGFR4 induction. This suggests that although iFGFR4 behaves differently than iFGFR1 in its effects on MAPK signalling and development, it has distinct and important effects upon neural development. There are also genes such as the novel putative iFGFR1 target, *ZSwim4,* found by RNA-seq which when knocked out produces cyclopia where FGFs mechanistic influence is more unclear. Similarly, *Nek6* affects mesodermal and neural development when knocked out but why this happens is still unclear. Further characterisation of these novel iFGFR1 and iFGFR4 targets will give greater insights into other ways FGF signalling impacts neural development.

7.2 Further work

7.2.1 Potential future additions to RNA-seq work

Ideally, all iFGFRs would have been investigated in this study, and a biologically replicated RNA-seq experiment performed in order to fully compare and contrast differences in signalling output between the different iFGFRs during early neural development. This may have in turn made for easier and more reliable dataset validation and the formation of stronger conclusions from ontological analyses. In particular, it would be interesting to compare the differences between iFGFR1 VT+ and VT- targets, as it is unclear if what role, if any, VT- isoforms of FGFRs have in *Xenopus* development. Furthermore, it is known that FGFR3 is expressed in the CNS in later neural development, but the microarray analysis suggested it predominantly functioned in other cellular processes during the time period investigated (Lea et al. 2009). Therefore, inducing iFGFRs during later periods of neural specification may reveal if iFGFR signalling in the CNS changes over time.

The RNA-seq data contains information that has not been analysed in this study, including the many ‘Unknown’ hits, and information relating to the ‘A’ and ‘B’ forms of each gene, as well as any non-coding mRNAs that may have been sequenced. Further analyses of A and B forms of each gene, which will be more feasible when the *laevis* genome improves would be interesting, and enable a better insight into

gene evolution and function. In order to analyse the 'unknown' files, the original sequence would have to be sourced. This proved difficult as the sequence data contributing to the Mayball longest cDNA library is no longer available, and the Mayball search engine only recognises the gene name, and not the read name attached to each gene. Due to time constraints, this was not investigated further although could yield interesting results and novel transcripts if investigated at a later date. As there was a high level of sequencing depth in this study, it is possible that miRNAs and ncRNAs are present in this data. To affirm this would require more in-depth data processing and re-alignment of the sequencing data, and may not yield optimal results as the fragmentation and library preparation protocols were optimised for longer fragments of RNA. The protocol for finding smaller RNAs selects RNA fragments of only ~24 bp and makes libraries of these, which would exclude the longer fragments which were used for library preparation in this study (Harding et al. 2014; Hafner et al. 2008). Nevertheless, it could be possible to see if miRNAs are present in their mature form in the sequenced fragments by aligning them to the *Xenopus tropicalis* collection of known miRNAs on miRBase (www.mirbase.org) to see if there are any miRNAs or other short RNAs present before proceeding further. Lastly, there may be different splice variants of genes present in the data, particularly those that feature in the genelists more than once. A disadvantage of using a non splice-aware read mapper during sequence alignment means that no novel splice junctions will be found, and use of a longest cDNA library to align reads to may make this impossible, but further investigation into this dataset could give an insight into how FGF signalling might regulate splicing during neural development, and what functional implications this has.

7.2.2 Characterisation of novel iFGFR signalling targets

In this project Nek6 has been identified as a novel FGFR1 target in *Xenopus. Nek6* knockout caused a loss of mesodermal and neuroectodermal genes, and a possible effect upon FGF signalling itself. Therefore *Nek6* has important developmental roles during *Xenopus* development in addition to its well-documented roles in the cell cycle. Further work to identify interacting pathways and *Nek6* knockout effect on mesodermal and neural gene function could give a better understanding of its role in *Xenopus* development. The aspect of *Nek6* phenotype that would be interesting to investigate further in this study was the defective movement phenotype which is probably caused by defective cilia. It would be interesting to find out if the knockout causes a loss of cilia, or defects such as shortening which render them unable to

beat. This could be done using an antibody against alpha tubulin to visualise cilia and their movement by live fluorescent imaging. It would be optimal to investigate cilia defects in the GRP, but TALENs would have to be targeted to this structure as the severe phenotype would make it difficult to study.

Characterisation of genes found in the RNA-seq dataset through knockout by CRISPR also produced phenotypes in novel FGF target genes *Snx10* and *Cited2* which displayed laterality defects, and *Zswim4* which when knocked out causes defects in head development. The next steps for *Snx10* and *Cited2* would be to try and increase their efficiency, and then see what effect CRISPR mediated knockout of these had on other cilia and nodal related genes. There were other genes implicated in cilia and left right patterning in this study, such as *Atp6V0c* and *Ift172* which would also be interesting to investigate by CRISPR. Lastly there are other examples of genes like *ZSwim4* which are very scarcely mentioned in the literature, such as *Ikzf2* and *Zfp36L1* of which their developmental functions are unknown. Further characterisation of *Zswim4* by investigation of its interaction with other signalling pathways, as well as other unknown targets would give a greater insight into the processes FGF signalling is involved with during neural development.

7.3 Can the effect of iFGFR induction in *Xenopus* be extrapolated to mammals?

Although manipulation of FGF signalling in this study was investigated in the frog, the function of individual FGFRs has also been investigated in mice in several knockout studies.

An FGFR1-/- mouse was made by Yamaguchi et al (1994), and was found to be embryonic lethal between E7.5 and E9.5, due to severe gastrulation defects and shortened egg cylinders. FGFR1 mutants were generally smaller, lacked somites and had smaller neural folds and heads than wild type controls. This is similar to dnFGFR1 *Xenopus* phenotypes (Enrique Amaya et al. 1991). Mesodermal cells in FGFR1 -/- mouse embryos accumulated in the primitive streak, and axial mesoderm was expanded at the expense of paraxial mesoderm (Yamaguchi et al. 1994). These morphological defects were found to be caused by a blockage of epidermal to mesenchymal transition in primitive streak cells through loss of FGFR1-mediated regulation of *Snail1* and *E-cadherin* (Ciruna & Rossant 2001). Interestingly in this RNA seq screen, *Snail1* was found downregulated by iFGFR1 -2.8x, and *E-cadherin*

downregulated by iFGFR4 -1.8x, which is different from the mouse data, although the regulation of these genes in neuralised ectoderm versus mesoderm may be different.

The phenotype of FGFR2 knockout mice is also severe, with homozygous embryos dying before implantation due to defects in visceral endoderm differentiation and a lack of growth of the inner cell mass (Arman et al. 1998). Conditional knockout of FGFR2 in radial glial cells – the primary progenitors of neurons in the dorsal diencephalus – is not lethal, but knockout mice display a decrease in hippocampal volume and have problems with learning and memory in later life (Stevens et al. 2012). Anatomical analysis of these knockout mice showed that FGFR2 is necessary for the formation of the correct number of excitatory neurons in the cerebral cortex and medial prefrontal cortex of the mouse brain (Stevens et al. 2010).

In comparison, FGFR3 knockout mice survive longer than FGFR1 and FGFR2 knockout mice, but are characterised by skeletal defects, such as kyphosis, scoliosis, crooked tails and curvature of long bones and vertebras (Colvin et al. 1996). FGFR3 has also been shown to be required for correct brain development, as FGFR3 knockout mice are characterised by having a smaller forebrain (particularly the telencephalon), cerebral cortex and hippocampus. These mice also had changes to the projections of their GABAergic neurons (Moldrich et al. 2011). It would be interesting to further characterise the phenotype of the CNS in induced iFGFR3 *Xenopus* embryos, as most embryos had misshapen heads, deformed eyes and larger cement glands compared to controls. The microarray and RNA seq based screens presented here did not reveal a role for FGFR3 in early neural development, possibly as the time window investigated was too early. From mid-neurula stages there is evidence to suggest that FGFR3 is concentrated in the developing brain in *Xenopus tropicalis* (Pope et al. 2010; Lea et al. 2009). Therefore, if iFGFR3 was induced later in development, its effect upon neural development might be easier to observe.

A major point of difference between the findings of this project in *Xenopus* and studies in mice is in the effects of disrupting FGFR4. Homozygous FGFR4 knockout mice consistently develop normally with only a small decrease in body weight at weaning found (Weinstein et al. 1998). The only detectable phenotype found in FGFR4 knockout mice is an arrest in muscle regeneration after injury and

replacement of injured muscle with fat and calcifications (Zhao et al. 2006). This agrees with findings in the chick where inhibition of FGFR4 lead to arrest of muscle progenitor differentiation (Marics et al. 2002). This contrasts with the severe developmental defects seen in *Xenopus* after injection of dnFGFR4a, including a failure of gastrulation, posterior truncations, as well as defects in telencephalon and eye development (Hardcastle et al. 2000; Hongo et al. 1999). dnFGFR4 also drastically altered the *Xenopus* transcriptome in a microarray based screen searching for mesodermal FGF targets (Branney et al. 2009). It is important to note that dnFGFR4 does not specifically knock down FGFR4, and so its effects may be due to the partial knockdown of other FGFRs (Ueno et al. 1992; Branney et al. 2009). However, although this investigation induced FGFR4-mediated signalling instead of repressing it, iFGFR4 induction caused definite changes to the embryonic transcriptome and phenotype, as embryos displayed misshapen heads, in some cases a failure of neural tube closure, defects in eye development and a shortened anteroposterior axis. This could mean that FGFR4 is only detrimental to development when constitutively active, or it is possible that the signalling role of FGFR4 is not conserved between *Xenopus* and mammals.

These possible discrepancies could be an example of a limitation of using Xenopus in the context of understanding mammalian development and FGF signalling. However, data from the other FGFR mouse knockout studies seem to be more in keeping with what is known already about *Xenopus* FGF signalling. Therefore, this work in *Xenopus* is hopefully useful for adding to knowledge about mammalian FGF signalling in development and disease.

7.4 FGF misregulation in human development

Understanding how FGF affects development on a molecular and anatomical scale is important for our understanding of a number of human developmental disorders which have been previously shown to centre on defective FGF signalling.

7.4.1.1 Gain-of-function of FGFR2 causes Craniosyntosis

Apert syndrome (AS) is characterised by craniosyntosis, which is the premature fusion of the coronal sutures. In babies, this causes facial abnormalities and megaencephaly, and effects on other parts of the body are seen such as syndactyly in both upper and lower limbs (Johnson & Wilkie 2011). Nearly 100% of people with

AS carry one of two mutations on FGFR2, with 70% carrying a S252W gain-of-function mutation (Aldridge et al. 2010; Yeh et al. 2013). A similar craniosyntosis syndrome without the syndactyly phenotype – Crouzon Syndrome – is also caused by over-activation of FGFR2 during development, by the formation of a disulphide bridge between receptor monomers causing constitutive dimerisation and activation of the receptor (Neilson & Friesel 1995). An AS mouse model has been made, with mice showing craniofacial dysmorphologies similar to humans diagnosed with AS. In addition to brain development being negatively impacted by defects in skull development, the AS FGFR2 mutation also caused aberrant brain morphologies independent of the skeletal defects. AS-mutant mouse brains had shorter rostrocaudal and longer dorsoventral axes, as well as showing severe cerebral asymmetry in some cases (Aldridge et al. 2010). Another group found that AS mutant FGFR2 expressed in endothelial cells of the blood vessels in the brain had defects in their vasculature, which the authors hypothesised contribute to the pathophysiology of AS (Yeh et al. 2013). Therefore a tight control of FGFR2 expression during brain development is needed for the coordination of skull and brain development, and investigation into FGFR2 targets could help us to understand how AS-associated pathologies develop.

7.4.1.2 FGFR3 gain-of-function in skeletal development

FGFR3 has been associated with bone development, as it is a key regulator of growth and differentiation during the process of endochondral ossification (Colvin et al. 1996). FGFR3 is expressed in resting and proliferating cartilage undergoing endochondral ossification and normally inhibits bone growth, with FGFR3 knockout mice displaying overgrowth of long bones due to an increase in chondrocyte proliferation (Colvin et al. 1996; Moldrich et al. 2011). A gain-of-function of FGFR3 is seen in humans with Achondroplasia. The mechanisms underpinning how this links to pathology has been investigated using a mouse model. In these AS-like mice, it was shown that FGFR3 inhibits chondrocyte differentiation through upregulation of *Smurf1.* In this RNA-seq based screen, *Smurf2* was found to be upregulated 2x by iFGFR1. Smurf1 causes an increase in the degradation of the BMP receptor BMPR1, which would otherwise stimulate the differentiation of chondrocytes (Qi et al. 2014). Thus, regulation of FGFR3 is important for correct skeletal development. Although outside the scope of this study, it would be interesting to see if *Xenopus* embryos treated with iFGFR3 display any skeletal defects as tadpoles, although it would be difficult to treat embryos with AP20187 as they grow large enough to swim and injected iFGFR mRNA and its protein would

eventually degrade. Thus a transgenesis approach may have to be employed in this instance.

7.4.2 Pathologies stemming from FGF misregulation in the human CNS

As can be seen from the phenotypes in *Xenopus* in this project, as well as in the mouse knockout studies described above, the disruption of FGF signalling causes problems with CNS development. Investigation of the long-term effects of iFGFR induction upon the brain and behaviour of feeding tadpoles was outside the scope of this project but as referenced above, FGFR knockout mice have smaller hippocampi, a region associated with mental illness. Several studies in mice and case studies in humans have shown a possible link between FGF mis-regulation in the hippocampus and FGF signalling in disorders such as schizophrenia, major depression and bipolar disorder.

An SNP upstream of human FGFR1 has been associated in a Genome Wide Association Study (GWAS) to confer a risk of developing schizophrenia (Shi et al. 2011). Other GWASs have identified two different SNPs upstream of FGFR2, one significantly associated with schizophrenia, and the other with Bipolar Disorder (O'Donovan et al. 2009; Wang et al. 2012). ISH on frontal cortices and hippocampi of human subjects that suffered from major depression and schizophrenia found there to be a higher percentage of *FGFR1*-positive cells in these regions in their brains (Gaughran et al. 2006).

Mice expressing dnFGFR1 under the control of an *Otx1* promoter displayed reductions in total brain size, particularly in the frontal and temporal regions, reminiscent of brains of people diagnosed with schizophrenia. The behaviour of these mice was also altered with hyperactivity and compulsive head movements (Shin et al. 2004). Other dnFGFR1 mutant mice displayed deficits in prepulse inhibition – a lack of response to a startle stimulus after a smaller previous stimulus. Deficits in Prepulse inhibition is another trait shared by schizophrenia patients, correlating with symptom severity (Terwisscha van Scheltinga et al. 2013). A functional reason for these traits is thought to be an imbalance between excitatory glutamergic neurons and inhibitory interneurons, as well as over-activation of the dopamine system, imbalances of which are found in those diagnosed with schizophrenia and autism (Shin et al. 2004; Marín 2012).

Therefore as well as the severe human pathologies of FGF signalling misregulation in the whole body during development, recent research has shown defective FGF signalling in the mammalian brain could contribute to serious illness. Therefore, the more that is known about FGF signalling networks during neural development, the more we might know about the reasons for FGF-related pathologies and potential therapeutic targets.

7.5 FGF signalling, cilia and laterality in the CNS

7.5.1 Consequences of defective ciliogenesis in human development

In both microarray and RNA-seq datasets, a number of genes associated with ciliogenesis and/or laterality were identified as putative iFGFR1 or iFGFR4 targets.

Ciliated cells are found throughout the body. Non-motile cilia function as mechano- or chemosensors and detect changes in the surrounding environment. Defects in non-motile cilia in humans are responsible for Polycystic Kidney Diseases in adults, and childhood-onset Autosomal recessive Polycystic Kidney Disease (ARPKD). These conditions are caused by mutations in the *Polycystin1/2* or *PKHD1* (reviewed in Badano et al. 2006). Renal mechanosensory cilia that are immotile as a result of these mutations cannot maintain homeostasis of renal epithelial cells or detect renal flow. It is thought this loss of environmental information causes abnormal cell proliferation and production of renal cysts, leading to eventual kidney failure (Nauli et al. 2003).

Motile cilia include those with planar motion and are present on a cell surface in large numbers, often beating in an uncoordinated manner. These are important in airways to waft mucus and foreign substances towards the mouth for removal, and in the reproductive system (Powles-Glover 2014). Primary Ciliary Dyskinesia (PCD) is a condition in humans caused by ciliary dysfunction due to absence of dynein arms in the axoneme. People with PCD are characterised with widening of the bronci (bronchiectasis), sinusitis and infertility. When these symptoms also coincide with laterality defects, it is known as Kartagener syndrome (reviewed in Badano et al. 2006). *Ruvbl2*, found by RNA-seq to be downregulated by iFGFR1, has been shown to be essential for cilia motility and to interact with the zebrafish PCD protein

- *Ruvbl2* mutant embryos contained axonemes with fewer dynein arms and embryos displayed kidney cysts (Zhao et al. 2013). As previously discussed, the laterality organs – the GRP in *Xenopus* – contain cells with a single polarised rotary cilia responsible for leftward fluid flow thought to break left right asymmetry. Mutations in *Nde1*, *Snx10*, and *Ift172* found by this RNA-seq based screen have been previously shown to cause laterality defects, so may also have implications in human development and ciliopathies (Kim et al. 2011; Chen et al. 2012; Gorivodsky et al. 2009).

7.5.2 Wnt and Shh signalling pathways, with possible FGF input, are needed for cilia function

Wnt and Shh signalling are also involved in, and require, cilia and ciliogenesis. The microarray and RNA-seq based screens undertaken in this project identified a number of components of these pathways previously implicated in cilia and/or laterality defects.

Non-canonical Wnt signalling is required for planar cell polarity (PCP) signalling at the level of Dishevelled, which is recruited to the basal body by *inversin* in response to activated Frz (Lienkamp et al. 2012). Both *Dvl3* and *Frz* were downregulated by iFGFR1 and iFGFR2 in the microarray-based screen. This interaction between *inversin* and *Dvl3* is required for polarisation of cilia at the plasma membrane, and *inversin* mutations in mouse embryos cause laterality defects (Okada et al. 1999). *Vangl2*, upregulated by iFGFR4 in the RNA-seq based screen is also a member of the PCP pathway, and shown to be responsible for the polarity of the KV cilia in zebrafish; *Xenopus Vangl2* morphants display heterotaxia as a result of PCP signalling disruption (Vandenberg et al. 2013; May-Simera et al. 2010). In zebrafish, Vangl2 has been shown to functionally interact with *Bbs8* at the basal body. Mutations in *Bbs8* cause Bardet‑Biedl syndrome in humans – a disorder that has many symptoms, but often includes those of ciliopathies such as *situs inversus* and reproductive tract anomalies (May-Simera et al. 2010).

Shh signalling is also localised to the cilium, as until Shh binds Ptch1, Ptch1 inhibits Smoothened by preventing its translocation to the cilium. Upon Shh binding, this inhibition is relieved allowing Smo to move to the tip of the cilium and signal (Powles-Glover 2014). *Shh*, *Ptch2*, and *Smo* were listed as upregulated by iFGFR1 and/or iFGFR2 in the microarray-based screen, and so FGF signalling could influence this process. Regulation of Shh signalling is important in the context of

ciliopathies as loss of cilia changes Shh signalling, and changes to Shh signalling itself causes skeletal abnormalities through changes to cilia intraflagellar transport proteins and basal body protein complexes (Powles-Glover 2014). Ciliary proteins are also required in neural tube development, and *Intraflagellar transport 2* (*Ift172*) – found upregulated by iFGFR4 and downregulated by iFGFR1 in this RNA-seq – was functionally characterised in a mouse mutagenesis screen to find targets of *Shh* signalling. *Ift172* mutants had greatly reduced *Ptch1* expression and as well as having laterality defects, embryos resembled *Shh* mutant embryos that lacked ventral neural cell types and an open neural tube (Huangfu et al. 2003).

There is evidence to suggest that embryonic asymmetry is set up much earlier than the formation of cilia, as maternal ion channels and proton pumps are found asymmetrically located in *Xenopus* embryos from the 4-cell stage. These propagate gradients in pH and voltage across the embryo (Vandenberg et al. 2013). *Atp6V0C*, a component of V-ATPase and found upregulated by iFGFR1 is also implicated in laterality in its own right, as it is asymmetrically located in the ventral right blastomere at the 4-cell stage, localised to Rab11 (Vandenberg et al. 2013). Expression of a dominant negative Rab11, or pharmacological inhibition of Atp6V0C both caused consistent heterotaxia in *Xenopus* embryos (Vandenberg et al. 2013; Adams et al. 2006).

Therefore, defects in cilia are important to understand as they are responsible for a variety of disorders in humans when they are non-functional. FGF signalling may feed into ciliogenesis at a number of steps, firstly in being directly important for cilia number and length in the node as described in previous chapters, as well as through targets identified in this RNA-seq screen and crosstalk with other signalling pathways.

7.6 FGF signalling and neural asymmetry

As the RNA-seq screen was based upon neuralised animal cap explants, perhaps the laterality-related genes found in this screen are also required for neural asymmetry. Laterality in the brain and CNS has been mainly studied in zebrafish embryos. Nodal signalling, as well as its role in breaking symmetry in the paraxial mesoderm, is also transiently activated on the left-hand side of the zebrafish brain (Rebagliati et al. 1998). Other Nodal pathway effectors such as *Lefty1* and *Pitx2* and in the fish, Nodal-related laterality genes such as *Cyclops* and *Oep,* are

expressed on the left side of the brain only (Rebagliati et al. 1998; Concha et al. 2000). A loss of Nodal and downstream signalling leads to randomisation of the laterality of the pineal organ, which is normally located on the left-hand side of the zebrafish epithalamus (Concha et al. 2000). In fish and amphibians, the pineal organ is photoreceptive and formed before the lateral eyes. In the adult organism the pineal organ has endocrine roles and involved in circadian rhythm. The parapineal organ of unknown function, is adjacent to the pineal organ and together they form the pineal complex (Halpern et al. 2005). The pineal complex asymmetrically influences the gene expression and development of the adjacent region of the brain, the left habenular. The habenular nuclei relay telencephalic input to the midbrain, and the left and right habenular nuclei project along distinct paths along the dorso-ventral axis (Sutherland 1982). There are also left/right differences in cell morphology and packing density in the left and right epithalamus, as well as differences in neuron calcium responsiveness and neurotransmitters emitted (Gamse et al. 2003). A loss of *Cyclops* or *Oep* expression in the epithalamus results in zebrafish embryos with bilaterally symmetric *Nodal* expression, and randomised orientation of the pineal and habenular complexes as a result (Concha et al. 2000; Gamse et al. 2003).

FGF signalling is thought to play a role in this laterality process, as FGFR4 is known to be expressed in the parapineal cells. In zebrafish FGF8 (*ace)* mutants, migration of the pineal complex to the left did not occur. This was rescued after the addition of an FGF8-soaked bead to the epithalamus (Regan et al. 2009). *Ace* mutants were also found to have fewer parapineal cells and an increase in the proportion of photoreceptor cell types. Therefore, as well as influencing the Nodal cascade and laterality in the brain, FGFs also influence cell fate (Clanton et al. 2013).

Neugebauer & Yost, (2014) recently found further evidence to support the requirement of FGF signalling for the asymmetry of the pineal complex. Inhibition of FGF signalling through application of the drug SU5402 caused bilateral expression of *Cyclops* and *Lefty1*, and a conditional constitutively active FGFR (caFGFR) caused a loss of *Lefty1* expression in the brain. Interestingly, this was independent of the earlier Nodal cascade signalling in the lateral plate mesoderm (Neugebauer & Yost 2014). FGF signalling in the zebrafish epithalamus was also found to regulate the transcription factors *Six3* and *Six7*, previously found to be required for zebrafish brain asymmetry (Inbal et al. 2007). Lastly, FGF signalling was found to have another role in the formation of a midline structure in the forebrain marked by β-

catenin. This is analogous to the physical midline provided by the neural tube and notochord in the left and right lateral plate mesoderm. Expression of caFGFR or inhibition of FGF signalling through application of SU5402 caused complete loss, or disruption and expansion of the telencephalic midline, respectively (Neugebauer & Yost 2014).

These findings suggest that genes found in this screen by RNA-seq, such as *Lefty* and other genes such as *Pitx2* found in the microarray-based screen may have roles in *Xenopus* neural asymmetry as well as in the lateral plate mesoderm, and FGF signalling may feed into this process at a number of levels. Although perhaps coincidental, the presence of FGFR4 in the pineal complex found by Regan et al. (2009) is also interesting, as 'Circadian Clock System' genes were significantly enriched in the iFGFR4-upregulated genelist as shown by PANTHER pathway analysis. Examining the role of FGF signalling later in neural development using iFGFRs could confirm this, as the time window of neural development investigated in this project is much earlier than the developmental events described here. There were other genes implicated in cilia and left right patterning in this study, such as *Atp6V0C* and *Ift172* which would also be interesting to investigate by CRISPR to see if they produced laterality or ciliary defects. More detailed analyses of the brains of *Snx10* and *Cited2* CRISPR embryos would be useful to see if brain laterality defects occurred as well as the randomised gut looping that suggested problems with laterality in the LPM.

Learning about laterality in the brain and the signalling processes involved is beneficial, as there is increasing evidence to suggest that alterations of L/R asymmetries in the human brain are correlated with autism, dyslexia, schizophrenia and depression (reviewed in Taylor et al. 2010). For example, a recent study on post-mortem brains of patients with depression revealed a right-sided reduction in habenular volume, cell number and cell area (Ranft et al. 2010). Therefore, the FGF-mediated asymmetry of the epithalamus described in the fish could have important implications for human mental health diagnoses and treatments. The more that is known about early signalling events and genes active in determining brain laterality, the better these pathologies and how to treat them could be understood.

7.7 Conclusions

The microarray and RNA-seq based screens undertaken in this project revealed many genes to be affected by FGF signalling during early neural development. Further characterisation of genes discussed here by TALEN/CRISPR could give a greater insight into FGF's roles in neural induction and patterning, as well other developmental processes occurring at the same time. It would also be interesting to investigate the effects of iFGFR2 and 3 in neuralised ectodermal explants as well as comparisons between the iFGFR1 VT- and iFGFR1 VT+ -affected transcriptome. Now that the depths of sequencing using the Illumina technology is known, biological repeats of the neuralised animal cap iFGFR induction assay using these other iFGFRs could be performed relatively quickly if time and resources allowed. These additional analyses would provide a more comprehensive view of FGF signalling in neural development, and further explore the differences in signalling output between the different FGFRs.

Knowledge about global FGF targets and gene networks it regulates could help give further insights into FGF signalling and associated developmental disorders in humans, of which there are still gaps in the understanding of how FGF misregulation contributes to phenotypes. Understanding cell signalling in development is also important to the understanding of cell signalling in stem cells, tissue regeneration and cancer. Therefore, research into how FGF signalling affects these processes, directly and through interaction with other signalling pathways could give clues as to how these phenomena arise and can be treated.

8 Appendices

8.1 Dynll1

Dynein light chain 1 (Dynll1) is a component of the Dynein motor complex and involved in the trafficking of molecules around the cell. In cytoplasmic dynein, two Dynll1 molecules interact with dynein intermediate chain, inducing dimerisation and organisation of the dynein complex (Regué et al. 2011). Dynll1 is also known as LC8, but this term also covers the highly similar Dynll2. Recently Dynll1 has been found to interact with myosin, cytoskeletal and motility proteins such as PAK and be essential for diverse processes such as nuclear transport, mitosis initiation, transcriptional regulation and post-synaptic density (Rapali et al. 2011)

Dynll1 was investigated because the preliminary microarray showed it to be upregulated 2.6-fold by iFGFR1 and 2.3-fold by iFGFR2. Furthermore, RNA-seq showed *Dynll1* to be 2.3-fold upregulated by iFGFR1 and 2.5-fold downregulated by iFGFR4 and so could be an example of a gene differentially regulated by FGFRs.

8.1.1 *Dynll1* is expressed in regions suggesting it could be involved in neural development and FGF signalling

The CDS of *Dynll1* was cloned into pGEM and *in-situ* probe synthesized. A range of *Xenopus tropicalis* developmental stages were collected and processed for ISH. *Dynll1* was first visible in late gastrula embryos in a dorsal triangle above the closing blastopore lip (Figure 8.1A). This corresponds to the Gastrocoel Roof Plate (GRP) region, which is populated with polarised cilia required for leftwards-fluid flow to break left/right symmetry in *Xenopus* (Schweickert et al. 2007). At neurula stages (Figure 8.1B and C) *Dynll1* is no longer visible in this region but is present in a punctate pattern on the epidermis. This is most obvious in the tailbud embryo (Figure 8.1D), and is reminiscent of ISH experiments for cilia marker genes such as α-tubulin (Dubaissi & Papalopulu 2011). As well as the epidermis, *Dynll1* was also present in the otic vesicle, the head and CNS. This is best shown by a cross section through the embryo (Figure 8.1D') which shows *Dynll1* expression in the neural tube. Even though the epidermal trunk cilia are unlikely to be under FGF

control, the presence of Dynll1 in the CNS and close to the GRP puts it in the right place to feasibly be an FGF target.

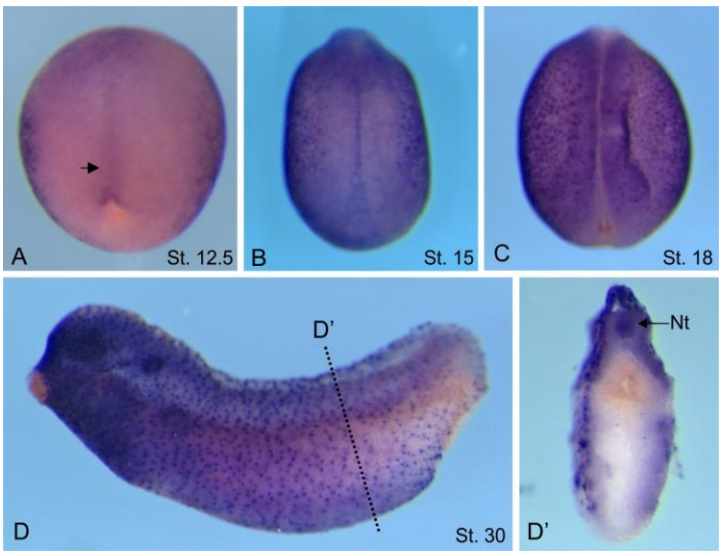

Figure 8.1 – *Dynll1* expression during *Xenopus tropicalis* development
Xenopus tropicalis embryos at various stages were processed for ISH with a probe against Dynll1. A shows faint Dynll1 staining above the dorsal blastopore lip of the late gastrula embryo (arrowed). In neurula stages (B and C), Dynll1 is expressed on the epidermis in a punctate pattern. This is most obvious in D, a tailbud embryo, where Dynll1 is expressed on the trunk at places corresponding to cilia. At the dotted line D' the embryo was cut and the cross section is shown in D, which shows Dynll1, is expressed in the neural tube (arrowed).

8.1.2 Dynll1 MO causes defects in cilia and movement of *Xenopus* embryos

A morpholino against *Dynll1* was designed with care so as to be specific to only *Dynll1*. BLAST searches revealed a site including, and upstream of, the transcriptional start site that was both specific to *Dynll1* only and suitable for a translation-blocking morpholino design.

The morpholino was injected bilaterally at the 1-2 cell stage at a number of concentrations into *Xenopus tropicalis* and embryos cultured to stage 42. 15ng of control morpholino was also injected into embryos, which appeared as wild type. At the time of imaging, embryos were at stage 42, when the heart and guts are looping (Figure 8.2, arrows). As the dose of Dynll1 morpholino is increased, morphants showed a progressively diminished ability for the hearts and guts to loop, leaving them in an immature, tubular state. Morphants also displayed oedema. The CNS was not as drastically affected by the loss of Dynll1, although at higher concentrations heads appeared smaller in the dorsal-anterior most region as there

appeared to be less space between the eyes and the front of the head. Embryos also failed to elongate posteriorly.

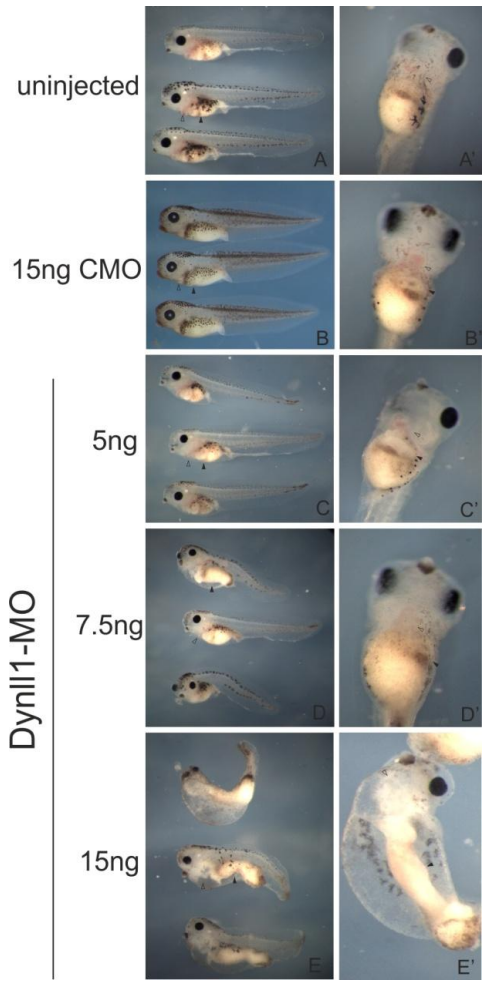

Figure 8.2 – Phenotype of *Xenopus tropicalis* embryos injected with *Dynll1* Morpholino
Xenopus tropicalis embryos were injected bilaterally with varying doses of Dynll1 morpholino at the 1-2 cell stage. 15ng of control morpholino was also injected and showed no ill effects. Embryos were cultured until stage 42 and imaged on their sides, and ventrally to show gut looping (black closed arrow) and heart development (position shown by open arrow).

This suggests that *Dynll1* has a role in organogenesis, and antero-posterior development. Further histology would be needed to see Dynll1's effects on the forebrain and CNS.

Another strong phenotype observed with these morphant embryos was that of movement ability– wild type and control-morpholino injected embryos 'coasted' across the culture dish, whereas morphants moved more slowly or not at all. Cilia are required in this region to help the developing embryo propel itself through medium, and circulate surrounding nutrients and oxygen around before it can swim. Movies showing a defective coasting phenotype in Dynll1 morphants are shown in

the Accompanying Material CD in Movies 4 and 5. 15ng Dynll1 Morpholino-injected embryos were almost completely stationary in the culture dish (Movie 5), compared to uninjected controls (Movie 4). These morphant embryos were categorised by their ability to coast as wild type, and to beat cellular debris away from themselves as a readout of epidermal cilia functionality. Results are shown in Figure 8.3.

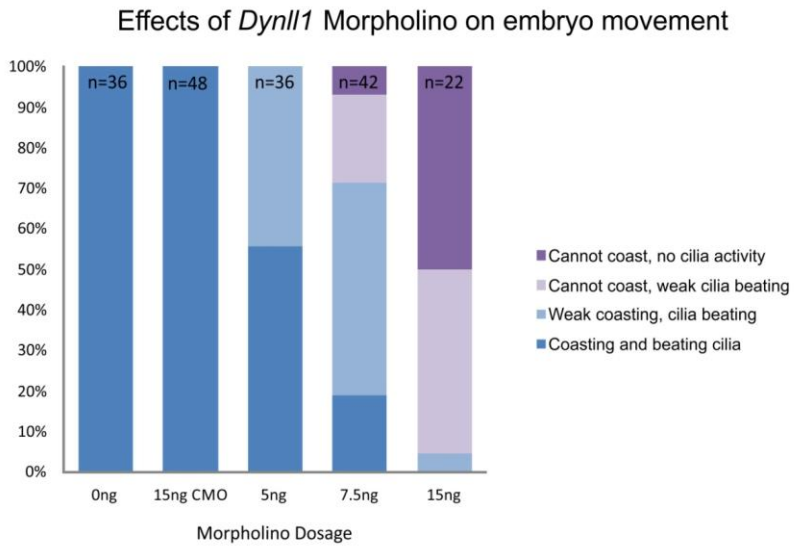

Figure 8.3 – Effects of *Dynll1* morpholino upon the ability of *Xenopus tropicalis* embryos to move.
Xenopus tropicalis embryos were injected bilaterally at the 1-2 cell stage with varying amounts of Dynll1 morpholino, or 15ng of control morpholino. Embryos were cultured until stage 30 and scored on the basis of their ability to move through medium, and also if they could beat away surrounding debris.

The most severely affected embryos were motionless and the beating action of cilia on cellular debris was not observed. Embryos injected with 5ng of morpholino largely moved as wild type, although some were noticeably slower than others. Most embryos injected with 7.5ng morpholino moved slower than wild type, with some embryos being unable to move at all. This movement category made up the majority of embryos injected with 15ng MO, with half of these unable to beat away cellular debris. This suggests a role for Dynll1 in ciliogenesis. Even though the trunk cilia, being far from FGF expression domains are probably not under FGF control, the negative effects on ciliogenesis in the trunk may be found in the GRP, although further experiments would be required to make this assertion.

8.1.3 RT-qPCR validation and RNA seq raw data shows *Dynll1* is not an FGF target

To validate the findings of the RNA-seq and iFGFR microarray to ascertain if *Dynll1* is indeed an FGF target, RT-qPCR was performed using primers against *Dynll1*. *Xenopus laevis* embryos were injected bilaterally with 20pg iFGFR1, cultured at 22°C to stage 10.5 and induced with AP20187 until stage 13, 15 or 17. Sibling embryos were injected with 1ng dnFGFR1 and cultured until the same stages. Figure 8.4 shows that at all three stages, relative to uninjected/uninduced controls *Dynll1* was not significantly or consistently affected by FGF induction or inhibition, which disagreed with the findings of the microarray.

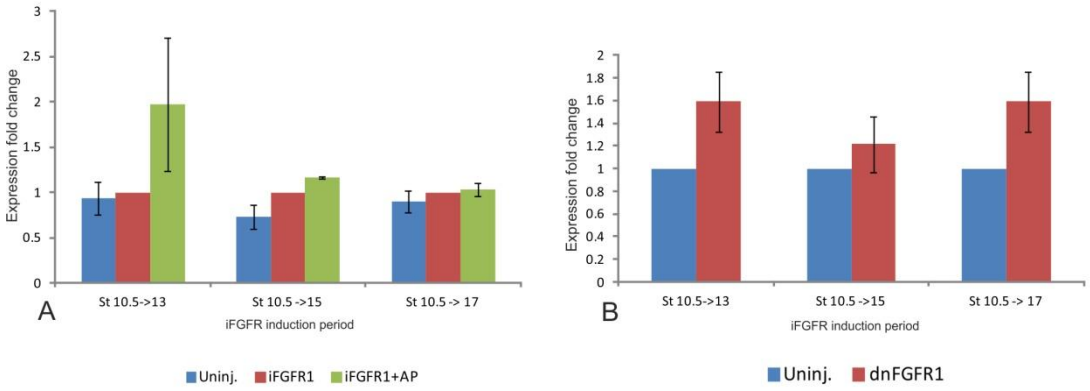

Figure 8.4 RT-qPCR shows that Dynll1 is not an FGF target
In A, whole *Xenopus laevis* embryos were injected bilaterally with 20pg iFGFR1 and cultured until stage 10.5. AP20187 was then added and sibling embryos cultured at 22°C until stage 13, 15 or 17. In B, 1ng dnFGFR1 was injected bilaterally into *Xenopus laevis* embryos and cultured until the same stages as A. Ct values were normalised against those of the housekeeping gene ODC and fold expression changes normalised against iFGFR1-injected uninduced embryos (A) or uninjected controls (B). Error bars represent SE from the mean of three biological replicates

The raw RNA-seq data was revisited, as it was hypothesised that maybe only a certain splice form of *Dynll1* was affected by iFGFR induction, as *Dynll1* was listed a number of times in the dataset and not always associated with a >2-fold expression change with either iFGFR. These two 'classes' of *Dynll1* were found to be associated with different sequences. Unfortunately a BLAST search revealed that the sequences of *Dynll1* that were listed as upregulated in both the microarray and RNA-seq were not in fact *Dynll1,* and were instead highly similar to apolipoprotein-C1. The origins of this clone sequence was from data used in Pollet et al. (2005), submitted to NCBI. The aim of this study was to perform a large semi-automated ISH screen of 8369 cDNA clones in *Xenopus laevis* embryos. One of these clone sequences, cnef01 mRNA, the precursor to Apoc1, was submitted to NCBI

database into the Dynll1 section despite sharing no significant similarities when aligned by BLAST. This ApoC1 sequence was presumably then mis-annotated as Dynll1 during processing of RNA-seq and microarray raw outputs. As this removes any connection between Dynll1 and FGF signalling, Dynll1 was not investigated further.

Figure 8.5. Geach et al. 2014 paper

© 2014. Published by The Company of Biologists Ltd | Development (2014) 141, 940-949 doi:10.1242/dev.104901

RESEARCH ARTICLE

An essential role for LPA signalling in telencephalon development

Timothy J. Geach[1], Laura Faas[2], Christelle Devader[1], Anai Gonzalez-Cordero[1,3], Jacqueline M. Tabler[1,4], Hannah Brunsdon[2], Harry V. Isaacs[2] and Leslie Dale[1,*]

ABSTRACT

Lysophosphatidic acid (LPA) has wide-ranging effects on many different cell types, acting through G-protein-coupled receptors such as LPAR6. We show that *Xenopus lpar6* is expressed from late blastulae and is enriched in the mesoderm and dorsal ectoderm of early gastrulae. Expression in gastrulae is an early response to FGF signalling. Transcripts for *lpar6* are enriched in the neural plate of *Xenopus* neurulae and loss of function caused forebrain defects, with reduced expression of telencephalic markers (*foxg1*, *emx1* and *nkx2-1*). Midbrain (*en2*) and hindbrain (*egr2*) markers were unaffected. *Foxg1* expression requires LPAR6 within ectoderm and not mesoderm. Head defects caused by LPAR6 loss of function were enhanced by co-inhibiting FGF signalling, with defects extending into the hindbrain (*en2* and *egr2* expression reduced). This is more severe than expected from simple summation of individual defects, suggesting that LPAR6 and FGF have overlapping or partially redundant functions in the anterior neural plate. We observed similar defects in forebrain development in loss-of-function experiments for ENPP2, an enzyme involved in the synthesis of extracellular LPA. Our study demonstrates a role for LPA in early forebrain development.

KEY WORDS: LPAR6, FGF, ENPP2, Forebrain, Telencephalon, *Xenopus*

INTRODUCTION

Lysophosphatidic acid (LPA) is a small ubiquitous phospholipid that acts as an extracellular signal and is believed to be involved in numerous physiological and pathological processes. It evokes a wide range of cellular responses from different cell types, including effects on cell proliferation, migration, adhesion, shape changes and death (Noguchi et al., 2009; Skoura and Hla, 2009; Choi et al., 2010). These diverse cellular functions are mediated by at least six members of the large superfamily of G-protein-coupled receptors (GPCR): LPA receptors 1 to 3 (LPAR1-3) belong to the Endothelial differentiation gene (EDG) subgroup, which also includes receptors for the bioactive lipid Sphingosine-1-phosphate, whereas LPA receptors 4 to 6 (LPAR4-6) belong to the Purinergic receptor (P2Y) subgroup, which includes receptors for extracellular Adenosine triphosphate (ATP) and Uridine triphosphate (UTP) (Choi et al., 2010). All six receptors couple to multiple G-protein subtypes that regulate multiple intracellular signalling pathways, including Cyclic adenosine monophosphate (cAMP), Ca^{2+}, Mitogen-activated protein (MAP) kinase, and Rho GTPases.

[1]Department of Cell and Developmental Biology, University College London, Anatomy Building, Gower Street, London, WC1E 6BT, UK. [2]Area 11, Department of Biology, University of York, Heslington, York, YO10 5DD, UK. [3]Department of Genetics, Institute of Ophthalmology, University College London, 11-43 Bath Street, London, EC1V 9EL, UK. [4]Section of Molecular Cell and Developmental Biology, University of Texas at Austin, Austin, TX 78712, USA.

*Author for correspondence (l.dale@ucl.ac.uk)

Received 15 October 2013; Accepted 25 November 2013

LPA receptors are widely expressed in vertebrate embryos, with distinct but overlapping expression patterns (Ohuchi et al., 2008; Massé et al., 2010a). Several LPA receptors are expressed in the developing nervous system (Ohuchi et al., 2008) but loss-of-function studies have provided few clues as to their role in neural development. Only minor phenotypic changes are observed, which presumably reflects redundant functions among LPA receptors (Contos et al., 2000; Contos et al., 2002; Ye et al., 2005; Lee et al., 2008). Abnormalities have been described in the cerebral cortex of *Lpar1*$^{-/-}$ mutant mice, including a reduction in neuronal progenitors (Estivill-Torrús et al., 2008) – a phenotype consistent with *Lpar1* expression in the ventricular zone of the developing cortex (Hecht et al., 1996). *Lpar5* is strongly expressed in a subset of neurons in dorsal root ganglia and loss-of-function studies have indicated a role in neuropathic pain (Lin et al., 2012). Severe neural defects have also been described in embryos lacking Ectonucleotide pyrophosphatase/phosphodiesterase 2 (ENPP2; also known as Autotaxin and Lysophospholipase D), a secreted enzyme involved in the synthesis of extracellular LPA (Tokumura et al., 2002; Umezu-Goto et al., 2002). *Enpp2*$^{-/-}$ mutant mice fail to complete cranial neural tube closure and exhibit defects in the forebrain and at the midbrain-hindbrain boundary (MHB) (Fotopoulou et al., 2010; Koike et al., 2010; Koike et al., 2011).

LPAR6 is the most recently characterised member of the family of LPA receptors (Chun et al., 2010). Identified as an orphan GPCR (Kaplan et al., 1993), it was subsequently named P2Y5 because of homology to nucleotide receptors (Webb et al., 1996). However, it failed to elicit detectable responses to extracellular nucleotides (Li et al., 1997). More recently, LPAR6 was shown to be a receptor for LPA, activating $G\alpha_i$ and $G\alpha_{12/13}$ G proteins, inhibiting Adenylyl cyclase, phosphorylating ERK1/2, and activating Rho GTPase (Pasternack et al., 2008; Lee et al., 2009; Pasternack et al., 2009; Yanagida et al., 2009). Little is known about the role of LPAR6 in cellular physiology except that it is required for human hair growth (Pasternack et al., 2008; Shimomura et al., 2008; Pasternack et al., 2009; Shimomura et al., 2009a). *LPAR6* is expressed in the inner root sheath of hair follicles (Pasternack et al., 2008; Shimomura et al., 2008) and loss-of-function mutations in this receptor are found in families with autosomal hair defects (Pasternack et al., 2008; Pasternack et al., 2009; Shimomura et al., 2008). Similar hair defects have been observed in families carrying loss-of-function mutations in the *Lipase H* (*LIPH*) gene, which is also expressed in the inner root sheath of hair follicles and encodes a secreted enzyme involved in the synthesis of extracellular LPA (Kazantseva et al., 2006; Shimomura et al., 2009b). However, both *LPAR6* and *LIPH* are widely expressed in human tissues, indicating that they have multiple roles.

In this study, we show that *lpar6* is expressed in *Xenopus* embryos, from late blastulae through to tadpoles, and that loss of function disrupts neural development. Embryos injected with antisense morpholinos (AMO) to *lpar6* had greatly reduced expression of telencephalic markers (*foxg1*, *emx1* and *nkx2-1*) and reduced expression of eyefield markers (*rax* and *pax6*). Midbrain (*en2*) and hindbrain (*egr2*) markers were not affected, demonstrating that defects were restricted to the developing forebrain. *Foxg1* expression requires LPAR6 within the ectoderm and not the mesoderm. Remarkably, defects caused by injecting *lpar6*-AMO were enhanced by also inhibiting FGF signalling, with midbrain (*en2*) and hindbrain (*egr2*) markers being greatly reduced in these embryos. This suggests that LPAR6 and FGF signalling interact in anterior neural development. Finally, we show that an AMO targeting *Xenopus* ENPP2 causes similar defects to those of *lpar6*-AMO. Our study indicates that LPA signalling is required to specifying cell fates in the anterior nervous system, a role that may involve cooperation with FGF signalling.

RESULTS

Lpar6 is expressed during embryonic development

Scanning expressed sequence tag (EST) databases, we identified *Xenopus* cDNAs encoding a protein of 345 amino acids, sharing 78% identity with human LPAR6 and only 15-51% identity with human LPAR1-5 (supplementary material Fig. S1). The corresponding gene is nested within the largest intron of the *Xenopus rb1* gene and transcribed in the opposite direction (supplementary material Fig. S2), an identical arrangement to that of human *LPAR6* and *RB1* (Herzog et al., 1996). Sequence conservation and genomic synteny demonstrate that we have identified *Xenopus lpar6*.

To determine whether *lpar6* is expressed during embryonic development we performed reverse transcription polymerase chain reaction (RT-PCR) on staged *Xenopus* embryos (Fig. 1A). Transcripts were detected from early gastrula (stage 10) through to tadpoles (stage 40), with reduced expression in late gastrulae (stage 13). Microarrays (Branney et al., 2009) showed that *lpar6* was transcribed from late blastulae (stage 9), on a similar timescale to *fgf8* but preceded the FGF target genes *bra* and *cdx4* (Fig. 1B). RT-PCR found that *lpar6* expression was greatest in the marginal zone of early gastrulae, with a low level of expression in the animal hemisphere and no expression in the vegetal hemisphere (Fig. 1C). Whole-mount *in situ* hybridisation confirmed that *lpar6* is expressed in the marginal zone of early gastrulae, with strongest expression above the dorsal blastopore lip (Fig. 2A-C). A bisected embryo shows that expression is localised to the involuting mesoderm (Fig. 2B). We also observed expression in the dorsal-animal hemisphere, the prospective neural plate, of early gastrulae (Fig. 2D). In neurulae, *lpar6* is expressed in the neural plate, with strongest expression in anterior regions (Fig. 2E-H). At tailbud stages, *lpar6* expression is strongest in the head, branchial arches, notochord and myotome (Fig. 2I,J).

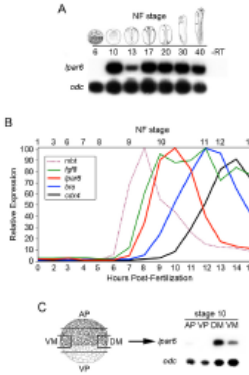

Fig. 1. Temporal expression of *lpar6*. (A) RT-PCR analysis for *lpar6* and ornithine decarboxylase (*odc*) in staged *Xenopus* embryos, showing *lpar6* expression from stage 10 (early gastrula) to stage 40 (tadpole). Note the drop in expression at stage 13 (late gastrula). Minus reverse transcriptase control (–RT) was performed at stage 40. (B) Microarray analysis for expression of *lpar6*, *fgf8*, *bra*, *cdx4* and a marker for the mid-blastula transition (*rbt1*). *Xenopus* embryos were collected 0-16 hours post-fertilisation (23°C). (C) RT-PCR analysis for *lpar6* and *odc* in dissected stage 10 embryos. AP, animal pole; DM, dorsal marginal zone; VM, ventral marginal zone; VP, vegetal pole.

Lpar6 is a direct target of FGF signalling

Lpar6 was previously shown to be positively regulated by FGF signalling (Branney et al., 2009), with expression levels 60-80% lower in gastrulae expressing dominant-negative FGF receptors (Fig. 3A). To confirm this, we isolated animal caps from blastulae (stage 8) and incubated them in media containing FGF4. RT-PCR showed that FGF4-induced expression of *lpar6*, consistent with the microarray data (Fig. 3B). *Lpar6* expression was also induced by Activin (Fig. 3B), a mesoderm-inducing factor belonging to the TGF-β family (Smith et al., 1990). To determine whether *lpar6* induction is an immediate-early response to FGF signalling, we incubated animal caps in media containing both FGF4 and cycloheximide (a protein synthesis inhibitor). However, cycloheximide alone induced strong expression of *lpar6* in animal caps (data not shown), replicating the effect previously described for chick *lpar6* in cultured spleen cells (Kaplan et al., 1993). As an alternative, we sought to determine how quickly induction of *lpar6* transcription occurs in response to FGF signalling. Animal caps were incubated in media containing FGF4, then removed at different time points and analysed by RT-PCR for *lpar6* transcripts. We detected weak expression of *lpar6* after 30 minutes of FGF4 exposure, with stronger expression after 60 minutes (Fig. 3C). Our results show that transcription of *lpar6* is an early response to FGF signalling.

Inhibition of LPAR6 disrupts head development

To determine the role of LPAR6 during development we adopted a loss-of-function approach, using antisense morpholino oligonucleotides (AMO1 and AMO2) that inhibit translation of *Xenopus lpar6* (Fig. 4A,B). *Xenopus* embryos were injected at the two-cell stage with 20 ng per blastomere of either AMO1 or AMO2 and the embryos were examined for developmental defects. Neither AMO had any effect on mesoderm formation in early gastrulae (supplementary material Fig. S3). The first defects were observed at early tailbud stages, with stage 28 embryos displaying a reduced anteroposterior axis length (3.4 mm compared with control length of 4.0 mm, *t*-test $P<0.005$) and head defects (Fig. 4C-E). Whole-

Development (2014) doi:10.1242/dev.104901

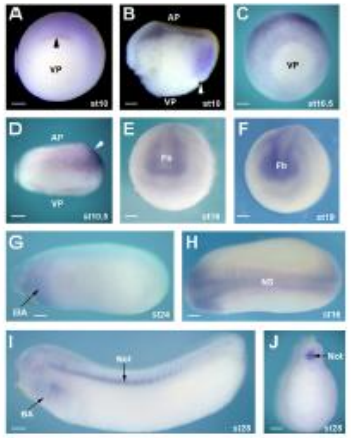

Fig. 2. Spatial expression of *lpar6*. Whole-mount *in situ* hybridisation with antisense probe for *lpar6*. (A) Stage 10, vegetal view, with dorsal blastopore lip (arrowhead). (B) Stage 10, bisected, with dorsal blastopore lip (arrowhead). (C) Stage 10.5, vegetal view. (D) Stage 10.5, lateral view, with dorsal-animal expression (arrowhead). (E) Stage 16, anterior view. (F) Stage 19, anterior view. (G) Stage 24, lateral view with head to the left. (H) Stage 16, dorsal view with head to the left. (I) Stage 28, lateral view with head to the left. (J) Stage 28, trunk section. Scale bars: 200 µm. AP, animal pole; BA, branchial arch; Fb, forebrain; Not, notochord; NS, nervous system; VP, vegetal pole.

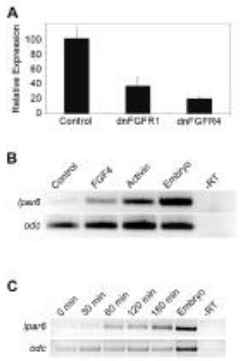

Fig. 3. FGF regulates expression of *lpar6*. (A) Microarray analysis for *lpar6* transcripts in early gastrulae expressing dnFGFR1 or dnFGFR4. (B) RT-PCR analysis for *lpar6* and *odc* in animal caps incubated for 5 hours (18°C) with either FGF4 or Activin. Sibling embryos were used for embryo and –RT controls. (C) RT-PCR analysis for *lpar6* and *odc* in animal caps incubated with FGF4 for up to 180 minutes (18°C). Sibling embryos were used for whole embryo and –RT controls.

mount *in situ* hybridisation showed that both AMO reduced telencephalic expression of *foxg1* (Fig. 4F-H). The frequency and severity of head defects were always greater with AMO2, which was used in all subsequent experiments. To demonstrate specificity, we attempted to rescue the head defect by co-injecting 40 ng of AMO2 with human *LPAR6* mRNA. Translation of this mRNA is not inhibited by AMO2 (Fig. 4B). Embryos co-injected with 200 pg of *LPAR6* mRNA failed to rescue the head defect and embryos injected with 600-800 pg usually died as gastrulae. In two experiments, embryos injected with 400 pg of *LPAR6* mRNA survived gastrulation and formed tailbud embryos with a normal head (Fig. 4I-K). We also injected *Xenopus tropicalis* embryos with a species-specific AMO for *lpar6* and obtained tadpoles with a smaller head and reduced *foxg1* expression (supplementary material Fig. S4). Our results suggest that forebrain defects are caused by specific inhibition of LPAR6 function.

Inhibition of LPAR6 disrupts neural development

Evidence from the use of the AMO injections suggested that LPAR6 has a role in anterior neural development. We therefore injected two-cell embryos with AMO2 and used whole-mount *in situ* hybridisation to study neural-specific gene expression. Initially, we injected a single blastomere with 20 ng of AMO2 and observed an increase in the width of *sox2* (Fig. 5A,B) and *cdx4* (Fig. 5I,J) expression on the injected side of neurulae, coupled with a reduction in epidermal keratin (*k81a1*) expression (Fig. 5C,D). We also observed loss in expression of *snai2*, a neural crest marker (Fig. 5E,F), whereas *myod1*, a mesodermal marker, was unaffected (Fig. 5G,H). Next, we injected 20 ng of AMO2 into each blastomere at the two-cell stage and analysed gene expression in the anterior neural plate. Expression of the telencephalon marker *foxg1* was greatly reduced in AMO2-injected neurulae (Fig. 5K,L), whereas the eye field markers *rax* and *pax6* were reduced to a lesser extent (Fig. 5Q-T). The MHB marker *en2* (Fig. 5O,P) and the hindbrain marker *egr2* (Fig. 5M,N) were expressed at normal levels, although their expression domains appear to have shifted towards the anterior neural plate border. Telencephalon development is regulated by signals from adjacent cells, including FGF8 from the anterior neural ridge (ANR) (Wilson and Houart, 2004; Hoch et al., 2009). We therefore analysed *fgf8* expression in AMO2-injected neurulae and observed that it was reduced, both in the ANR and more posteriorly at the MHB (Fig. 5U,V). There was also a reduction in diphospho-ERK (dpERK) staining in the anterior neural plate (Fig. 5W,X), demonstrating that FGF signalling was reduced in AMO2-injected embryos. Loss-of-function experiments demonstrate that LPAR6 is required for forebrain development in *Xenopus* embryos, perhaps by regulating FGF signalling.

To investigate forebrain development in more detail, we allowed AMO2-injected embryos to develop until tailbud stages (stage 26) and analysed them for telencephalon-specific gene expression (Fig. 6). In addition to *foxg1*, we also analysed expression of *nkx2-1*, a marker for the ventral telencephalon, and *emx1*, a marker for the

Development (2014) doi:10.1242/dev.104901

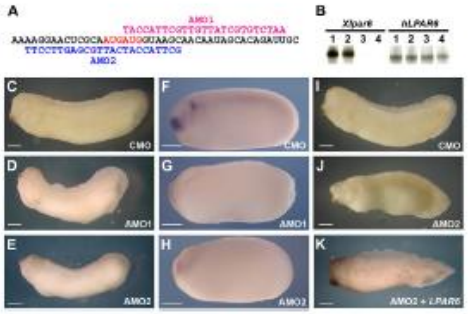

Fig. 4. LPAR6 is required for forebrain development. (A) Sequence (black letters, 5′-3′) of *Xenopus lpar6* mRNA (translational start site in red) aligned with sequence for both AMO1 (pink letters 3′-5′) and AMO2 (blue letters 3′-5′). (B) *In vitro* translation of *Xenopus lpar6* and human *LPAR6* in the presence of morpholinos. Lane 1, no MO. Lane 2, control MO. Lane 3, AMO1. Lane 4, AMO2. (C-E) Stage 28, lateral view (head to left), injected with 40 ng of morpholino. (C) Normal embryo injected with control MO (100%, *n*=90). (D) AMO1-injected embryo with head defect (80%, *n*=95). (E) AMO2-injected embryo with head defect (93%, *n*=75). Anteroposterior axis length of control-MO-injected embryos was 4.0 mm (s.d.=0.21, *n*=44) and that of AMO-injected embryos 3.4 mm (s.d.=0.17, *n*=44). Defects in D and E are statistically significant (Fisher's exact test, *P*<0.001). (F-H) Whole-mount *in situ* hybridisation, with antisense *foxg1* probe. Stage 24, lateral view (head to left), injected with 40 ng of morpholino. (F) Normal embryo injected with control MO (100%, *n*=30). (G) AMO1-injected embryo with reduced *foxg1* expression (80%, *n*=30). (H) AMO2-injected embryo with reduced *foxg1* expression (87%, *n*=30). Defects in G and H are statistically significant (Fisher's exact test, *P*<0.001). (I-K) Stage 28, lateral view (head to left), injected with 40 ng of AMO2 and 400 pg of human *LPAR6* mRNA. (I) Normal embryo injected with control MO (100%, *n*=30). (J) AMO2-injected embryo with head defect (80%, *n*=35). (K) AMO2 plus *hLPAR6* mRNA-injected embryo with normal head (66%, *n*=35). Rescue of head development in K is statistically significant (Fisher's exact test, *P*<0.001). Scale bars: 400 µm.

dorsal telencephalon (Small et al., 2000; Bachy et al., 2002). Transcripts for *foxg1* (Fig. 6A,B) and *emx1* (Fig. 6E,F) were not detected in AMO2-injected embryos, and only faint signals were detected for *nkx2-1* (Fig. 6C,D). Our results suggest that LPAR6 is required for the development of both dorsal and ventral regions of the *Xenopus* telencephalon.

LPAR6 is required in the ectoderm for telencephalon development

As *lpar6* is expressed in both mesoderm and ectoderm, we wished to determine its germ layer requirement for telencephalon development and initially targeted AMO injections to pairs of blastomeres (5 ng per blastomere) at the eight-cell stage (Fig. 7A). Fate maps (Dale and Slack, 1987; Moody, 1987) have shown that the nervous system is predominantly formed by dorsal-animal blastomeres, whereas the mesoderm that underlies the forebrain is formed by dorsal-vegetal blastomeres (Fig. 7A). AMO2 disrupted tadpole morphology in all four injection sets, but forebrain defects were confined to dorsal-animal injections (Fig. 7B-F). This suggests that LPAR6 is required in the ectoderm for forebrain development. Next, we exploited the ability of dorsal mesoderm to induce *foxg1* expression in animal cap ectoderm (Lupo et al., 2002). Embryos were injected at the four-cell stage, with 10 ng per blastomere of AMO2, and both the dorsal marginal zone (DMZ) and animal cap isolated from early gastrulae (stage 10). They were grafted together (Fig. 7G) and incubated until sibling embryos were late neurulae (stage 18). RT-PCR showed that *foxg1* expression was reduced when an AMO2-injected animal cap was grafted with a control DMZ, but not when a control animal cap was combined with an AMO2-injected DMZ (Fig. 7H). Expression of the general neural plate marker *sox2* was similar in all grafts. Our results demonstrate that LPAR6 is required in ectoderm, and not mesoderm, for telencephalon development. A requirement for LPAR6 in the ectoderm was also demonstrated in animal caps expressing Noggin, a Bone morphogenetic protein (BMP) inhibitor that induces *foxg1* expression (Papalopulu and Kintner, 1996). AMO2 reduced Noggin-induced expression of *foxg1* without affecting *sox2* expression (supplementary material Fig. S5). As mesoderm is not induced by Noggin, the inhibitory effect of AMO2 must reside within the ectoderm.

LPAR6 and FGFs act together in head development

While looking at the control of *lpar6* expression by FGF signalling, we observed enhanced head defects when embryos were co-injected with 40 ng of AMO2 and dominant-negative FGFR1 (*dnfgfr1*) mRNA (Fig. 8). Injection of AMO2 alone gave the expected forebrain defects (Fig. 8B), whereas *dnfgfr1* mRNA (plus control MO) disrupted posterior development but had no discernible effect on head development (Fig. 8C). Remarkably, embryos co-injected with AMO2 and *dnfgfr1* mRNA appeared to lack all head structures (Fig. 8D). This is a more severe phenotype than expected from the individual defects, indicating that LPA and FGF signalling might interact during the development of the anterior nervous system. We repeated this experiment using SU5402, a chemical inhibitor of FGF receptors (Mohammadi et al., 1997). Embryos injected with 40 ng of AMO2 were incubated in 10 µM SU5402, from late blastulae through early tailbud stages. This concentration of SU5402 alone gave an almost identical phenotype to injecting *dnfgfr1* mRNA. We also noted that it did not affect expression of *lpar6* (data not shown), which we attribute to the late application of the reagent. Embryos were analysed by RT-PCR for expression of the neural plate markers

Development (2014) doi:10.1242/dev.104901

Fig. 5. LPAR6 is required for neural development. Whole-mount *in situ* hybridisation analysis of MO injected neurulae. (A–J) Dorsal views of neurulae injected with 20 ng of morpholino into a single blastomere at the two-cell stage. Head at the top and injected side (asterisk) on the right. (A,B) Neural plate marker *sox2*, with increased width on the AMO2-injected side (70%, *n*=40). (C,D) Epidermal marker *slit1a1*, with decreased expression on the AMO2-injected side (75%, *n*=40). (E,F) Neural crest marker *snai2*, with reduced expression on the AMO2-injected side (69%, *n*=35). (G,H) Skeletal muscle marker *myod1*, with no defect (100%, *n*=38). (I,J) Posterior neural plate marker *cdx4*, with increased width on the AMO2-injected side (80%, *n*=40). (K–X) Anterodorsal views of neurulae injected with 40 ng of morpholino. (K,L) Telencephalon marker *foxg1*, with reduced expression in the AMO2-injected embryo (79%, *n*=38). (M,N) Hindbrain marker *egr2*, with normal expression in the AMO2-injected embryo (100%, *n*=35). (O,P) MHB marker *en2*, with normal expression in the AMO2-injected embryo (100%, *n*=35). Expression usually moved anteriorly (74%, *n*=35). (Q,R) Eyefield marker *rax*, with reduced expression in the AMO2-injected embryo (70%, *n*=40). (S,T) Eyefield marker *pax6*, with reduced expression in the AMO2-injected embryo (80%, *n*=30). (U,V) Anterior neural plate marker *fgf8*, with reduced expression in AMO2-injected embryos at the ANR (black arrow) and MHB (white arrow) (100%, *n*=23). (W,X) Whole-mount immunostaining for dpERK, with reduced ERK activity in AMO2-injected embryos at the ANR (black arrow), MHB (white arrow) and branchial arches (white arrowhead) (92%, *n*=36). All defects are statistically significant (Fisher's exact test, $P<0.001$). Scale bars: 200 µm.

foxg1, *otx2*, *rax*, *en2*, *egr2* and *sox2*, and the muscle marker *myod1* (Fig. 8E). SU5402 alone had no effect on the expression of any of the neural plate markers tested but greatly reduced expression of *myod1*, a gene known to be regulated by FGF signalling (Standley et al., 2001; Fisher et al., 2002). AMO2 alone only reduced expression of *foxg1* and *otx2*, the most anteriorly expressed genes tested. By contrast, AMO2-injected embryos treated with SU5402 displayed reduced expression of all five anterior neural plate markers (*foxg1*, *otx2*, *rax*, *en2* and *egr2*), but not the general neural plate marker *sox2*. Our results indicate that signalling pathways activated by LPAR6 and FGF interact in a redundant fashion to pattern the anterior nervous system.

Inhibition of ENPP2 disrupts forebrain development

To further test the role of LPA in forebrain development we turned to loss-of-function experiments for ENPP2, a secreted phospholipase

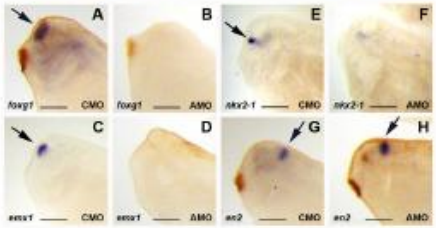

Fig. 6. LPAR6 is required for telencephalic development. Whole-mount *in situ* hybridisation of tailbud embryos injected with 40 ng of morpholinos; lateral views of the head. (A,B) Telencephalon marker *foxg1*, with loss of expression in the AMO2-injected embryo (71%, *n*=35). (C,D) Dorsal telencephalon marker *emx1*, with loss of expression in the AMO2-injected embryo (75%, *n*=32). (E,F) Ventral telencephalon marker *nkx2-1*, with reduced expression in the AMO2-injected embryo (67%, *n*=33). (G,H) MHB marker *en2*, with normal expression in the AMO2-injected embryo (100%, *n*=32). All defects are statistically significant (Fisher's exact test, $P<0.001$). Scale bars: 200 µm.

Development (2014) doi:10.1242/dev.104901

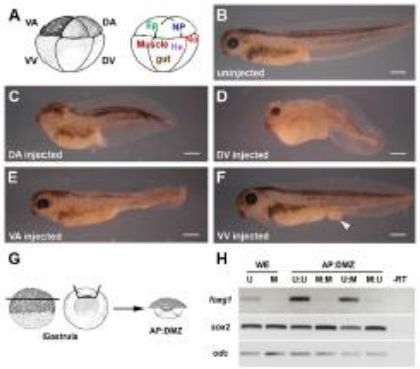

Fig. 7. LPAR6 is required in the ectoderm. (A) Schematic diagrams of an eight-cell *Xenopus* embryo, indicating injected blastomere pairs and their normal fate. (B–F) Stage 40 embryos, lateral view (head to left), injected with 5 ng per blastomere of AMO2. (B) Uninjected normal embryo (*n*=50). (C) DA injected embryo with head defect (88%, *n*=69). (D) DV injected embryo with dorsal defect but a normal head (81%, *n*=64). (E) VA injected embryo with tail defect but a normal head (78%, *n*=66). (F) VV injected embryo with defect in the posterior endoderm (arrowhead) but a normal head (80%, *n*=60). All defects are statistically significant (Fisher's exact test, $P<0.001$). (G) Schematic diagram of animal pole (AP) and dorsal marginal zone grafts. (H) RT-PCR analysis for *foxg1*, *sox2* and *odc* expression in AP:DMZ grafts. Grafts were made between uninjected (U) and AMO2-injected (M) fragments. Scale bars: 500 µm. –RT, minus reverse transcriptase control, uninjected stage 19 embryos; AP, animal pole; DA, dorsal-animal; DV, dorsal-vegetal; Ep, epidermis; He, heart; M:M, AMO2-injected AP and AMO2-injected DMZ; M:U, AMO2-injected AP and uninjected DMZ; No, notochord; NP, neural plate; U:M, uninjected AP and AMO2-injected DMZ; U:U, uninjected AP and uninjected DMZ; VA, ventral-animal; VV, ventral-vegetal; WE, stage 19 embryo.

that synthesises extracellular LPA (Tokumura et al., 2002; Umezu-Goto et al., 2002). *Xenopus enpp2* is expressed throughout development and transcripts are enriched in the nervous system of neurulae (Massé et al., 2010b). An AMO targeting the translational start site of both *enpp2a* and *enpp2b* was designed (Fig. 9A) and injected into *Xenopus* embryos with *enpp2a* mRNA. Western blot analysis showed that this AMO efficiently inhibited translation of co-injected mRNA (Fig. 9B). Next, we injected 10 ng of *enpp2* AMO into each blastomere at the two-cell stage and the first defects were detected at the end of neurulation, when AMO-injected embryos were found to be shorter than controls (Fig. 9C,D). The average anteroposterior axis length of AMO-injected embryos was only 72% of that of control embryos (2.9 mm compared to 4.0 mm, *t*-test, $P<0.005$). It was also clear that the anterior neural plate had failed to close in most AMO-injected embryos (74%, *n*=105), consistent with loss-of-function studies in mice (van Meeteren et al., 2006; Fotopoulou et al., 2010; Koike et al., 2011). To determine whether ENPP2 is required for forebrain development, we used whole-mount *in situ* hybridisation to analyse expression of anterior neural plate markers. Expression of the telencephalic markers *foxg1* (Fig. 9E,F), *nkx2-1* (Fig. 9G,H) and *emx1* (Fig. 9I,J) were greatly reduced in AMO-injected neurulae, whereas expression of the eyefield marker *rax* (Fig. 9K,L) was unaffected. Expression of the midbrain-hindbrain marker *en2* was normal in most embryos but reduced in a small number (Fig. 9M,N). We also observed a reduction in expression of *fgf8* in the ANR and MHB (Fig. 9O,P),

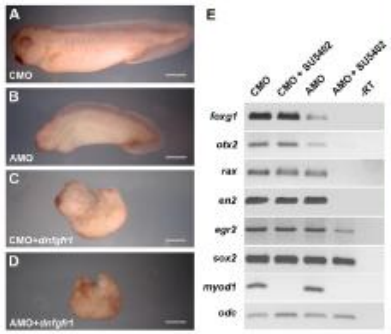

Fig. 8. LPAR6 and FGF co-regulate neural development. (A–D) stage 32, lateral view (head to left), injected with 40 ng per blastomere of MO plus or minus 1 ng of dominant-negative FGFR1 (dnfgfr1) mRNA. (A) Normal embryo injected with control MO (100%, *n*=27). (B) AMO2-injected embryo with head defect (81%, *n*=37). (C) Control MO plus dnfgfr1-injected embryo with posterior defect but normal head (92%, *n*=25). (D) AMO2 plus dnfgfr1-injected embryo with both head and posterior defects (100%, *n*=28). Note that the head defect is more severe than with AMO alone. All defects are statistically significant (Fisher's exact test, $P<0.001$). (E) RT-PCR analysis of MO-injected embryos incubated with or without 10 µM SU5402, from stage 9 to stage 18. Embryos were analysed for expression of the *foxg1* and *otx2* (forebrain), *rax* (eyefield), *en2* (MHB), *egr2* (hindbrain), *sox2* (neural plate), *myod1* (skeletal muscle) and *odc* (control). Scale bars: 500 µm. –RT, control-morpholino-injected embryos.

Development (2014) doi:10.1242/dev.104901

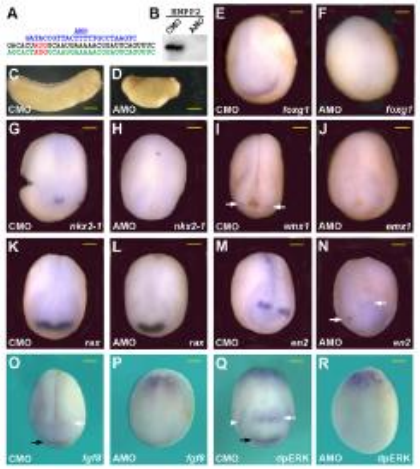

Fig. 9. ENPP2 is required for forebrain development. (A) Sequence of *Xenopus* enpp2a (black lettering, 5′-3′) and enpp2b (green lettering, 5-3′), translational start site in red, aligned with sequence for AMO (blue letters, 3′-5′). (B) Western blot analysis of *Xenopus* embryos injected with 1 µg of enpp2a.myc mRNA and 40 ng of morpholino. (C,D) Stage 28, lateral views (head to right) injected with 20 ng of either control MO or enpp2-AMO. Anteroposterior axis length of control-morpholino-injected embryos was 4.0 mm (s.d.=0.13, *n*=45) and that of AMO-injected embryos 2.9 mm (s.d.=0.22, *n*=45). (E-P) Whole-mount *in situ* hybridisation analysis of neurulae injected with 20 ng of either control (CMO) or enpp2-AMO. All embryos are viewed from anterodorsal perspective. (E,F) Telencephalon marker *foxg1*, with reduced expression in AMO-injected embryo (57%, *n*=62) (G,H) Ventral telencephalon marker *nkx2-1*, with reduced expression in AMO-injected embryo (59%, *n*=70). (I,J) Dorsal telencephalon marker *emx1*, with reduced expression in AMO-injected embryo (72%, *n*=63). (K,L) Eyefield marker *rax*, with normal expression in AMO-injected embryo (100%, *n*=77). (M,N) MHB marker *en2*, with reduced expression in AMO-injected embryo (16%, *n*=73 – 5% in controls, *n*=60). (O,P) Anterior neural plate marker *fgf8*, with reduced expression in AMO-injected embryo in both ANR (black arrow) and MHB (white arrow) (71%, *n*=21). (Q,R) Whole-mount immunolocalisation for dpERK. Note reduced ERK activity in AMO-injected embryos in the ANR (black arrow), the MHB (white arrow) and the branchial arches (white arrowhead) (98%, *n*=26). All defects are statistically significant (Fisher's exact test, $P<0.001$) except for *en2* (M,N). Scale bars: 600 µm in C,D; 200 µm in E-P.

as well as a reduction in dpERK staining in the anterior neural plate (Fig. 9Q,R). Our results demonstrate a role for ENPP2 in anterior neural plate development. These defects are similar to those caused by LPAR6 loss of function (above), confirming a role for LPA signalling in forebrain development.

DISCUSSION

Xenopus LPAR6

In this study we describe *Xenopus* LPAR6, a GPCR for the bioactive lipid LPA (Choi et al., 2010; Chun et al., 2010). We have shown that it is transcribed from late blastulae and enriched in the mesoderm of early gastrulae, with transcription regulated by FGF signalling. The distribution of *lpar6* transcripts in early gastrulae is very similar to that of *fgf4* and *fgf8* (Isaacs et al., 1995; Christen and Slack, 1997; Lea et al., 2009), and to FGF-dependent Extracellular-signal-related kinase (ERK) activity (Christen and Slack, 1999). Transcription is rapidly induced (30 minutes to 1 hour) by FGF4 in blastula stage animal caps and inhibited in early gastrulae by dominant-negative FGF receptors. We also find that *lpar6* is one of the first FGF responsive genes to be transcribed in late blastulae, suggesting that it is transcribed as an immediate-early response to FGF signalling. Inhibition of FGF signalling causes specific defects in posterior mesoderm formation (Amaya et al., 1991; Isaacs et al., 1998) and similar defects have been observed following inhibition of a number of FGF target genes, including *bra* and *cdx4* (Conlon et al., 1996; Isaacs et al., 1998). Surprisingly, we were unable to detect any effect of inhibiting LPAR6 function on mesoderm formation. Either LPAR6 is not an effector of FGF signalling in these processes, or different LPA receptor subtypes can compensate for defective LPAR6 signalling. Transcripts for *lpar1*, *lpar2*, *lpar4* and *lpar5* have been detected in *Xenopus* embryos (Lloyd et al., 2005; Massé et al., 2010a). As different LPA receptor subtypes have been shown to activate similar intracellular signalling pathways within a single cell (Dubin et al., 2010), it is possible that one or more of these *Xenopus* receptors could compensate for defective LPAR6 function at this stage.

LPA is required for anterior neural development

Xenopus lpar6 is expressed in the neural ectoderm of both early gastrulae and neurulae, and it is in the ectoderm of neurulae that we observed the first defects in loss-of-function experiments. We found that the width of the neural plate was increased throughout its length, as demonstrated by *sox2* and *cdx4* expression. This may be caused by defects in convergent-extension, coordinated cell intercalation that both narrows and extends the neural plate (Ehul and Keller, 2000). Further studies will be required to confirm this, but we observed a reduced anteroposterior axis length in *lpar6*-AMO-injected embryos, expected of embryos with defective convergent-extension. However, we note that the neural tube of *lpar6*-AMO-injected embryos is fully closed, whereas neural tube defects are common in embryos with disrupted convergent-extension movements (Wallingford and Harland, 2002). A reduction in the size of the forebrain was also observed in *lpar6*-AMO-injected embryos, as demonstrated by reduced expression of the telencephalic marker *foxg1*. Both dorsal (*emx1* expression) and ventral (*nkx2-1* expression) regions of the telencephalon were affected. We also observed reduced *fgf8* expression and ERK activity (in the ANR and MHB), as well as reduced *rax* and *pax6* expression (in the eyefield). More posterior regions of the brain (*en2* and egr2 expression) were not affected. Reduced *foxg1* expression was dependent upon

Development (2014) doi:10.1242/dev.104901

inhibiting LPAR6 within the ectoderm, indicating that the role of LPAR6 is intrinsic to the developing forebrain. Our results suggest that LPA signalling through LPAR6 is required in the anterior neural ectoderm for telencephalic development.

We observed similar defects in embryos injected with an AMO for ENPP2, a secreted enzyme that synthesises extracellular LPA (Tokumura et al., 2002; Umezu-Goto et al., 2002). *Enpp2* is expressed throughout *Xenopus* development and enriched in the neural plate of neurulae, then the anterior nervous system and neural crest following the completion of neurulation (Massé et al., 2010b). The most obvious defect that we observed following AMO injection was truncation of the anteroposterior axis, which was often accompanied by defects in anterior neural tube closure. Both defects are consistent with a role for ENPP2 in regulating convergent-extension in the neural plate. Further studies will be required to confirm this. We also observed reduced expression of the telencephalic markers *foxg1*, *emx1* and *nkx2-1* in neurulae, indicating that both dorsal and ventral regions of the telencephalon were affected. Both *fgf8* expression and ERK activity was reduced in the anterior neural plate of AMO-injected embryos. In contrast to *lpar6*-AMO-injected embryos, we did not observe reduced expression of the eyefield marker *rax*. Our results are consistent with studies on mice homozygous for mutations in *Enpp2*. E8.5 homozygous mutant embryos display defects in the anterior nervous system, both neural tube defects and reduced expression of anterior neural markers (van Meeteren et al., 2006; Fotopoulou et al., 2010). Reduced expression was described for *Otx2*, *Six3*, *Tcf4* and *Fgf8*, indicating defects in forebrain development (Koike et al., 2011). In contrast to our results in *Xenopus*, expression of the ventral telencephalic marker *Nkx2-1* was not reduced in *Enpp2*$^{-/-}$ mice (Koike et al., 2011). However, we note that reduced expression of *nkx2-1* (but not *foxg1* or *emx1*) in *enpp2*-AMO-injected *Xenopus* embryos was only transient, with expression restored by early tailbud stages (supplementary material Fig. S6). The similarities between the results of loss-of-function studies in *Xenopus* and the mouse suggest a key role for LPA in regulating telencephalon development. Moreover, they suggest that *Xenopus* is an ideal organism for studying these defects. *Xenopus* embryos are accessible at all stages of development and can survive with the vascular defects that kill *Enpp2*$^{-/-}$ mouse embryos by embryonic day (E) 9.5-10.5 (van Meeteren et al., 2006; Fotopoulou et al., 2010).

Functional cooperation between LPAR6 and FGF signalling

The telencephalon is the most anterior region of the vertebrate forebrain and will eventually form the cerebrum, including cerebral hemispheres, olfactory system and basal ganglia. Its development is regulated by numerous signals from organising centres in adjacent regions of the embryo, including the ANR (Hébert and Fishell, 2008; Hoch et al., 2009). This region is a source for a number of FGF signals, including FGF8, and FGF will induce ectopic *foxg1* expression in the anterior neural plate (Shimamura and Rubenstein, 1997; Eagleson and Dempewolf, 2002). Furthermore, *fgf8* mutant zebrafish and mouse embryos display telencephalic defects (Meyers et al., 1998; Shanmugalingam et al., 2000; Walshe and Mason, 2003). In addition, progressively more severe telencephalic defects have been described in mouse embryos with single, double and triple mutations for *Fgfr1*, *Fgfr2* and *Fgfr3* (Paek et al., 2009). These results highlight the importance of FGF signalling for telencephalon development. We note that AMO for both *lpar6* and *enpp2* reduce *fgf8* expression in the ANR of *Xenopus* neurulae and dpERK in the anterior neural plate, demonstrating reduced FGF signalling in the presumptive telencephalon. This suggests an explanation for our results in which LPA signalling is required for *fgf8* expression in the ANR, with reduced expression of *fgf8* being responsible for defects in telencephalic development. However, *fgf8*-AMO injection experiments in *Xenopus* have failed to detect a role for FGF8 in forebrain development (Fletcher et al., 2006). This might reflect redundant functions among different FGFs, as both *fgf3* and *fgf8* are required for telencephalon development in zebrafish (Walshe and Mason, 2003).

A link between LPAR6 and FGF signalling in anterior neural development was also demonstrated in experiments in which we inhibited both pathways. dnFGFR1 disrupts the development of the trunk and tail of *Xenopus* embryos but has very little effect on the head (Amaya et al., 1991; Isaacs et al., 1998). Yet, when combined with inhibition of LPAR6 we observed a dramatic reduction in head development, far greater than the forebrain defects observed by inhibiting LPAR6 alone. We observed the same effect when FGF signalling was inhibited by SU5402, a small molecule inhibitor of FGF receptors (Mohammadi et al., 1997). Phenotypic enhancement, as observed here, is usually an indicator of genetic interaction and probably reflects a degree of functional redundancy. We suggest that LPAR6 and FGF signalling are required throughout the developing brain but only the telencephalon is sensitive to reductions in signalling by LPAR6 alone. Only by inhibiting both pathways is a broader role in brain development revealed. Further studies are required to determine the level at which these signalling pathways interact, but ERK1/2 is a potential candidate. ERK1/2 is a key component of the canonical FGF signalling pathway (Dorey and Amaya, 2010; Pownall and Isaacs, 2010) and also a target of LPAR6 signalling (Lee et al., 2009). Although activation of ERK1/2 in early *Xenopus* embryos is predominantly FGF dependent (LaBonne and Whitman, 1997; Christen and Slack, 1999) a degree of LPAR6 dependency cannot be excluded. How LPA signalling regulates ERK activity in *Xenopus* embryos needs to be explored but it might involve the G protein $G\alpha_i$, as LPA-induced ERK activation in hBRIE 308i cells was blocked by the $G\alpha_i$ inhibitor pertussis toxin (Lee et al., 2009). An alternative mechanism is suggested by a study on hair follicle development in mice, which showed that LPAR6 acts through $G\alpha_{13}$ to stimulate TNFα converting enzyme (TACE)-mediated ectodomain shedding of TGFα (Inoue et al., 2011). TGFα stimulates ERK activity via the Epidermal growth factor (EGF) receptor. It is of interest that AMO for the EGF-like receptor ERBB4 generates posterior defects similar to those caused by dnFGFR1, defects rescued by increasing ERK activity (Nie and Chang, 2007).

Conclusions

Our results show that LPA signalling, acting through the LPAR6 receptor, is required in the initial specification and/or maintenance of the telencephalon, the most anterior region of the vertebrate brain. This is only the second LPAR receptor, after LPAR1 (Estivill-Torrús et al., 2008), that has been shown to have a role in early neural development, even though multiple receptor subtypes are expressed in the developing nervous system (Ohuchi et al., 2008; Massé et al., 2010a). The cellular and molecular basis of this role will require further studies, as will identifying the source of the LPA signals. Previous studies have shown that LPAR6 is required for hair growth in humans, but no evidence for a role in brain function was obtained. Either LPAR6 has evolved different roles in amphibians and mammals, or functional redundancy among the different LPA receptor subtypes masks the role of LPAR6 in mammalian forebrain development.

Development (2014) doi:10.1242/dev.104901

MATERIALS AND METHODS

Embryo methods

Xenopus laevis embryos were injected at either the two, four or eight-cell stage and incubated at 14-18°C. Animal caps were isolated at stage 8 and cultured in 50% Normal Amphibian Medium containing either 10 u/ml of *Xenopus* FGF4 (Isaacs et al., 1992) or 10 u/ml human Activin A (Sigma). Stage 10.5 DMZ and animal cap explants were grafted together and cultured until stage 18. Embryos were incubated in 10 µM SU5402 (Calbiochem) from stage 9 to stage 16. Whole-mount *in situ* hybridisation was performed using digoxigenin-labelled antisense probes (Sive et al., 2000). Immunostaining was performed using anti-diphospho-ERK (Sigma) (Christen and Slack, 1999). Animal procedures were performed under license, as required by the Animals (Scientific Procedures) Act 1986 (UK).

Sequences and AMO

EST for *Xenopus laevis lpar6* (IMAGE:3420557; Accession number BG552112) and *enpp2* (IMAGE:5570505; Accession number BQ736035) were purchased from Geneservice (Cambridge, UK) and sequenced. The Accession number for *lpar6* is HF558446, and *enpp2* is identical to NM_001087057. *Lpar6* was inserted into pCS2+ and *enpp2* into pCS2+myc. AMO for *lpar6* (AMO1, 5′-TACCATTGCTTGTTATCGTGTCTAA-3′; AMO2, 5′-TTCCTTGAGCGTTACTACCATTGC-3′), *enpp2* (5′-CTGAATCCGTTTTTCATTGCCATAG-3′), and standard control (5′-CTGAATCCGTTTTTCATTGCCATAG-3′) were purchased from Gene Tools. *Lpar6* AMO were tested by adding 1 µg to an SP6 TNT coupled reticulocyte lysate cell free translation system (Promega), loaded with 1 µg of *lpar6* cDNA and ^{35}S-methionine (GE Healthcare). Products were separated on NuPAGE 4-12% bis-Tris gels (Invitrogen) and exposed to autoradiographic film (GE Healthcare). *Enpp2* AMO was tested by co-injecting *Xenopus* embryos with 40 ng of AMO and 1 µg of *enpp2.myc* mRNA. Proteins were isolated at stage 9 and ENPP2 detected by western blot using 9E10 monoclonal antibody (Santa Cruz Biotechnology) (Gnach and Dale, 2008). Capped mRNA for human LPAR6 (Janssens et al., 1997), ENPP2.myc, dnFGFR1 (Amaya et al., 1991) and dnFGFR4 (Hongo et al., 1999) were transcribed using the SP6 mMessage mMachine kit (Ambion).

RT-PCR

Total RNA was purified using RNeasy columns (Qiagen) and cDNA synthesised using ImProm II reverse transcriptase and random primers (Promega). PCR was performed with Taq polymerase (New England Biolabs), using 0.5 µl of cDNA in a final volume of 25 µl for 26-28 cycles. Primers (5′-3′) used were: *egr2* (CCGGCCCATCCTCAGACCCAGAAA and CGCC-AGGCCGCTGTTGCCGAGTTC), *en2* (ATGAGCAGAATAACAGGGA-AGTGGA and CCTCGGGGACATTGACTCGGTGGTG), *fzzg1* (AAAG-TGGACGGCAAAGACGGTG and CCAATGAACACATCGTCGCTGC), *lpar6* (AGCATCTATCACCAGCAGCAGG and TGCCGCAACCTTACTG-AGACAG), *myod1* (AGGTCCAACTGCTCCGACGGCATGAA and AGGAGAGAATCCAGTTGATGGAAACA), *odc* (CAGCTAGCTGTGGT-GTGG and CAACATGGAAACTCACACC), *otx2* (GGATGGATTTGT-TGCACCAGTC and CACTCTCCGAGCTCACTTCTC), *rax* (AGACTG-GTGGCTATGGAG and ATACCTGCACCCTGACTT), *sox2* (GAGG-ATGGACACTTATGCCCAC and GGACATGCTGTAGGTAGGCGA).

Microarray assays

Microarray data were derived from published data sets (Branney et al., 2009). Affymetrix Cel files are available at EMBL ArrayExpress, accession numbers E-MEXP-2058 and E-MEXP-2059.

Acknowledgements

We thank Carlos Carmona-Fontaine, Philippa Francis-West, Sandip Patel, Ben Steventon, Andrea Townsend-Nicholson, Anne Warner and Steve Wilson for advice or helpful comments on the manuscript.

Competing interests

The authors declare no competing financial interests.

Author contributions

The project was designed by T.J.G., C.D., H.V.I. and L.D. Experiments were performed in the laboratories of L.D. and H.V.I. All authors contributed to the figures presented and interpreted the results. L.D., H.V.I. and T.J.G. wrote the manuscript, with remaining authors commenting on the manuscript.

Funding

The work was supported by project grants from the Biotechnology and Biological Sciences Research Council [BB/I/M/06861X to L.D. and BB/D010039/1 to H.V.I.].

Supplementary material

Supplementary material available online at http://dev.biologists.org/lookup/suppl/doi:10.1242/dev.104901/-/DC1

References

Amaya, E., Musci, T. J. and Kirschner, M. W. (1991). Expression of a dominant negative mutant of the FGF receptor disrupts mesoderm formation in *Xenopus* embryos. *Cell* **66**, 257-270.

Bachy, I., Berthon, J. and Rétaux, S. (2002). Defining pallial and subpallial divisions in the developing *Xenopus* forebrain. *Mech. Dev.* **117**, 163-172.

Branney, P. A., Faas, L., Steane, S. E., Pownall, M. E. and Isaacs, H. V. (2009). Characterisation of the fibroblast growth factor dependent transcriptome in early development. *PLoS ONE* **4**, e4951.

Choi, J. W., Herr, D. R., Noguchi, K., Yung, Y. C., Lee, C. W., Mutoh, T., Lin, M. E., Teo, S. T., Park, K. E., Mosley, A. N. et al. (2010). LPA receptors: subtypes and biological actions. *Annu. Rev. Pharmacol. Toxicol.* **50**, 157-186.

Christen, B. and Slack, J. M. (1997). FGF-8 is associated with anteroposterior patterning and limb regeneration in *Xenopus*. *Dev. Biol.* **192**, 455-466.

Christen, B. and Slack, J. M. (1999). Spatial response to fibroblast growth factor signalling in *Xenopus* embryos. *Development* **126**, 119-125.

Chun, J., Hla, T., Lynch, K. R., Spiegel, S. and Moolenaar, W. H. (2010). International Union of Basic and Clinical Pharmacology. LXXVIII. Lysophospholipid receptor nomenclature. *Pharmacol. Rev.* **62**, 579-587.

Conlon, F. L., Sedgwick, S. G., Weston, K. M. and Smith, J. C. (1996). Inhibition of Xbra transcription activation causes defects in mesodermal patterning and reveals autoregulation of Xbra in dorsal mesoderm. *Development* **122**, 2427-2435.

Cortes, J. J., Fukushima, N., Weiner, J. A., Kaushal, D. and Chun, J. (2000). Requirement for the lpA1 lysophosphatidic acid receptor gene in normal suckling behavior. *Proc. Natl. Acad. Sci. USA* **97**, 13384-13389.

Cortes, J. J., Ishii, I., Fukushima, N., Kingsbury, M. A., Ye, X., Kawamura, S., Brown, J. H. and Chun, J. (2002). Characterization of lpa(2) (Edg4) and lpa(1)/lpa(2) (Edg2/Edg4) lysophosphatidic acid receptor knockout mice: signaling deficits without obvious phenotypic abnormality attributable to lpa(2). *Mol. Cell. Biol.* **22**, 6621-6629.

Dale, L. and Slack, J. M. (1987). Fate map for the 32-cell stage of *Xenopus laevis*. *Development* **99**, 527-551.

Dorey, K. and Amaya, E. (2010). FGF signalling: diverse roles during early vertebrate embryogenesis. *Development* **137**, 3731-3742.

Dubin, A. E., Herr, D. R. and Chun, J. (2010). Diversity of lysophosphatidic acid receptor-mediated intracellular calcium signaling in early cortical neurogenesis. *J. Neurosci.* **30**, 7300-7309.

Eagleson, G. W. and Dempewolff, R. D. (2002). The role of the anterior neural ridge and Fgf-8 in early forebrain patterning and regionalization in *Xenopus laevis*. *Comp. Biochem. Physiol.* **132B**, 179-189.

Ebisi, T. and Keller, R. (2000). Monopolar protrusive activity: a new morphogenic cell behavior in the neural plate dependent on vertical interactions with the mesoderm in *Xenopus*. *Dev. Biol.* **224**, 3-19.

Erthill-Tomás, G., Llebrez-Zayas, P., Matos-Rico, E., Santín, L., Pedraza, C., De Diego, I., Del Arco, I., Fernández-Llebrez, P., Chun, J. and De Fonseca, F. R. (2008). Absence of LPA1 signaling results in defective cortical development. *Cereb. Cortex* **18**, 938-950.

Fisher, M. E., Isaacs, H. V. and Pownall, M. E. (2002). eFGF is required for activation of XmyoD expression in the myogenic cell lineage of *Xenopus laevis*. *Development* **129**, 1307-1315.

Fletcher, R. B., Baker, J. C. and Harland, R. M. (2006). FGF8 spliceforms mediate early mesoderm and posterior neural tissue formation in *Xenopus*. *Development* **133**, 1703-1714.

Fotopoulou, S., Oikonomou, N., Grigoriava, E., Nikitopoulou, I., Paparountas, T., Thanassopoulou, A., Zhao, Z., Xu, Y., Kontoyiannis, D. L., Remboutsika, E. et al. (2010). ATX expression and LPA signalling are vital for the development of the nervous system. *Dev. Biol.* **339**, 451-464.

Geach, T. J. and Dale, L. (2008). Molecular determinants of Xotch6 action in vivo. *J. Biol. Chem.* **283**, 27057-27063.

Hébert, J. M. and Fishell, G. (2008). The genetics of early telencephalon patterning: some assembly required. *Nat. Rev. Neurosci.* **9**, 678-685.

Hecht, J. H., Weiner, J. A., Post, S. R. and Chun, J. (1996). Ventricular zone gene-1 (vzg-1) encodes a lysophosphatidic acid receptor expressed in neurogenic regions of the developing cerebral cortex. *J. Cell Biol.* **135**, 1071-1083.

Herzog, H., Darby, K., Hort, Y. J. and Shine, J. (1996). Intron 17 of the human retinoblastoma susceptibility gene encodes an actively transcribed G protein-coupled receptor gene. *Genome Res.* **6**, 953-961.

Hoch, R. V., Rubenstein, J. L. and Pleasure, S. (2009). Genes and signaling events that establish regional patterning of the mammalian forebrain. *Semin. Cell Dev. Biol.* **20**, 378-386.

Hongo, I., Kengaku, M. and Okamoto, H. (1999). FGF signaling and the anterior neural induction in *Xenopus*. *Dev. Biol.* **216**, 561-581.

Inoue, A., Arima, N., Ishiguro, J., Prestwich, G. D., Arai, H. and Aoki, J. (2011). LPA-producing enzyme PA-PLA$_1\alpha$ regulates hair follicle development by modulating EGFR signalling. *EMBO J.* **30**, 4248-4260.

Isaacs, H. V., Tannahill, D. and Slack, J. M. (1992). Expression of a novel FGF in the *Xenopus* embryo. A new candidate inducing factor for mesoderm formation and anteroposterior specification. *Development* **114**, 711-720.

Isaacs, H. V., Pownall, M. E. and Slack, J. M. (1998). eFGF is expressed in the dorsal midline of *Xenopus laevis*. *Int. J. Dev. Biol.* **38**, 575-579.

Isaacs, H. V., Pownall, M. E. and Slack, J. M. (1998). Regulation of Hox gene expression and posterior development by the *Xenopus* caudal homologue Xcad3. *EMBO J.* **17**, 3413-3427.

Janssens, R., Boeynaems, J. M., Godart, M. and Communi, D. (1997). Cloning of a human heptahelical receptor closely related to the P2Y5 receptor. *Biochem. Biophys. Res. Commun.* **236**, 106-112.

Kaplan, M. H., Smith, D. I. and Sundick, R. S. (1993). Identification of a G protein coupled receptor induced in activated T cells. *J. Immunol.* **151**, 628-636.

Kazanskaya, A., Golitsov, A., Zinchenko, R., Grigorienko, A. P., Abrukova, A. V., Mollaka, Y. K., Kirillov, A. G., Guo, Z., Lyle, S., Ginter, E. K. et al. (2006). Human hair growth deficiency is linked to a genetic defect in the phospholipase gene LIPH. *Science* **314**, 982-985.

Kolko, S., Kelno-Masu, K. and Masu, M. (2010). Deficiency of autotaxin/lysophospholipase D results in head cavity formation in mouse embryos through the LPA/rac-rho-ROCK pathway. *Biochem. Biophys. Res. Commun.* **402**, 66-71.

Kolko, S., Yutoh, Y., Kelno-Masu, K., Noji, S., Masu, M. and Ohuchi, H. (2011). Autotaxin is required for the cranial neural tube closure and establishment of the midbrain-hindbrain boundary during mouse development. *Dev. Dyn.* **240**, 413-421.

LaBonne, C. and Whitman, M. (1997). Localization of MAP kinase activity in early *Xenopus* embryos: implications for endogenous FGF signaling. *Dev. Biol.* **183**, 9-20.

Lea, R., Papalopulu, N., Amaya, E. and Dorey, K. (2009). Temporal and spatial expression of FGF ligands and receptors during *Xenopus* development. *Dev. Dyn.* **238**, 1467-1479.

Lee, Z., Cheng, C. T., Zhang, H., Subler, M. A., Wu, J., Mukherjee, A., Windle, J. J., Chen, C. K. and Fang, X. (2008). Role of LPA4/p2y9/GPR23 in negative regulation of cell motility. *Mol. Biol. Cell* **19**, 5435-5445.

Lee, M., Choi, S., Halldén, G., Yo, S. J., Schilchoss, D. and Aponte, G. W. (2009). P2Y5 is a G(alpha)i, G(alpha)12/13 G protein-coupled receptor activated by lysophosphatidic acid that reduces intestinal cell adhesion. *Am. J. Physiol.* **297**, G641-G654.

Li, Q., Schachter, J. B., Harder, T. K. and Nicholas, R. A. (1997). The 6H1 orphan receptor, claimed to be the p2y5 receptor, does not mediate nucleotide-promoted second messenger responses. *Biochem. Biophys. Res. Commun.* **236**, 458-460.

Lin, M. E., Rivera, R. R. and Chun, J. (2012). Targeted deletion of LPA5 identifies novel roles for lysophosphatidic acid signaling in development of neuropathic pain. *J. Biol. Chem.* **287**, 17608-17617.

Lloyd, B., Tao, Q., Lang, S. and Wylie, C. (2005). Lysophosphatidic acid signalling controls cortical actin assembly and cytoarchitecture in *Xenopus* embryos. *Development* **132**, 805-816.

Lupo, G., Harris, W. A., Barsacchi, G. and Vignali, R. (2002). Induction and patterning of the telencephalon in *Xenopus laevis*. *Development* **129**, 5421-5436.

Masek, K., Kyuno, J., Sharma, S. and Jones, E. A. (2010a). The lysophosphatidic acid (LPA) and sphingosine-1-phosphate (S1P) receptor gene families: cloning and comparative expression analysis in *Xenopus laevis*. *Int. J. Dev. Biol.* **54**, 1361-1374.

Masek, K., Sharma, S., Allsop, G., Dale, K. and Jones, E. A. (2010b). Ectophosphodiesterase/nucleotide phosphohydrolase (Enpp) nucleotidases: cloning, conservation and developmental restriction. *Int. J. Dev. Biol.* **54**, 181-193.

Meyers, E. N., Lewandoski, M. and Martin, G. R. (1998). An Fgf8 mutant allelic series generated by Cre- and Flp-mediated recombination. *Nat. Genet.* **18**, 136-141.

Mohammadi, M., McMahon, G., Sun, L., Tang, C., Hirth, P., Yeh, B. K., Hubbard, S. R. and Schlessinger, J. (1997). Structures of the tyrosine kinase domain of fibroblast growth factor receptor in complex with inhibitors. *Science* **276**, 955-960.

Moody, S. A. (1987). Fates of the blastomeres of the 32-cell-stage *Xenopus* embryo. *Dev. Biol.* **122**, 300-319.

Nie, S. and Chang, C. (2007). PI3K and Erk MAPK mediate Erbl3 signaling in *Xenopus* gastrulation. *Mech. Dev.* **124**, 657-667.

Noguchi, K., Herr, D., Mutoh, T. and Chun, J. (2009). Lysophosphatidic acid (LPA) and its receptors. *Curr. Opin. Pharmacol.* **9**, 15-23.

Ohuchi, H., Hamada, A., Matsuda, H., Takagi, A., Tanaka, M., Aoki, J., Arai, H. and Noji, S. (2008). Expression patterns of the lysophospholipid receptor genes during mouse early development. *Dev. Dyn.* **237**, 3280-3294.

Paek, H., Gutin, G. and Hébert, J. M. (2009). FGF signaling is strictly required to maintain early telencephalic precursor cell survival. *Development* **136**, 2457-2465.

Papalopulu, N. and Kintner, C. (1996). A Xenopus gene, Xbr-1, defines a novel class of homeobox genes and is expressed in the dorsal ciliary margin of the eye. *Dev. Biol.* **174**, 104-114.

Pasternack, S. M., von Kügelgen, I., Al Aboud, K., Lee, Y. A., Rüschendorf, F., Voss, K., Hillmer, A. M., Molderings, G. J., Franz, T., Ramirez, A. et al. (2008). G protein-coupled receptor P2Y5 and its ligand LPA are involved in maintenance of human hair growth. *Nat. Genet.* **40**, 329-334.

Pasternack, S. M., Murugasundram, S., Elgabsheen, S., Müller, M., Kruse, R., Lehmann, P. and Betz, R. C. (2009). Novel mutations in the P2RY5 gene in one Turkish and two Indian patients presenting with hypotrichosis and woolly hair. *Arch. Dermatol. Res.* **301**, 621-624.

Pownall, M. E. and Isaacs, H. V. (2010). *FGF Signalling in Vertebrate Development*. San Rafael, CA, USA: Morgan & Claypool Life Sciences.

Shanmugalingam, S., Houart, C., Picker, A., Reifers, F., Macdonald, R., Barth, A., Griffin, K., Brand, M. and Wilson, S. W. (2000). Ace/Fgf8 is required for forebrain commissure formation and patterning of the telencephalon. *Development* **127**, 2549-2561.

Shimamura, K. and Rubenstein, J. L. (1997). Inductive interactions direct early regionalization of the mouse forebrain. *Development* **124**, 2709-2718.

Shimomura, Y., Wajid, M., Ishii, Y., Shapiro, L., Petukhova, L., Gordon, D. and Christiano, A. M. (2008). Disruption of P2RY5, an orphan G protein-coupled receptor, underlies autosomal recessive woolly hair. *Nat. Genet.* **40**, 335-339.

Shimomura, Y., Garzon, M. C., Kristal, L., Shapiro, L. and Christiano, A. M. (2009a). Autosomal recessive woolly hair with hypotrichosis caused by a novel homozygous mutation in the P2RY5 gene. *Exp. Dermatol.* **18**, 218-221.

Shimomura, Y., Wajid, M., Petukhova, L., Shapiro, L. and Christiano, A. M. (2009b). Mutations in the lipase H gene underlie autosomal recessive woolly hair/hypotrichosis. *J. Invest. Dermatol.* **129**, 622-628.

Sive, H. L., Grainger, R. M. and Harland, R. M. (2000). *Early Development of Xenopus laevis: a Laboratory Manual*. Cold Spring Harbor, NY: Cold Spring Harbor Laboratory Press.

Skoura, A. and Hla, T. (2009). Lysophospholipid receptors in vertebrate development, physiology, and pathology. *J. Lipid Res.* **50 Suppl.**, S293-S298.

Small, E. M., Vokes, S. A., Garriock, R. J., Li, D. and Krieg, P. A. (2005). Developmental expression of the *Xenopus* Nkx2-1 and Nkx2-4 genes. *Mech. Dev.* **90**, 259-262.

Smith, J. C., Price, B. M., Van Nimmen, K. and Huylebroeck, D. (1990). Identification of a potent Xenopus mesoderm-inducing factor as a homologue of activin A. *Nature* **345**, 729-731.

Standley, H. J., Zorn, A. M. and Gurdon, J. B. (2001). eFGF and its mode of action in the community effect during Xenopus myogenesis. *Development* **128**, 1347-1357.

Tokumura, A., Majima, E., Kariya, Y., Tominaga, K., Kogure, K., Yasuda, K. and Fukuzawa, K. (2002). Identification of human plasma lysophospholipase D, a lysophosphatidic acid-producing enzyme, as autotaxin, a multifunctional phosphodiesterase. *J. Biol. Chem.* **277**, 39436-39442.

Umezu-Goto, M., Kishi, Y., Taira, A., Hama, K., Dohmae, N., Takio, K., Yamori, T., Mills, G. B., Inoue, K., Aoki, J. et al. (2002). Autotaxin has lysophospholipase D activity leading to tumor cell growth and motility by lysophosphatidic acid production. *J. Cell Biol.* **158**, 227-233.

van Meeteren, L. A., Ruurs, P., Stortelers, C., Bouwman, P., van Rooijen, M. A., Pradère, J. P., Pettit, T. R., Wakelam, M. J., Saulnier-Blache, J. S., Mummery, C. L. et al. (2006). Autotaxin, a secreted lysophospholipase D, is essential for blood vessel formation during development. *Mol. Cell. Biol.* **26**, 5015-5022.

Wallingford, J. B. and Harland, R. M. (2002). Neural tube closure requires Dishevelled-dependent convergent extension of the midline. *Development* **129**, 5815-5825.

Walshe, J. and Mason, I. (2003). Unique and combinatorial functions of Fgf3 and Fgf8 during zebrafish forebrain development. *Development* **130**, 4337-4349.

Webb, T. E., Kaplan, M. G. and Barnard, E. A. (1996). Identification of 6H1 as a P2Y purinoceptor P2Y5. *Biochem. Biophys. Res. Commun.* **219**, 105-110.

Wilson, S. W. and Houart, C. (2004). Early steps in the development of the forebrain. *Dev. Cell* **6**, 167-181.

Yanagida, K., Masago, K., Nakanishi, H., Kihara, Y., Hamano, F., Tajima, Y., Taguchi, R., Shimizu, T. and Ishii, S. (2009). Identification and characterization of a novel lysophosphatidic acid receptor, p2y5/LPA6. *J. Biol. Chem.* **284**, 17731-17741.

Ye, X., Hama, K., Contos, J. J., Anliker, B., Inoue, A., Skinner, M. K., Suzuki, H., Amano, T., Kennedy, G., Arai, H. et al. (2005). LPA3-mediated lysophosphatidic acid signalling in embryo implantation and spacing. *Nature* **435**, 104-108.

List of Abbreviations

ACTC1	actin, alpha, cardiac muscle 1
AGR2	Anterior Gradient 2
ANB	Anterior Neural Border
APS	Ammonium Persulphate
AS	Apert Syndrome
ATP6V0C	ATPase, H+ transporting, lysosomal
BHLH	basic helix-loop-helix
BMP	Bone Morphogenetic Protein
BSA	Bovine Serum Albumin
CAMKL1	Calmodulin kinase-like 1
C-CBL	Casitas B-lineage Lymphoma
CDH…	cadherin 2, type 1, N-cadherin (neuronal)
CDX…	Caudal type homeobox
CHMP1	charged multivesicular body protein 1A
CIP	Calf Intestinal alkaline phosphatase
CITED2	Cbp/p300-interacting transactivator, with Glu/ Asp-rich carboxy-terminal domain 2
CRABP2	cellular retinoic acid binding protein 2
CRISPR	clustered regularly interspaced short palindromic repeats
CYP26A1	cytochrome P450, family 26, subfamily A, polypeptide 1
DAG	Diacylglycerol
DAVID	Database for Annotation, Visualization and Integrated Discovery
DAZAP	DAZ-associated protein
DIG	Digoxygenin
DLX…	Distal-less Homeobox
DSB	Double-stranded Break
DTT	Dithiothreitol
DUSP	Dual-specificity phosphatase
DYNLL1	Dynein Light Chain 1
EDTA	Ethylenediaminetetraacetic acid
EGR1	early growth response 1
EMX	Empty spiracles homeobox
EN2	Engrailed 2
ENPP2	ectonucleotide pyrophosphatase/phosphodiesterase 2
EPHA	Ephrin A
ERK	Extracellular signal-Related Kinase
ETS	E26 transformation-specific
ETV	ETS variant 3
FGF	Fibroblast Growth Factor
FGFR	Fibroblast Growth Factor Receptor
FGFRL1	FGFR-like 1
FHF	Fibroblast Homologous Factor
LPAR6	Lysophosphatidic acid receptor 6
MAB(T)	Maleic Acid Buffer (Tween)
MAFB	musculoaponeurotic fibrosarcoma oncogene homolog B
MAPK	Mitogen Activated Protein kinase
MBT	Mid-Blastula Transition
FLRT3	fibronectin leucine rich transmembrane protein 3
FOX…	forkhead box…
FRS	FGF Receptor Substrate
FRZ…	Frizzled
GAB1	GRB2-associated binding protein 1
GAPDH	glyceraldehyde-3-phosphate dehydrogenase
GBX	Gastrulation Brain Homeobox
GDP/GTP	Guanosine di/tri phosphate
GFP	Green Fluorescent Protein
GRB2	Growth factor receptor-bound 2
GRHL…	grainyhead-like
GRP	Gastrocoel Roof Plate
GSKB	Glycogen Synthase Kinase β
GWAS	Genome Wide Association Studies
HA	haemagglutinin
HCG	Human Chorionic Gonadotrophin
HESX1	Hesx homeobox 1
HH	Hedgehog (Drosophila)
HMX3	H6 family homeobox 3
HOX…	Homeobox
HS	Heparan Sulphate
HSPG	Heparan Sulphate Proteoglycan
HTR1	5-hydroxytryptamine (serotonin) receptor
IER2	Immediate Early Response 2
IFGFR	Inducible FGFR
IFT172	Intraflaggelar Transport 172
IG	Immunoglobulin
IGF(R)	Insulin-like Growth Factor (Receptor)
IP3	Inositol Triphosphate
IRG	Immunity Related Guanosine Triphosphatases
ISH	In Situ Hybridisation
ISO	Isthmic Organiser
JNK	c-Jun N-terminal kinase
KEA	Kinase Enrichment Analysis
KROX20 aka EGR2	Early Growth Response 2
KRT12	Keratin 12
KV	Kupffer's Vesicle
LHX1	LIM homeobox 1
LIN28A	LIN-28 homologue A
LMBRD2	LMBR1 domain containing 2
RA	Retinoic Acid
RAF	Rapidly Accelerated Fibrosarcoma
RALDH	Retinaldehyde dehydrogenase 2
RARRES	retinoic acid receptor responder (tazarotene induced) 1

MED9	Mediator 9
MEK	Mitogen Activated Protein kinase kinase
MENF	mesendoderm nuclear factor, gene 1
MHB	Mid Hindbrain Boundary
MIX1	Mix paired like homeobox
MKP	MAPK phosphatase
MRS	Modified Ringers Solution
MYOD	Myogenic differentiation
NAM	Normal Amphibian Medium
NCAM	Neural Cell Adhesion Molecule
NDE1	nudE neurodevelopment protein 1
NEK6	NIMA-related kinase 6
NF	Nieukwoop Faber
NGN..	Neurogenin
NHEJ	Non homologous End Joining
NIMA	Never In Mitosis A
NLS	Nuclear Localisation Signal
NOT-B	Notochord homeobox
OCT…	Octamer transcription factor
OCT…	Octamer transcription factor
ODC	ornithine decarboxylase
OTX2	Orthodenticle homeobox 2
PAM	Protospacer-adjacent Motif
PANTHEF	Protein ANalysis THrough Evolutionary Re lationships
PAX…	Paired Box 6
PBS(T)	Phospho Buffered Saline (Tween)
PCDH10	Protocadherin 10
PCP	Planar Cell Polarity
PCR	Polymerase Chain Reaction
PDX1	Pancreatic and duodenal homeobox 1
PI3K	Phosphatidylinositol-4,5-bisphosphate 3-kinase
PIP2(3)	Phosphatidylinositol (3) 4,5-bisphosphate
PITX1	paired-like homeodomain 1
PKB	Protein kinase B, aka Akt
PKC	Protein kinase C
PLCY	Phospholipase C gamma
POC5	POC5 centriolar protein
PP2A	protein phosphatase 2
PSM	Presomitic mesoderm
PTCH2	Patched 2
RAS	Rat sarcoma
RAS-DVA	Ras dorso ventral anterior localisation
RAX	Retina and anterior neural fold homeobox
RT-QPCR	Reverse Transcription Quantitative PCR
RVD	repeat-variable diresidue
RXR	Retinoid X Receptor
SDS	sodium dodecyl sulfate
SH2	Src-homology 2
SHH	Sonic Hedgehog
SLC12A3	solute carrier family 12 (potassium/chloride transporter), member 3
SMAD…	Mothers Against Decepentaplegic homologue
SMO	Smoothened
SNP	Single Nucleotide Polymorphism
SNX10	Sortin Nexin 10
SOS	Son of Sevenless
SOX…	SRY (sex determining region Y)-box
SPRED	Sprouty-related, EVH1 domain-containing protein
SPRY	Sprouty
SRFP2	secreted frizzled-related protein 2
SSC	Sodium Citrate/chloride
SUFU	Suppressor of Fused Homologue
SULF…	Sulphatase…
TAE	Tris-acetate-EDTA
TALEN	Transcription activator-like effector nucleases
TEMED	Tetramethylethylenediamine
TGFB	Transforming Growth Factor β
TNNC2	troponin C type 2 (fast)
TSPAN1	tetraspanin 1
TUBA1A	tubulin, alpha 1a
VANGL2	VANGL planar cell polarity protein 2
VEG1	Vegetally localised T box
VG1 (GDF1)	Growth Differention Factor 1
WG	Wingless (Drosophila)
WNT	Wingless-type MMTV integration site family
XBRA	Xenopus Brachyury
XNR	Xenopus Nodal Related
ZEB2	zinc finger E-box binding homeobox 2
ZFP36L1	Zinc Finger Protein 36 like 1
ZIC1	Zic family member 1

References

Adachi, S. et al., 2014. ZFP36L1 and ZFP36L2 control LDLR mRNA stability via the ERK-RSK pathway. *Nucleic acids research*, 42(15), pp.10037–49.

Adams, D.S. et al., 2006. Early, H+-V-ATPase-dependent proton flux is necessary for consistent left-right patterning of non-mammalian vertebrates. *Development (Cambridge, England)*, 133(9), pp.1657–1671.

Adamska, M. et al., 2001. FGFs control the patterning of the inner ear but are not able to induce the full ear program. *Mechanisms of Development*, 109(2), pp.303–313.

Akai, J., Halley, P.A. & Storey, K.G., 2005. FGF-dependent Notch signaling maintains the spinal cord stem zone. *Genes & development*, 19(23), pp.2877–87.

Albertson, R.C. & Yelick, P.C., 2005. Roles for fgf8 signaling in left-right patterning of the visceral organs and craniofacial skeleton. *Developmental biology*, 283(2), pp.310–21.

Aldridge, K. et al., 2010. Brain phenotypes in two FGFR2 mouse models for Apert syndrome. *Developmental dynamics : an official publication of the American Association of Anatomists*, 239(3), pp.987–97.

Allen, N.P.C. et al., 2007. RASSF6 is a novel member of the RASSF family of tumor suppressors. *Oncogene*, 26(42), pp.6203–11.

Amaya, E. et al., 1993. FGF signalling in the early specification of mesoderm in Xenopus. *Development (Cambridge, England)*, 118(2), pp.477–87.

Amaya, E., Musci, T.J. & Kirschner, M.W., 1991. Expression of a dominant negative mutant of the FGF receptor disrupts mesoderm formation in xenopus embryos. *Cell*, 66(2), pp.257–270.

Amaya, E., Musci, T.J. & Kirschner, M.W., 1991. Expression of a dominant negative mutant of the FGF receptor disrupts mesoderm formation in Xenopus embryos. *Cell*, 66(2), pp.257–70.

Amin, N.M. et al., 2014. RNA-seq in the tetraploid Xenopus laevis enables genome-wide insight in a classic developmental biology model organism. *Methods*, 66(3), pp.398–409.

Aquino, J.B. et al., 2009. The retinoic acid inducible Cas-family signaling protein Nedd9 regulates neural crest cell migration by modulating adhesion and actin dynamics. *Neuroscience*, 162(4), pp.1106–19.

Arima, K. et al., 2005. Global analysis of RAR-responsive genes in the Xenopus neurula using cDNA microarrays. *Developmental Dynamics*, 232(December 2004), pp.414–431.

Arman, E. et al., 1998. Targeted disruption of fibroblast growth factor (FGF) receptor 2 suggests a role for FGF signaling in pregastrulation mammalian development. *Proceedings of the National Academy of Sciences of the United States of America*, 95(9), pp.5082–5087.

Atkinson-Leadbeater, K. et al., 2009. FGF receptor dependent regulation of Lhx9 expression in the developing nervous system. *Developmental dynamics : an official publication of the American Association of Anatomists*, 238(2), pp.367–75.

Azimzadeh, J. et al., 2009. hPOC5 is a centrin-binding protein required for assembly of full-length centrioles. *The Journal of cell biology*, 185(1), pp.101–14.

Bachiller, D. et al., 2000. The organizer factors Chordin and Noggin are required for mouse forebrain development. *Nature*, 403(6770), pp.658–61.

Badano, J.L. et al., 2006. The ciliopathies: an emerging class of human genetic disorders. *Annual review of genomics and human genetics*, 7, pp.125–148.

Bai, Y. et al., 2014. Ror2 receptor mediates Wnt11 ligand signaling and affects convergence and extension movements in zebrafish. *The Journal of biological chemistry*, 289(30), pp.20664–76.

Baker, JC, Beddington, Rosa, Harland, R., 1999. Wnt signaling in Xenopus embryos inhibits bmp4 expression and activates neural development. *… & development*, pp.3149–3159.

Bamforth, S.D. et al., 2004. Cited2 controls left-right patterning and heart development through a Nodal-Pitx2c pathway. *Nature genetics*, 36(11), pp.1189–96.

Barreto, G. et al., 2003. The function of Xenopus germ cell nuclear factor (xGCNF) in morphogenetic movements during neurulation. *Developmental Biology*, 257(2), pp.329–342.

Barrios-Rodiles, M. et al., 2005. High-throughput mapping of a dynamic signaling network in mammalian cells. *Science (New York, N.Y.)*, 307(5715), pp.1621–1625.

Barrow, J.R., Stadler, H.S. & Capecchi, M.R., 2000. Roles of Hoxa1 and Hoxa2 in patterning the early hindbrain of the mouse. *Development (Cambridge, England)*, 127(5), pp.933–44.

Bassett, A.R. et al., 2013. Highly efficient targeted mutagenesis of Drosophila with the CRISPR/Cas9 system. *Cell reports*, 4(1), pp.220–8.

Basson, M.A. et al., 2008. Specific regions within the embryonic midbrain and cerebellum require different levels of FGF signaling during development. *Development (Cambridge, England)*, 135(5), pp.889–98.

Basu, B. & Brueckner, M., 2009. Fibroblast “cilia growth” factor in the development of left-right asymmetry. *Developmental cell*, 16(4), pp.489–90.

Bayramov, A. V. et al., 2004. The homeodomain-containing transcription factor X-nkx-5.1 inhibits expression of the homeobox gene Xanf-1 during the Xenopus laevis forebrain development. *Mechanisms of Development*, 121, pp.1425–1441.

Belo, J.A. et al., 2000. Cerberus-like is a secreted BMP and nodal antagonist not essential for mouse development. *Genesis (New York, N.Y. : 2000)*, 26(4), pp.265–70.

Bel-Vialar, S., Itasaki, N. & Krumlauf, R., 2002. Initiating Hox gene expression: in the early chick neural tube differential sensitivity to FGF and RA signaling subdivides the HoxB genes in two distinct groups. *Development*, 129(22), pp.5103–5115.

Bénazet, J.-D. & Zeller, R., 2009. Vertebrate limb development: moving from classical morphogen gradients to an integrated 4-dimensional patterning system. *Cold Spring Harbor perspectives in biology*, 1(4), p.a001339.

Bertran, M.T. et al., 2011. Nek9 is a Plk1-activated kinase that controls early centrosome separation through Nek6/7 and Eg5. *The EMBO journal*, 30(13), pp.2634–47.

Bertrand, V. et al., 2003. Neural tissue in ascidian embryos is induced by FGF9/16/20, acting via a combination of maternal GATA and Ets transcription factors. *Cell*, 115(5), pp.615–27.

Boije, H. et al., 2013. Forkheadbox N4 (FoxN4) triggers context-dependent differentiation in the developing chick retina and neural tube. *Differentiation; research in biological diversity*, 85(1-2), pp.11–9.

Böttcher, R.T. et al., 2004. The transmembrane protein XFLRT3 forms a complex with FGF receptors and promotes FGF signalling. *Nature cell biology*, 6(1), pp.38–44.

Böttcher, R.T. & Niehrs, C., 2005. Fibroblast growth factor signaling during early vertebrate development. *Endocrine reviews*, 26(1), pp.63–77.

Branney, P. a et al., 2009. Characterisation of the fibroblast growth factor dependent transcriptome in early development. *PloS one*, 4(3), p.e4951.

Briscoe, J. & Novitch, B.G., 2008. Regulatory pathways linking progenitor patterning, cell fates and neurogenesis in the ventral neural tube. *Philosophical transactions of the Royal Society of London. Series B, Biological sciences*, 363(1489), pp.57–70.

Broccoli, V., Boncinelli, E. & Wurst, W., 1999. The caudal limit of Otx2 expression positions the isthmic organizer. *Nature*, 401(6749), pp.164–8.

Bundschu, K., Walter, U. & Schuh, K., 2007. Getting a first clue about SPRED functions. *BioEssays*, 29(9), pp.897–907.

Burgar, H.R. et al., 2002. Association of the signaling adaptor FRS2 with fibroblast growth factor receptor 1 (Fgfr1) is mediated by alternative splicing of the juxtamembrane domain. *The Journal of biological chemistry*, 277(6), pp.4018–23.

Busnadiego, O. et al., 2013. LOXL4 is induced by transforming growth factor β1 through Smad and JunB/Fra2 and contributes to vascular matrix remodeling. *Molecular and cellular biology*, 33(12), pp.2388–401.

Caron, A., Xu, X. & Lin, X., 2012. Wnt/β-catenin signaling directly regulates Foxj1 expression and ciliogenesis in zebrafish Kupffer's vesicle. *Development (Cambridge, England)*, 139(3), pp.514–24.

Catela, C. et al., 2009. Multiple congenital malformations of Wolf-Hirschhorn syndrome are recapitulated in Fgfrl1 null mice. *Disease models & mechanisms*, 2(5-6), pp.283–94.

Chang, N. et al., 2013. Genome editing with RNA-guided Cas9 nuclease in zebrafish embryos. *Cell research*, 23(4), pp.465–72.

Chen, J. et al., 2006. Interaction of Pin1 with Nek6 and characterization of their expression correlation in Chinese hepatocellular carcinoma patients. *Biochemical and biophysical research communications*, 341(4), pp.1059–65.

Chen, Y. et al., 2012. A SNX10/V-ATPase pathway regulates ciliogenesis in vitro and in vivo. *Cell research*, 22(2), pp.333–45.

Chen, Y., Mohammadi, M. & Flanagan, J.G., 2009. Graded levels of FGF protein span the midbrain and can instruct graded induction and repression of neural mapping labels. *Neuron*, 62(6), pp.773–80.

Cheng, J.Q. et al., 1997. Transforming activity and mitosis-related expression of the AKT2 oncogene: evidence suggesting a link between cell cycle regulation and oncogenesis. *Oncogene*, 14(23), pp.2793–801.

Chi, C.L. et al., 2003. The isthmic organizer signal FGF8 is required for cell survival in the prospective midbrain and cerebellum. *Development*, 130(12), pp.2633–2644.

Chiu, W.T. et al., 2014. Genome-wide view of TGF /Foxh1 regulation of the early mesendoderm program. *Development*, 141, pp.4537–4547.

Cho, G.-S., Choi, S.-C. & Han, J.-K., 2013. BMP signal attenuates FGF pathway in anteroposterior neural patterning. *Biochemical and biophysical research communications*, (April).

Chourrout, D. et al., 2006. Minimal ProtoHox cluster inferred from bilaterian and cnidarian Hox complements. *Nature*, 442(7103), pp.684–7.

Christen, B. & Slack, J.M., 1999. Spatial response to fibroblast growth factor signalling in Xenopus embryos. *Development (Cambridge, England)*, 126(1), pp.119–25.

Chung, A.-Y. et al., 2010. Neuron-specific expression of atp6v0c2 in zebrafish CNS. *Developmental dynamics : an official publication of the American Association of Anatomists*, 239(9), pp.2501–8.

Chung, H.A. et al., 2004. Screening of FGF target genes in Xenopus by microarray: temporal dissection of the signalling pathway using a chemical inhibitor. *Genes to cells : devoted to molecular & cellular mechanisms*, 9(8), pp.749–61.

Ciruna, B. & Rossant, J., 2001. FGF signaling regulates mesoderm cell fate specification and morphogenetic movement at the primitive streak. *Developmental cell*, 1(1), pp.37–49.

Clackson, T. et al., 1998. Redesigning an FKBP-ligand interface to generate chemical dimerizers with novel specificity. *Proceedings of the National Academy of Sciences of the United States of America*, 95(18), pp.10437–42.

Clanton, J.A., Hope, K.D. & Gamse, J.T., 2013. Fgf signaling governs cell fate in the zebrafish pineal complex. *Development (Cambridge, England)*, 140(2), pp.323–32.

Clarke, J.D. & Lumsden, A., 1993. Segmental repetition of neuronal phenotype sets in the chick embryo hindbrain. *Development (Cambridge, England)*, 118(1), pp.151–62.

Collart, C. et al., 2014. High-resolution analysis of gene activity during the Xenopus mid-blastula transition. *Development (Cambridge, England)*, 141(1927), pp.1927–39.

Colli, L.M. et al., 2013. Components of the canonical and non-canonical Wnt pathways are not mis-expressed in pituitary tumors. *PloS one*, 8(4), p.e62424.

Colvin, J.S. et al., 2001. Lung hypoplasia and neonatal death in Fgf9-null mice identify this gene as an essential regulator of lung mesenchyme. *Development (Cambridge, England)*, 128(11), pp.2095–106.

Colvin, J.S. et al., 1996. Skeletal overgrowth and deafness in mice lacking fibroblast growth factor receptor 3. *Nat Genet*, 12(4), pp.390–397.

Concha, M.L. et al., 2000. A nodal signaling pathway regulates the laterality of neuroanatomical asymmetries in the zebrafish forebrain. *Neuron*, 28(2), pp.399–409.

Conlon, F.L. et al., 1996. Inhibition of Xbra transcription activation causes defects in mesodermal patterning and reveals autoregulation of Xbra in dorsal mesoderm. *Development (Cambridge, England)*, 122, pp.2427–2435.

Cornell, R. a & Kimelman, D., 1994. Activin-mediated mesoderm induction requires FGF. *Development (Cambridge, England)*, 120(2), pp.453–462.

Del Corral, R.D. et al., 2003. Opposing FGF and Retinoid Pathways Control Ventral Neural Pattern, Neuronal Differentiation, and Segmentation during Body Axis Extension. *Neuron*, 40(1), pp.65–79.

Del Corral, R.D., Breitkreuz, D.N. & Storey, K.G., 2002. Onset of neuronal differentiation is regulated by paraxial mesoderm and requires attenuation of FGF signalling. *Development*, 129(7), pp.1681–1691.

Cox, W.G. & Hemmati-Brivanlou, A., 1995. Caudalization of neural fate by tissue recombination and bFGF. *Development (Cambridge, England)*, 121(12), pp.4349–58.

Crossley, P.H., Martinez, S. & Martin, G.R., 1996. Midbrain development induced by FGF8 in the chick embryo. *Nature*, 380(6569), pp.66–68.

Cullen, P.J., 2008. Endosomal sorting and signalling: an emerging role for sorting nexins. *Nature reviews. Molecular cell biology*, 9(7), pp.574–82.

Dasen, J.S., Liu, J.-P. & Jessell, T.M., 2003. Motor neuron columnar fate imposed by sequential phases of Hox-c activity. *Nature*, 425(6961), pp.926–933.

Davidson, A.J. et al., 2003. Cdx4 Mutants Fail To Specify Blood Progenitors and Can Be Rescued By Multiple Hox Genes. *Nature*, 425(6955), pp.300–306.

Davidson, A.J. & Zon, L.I., 2006. The caudal-related homeobox genes cdx1a and cdx4 act redundantly to regulate hox gene expression and the formation of putative hematopoietic stem cells during zebrafish embryogenesis. *Developmental Biology*, 292(2), pp.506–518.

Delaune, E., Lemaire, P. & Kodjabachian, L., 2005. Neural induction in Xenopus requires early FGF signalling in addition to BMP inhibition. *Development (Cambridge, England)*, 132(2), pp.299–310.

Dessaud, E., McMahon, A.P. & Briscoe, J., 2008. Pattern formation in the vertebrate neural tube: a sonic hedgehog morphogen-regulated transcriptional network. *Development (Cambridge, England)*, 135(15), pp.2489–503.

Diez del Corral, R. et al., 2003. Opposing FGF and retinoid pathways control ventral neural pattern, neuronal differentiation, and segmentation during body axis extension. *Neuron*, 40(1), pp.65–79.

Donizetti, A. et al., 2008. Differential expression of duplicated genes for prothymosin alpha during zebrafish development. *Developmental dynamics : an official publication of the American Association of Anatomists*, 237(4), pp.1112–8.

Dorey, K. & Amaya, E., 2010. FGF signalling: diverse roles during early vertebrate embryogenesis. *Development (Cambridge, England)*, 137(22), pp.3731–42.

Dow, A.L. et al., 2015. Sprouty2 in the Dorsal Hippocampus Regulates Neurogenesis and Stress Responsiveness in Rats. *Plos One*, 10(3), p.e0120693.

Duan, D.S., Werner, S. & Williams, L.T., 1992. A naturally occurring secreted form of fibroblast growth factor (FGF) receptor 1 binds basic FGF in preference over acidic FGF. *The Journal of biological chemistry*, 267(23), pp.16076–80.

Dubaissi, E. & Papalopulu, N., 2011. Embryonic frog epidermis: a model for the study of cell-cell interactions in the development of mucociliary disease. *Disease models & mechanisms*, 4(2), pp.179–92.

Dubrulle, J., McGrew, M.J. & Pourquié, O., 2001. FGF signaling controls somite boundary position and regulates segmentation clock control of spatiotemporal Hox gene activation. *Cell*, 106(2), pp.219–232.

Dubrulle, J. & Pourquié, O., 2004. fgf8 mRNA decay establishes a gradient that couples axial elongation to patterning in the vertebrate embryo. *Nature*, 427(6973), pp.419–422.

Dunn, M.K., Mercola, M. & Moore, D.D., 1995. Cyclopamine, a steroidal alkaloid, disrupts development of cranial neural crest cells in Xenopus. *Developmental dynamics : an official publication of the American Association of Anatomists*, 202(3), pp.255–270.

Dyer, C. et al., 2014. A bi-modal function of Wnt signalling directs an FGF activity gradient to spatially regulate neuronal differentiation in the midbrain. *Development (Cambridge, England)*, 141(1), pp.63–72.

Eagleson, G.W. & Dempewolf, R.D., 2002. The role of the anterior neural ridge and Fgf-8 in early forebrain patterning and regionalization in Xenopus laevis. *Comparative biochemistry and physiology. Part B, Biochemistry & molecular biology*, 132(1), pp.179–89.

Eblaghie, M.C. et al., 2003. Negative feedback regulation of FGF signaling levels by Pyst1/MKP3 in chick embryos. *Current biology : CB*, 13(12), pp.1009–18.

Ermakova, G. V et al., 1999. The homeobox gene, Xanf-1, can control both neural differentiation and patterning in the presumptive anterior neurectoderm of the Xenopus laevis embryo. *Development (Cambridge, England)*, 126, pp.4513–4523.

Ermakova, G. V et al., 2007. The homeodomain factor Xanf represses expression of genes in the presumptive rostral forebrain that specify more caudal brain regions. *Developmental biology*, 307(2), pp.483–97.

Esko, J.D. & Selleck, S.B., 2002. Order out of chaos: assembly of ligand binding sites in heparan sulfate. *Annual review of biochemistry*, 71, pp.435–71.

Eswarakumar, V.P., Lax, I. & Schlessinger, J., 2005. Cellular signaling by fibroblast growth factor receptors. *Cytokine & growth factor reviews*, 16(2), pp.139–49.

Faas, L. et al., 2013. Lin28 proteins are required for germ layer specification in Xenopus. *Development (Cambridge, England)*, 986(January), pp.976–986.

Faas, L. & Isaacs, H. V, 2009. Overlapping functions of Cdx1, Cdx2, and Cdx4 in the development of the amphibian Xenopus tropicalis. *Developmental dynamics : an official publication of the American Association of Anatomists*, 238(4), pp.835–52.

Fang, H., Marikawa, Y. & Elinson, R.P., 2000. Ectopic expression of Xenopus noggin RNA induces complete secondary body axes in embryos of the direct developing frog Eleutherodactylus coqui. *Development, Genes and Evolution*, 210(1), pp.21–27.

Fang, X. et al., 2005. Control of CREB-binding protein signaling by nuclear fibroblast growth factor receptor-1: a novel mechanism of gene regulation. *The Journal of biological chemistry*, 280(31), pp.28451–62.

Fang, Z. & Cui, X., 2011. Design and validation issues in RNA-seq experiments. *Briefings in Bioinformatics*, 12(3), pp.280–287.

Faux, C.H. et al., 2001. Interactions between fibroblast growth factors and Notch regulate neuronal differentiation. *The Journal of neuroscience : the official journal of the Society for Neuroscience*, 21(15), pp.5587–5596.

Feige, E. & Motro, B., 2002. The related murine kinases, Nek6 and Nek7, display distinct patterns of expression. *Mechanisms of development*, 110(1-2), pp.219–23.

Feng, Y. & Xu, Q., 2010. Pivotal role of hmx2 and hmx3 in zebrafish inner ear and lateral line development. *Developmental biology*, 339(2), pp.507–18.

Fish, M.B. et al., 2014. Xenopus mutant reveals necessity of rax for specifying the eye field which otherwise forms tissue with telencephalic and diencephalic character. *Developmental Biology*, 395(2), pp.317–330.

Fisher, M.E., Isaacs, H. V & Pownall, M.E., 2002. eFGF is required for activation of XmyoD expression in the myogenic cell lineage of Xenopus laevis. *Development (Cambridge, England)*, 129(6), pp.1307–15.

Fletcher, R.B. & Harland, R.M., 2008. The role of FGF signaling in the establishment and maintenance of mesodermal gene expression in Xenopus. *Developmental dynamics : an official publication of the American Association of Anatomists*, 237(5), pp.1243–54.

Forde, N. et al., 2012. Evidence for an early endometrial response to pregnancy in cattle: both dependent upon and independent of interferon tau. *Physiological Genomics*, 44(16), pp.799–810.

Freeman, S.D. et al., 2008. Extracellular regulation of developmental cell signaling by XtSulf1. *Developmental biology*, 320(2), pp.436–45.

Fry, A.M. et al., 2012. Cell cycle regulation by the NEK family of protein kinases. *Journal of cell science*, 125(Pt 19), pp.4423–33.

Fuentealba, L.C. et al., 2007. Integrating patterning signals: Wnt/GSK3 regulates the duration of the BMP/Smad1 signal. *Cell*, 131(5), pp.980–93.

Furdui, C.M. et al., 2006. Autophosphorylation of FGFR1 kinase is mediated by a sequential and precisely ordered reaction. *Molecular cell*, 21(5), pp.711–7.

Fürthauer, M. et al., 2004. Fgf signalling controls the dorsoventral patterning of the zebrafish embryo. *Development (Cambridge, England)*, 131(12), pp.2853–64.

Furukawa, T. et al., 2000. rax, Hes1, and notch1 Promote the Formation of Müller Glia by Postnatal Retinal Progenitor Cells. *Neuron*, 26(2), pp.383–394.

Gagnon, J.A. et al., 2014. Efficient mutagenesis by Cas9 protein-mediated oligonucleotide insertion and large-scale assessment of single-guide RNAs. *PloS one*, 9(5), p.e98186.

Gaj, T., Gersbach, C. a. & Barbas, C.F., 2013. ZFN, TALEN, and CRISPR/Cas-based methods for genome engineering. *Trends in Biotechnology*, 31(7), pp.397–405.

Galceran, J. et al., 1999. Wnt3a-/--like phenotype and limb deficiency in Lef1(-/-)Tcf1(-/-) mice. *Genes & development*, 13(6), pp.709–17.

Gamse, J.T. et al., 2003. The parapineal mediates left-right asymmetry in the zebrafish diencephalon. *Development (Cambridge, England)*, 130(6), pp.1059–1068.

Ganoth, D. et al., 2001. The cell-cycle regulatory protein Cks1 is required for SCF(Skp2)-mediated ubiquitinylation of p27. *Nature cell biology*, 3(3), pp.321–4.

Garcia-Fernàndez, J., 2005. The genesis and evolution of homeobox gene clusters. *Nature reviews. Genetics*, 6(12), pp.881–92.

Garnett, A.T., Square, T.A. & Medeiros, D.M., 2012. BMP, Wnt and FGF signals are integrated through evolutionarily conserved enhancers to achieve robust expression of Pax3 and Zic genes at the zebrafish neural plate border. *Development (Cambridge, England)*.

Gaughran, F. et al., 2006. Hippocampal FGF-2 and FGFR1 mRNA expression in major depression, schizophrenia and bipolar disorder. *Brain Research Bulletin*, 70(3), pp.221–227.

Gaunt, S.J., Drage, D. & Cockley, A., 2003. Vertebrate caudal gene expression gradients investigated by use of chick cdx-A/lacZ and mouse cdx-1/lacZ reporters in transgenic mouse embryos: evidence for an intron enhancer. *Mechanisms of Development*, 120(5), pp.573–586.

Gaunt, S.J., Drage, D. & Trubshaw, R.C., 2005. cdx4/lacZ and cdx2/lacZ protein gradients formed by decay during gastrulation in the mouse. *International Journal of Developmental Biology*, 49(8), pp.901–908.

Geach, T.J. et al., 2014. An essential role for LPA signalling in telencephalon development. *Development (Cambridge, England)*, 141(4), pp.940–9.

Gillespie, L.L., Chen, G. & Paterno, G.D., 1995. Cloning of a fibroblast growth factor receptor 1 splice variant from Xenopus embryos that lacks a protein kinase C site important for the regulation of receptor activity. *Journal of Biological Chemistry*, 270, pp.22758–22763.

Giudetti, G. et al., 2014. Characterization of the Rx1 dependent transcriptome during early retinal development. *Developmental dynamics : an official publication of the American Association of Anatomists*, pp.1352–1361.

Giudicelli, F. et al., 2003. Novel activities of Mafb underlie its dual role in hindbrain segmentation and regional specification. *Developmental biology*, 253(1), pp.150–162.

Glavic, A., Gómez-Skarmeta, J.L. & Mayor, R., 2002. The homeoprotein Xiro1 is required for midbrain-hindbrain boundary formation. *Development (Cambridge, England)*, 129(7), pp.1609–21.

Goda, T., Takagi, C. & Ueno, N., 2009. Xenopus Rnd1 and Rnd3 GTP-binding proteins are expressed under the control of segmentation clock and required for somite formation. *Developmental dynamics : an official publication of the American Association of Anatomists*, 238(11), pp.2867–76.

Godsave, S.F. & Slack, J.M., 1989. Clonal analysis of mesoderm induction in Xenopus laevis. *Developmental biology*, 134(2), pp.486–90.

Goetz, R. et al., 2007. Molecular insights into the klotho-dependent, endocrine mode of action of fibroblast growth factor 19 subfamily members. *Molecular and cellular biology*, 27(9), pp.3417–28.

Goetz, R. & Mohammadi, M., 2013. Exploring mechanisms of FGF signalling through the lens of structural biology. *Nature reviews. Molecular cell biology*, 14(3), pp.166–80.

Goggolidou, P. et al., 2014. ATMIN is a transcriptional regulator of both lung morphogenesis and ciliogenesis. *Development (Cambridge, England)*, 141(20), pp.3966–77.

Goldfarb, M. et al., 2007. Fibroblast growth factor homologous factors control neuronal excitability through modulation of voltage-gated sodium channels. *Neuron*, 55(3), pp.449–63.

Gómez, A.R. et al., 2005. Conserved cross-interactions in Drosophila and Xenopus between Ras/MAPK signaling and the dual-specificity phosphatase MKP3. *Developmental dynamics : an official publication of the American Association of Anatomists*, 232(3), pp.695–708.

Gong, S.-G., 2014. Isoforms of Receptors of Fibroblast Growth Factors. *Journal of cellular physiology*, (August 2013), pp.1–28.

Gorivodsky, M. et al., 2009. Intraflagellar transport protein 172 is essential for primary cilia formation and plays a vital role in patterning the mammalian brain. *Developmental biology*, 325(1), pp.24–32.

Gospodarowicz, D., 1975. PURIFICATION OF A FIBROBLAST GROWTH-FACTOR FROM BOVINE PITUITARY. *Endocrinology*, 250(7), pp.2515–20.

Grand, E.K. et al., 2004. Identification of a novel gene, FGFR1OP2, fused to FGFR1 in 8p11 myeloproliferative syndrome. *Genes, chromosomes & cancer*, 40(1), pp.78–83.

Gross, I. et al., 2007. Sprouty2 inhibits BDNF-induced signaling and modulates neuronal differentiation and survival. *Cell death and differentiation*, 14(10), pp.1802–12.

Grothe, C. et al., 2008. Expression and regulation of Sef, a novel signaling inhibitor of receptor tyrosine kinases-mediated signaling in the nervous system. *Acta Histochemica*, 110(2), pp.155–162.

Van Grunsven, L. a et al., 2007. XSip1 neuralizing activity involves the co-repressor CtBP and occurs through BMP dependent and independent mechanisms. *Developmental biology*, 306(1), pp.34–49.

Grunz, H. & Tacke, L., 1989. Neural differentiation of Xenopus laevis ectoderm takes place after disaggregation and delayed reaggregation without inducer. *Cell differentiation and development : the official journal of the International Society of Developmental Biologists*, 28(3), pp.211–7.

Guo, X. et al., 2014. Efficient RNA/Cas9-mediated genome editing in Xenopus tropicalis. *Development (Cambridge, England)*, 141(3), pp.707–14.

Hafner, M. et al., 2008. Identification of microRNAs and other small regulatory RNAs using cDNA library sequencing. *Methods (San Diego, Calif.)*, 44(1), pp.3–12.

Halpern, M.E. et al., 2005. Lateralization of the vertebrate brain: taking the side of model systems. *The Journal of neuroscience : the official journal of the Society for Neuroscience*, 25(45), pp.10351–10357.

Hanafusa, H. et al., 2002. Sprouty1 and Sprouty2 provide a control mechanism for the Ras/MAPK signalling pathway. *Nature cell biology*, 4(11), pp.850–8.

Harada, H. et al., 1999. Localization of putative stem cells in dental epithelium and their association with Notch and FGF signaling. *The Journal of cell biology*, 147(1), pp.105–20.

Harbers, M. & Carninci, P., 2005. Tag-based approaches for transcriptome research and genome annotation. *Nature methods*, 2(7), pp.495–502.

Hardcastle, Z., Chalmers, A.D. & Papalopulu, N., 2000. FGF-8 stimulates neuronal differentiation through FGFR-4a and interferes with mesoderm induction in Xenopus embryos. *Current Biology*, 10(23), pp.1511–1514.

Harding, J.L. et al., 2014. Small RNA profiling of Xenopus embryos reveals novel miRNAs and a new class of small RNAs derived from intronic transposable elements Small RNA profiling of Xenopus embryos reveals novel miRNAs and a new class of small RNAs derived from intronic transposa. *Genome Research*, pp.96–106.

Harvey, R.P., 1991. Widespread expression of MyoD genes in Xenopus embryos is amplified in presumptive muscle as a delayed response to mesoderm induction. *Proceedings of the National Academy of Sciences of the United States of America*, 88(October), pp.9198–9202.

Hashimoto, M. et al., 2002. Fibroblast growth factor 1 regulates signaling via the glycogen synthase kinase-3beta pathway. Implications for neuroprotection. *The Journal of biological chemistry*, 277(36), pp.32985–91.

Hawley, S.H. et al., 1995. Disruption of BMP signals in embryonic Xenopus ectoderm leads to direct neural induction. *Genes & Development*, 9(23), pp.2923–2935.

Hayashi, S. et al., 2004. Expression patterns of Xenopus FGF receptor-like 1/nou-darake in early Xenopus development resemble those of planarian nou-darake and Xenopus FGF8. *Developmental dynamics : an official publication of the American Association of Anatomists*, 230(4), pp.700–7.

Hayata, T. et al., 2009. Identification of embryonic pancreatic genes using Xenopus DNA microarrays. *Developmental dynamics : an official publication of the American Association of Anatomists*, 238(6), pp.1455–66.

Hébert, J.M. & Fishell, G., 2008. The genetics of early telencephalon patterning: some assembly required. *Nature reviews. Neuroscience*, 9(9), pp.678–85.

Heigwer, F., Kerr, G. & Boutros, M., 2014. E-CRISP: fast CRISPR target site identification. *Nature methods*, 11(2), pp.122–3.

Hemmati-Brivanlou, a & Melton, D. a, 1994. Inhibition of activin receptor signaling promotes neuralization in Xenopus. *Cell*, 77(2), pp.273–81.

Hemmati-Brivanlou, A. & Melton, D., 1997a. Vertebrate embryonic cells will become nerve cells unless told otherwise. *Cell*, 88, pp.13–17.

Hemmati-Brivanlou, A. & Melton, D., 1997b. Vertebrate Embryonic Cells Will Become Nerve Cells Unless Told Otherwise. *Cell*, 88(1), pp.13–17.

Hirata, H. et al., 2001. Hes1 and Hes3 regulate maintenance of the isthmic organizer and development of the mid/hindbrain. *The EMBO journal*, 20(16), pp.4454–66.

Holland, P.W.H. & Takahashi, T., 2005. The evolution of homeobox genes: Implications for the study of brain development. *Brain research bulletin*, 66(4-6), pp.484–90.

Hollenhorst, P.C., McIntosh, L.P. & Graves, B.J., 2011. Genomic and biochemical insights into the specificity of ETS transcription factors. *Annual review of biochemistry*, 80, pp.437–71.

Hong, S.-K. & Dawid, I.B., 2009. FGF-dependent left-right asymmetry patterning in zebrafish is mediated by Ier2 and Fibp1. *Proceedings of the National Academy of Sciences of the United States of America*, 106(7), pp.2230–5.

Hongo, I., Kengaku, M. & Okamoto, H., 1999. FGF signaling and the anterior neural induction in Xenopus. *Developmental biology*, 216(2), pp.561–81.

Hou, S. et al., 2007. The secreted serine protease xHtrA1 stimulates long-range FGF signaling in the early Xenopus embryo. *Developmental cell*, 13(2), pp.226–41.

Houart, C., Westerfield, M. & Wilson, S.W., 1998. A small population of anterior cells patterns the forebrain during zebrafish gastrulation. *Nature*, 391(6669), pp.788–92.

Howell, G.R. et al., 2007. Mutation of a ubiquitously expressed mouse transmembrane protein (Tapt1) causes specific skeletal homeotic transformations. *Genetics*, 175(2), pp.699–707.

Huangfu, D. et al., 2003. Hedgehog signalling in the mouse requires intraflagellar transport proteins. *Nature*, 426(6962), pp.83–7.

Hudson, C., Darras, S., Caillol, D., Yasuo, H., Lemaire, P., 2003. A conserved role for the MEK signalling pathway in neural tissue specification and posteriorisation in the invertebrate chordate, the ascidian Ciona intestinalis. *Development*, 130(1), pp.147–159.

Illes, J.C., Winterbottom, E. & Isaacs, H. V, 2009. Cloning and expression analysis of the anterior parahox genes, Gsh1 and Gsh2 from Xenopus tropicalis. *Developmental dynamics : an official publication of the American Association of Anatomists*, 238(1), pp.194–203.

Inagaki, T. et al., 2005. Fibroblast growth factor 15 functions as an enterohepatic signal to regulate bile acid homeostasis. *Cell metabolism*, 2(4), pp.217–25.

Inbal, A. et al., 2007. Six3 represses nodal activity to establish early brain asymmetry in zebrafish. *Neuron*, 55(3), pp.407–15.

Inoue, Y. & Imamura, T., 2008. Regulation of TGF-beta family signaling by E3 ubiquitin ligases. *Cancer science*, 99(11), pp.2107–12.

Isaacs, H. V, Pownall, M.E. & Slack, J.M., 1994. eFGF regulates Xbra expression during Xenopus gastrulation. *The EMBO journal*, 13(19), pp.4469–81.

Isaacs, H. V, Pownall, M.E. & Slack, J.M., 1998. Regulation of Hox gene expression and posterior development by the Xenopus caudal homologue Xcad3. *The EMBO journal*, 17(12), pp.3413–27.

Isaacs, H. V, Tannahill, D. & Slack, J.M., 1992. Expression of a novel FGF in the Xenopus embryo. A new candidate inducing factor for mesoderm formation and anteroposterior specification. *Development (Cambridge, England)*, 114(3), pp.711–720.

Ishibashi, S., Cliffe, R. & Amaya, E., 2012. Highly efficient bi-allelic mutation rates using TALENs in Xenopus tropicalis. *Biology open*, 1(12), pp.1273–6.

Itoh, K. & Sokol, S.Y., 1994. Heparan sulfate proteoglycans are required for mesoderm formation in Xenopus embryos. *Development (Cambridge, England)*, 120(9), pp.2703–11.

Itoh, N. & Ornitz, D.M., 2004. Evolution of the Fgf and Fgfr gene families. *Trends in genetics : TIG*, 20(11), pp.563–9.

Itoh, N. & Ornitz, D.M., 2011. Fibroblast growth factors: From molecular evolution to roles in development, metabolism and disease. *Journal of Biochemistry*, 149(2), pp.121–130.

Itoh, N. & Ornitz, D.M., 2008. Functional evolutionary history of the mouse Fgf gene family. *Developmental dynamics : an official publication of the American Association of Anatomists*, 237(1), pp.18–27.

Janssens, S. et al., 2010. Direct control of Hoxd1 and Irx3 expression by Wnt/beta-catenin signaling during anteroposterior patterning of the neural axis in Xenopus. *The International journal of developmental biology*, 54(10), pp.1435–42.

Jessell, T.M., 2000. Neuronal specification in the spinal cord: inductive signals and transcriptional codes. *Nature reviews. Genetics*, 1(1), pp.20–9.

Johnson, D. & Wilkie, A.O.M., 2011. Craniosynostosis. *European Journal of Human Genetics*, 19(4), pp.369–376.

Kalinina, J. et al., 2012. The alternatively spliced acid box region plays a key role in FGF receptor autoinhibition. *Structure (London, England : 1993)*, 20(1), pp.77–88.

Kalkan, T. et al., 2009. Tumor necrosis factor-receptor-associated factor-4 is a positive regulator of transforming growth factor-beta signaling that affects neural crest formation. *Molecular biology of the cell*, 20(14), pp.3436–50.

Karpinka, J.B. et al., 2014. Xenbase, the Xenopus model organism database; new virtualized system, data types and genomes. *Nucleic acids research*, 43(Database issue), pp.D756–63.

Katoh, M. & Katoh, M., 2006. FGF signaling inhibitor, SPRY4, is evolutionarily conserved target of WNT signaling pathway in progenitor cells. *International Journal of Molecular Medicine*, 17, pp.529–532.

Keenan, I.D., Sharrard, R.M. & Isaacs, H. V, 2006. FGF signal transduction and the regulation of Cdx gene expression. *Developmental biology*, 299(2), pp.478–88.

Kelly, L.E., Nekkalapudi, S. & El-Hodiri, H.M., 2007. Expression of the forkhead transcription factor FoxN4 in progenitor cells in the developing Xenopus laevis retina and brain. *Gene expression patterns : GEP*, 7(3), pp.233–8.

Kennedy, M.W. et al., 2010. A co-dependent requirement of xBcl9 and Pygopus for embryonic body axis development in Xenopus. *Developmental Dynamics*, 239(October 2009), pp.271–283.

Kessaris, N. et al., 2004. Cooperation between sonic hedgehog and fibroblast growth factor/MAPK signalling pathways in neocortical precursors. *Development (Cambridge, England)*, 131(6), pp.1289–98.

Kharitonenkov, A. et al., 2005. FGF-21 as a novel metabolic regulator. *The Journal of clinical investigation*, 115(6), pp.1627–35.

Khokha, M.K. et al., 2005. Depletion of three BMP antagonists from Spemann's organizer leads to a catastrophic loss of dorsal structures. *Developmental cell*, 8(3), pp.401–11.

Kiecker, C. & Niehrs, C., 2001. A morphogen gradient of Wnt/{beta}-catenin signalling regulates anteroposterior neural patterning in Xenopus. *Development*, 128(21), pp.4189–4201.

Kim, G.S. et al., 2015. Cdc6 localizes to S- and G2-phase centrosomes in a cell cycle-dependent manner. *Biochemical and biophysical research communications*, 456(3), pp.763–7.

Kim, S. et al., 2011. Nde1-mediated inhibition of ciliogenesis affects cell cycle re-entry. *Nature cell biology*, 13(4), pp.351–60.

Kim, Y.-J. et al., 2015. Xenopus laevis FGF receptor substrate 3 (XFrs3) is important for eye development and mediates Pax6 expression in lens placode through its Shp2-binding sites. *Developmental biology*, 397(1), pp.129–39.

Kimelman, D. & Kirschner, M., 1987. Synergistic induction of mesoderm by FGF and TGF-beta and the identification of an mRNA coding for FGF in the early Xenopus embryo. *Cell*, 51(5), pp.869–877.

Klisch, T.J. et al., 2006. Mxi1 is essential for neurogenesis in Xenopus and acts by bridging the pan-neural and proneural genes. *Developmental biology*, 292(2), pp.470–85.

Ko, J.Y. et al., 2013. Inactivation of max-interacting protein 1 induces renal cilia disassembly through reduction in levels of intraflagellar transport 20 in polycystic kidney. *The Journal of biological chemistry*, 288(9), pp.6488–97.

Kole, D. et al., 2014. Maintenance of multipotency in human dermal fibroblasts treated with Xenopus laevis egg extract requires exogenous fibroblast growth factor-2. *Cellular reprogramming*, 16(1), pp.18–28.

Kolm, P.J. & Sive, H.L., 1995. Efficient hormone-inducible protein function in Xenopus laevis. *Developmental biology*, 171, pp.267–272.

Kolupaeva, V. & Basilico, C., 2012. Overexpression of cyclin E/CDK2 complexes overcomes FGF-induced cell cycle arrest in the presence of hypophosphorylated Rb proteins. *Cell cycle (Georgetown, Tex.)*, 11(13), pp.2557–66.

Kostrzewa, M. & Müller, U., 1998. Genomic structure and complete sequence of the human FGFR4 gene. *Mammalian Genome*, 9(2), pp.131–135.

Kouhara, H. et al., 1997. A lipid-anchored Grb2-binding protein that links FGF-receptor activation to the Ras/MAPK signaling pathway. *Cell*, 89(5), pp.693–702.

Kovalenko, D. et al., 2003. Sef inhibits fibroblast growth factor signaling by inhibiting FGFR1 tyrosine phosphorylation and subsequent ERK activation. *The Journal of biological chemistry*, 278(16), pp.14087–91.

Kretzschmar, M., Doody, J. & Massagué, J., 1997. Opposing BMP and EGF signalling pathways converge on the TGF-beta family mediator Smad1. *Nature*, 389(6651), pp.618–22.

Kroll, K.L. & Amaya, E., 1996. Transgenic Xenopus embryos from sperm nuclear transplantations reveal FGF signaling requirements during gastrulation. *Development (Cambridge, England)*, 122(1996), pp.3173–3183.

Kudoh, T. et al., 2004. Combinatorial Fgf and Bmp signalling patterns the gastrula ectoderm into prospective neural and epidermal domains. *Development (Cambridge, England)*, 131(15), pp.3581–92.

Kudoh, T., Wilson, S.W. & Dawid, I.B., 2002. Distinct roles for Fgf, Wnt and retinoic acid in posteriorizing the neural ectoderm. *Development (Cambridge, England)*, 129(18), pp.4335–46.

Kuhns, S. et al., 2013. The microtubule affinity regulating kinase MARK4 promotes axoneme extension during early ciliogenesis. *The Journal of cell biology*, 200(4), pp.505–22.

Kumano, G. & Smith, W.C., 2002. The nodal target gene Xmenf is a component of an FGF-independent pathway of ventral mesoderm induction in Xenopus. *Mechanisms of development*, 118(1-2), pp.45–56.

Kuroda, H. et al., 2005. Default neural induction: neuralization of dissociated Xenopus cells is mediated by Ras/MAPK activation. *Genes & development*, 19(9), pp.1022–7.

Kwon, H.-J. & Chung, H.-M., 2003. Yin Yang 1, a vertebrate polycomb group gene, regulates antero-posterior neural patterning. *Biochemical and biophysical research communications*, 306(4), pp.1008–13.

Kwon, T. et al., 2014. Identifying direct targets of transcription factor Rfx2 that coordinate ciliogenesis and cell movement. *Genomics Data*, 2, pp.192–194.

LaBonne, C. & Whitman, M., 1994. Mesoderm induction by activin requires FGF-mediated intracellular signals. *Development (Cambridge, England)*, 120(2), pp.463–472.

Ladher, R.K. et al., 2000. Cloning and expression of the Wnt antagonists Sfrp-2 and Frzb during chick development. *Developmental biology*, 218(2), pp.183–98.

Lai, C.J. et al., 1995. Patterning of the neural ectoderm of Xenopus laevis by the amino-terminal product of hedgehog autoproteolytic cleavage. *Development (Cambridge, England)*, 121(8), pp.2349–60.

Lai, W.-T., Krishnappa, V. & Phinney, D.G., 2011. Fgf2 Inhibits Differentiation of Mesenchymal Stem Cells by Inducing Twist2 Spry4, Blocking Extracellular Regulated Kinase Activation and Altering Fgfr Expression Levels. *Stem cells (Dayton, Ohio)*, 2, pp.1102–1111.

Lamb, T.M. & Harland, R.M., 1995. Fibroblast growth factor is a direct neural inducer, which combined with noggin generates anterior-posterior neural pattern. *Development (Cambridge, England)*, 121(11), pp.3627–36.

Lamborghini, J.E., 1980. Rohon-beard cells and other large neurons in Xenopus embryos originate during gastrulation. *The Journal of comparative neurology*, 189(2), pp.323–333.

Lanctot, A.A. et al., 2013. Spatially dependent dynamic MAPK modulation by the Nde1-Lis1-Brap complex patterns mammalian CNS. *Developmental cell*, 25(3), pp.241–55.

Lanner, F. et al., 2010. Heparan sulfation-dependent fibroblast growth factor signaling maintains embryonic stem cells primed for differentiation in a heterogeneous state. *Stem cells (Dayton, Ohio)*, 28(2), pp.191–200.

Lappin, T.R.J. et al., 2006. HOX genes: seductive science, mysterious mechanisms. *The Ulster medical journal*, 75(1), pp.23–31.

Lea, R. et al., 2009. Temporal and spatial expression of FGF ligands and receptors during Xenopus development. *Developmental dynamics : an official publication of the American Association of Anatomists*, 238(6), pp.1467–79.

Lee, J.Y. & Stearns, T., 2013. FOP is a centriolar satellite protein involved in ciliogenesis. *PloS one*, 8(3), p.e58589.

Lee, S.-Y. et al., 2012. The role of heterodimeric AP-1 protein comprised of JunD and c-Fos proteins in hematopoiesis. *The Journal of biological chemistry*, 287(37), pp.31342–8.

Lei, Y. et al., 2012. Efficient targeted gene disruption in Xenopus embryos using engineered transcription activator-like effector nucleases (TALENs). *Proceedings of the National Academy of Sciences*, 109(43), pp.17484–17489.

Li, C. et al., 2007. Dusp6 (Mkp3) is a negative feedback regulator of FGF-stimulated ERK signaling during mouse development. *Development (Cambridge, England)*, 134(1), pp.167–76.

Li, H. et al., 2009. The Sequence Alignment/Map format and SAMtools. *Bioinformatics*, 25(16), pp.2078–2079.

Li, H. & Durbin, R., 2009. Fast and accurate short read alignment with Burrows-Wheeler transform. *Bioinformatics*, 25(14), pp.1754–1760.

Li, R. et al., 2014. Isl1 and Pou4f2 form a complex to regulate target genes in developing retinal ganglion cells. *PloS one*, 9(3), p.e92105.

Lienkamp, S., Ganner, A. & Walz, G., 2012. Inversin, Wnt signaling and primary cilia. *Differentiation; research in biological diversity*, 83(2), pp.S49–55.

Lin, X. et al., 1999. Heparan sulfate proteoglycans are essential for FGF receptor signaling during Drosophila embryonic development. *Development (Cambridge, England)*, 126(17), pp.3715–23.

Lin, X. & Perrimon, N., 1999. Dally cooperates with Drosophila Frizzled 2 to transduce Wingless signalling. *Nature*, 400(6741), pp.281–4.

Linker, C. & Stern, C.D., 2004. Neural induction requires BMP inhibition only as a late step, and involves signals other than FGF and Wnt antagonists. *Development (Cambridge, England)*, 131(22), pp.5671–81.

Liu, A. et al., 2003. FGF17b and FGF18 have different midbrain regulatory properties from FGF8b or activated FGF receptors. *Development (Cambridge, England)*, 130(25), pp.6175–85.

Liu, J.-P., Laufer, E. & Jessell, T.M., 2001. Assigning the Positional Identity of Spinal Motor Neurons. *Neuron*, 32(6), pp.997–1012.

Liu, X.-J. et al., 2014. Up-regulating of RASD1 and apoptosis of DU-145 human prostate cancer cells induced by formononetin in vitro. *Asian Pacific journal of cancer prevention : APJCP*, 15(6), pp.2835–9.

Lizcano, J.M. et al., 2002. Molecular basis for the substrate specificity of NIMA-related kinase-6 (NEK6). Evidence that NEK6 does not phosphorylate the hydrophobic motif of ribosomal S6 protein kinase and serum- and glucocorticoid-induced protein kinase in vivo. *The Journal of biological chemistry*, 277(31), pp.27839–49.

Lloret-Vilaspasa, F. et al., 2010. Retinoid signalling is required for information transfer from mesoderm to neuroectoderm during gastrulation. *International Journal of Developmental Biology*, 54(December 2009), pp.599–608.

Lombardo, A., Isaacs, H. V. & Slack, J.M.W., 1998. Expression and functions of FGF-3 in Xenopus development. *International Journal of Developmental Biology*, 42, pp.1101–1107.

Lopes Floro, K. et al., 2011. Loss of Cited2 causes congenital heart disease by perturbing left-right patterning of the body axis. *Human molecular genetics*, 20(6), pp.1097–110.

López-Perrote, A. et al., 2014. Structure of Yin Yang 1 oligomers that cooperate with RuvBL1-RuvBL2 ATPases. *The Journal of biological chemistry*, 289(33), pp.22614–29.

Lüders, F. et al., 2003. Slalom encodes an adenosine 3'-phosphate 5'-phosphosulfate transporter essential for development in Drosophila. *The EMBO journal*, 22(14), pp.3635–44.

Lundin, L. et al., 2000. Selectively desulfated heparin inhibits fibroblast growth factor-induced mitogenicity and angiogenesis. *The Journal of biological chemistry*, 275(32), pp.24653–60.

Luo, T. et al., 2007. Inca: a novel p21-activated kinase-associated protein required for cranial neural crest development. *Development (Cambridge, England)*, 134(7), pp.1279–89.

Lupo, G. et al., 2005. Dorsoventral patterning of the Xenopus eye: a collaboration of Retinoid, Hedgehog and FGF receptor signaling. *Development (Cambridge, England)*, 132(7), pp.1737–48.

Maecker, H.T., Todd, S.C. & Levy, S., 1997. The tetraspanin superfamily: molecular facilitators. *FASEB journal : official publication of the Federation of American Societies for Experimental Biology*, 11(6), pp.428–42.

Majumdar, D. et al., 2011. An APPL1/Akt signaling complex regulates dendritic spine and synapse formation in hippocampal neurons. *Molecular and cellular neurosciences*, 46(3), pp.633–44.

Makarenkova, H.P. et al., 2009. Differential interactions of FGFs with heparan sulfate control gradient formation and branching morphogenesis. *Science signaling*, 2(88), p.ra55.

Manzanares, M. et al., 1999. The role of kreisler in segmentation during hindbrain development. *Developmental biology*, 211(2), pp.220–37.

Marchal, L. et al., 2009. BMP inhibition initiates neural induction via FGF signaling and Zic genes. *Proceedings of the National Academy of Sciences of the United States of America*, 106(41), pp.17437–42.

Marguerat, S. & Bähler, J., 2010. RNA-seq: From technology to biology. *Cellular and Molecular Life Sciences*, 67, pp.569–579.

Marics, I. et al., 2002. FGFR4 signaling is a necessary step in limb muscle differentiation. *Development*, 129(19), pp.4559–4569.

Marín, F. & Charnay, P., 2000. Positional regulation of Krox-20 and mafB/kr expression in the developing hindbrain: potentialities of prospective rhombomeres. *Developmental biology*, 218(2), pp.220–234.

Marín, O., 2012. Interneuron dysfunction in psychiatric disorders. *Nature reviews. Neuroscience*, 13(2), pp.107–20.

Marioni, J.C. et al., 2008. RNA-seq : An assessment of technical reproducibility and comparison with gene expression arrays. , pp.1509–1517.

Martin, B.L. & Kimelman, D., 2009. Regulation of canonical Wnt signaling by Brachury is essential for posterior mesoderm formation. *Dev. Cell*, 15(1), pp.121–133.

Martinez, S. et al., 1999. FGF8 induces formation of an ectopic isthmic organizer and isthmocerebellar development via a repressive effect on Otx2 expression. *Development (Cambridge, England)*, 126(6), pp.1189–200.

Martinez, S., Wassef, M. & Alvarado-Mallart, R.M., 1991. Induction of a mesencephalic phenotype in the 2-day-old chick prosencephalon is preceded by the early expression of the homeobox gene en. *Neuron*, 6(6), pp.971–81.

Martín-Ibáñez, R. et al., 2012. Helios transcription factor expression depends on Gsx2 and Dlx1&2 function in developing striatal matrix neurons. *Stem cells and development*, 21(12), pp.2239–51.

Martynoga, B. et al., 2005. Foxg1 is required for specification of ventral telencephalon and region-specific regulation of dorsal telencephalic precursor proliferation and apoptosis. *Developmental biology*, 283(1), pp.113–27.

Martynova, N. et al., 2004. Patterning the forebrain: FoxA4a/Pintallavis and Xvent2 determine the posterior limit of Xanf1 expression in the neural plate. *Development (Cambridge, England)*, 131(10), pp.2329–38.

Matsuda, K. & Kondoh, H., 2014. Dkk1-dependent inhibition of Wnt signaling activates Hesx1 expression through its 5' enhancer and directs forebrain precursor development. *Genes to cells : devoted to molecular & cellular mechanisms*, 19(5), pp.374–85.

Maves, L., Jackman, W. & Kimmel, C.B., 2002. FGF3 and FGF8 mediate a rhombomere 4 signaling activity in the zebrafish hindbrain. *Development (Cambridge, England)*, 129(16), pp.3825–3837.

May-Simera, H.L. et al., 2010. Bbs8, together with the planar cell polarity protein Vangl2, is required to establish left-right asymmetry in zebrafish. *Developmental biology*, 345(2), pp.215–25.

McGrath, J. et al., 2003. Two populations of node monocilia initiate left-right asymmetry in the mouse. *Cell*, 114(1), pp.61–73.

McGrew, L.L., Hoppler, S. & Moon, R.T., 1997. Wnt and FGF pathways cooperatively pattern anteroposterior neural ectoderm in Xenopus. *Mechanisms of Development*, 69(1-2), pp.105–114.

McKay, M.M. & Morrison, D.K., 2007. Integrating signals from RTKs to ERK/MAPK. *Oncogene*, 26(2007), pp.3113–3121.

McMahon, A.P. & Moon, R.T., 1989. Ectopic expression of the proto-oncogene int-1 in Xenopus embryos leads to duplication of the embryonic axis. *Cell*, 58(6), pp.1075–84.

McMahon, J.A. et al., 1998. Noggin-mediated antagonism of BMP signaling is required for growth and patterning of the neural tube and somite. *Genes & development*, 12(10), pp.1438–52.

Meyers, E.N. & Martin, G.R., 1999. Differences in left-right axis pathways in mouse and chick: functions of FGF8 and SHH. *Science (New York, N.Y.)*, 285(5426), pp.403–6.

Mi, H., Muruganujan, A. & Thomas, P.D., 2013. PANTHER in 2013: modeling the evolution of gene function, and other gene attributes, in the context of phylogenetic trees. *Nucleic acids research*, 41(Database issue), pp.D377–86.

Miller, J.C. et al., 2011. A TALE nuclease architecture for efficient genome editing. *Nature biotechnology*, 29(2), pp.143–8.

Min, T.H. et al., 2011. The dual regulator Sufu integrates Hedgehog and Wnt signals in the early Xenopus embryo. *Developmental biology*, 358(1), pp.262–76.

Mitsiadis, T.A. et al., 2010. BMPs and FGFs target Notch signalling via jagged 2 to regulate tooth morphogenesis and cytodifferentiation. *Development (Cambridge, England)*, 137(18), pp.3025–35.

Mlodzik, M. & Gehring, W.J., 1987. Expression of the caudal gene in the germ line of Drosophila: Formation of an RNA and protein gradient during early embryogenesis. *Cell*, 48(3), pp.465–478.

Mohammadi, M. et al., 1991. A tyrosine-phosphorylated carboxy-terminal peptide of the fibroblast growth factor receptor (Flg) is a binding site for the SH2 domain of phospholipase C-gamma 1. *Molecular and cellular biology*, 11(10), pp.5068–78.

Mohammadi, M. et al., 1996. Identification of six novel autophosphorylation sites on fibroblast growth factor receptor 1 and elucidation of their importance in receptor activation and signal transduction. *Molecular and cellular biology*, 16(3), pp.977–89.

Mohammadi, M. et al., 1997. Structures of the tyrosine kinase domain of fibroblast growth factor receptor in complex with inhibitors. *Science (New York, N.Y.)*, 276(5314), pp.955–60.

Mohammadi, M., Olsen, S.K. & Ibrahimi, O. a, 2005. Structural basis for fibroblast growth factor receptor activation. *Cytokine & growth factor reviews*, 16(2), pp.107–37.

Moldrich, R.X. et al., 2011. Fgfr3 regulates development of the caudal telencephalon. *Developmental Dynamics*, 240(6), pp.1586–1599.

Molina, G. et al., 2009. Zebrafish chemical screening reveals an inhibitor of Dusp6 that expands cardiac cell lineages. *Nature chemical biology*, 5(9), pp.680–7.

Monsoro-Burq, A.-H., Fletcher, R.B. & Harland, R.M., 2003. Neural crest induction by paraxial mesoderm in Xenopus embryos requires FGF signals. *Development*, 130(>14), pp.3111–3124.

Montavon, T. & Soshnikova, N., 2014. Hox gene regulation and timing in embryogenesis. *Seminars in cell & developmental biology*, 34C(2014), pp.76–84.

Moody, S.A., 1987. Fates of the blastomeres of the 16-cell stage Xenopus embryo. *Developmental Biology*, 119(2), pp.560–578.

Morgan, M.J. et al., 2004. YY1 regulates the neural crest-associated slug gene in Xenopus laevis. *The Journal of biological chemistry*, 279(45), pp.46826–34.

Morozova, O. & Marra, M. a., 2008. Applications of next-generation sequencing technologies in functional genomics. *Genomics*, 92(5), pp.255–264.

Mukhopadhyay, M. et al., 2001. Dickkopf1 is required for embryonic head induction and limb morphogenesis in the mouse. *Developmental cell*, 1(3), pp.423–34.

Murato, Y. et al., 2007. Two alloalleles of Xenopus laevis hairy2 gene—evolution of duplicated gene function from a developmental perspective. *Development Genes and Evolution*, 217(9), pp.665–673.

Murgan, S. et al., 2014. FoxA4 favours notochord formation by inhibiting contiguous mesodermal fates and restricts anterior neural development in Xenopus embryos. *PloS one*, 9(10), p.e110559.

Nagalakshmi, U., Waern, K. & Snyder, M., 2010. RNA-seq: A method for comprehensive transcriptome analysis. *Current Protocols in Molecular Biology*, (SUPPL. 89), pp.1–13.

Nagano, T. et al., 2006. Shisa2 promotes the maturation of somitic precursors and transition to the segmental fate in Xenopus embryos. *Development (Cambridge, England)*, 133(23), pp.4643–54.

Nagaoka, T. et al., 2014. Vangl2 regulates E-cadherin in epithelial cells. *Scientific reports*, 4, p.6940.

Nakajima, K. & Yaoita, Y., 2015. Highly efficient gene knockout by injection of TALEN mRNAs into oocytes and host transfer in Xenopus laevis. *Biology Open*, 4(2), pp.180–185.

Nakayama, T. et al., 2013. Simple and efficient CRISPR/Cas9-mediated targeted mutagenesis in Xenopus tropicalis. *Genesis (New York, N.Y. : 2000)*, 51(12), pp.835–43.

Nauli, S.M. et al., 2003. Polycystins 1 and 2 mediate mechanosensation in the primary cilium of kidney cells. *Nature genetics*, 33(2), pp.129–37.

Neilson, K.M. et al., 2012. Specific domains of FoxD4/5 activate and repress neural transcription factor genes to control the progression of immature neural ectoderm to differentiating neural plate. *Developmental biology*, 365(2), pp.363–75.

Neilson, K.M. & Friesel, R.E., 1995. Constitutive activation of fibroblast growth factor receptor-2 by a point mutation associated with Crouzon syndrome. *The Journal of biological chemistry*, 270(22), pp.26037–26040.

Neugebauer, J.M. et al., 2009. FGF Signaling during embryo development regulates cilia length in diverse epithelia. *October*, 458(7238), pp.651–654.

Neugebauer, J.M. & Yost, H.J., 2014. FGF Signaling is Required for Brain Left-Right Asymmetry and Brain Midline Formation. *Developmental biology*, 1(3), pp.123–134.

Nichane, M. et al., 2008. Hairy2-Id3 interactions play an essential role in Xenopus neural crest progenitor specification. *Developmental biology*, 322(2), pp.355–67.

Nichane, M., Ren, X. & Bellefroid, E.J., 2010. Self-regulation of Stat3 activity coordinates cell-cycle progression and neural crest specification. *The EMBO journal*, 29(1), pp.55–67.

Nicholson, K.M. & Anderson, N.G., 2002. The protein kinase B/Akt signalling pathway in human malignancy. *Cellular Signalling*, 14(5), pp.381–395.

Nicoli, S. et al., 2005. Regulated expression pattern of gremlin during zebrafish development. *Gene expression patterns : GEP*, 5(4), pp.539–44.

Nie, X., Luukko, K. & Kettunen, P., 2006. FGF signalling in craniofacial development and developmental disorders. *Oral diseases*, 12(2), pp.102–11.

Niehrs, C. & Feld, I.N., 1999. Head in the WNT the molecular nature of Spemann ' s head organizer. , 9525(99).

Nieuwkoop, P. & Nigtevecht, G., 1954. Neural activation and transformation in explants of competent ectoderm under the influence of fragments of anterior notochord in urodeles. *Journal of Embryology and …*, 2(September), pp.175–193.

Niswander, L. et al., 1993. FGF-4 replaces the apical ectodermal ridge and directs outgrowth and patterning of the limb. *Cell*, 75(3), pp.579–87.

Nitta, K.R. et al., 2004. XSIP1 is essential for early neural gene expression and neural differentiation by suppression of BMP signaling. *Developmental biology*, 275(1), pp.258–67.

Nolte, C. & Krumlauf, R., 2000. Expression of Hox Genes in the Nervous System of Vertebrates.

Nonaka, S. et al., 1998. Randomization of left-right asymmetry due to loss of nodal cilia generating leftward flow of extraembryonic fluid in mice lacking KIF3B motor protein. *Cell*, 95(6), pp.829–37.

Nordström, U. et al., 2006. An early role for Wnt signaling in specifying neural patterns of Cdx and Hox gene expression and motor neuron subtype identity. *PLoS Biology*, 4(8), pp.1438–1452.

O'Donovan, M.C. et al., 2009. Analysis of 10 independent samples provides evidence for association between schizophrenia and a SNP flanking fibroblast growth factor receptor 2. *Molecular psychiatry*, 14(1), pp.30–6.

O'Regan, L. & Fry, A.M., 2009. The Nek6 and Nek7 protein kinases are required for robust mitotic spindle formation and cytokinesis. *Molecular and cellular biology*, 29(14), pp.3975–90.

Ohta, N. & Satou, Y., 2013. Multiple signaling pathways coordinate to induce a threshold response in a chordate embryo. *PLoS genetics*, 9(10), p.e1003818.

Oishi, I. et al., 2003. The receptor tyrosine kinase Ror2 is involved in non-canonical Wnt5a/JNK signalling pathway. *Genes to cells : devoted to molecular & cellular mechanisms*, 8(7), pp.645–54.

Okada, Y. et al., 1999. Abnormal nodal flow precedes situs inversus in iv and inv mice. *Molecular cell*, 4(4), pp.459–68.

Okada, Y. et al., 2005. Mechanism of nodal flow: a conserved symmetry breaking event in left-right axis determination. *Cell*, 121(4), pp.633–44.

Olivera-Martinez, I. & Storey, K.G., 2007. Wnt signals provide a timing mechanism for the FGF-retinoid differentiation switch during vertebrate body axis extension. *Development (Cambridge, England)*, 134(11), pp.2125–35.

Olsen, S.K. et al., 2006. Structural basis by which alternative splicing modulates the organizer activity of FGF8 in the brain. *Genes & development*, 20(2), pp.185–98.

Ong, S.H. et al., 2000. FRS2 Proteins Recruit Intracellular Signaling Pathways by Binding to Diverse Targets on Fibroblast Growth Factor and Nerve Growth Factor Receptors. *Molecular and Cellular Biology*, 20(3), pp.979–989.

Ornitz, D.M. et al., 1992. Heparin is required for cell-free binding of basic fibroblast growth factor to a soluble receptor and for mitogenesis in whole cells. *Molecular and cellular biology*, 12(1), pp.240–7.

Ornitz, D.M. & Itoh, N., 2001. Protein family review Fibroblast growth factors Gene organization and evolutionary history. *Genome*, pp.1–12.

Osipovich, A.B. et al., 2014. Insm1 promotes endocrine cell differentiation by modulating the expression of a network of genes that includes Neurog3 and Ripply3. *Development (Cambridge, England)*, 141(15), pp.2939–49.

Ossipova, O. et al., 2015. Vangl2 cooperates with Rab11 and Myosin V to regulate apical constriction during vertebrate gastrulation. *Development*, 142, pp.99–107.

Ota, S., Tonou-Fujimori, N. & Yamasu, K., 2009. The roles of the FGF signal in zebrafish embryos analyzed using constitutive activation and dominant-negative suppression of different FGF receptors. *Mechanisms of development*, 126(1-2), pp.1–17.

Paek, H., Gutin, G. & Hébert, J.M., 2009. FGF signaling is strictly required to maintain early telencephalic precursor cell survival. *Development (Cambridge, England)*, 136(14), pp.2457–65.

Paterno, G.D. et al., 2000. The VT+ and VT- isoforms of the fibroblast growth factor receptor type 1 are differentially expressed in the presumptive mesoderm of Xenopus embryos and differ in their ability to mediate mesoderm formation. *The Journal of biological chemistry*, 275(13), pp.9581–6.

Pellegrini, L. et al., 2000. Crystal structure of fibroblast growth factor receptor ectodomain bound to ligand and heparin. *Nature*, 407(6807), pp.1029–34.

Peng, Y. et al., 2006. Cold-inducible RNA binding protein is required for the expression of adhesion molecules and embryonic cell movement in Xenopus laevis. *Biochemical and biophysical research communications*, 344(1), pp.416–24.

Pera, E. & Ikeda, A., 2003. Integration of IGF, FGF, and anti-BMP signals via Smad1 phosphorylation in neural induction. *Genes & …*, (310), pp.3023–3028.

Pera, E.M. et al., 2014. Active signals, gradient formation and regional specificity in neural induction. *Experimental cell research*, 321(1), pp.25–31.

Pézeron, G. et al., 2008. Rasl11b knock down in zebrafish suppresses one-eyed-pinhead mutant phenotype. *PloS one*, 3(1), p.e1434.

Piccolo, S. et al., 1996. Dorsoventral patterning in Xenopus: inhibition of ventral signals by direct binding of chordin to BMP-4. *Cell*, 86(4), pp.589–98.

Pignatelli, M. et al., 2003. The transcription factor early growth response factor-1 (EGR-1) promotes apoptosis of neuroblastoma cells. *The Biochemical journal*, 373, pp.739–746.

Pinho, S. et al., 2011. Distinct steps of neural induction revealed by Asterix, Obelix and TrkC, genes induced by different signals from the organizer. *PloS one*, 6(4), p.e19157.

Plotnikov, A.N. et al., 2001. Crystal structure of fibroblast growth factor 9 reveals regions implicated in dimerization and autoinhibition. *The Journal of biological chemistry*, 276(6), pp.4322–9.

Pollet, N. et al., 2005. An atlas of differential gene expression during early Xenopus embryogenesis. *Mechanisms of Development*, 122(3), pp.365–439.

Pope, A.P. et al., 2010. FGFR3 expression in Xenopus laevis. *Gene Expression Patterns*, 10(2-3), pp.87–92.

Powles-Glover, N., 2014. Cilia and ciliopathies: Classic examples linking phenotype and genotype-An overview. *Reproductive Toxicology*, 48, pp.98–105.

Pownall & Isaacs, 2010. *FGF Signalling in Vertebrate Development* D. S. Kessler, ed., Morgan & Claypool Life Sciences Publishers.

Pownall, M. et al., 2003. An inducible system for the study of FGF signalling in early amphibian development. *Developmental Biology*, 256(1), pp.90–100.

Pownall, M.E. et al., 1996. eFGF, Xcad3 and Hox genes form a molecular pathway that establishes the anteroposterior axis in Xenopus. *Development (Cambridge, England)*, 122(12), pp.3881–92.

Pownall, M.E., Isaacs, H. V & Slack, J.M., 1998. Two phases of Hox gene regulation during early Xenopus development. *Current biology : CB*, 8(11), pp.673–6.

Pye, D.A. et al., 2000. Regulation of FGF-1 mitogenic activity by heparan sulfate oligosaccharides is dependent on specific structural features: differential requirements for the modulation of FGF-1 and FGF-2. *Glycobiology*, 10(11), pp.1183–1192.

Qi, H. et al., 2014. FGFR3 induces degradation of BMP type I receptor to regulate skeletal development. *Biochimica et Biophysica Acta - Molecular Cell Research*, 1843(7), pp.1237–1247.

Qin, B. et al., 2006. Sorting nexin 10 induces giant vacuoles in mammalian cells. *The Journal of biological chemistry*, 281(48), pp.36891–6.

Quarmby, L.M. & Mahjoub, M.R., 2005. Caught Nek-ing: cilia and centrioles. *Journal of cell science*, 118(Pt 22), pp.5161–9.

Raffioni, S. et al., 1999. Comparison of the intracellular signaling responses by three chimeric fibroblast growth factor receptors in PC12 cells. *Proceedings of the National Academy of Sciences of the United States of America*, 96(June), pp.7178–7183.

Ramsdell, a F. & Yost, H.J., 1998. Molecular mechanisms of vertebrate left-right development. *Trends in genetics : TIG*, 14(11), pp.459–65.

Ranft, K. et al., 2010. Evidence for structural abnormalities of the human habenular complex in affective disorders but not in schizophrenia. *Psychological medicine*, 40(4), pp.557–67.

Rapali, P. et al., 2011. DYNLL/LC8: a light chain subunit of the dynein motor complex and beyond. *The FEBS journal*, 278(17), pp.2980–96.

Rash, B.G. & Grove, E.A., 2007. Patterning the dorsal telencephalon: a role for sonic hedgehog? *The Journal of neuroscience : the official journal of the Society for Neuroscience*, 27(43), pp.11595–603.

Rebagliati, M.R. et al., 1998. Zebrafish nodal-related genes are implicated in axial patterning and establishing left-right asymmetry. *Developmental biology*, 199(2), pp.261–72.

Regan, J.C. et al., 2009. An Fgf8-dependent bistable cell migratory event establishes CNS asymmetry. *Neuron*, 61(1), pp.27–34.

Regué, L. et al., 2011. DYNLL/LC8 protein controls signal transduction through the Nek9/Nek6 signaling module by regulating Nek6 binding to Nek9. *The Journal of biological chemistry*, 286(20), pp.18118–29.

Reifers, F. et al., 1998. Fgf8 is mutated in zebrafish acerebellar (ace) mutants and is required for maintenance of midbrain-hindbrain boundary development and somitogenesis. *Development (Cambridge, England)*, 125(13), pp.2381–95.

Ren, Y. et al., 2007. Tyrosine 330 in hSef is critical for the localization and the inhibitory effect on FGF signaling. *Biochemical and biophysical research communications*, 354(3), pp.741–6.

Reversade, B. & De Robertis, E., 2005. Regulation of ADMP and BMP2/4/7 at Opposite Embroynic Poles Generates a Self-Regulating Morphogenetic Field. *Cell*, 123(6), pp.1147–1160.

Revest, J.-M., 2000. Fibroblast Growth Factor 9 Secretion Is Mediated by a Non-cleaved Amino-terminal Signal Sequence. *Journal of Biological Chemistry*, 275(11), pp.8083–8090.

Revollo, L. et al., 2015. N-cadherin restrains PTH activation of Lrp6/β-catenin signaling and osteoanabolic action. *Journal of bone and mineral research : the official journal of the American Society for Bone and Mineral Research*, 30(2), pp.274–85.

Rhinn, M. & Dollé, P., 2012. Retinoic acid signalling during development. *Development (Cambridge, England)*, 139(5), pp.843–58.

Ribisi, S. et al., 2000. Ras-mediated FGF signaling is required for the formation of posterior but not anterior neural tissue in Xenopus laevis. *Developmental biology*, 227(1), pp.183–96.

Ritchey, E.R. et al., 2010. The pattern of expression of guanine nucleotide-binding protein beta3 in the retina is conserved across vertebrate species. *Neuroscience*, 169(3), pp.1376–91.

Robbins, M.J. et al., 2000. Molecular cloning and characterization of two novel retinoic acid-inducible orphan G-protein-coupled receptors (GPRC5B and GPRC5C). *Genomics*, 67(1), pp.8–18.

Robert-Moreno, À. et al., 2010. Characterization of new otic enhancers of the pou3f4 gene reveal distinct signaling pathway regulation and spatio-temporal patterns. *PloS one*, 5(12), p.e15907.

Roche, D.D. et al., 2009. Dazap2 is required for FGF-mediated posterior neural patterning, independent of Wnt and Cdx function. *Developmental biology*, 333(1), pp.26–36.

Rodríguez Esteban, C. et al., 1999. The novel Cer-like protein Caronte mediates the establishment of embryonic left-right asymmetry. *Nature*, 401, pp.243–251.

Rogers, C.D., Ferzli, G.S. & Casey, E.S., 2011. The response of early neural genes to FGF signaling or inhibition of BMP indicate the absence of a conserved neural induction module. *BMC developmental biology*, 11, p.74.

Ryu, M.S. et al., 2004. TIS21/BTG2/PC3 is expressed through PKC-delta pathway and inhibits binding of cyclin B1-Cdc2 and its activity, independent of p53 expression. *Experimental cell research*, 299(1), pp.159–70.

Saka, Y., Tada, M. & Smith, J.., 2000. A screen for targets of the Xenopus T-box gene Xbra. *Mechanisms of Development*, 93(1-2), pp.27–39.

Santiago, Y. et al., 2008. Targeted gene knockout in mammalian cells by using engineered zinc-finger nucleases. *Proceedings of the National Academy of Sciences of the United States of America*, 105(15), pp.5809–5814.

Sasai, Y. et al., 1995. Regulation of neural induction by the Chd and Bmp-4 antagonistic patterning signals in Xenopus. *Nature*.

Sasaki, A. et al., 2003. Mammalian Sprouty4 suppresses Ras-independent ERK activation by binding to Raf1. *Nature cell biology*, 5(5), pp.427–32.

Sato, T., Araki, I. & Nakamura, H., 2001. Inductive signal and tissue responsiveness defining the tectum and the cerebellum. *Development (Cambridge, England)*, 128(13), pp.2461–9.

Sato, T., Joyner, A.L. & Nakamura, H., 2004. How does Fgf signaling from the isthmic organizer induce midbrain and cerebellum development? *Development, growth & differentiation*, 46(6), pp.487–94.

Schlessinger, J. et al., 2000. Crystal Structure of a Ternary FGF-FGFR-Heparin Complex Reveals a Dual Role for Heparin in FGFR Binding and Dimerization. *Molecular Cell*, 6(3), pp.743–750.

Schlosser, G., Koyano-Nakagawa, N. & Kintner, C., 2002. Thyroid hormone promotes neurogenesis in the Xenopus spinal cord. *Developmental Dynamics*, 225(4), pp.485–498.

Schmid-Burgk, J.L. et al., 2013. A ligation-independent cloning technique for high-throughput assembly of transcription activator–like effector genes. *Nature biotechnology*, 31(1), pp.76–81.

Schuff, M. et al., 2006. Temporal and spatial expression patterns of FoxN genes in Xenopus laevis embryos. *The International journal of developmental biology*, 50(4), pp.429–34.

Schulte-Merker, S. & Smith, J.C., 1995. Mesoderm formation in response to Brachyury requires FGF signalling. *Current Biology*, 5(1), pp.62–67.

Schweickert, A. et al., 2007. Cilia-driven leftward flow determines laterality in Xenopus. *Current biology : CB*, 17(1), pp.60–6.

Schweickert, A. et al., 2012. Linking early determinants and cilia-driven leftward flow in left-right axis specification of Xenopus laevis: a theoretical approach. *Differentiation; research in biological diversity*, 83(2), pp.S67–77.

Schweickert, A. et al., 2010. The nodal inhibitor Coco is a critical target of leftward flow in Xenopus. *Current biology : CB*, 20(8), pp.738–43.

Sdelci, S., Bertran, M.T. & Roig, J., 2011. Nek9, Nek6, Nek7 and the separation of centrosomes. *Cell Cycle*, 10, pp.3816–3817.

Selvaraj, N., Kedage, V. & Hollenhorst, P.C., 2015. Comparison of MAPK specificity across the ETS transcription factor family identifies a high-affinity ERK interaction required for ERG function in prostate cells. *Cell communication and signaling : CCS*, 13(1), p.12.

Shanmugalingam, S. et al., 2000. Ace/Fgf8 is required for forebrain commissure formation and patterning of the telencephalon. *Development (Cambridge, England)*, 127(12), pp.2549–61.

Shi, Y. et al., 2011. Common variants on 8p12 and 1q24.2 confer risk of schizophrenia. *Nature genetics*, 43(12), pp.1224–7.

Shimada, T. et al., 2004. Targeted ablation of Fgf23 demonstrates an essential physiological role of FGF23 in phosphate and vitamin D metabolism. *The Journal of clinical investigation*, 113(4), pp.561–8.

Shimamura, K. & Rubenstein, J.L., 1997. Inductive interactions direct early regionalization of the mouse forebrain. *Development (Cambridge, England)*, 124(14), pp.2709–18.

Shimizu, T., Bae, Y.-K. & Hibi, M., 2006. Cdx-Hox code controls competence for responding to Fgfs and retinoic acid in zebrafish neural tissue. *Development (Cambridge, England)*, 133(23), pp.4709–19.

Shin, D.M. et al., 2004. Loss of glutamatergic pyramidal neurons in frontal and temporal cortex resulting from attenuation of FGFR1 signaling is associated with spontaneous hyperactivity in mice. *The Journal of neuroscience : the official journal of the Society for Neuroscience*, 24(9), pp.2247–2258.

Shiotsugu, J. et al., 2004. Multiple points of interaction between retinoic acid and FGF signaling during embryonic axis formation. *Development (Cambridge, England)*, 131(11), pp.2653–67.

Sirbu, I.O. et al., 2005. Shifting boundaries of retinoic acid activity control hindbrain segmental gene expression. *Development (Cambridge, England)*, 132(11), pp.2611–22.

Sivak, J.M., Petersen, L.F. & Amaya, E., 2005. FGF signal interpretation is directed by Sprouty and Spred proteins during mesoderm formation. *Developmental cell*, 8(5), pp.689–701.

Skromne, I. et al., 2007. Repression of the hindbrain developmental program by Cdx factors is required for the specification of the vertebrate spinal cord. *Development (Cambridge, England)*, 134(11), pp.2147–2158.

Slack, J. et al., 1987a. Mesoderm induction in early Xenopus embryos by heparin-binding growth factors. *Nature*, 326(6109), pp.197–200.

Slack, J. et al., 1987b. Mesoderm induction in early Xenpus embryos by heparin-binding growth factors. *Nature*, pp.197–200. Available at: http://www.nature.com/nature/journal/v326/n6109/pdf/326197a0.pdf [Accessed December 21, 2011].

Slack, J.M. et al., 1987. Mesoderm induction in early Xenopus embryos by heparin-binding growth factors. *Nature*, 326(6109), pp.197–200.

Slack, J.M. & Forman, D., 1980. An interaction between dorsal and ventral regions of the marginal zone in early amphibian embryos. *Journal of embryology and experimental morphology*, 56, pp.283–299.

Smith, W.C. & Harland, R.M., 1992. Expression cloning of noggin, a new dorsalizing factor localized to the Spemann organizer in Xenopus embryos. *Cell*, 70(5), pp.829–40.

Sölter, M. et al., 2006. Characterization and function of the bHLH-O protein XHes2: insight into the mechanisms controlling retinal cell fate decision. *Development (Cambridge, England)*, 133, pp.4097–4108.

Spencer, D.M. et al., 1993. Controlling signal transduction with synthetic ligands. *Science (New York, N.Y.)*, 262(5136), pp.1019–1024.

Stachowiak, M.K. et al., 2003. Integrative Nuclear FGFR1 Signaling (INFS) as a Part of a Universal "Feed-Forward-And-Gate" Signaling Module That Controls Cell Growth and Differentiation. *Journal of Cellular Biochemistry*, 90(4), pp.662–691.

Stachowiak, M.K. et al., 1996. Nuclear accumulation of fibroblast growth factor receptors is regulated by multiple signals in adrenal medullary cells. *Molecular biology of the cell*, 7(8), pp.1299–317.

Stachowiak, M.K., Maher, P. a & Stachowiak, E.K., 2007. Integrative nuclear signaling in cell development--a role for FGF receptor-1. *DNA and cell biology*, 26(12), pp.811–826.

Steinberg, F. et al., 2010. The FGFRL1 receptor is shed from cell membranes, binds fibroblast growth factors (FGFs), and antagonizes FGF signaling in Xenopus embryos. *The Journal of biological chemistry*, 285(3), pp.2193–202.

Stern, C.D., 2001. Initial patterning of the central nervous system: how many organizers? *Nature reviews. Neuroscience*, 2(2), pp.92–8.

Stevens, H.E. et al., 2010. Fgfr2 is required for the development of the medial prefrontal cortex and its connections with limbic circuits. *The Journal of neuroscience : the official journal of the Society for Neuroscience*, 30(16), pp.5590–5602.

Stevens, H.E. et al., 2012. Learning and memory depend on fibroblast growth factor receptor 2 functioning in hippocampus. *Biological psychiatry*, 71(12), pp.1090–8.

Streit, a et al., 2000. Initiation of neural induction by FGF signalling before gastrulation. *Nature*, 406(6791), pp.74–8.

Streit, A. et al., 1998. Chordin regulates primitive streak development and the stability of induced neural cells, but is not sufficient for neural induction in the chick embryo. *Development (Cambridge, England)*, 125(3), pp.507–19.

Streit, A. et al., 2000. Initiation of neural induction by FGF signalling before gastrulation. *Nature*, 406(6791), pp.74–8.

Su, Y. et al., 2008. APC is essential for targeting phosphorylated beta-catenin to the SCFbeta-TrCP ubiquitin ligase. *Molecular cell*, 32(5), pp.652–61.

Subramanian, V., Meyer, B.I. & Gruss, P., 1995. Disruption of the murine homeobox gene Cdx1 affects axial skeletal identities by altering the mesodermal expression domains of Hox genes. *Cell*, 83(4), pp.641–653.

Sugimoto, K. et al., 2007. The role of XBtg2 in Xenopus neural development. *Developmental neuroscience*, 29(6), pp.468–79.

Sun, L. et al., 1999. Design, Synthesis, and Evaluations of Substituted 3-[(3- or 4-Carboxyethylpyrrol-2-yl)methylidenyl]indolin-2-ones as Inhibitors of VEGF, FGF, and PDGF Receptor Tyrosine Kinases. *Journal of Medicinal Chemistry*, 42(25), pp.5120–5130.

Sun, Z. et al., 2006. Sp5l is a mediator of Fgf signals in anteroposterior patterning of the neuroectoderm in zebrafish embryo. *Developmental dynamics : an official publication of the American Association of Anatomists*, 235(11), pp.2999–3006.

Suri, C., Haremaki, T. & Weinstein, D.C., 2005. Xema, a foxi-class gene expressed in the gastrula stage Xenopus ectoderm, is required for the suppression of mesendoderm. *Development (Cambridge, England)*, 132(12), pp.2733–42.

Sutherland, R.J., 1982. The dorsal diencephalic conduction system: a review of the anatomy and functions of the habenular complex. *Neuroscience and biobehavioral reviews*, 6(1), pp.1–13.

Suzuki, K.-I.T. et al., 2013. High efficiency TALENs enable F0 functional analysis by targeted gene disruption in Xenopus laevis embryos. *Biology open*, 2(5), pp.448–52.

Suzuki-Hirano, A., Sato, T. & Nakamura, H., 2005. Regulation of isthmic Fgf8 signal by sprouty2. *Development (Cambridge, England)*, 132(2), pp.257–65.

Takayama, H. et al., 2008. High-level expression, single-step immunoaffinity purification and characterization of human tetraspanin membrane protein CD81. *PloS one*, 3(6), p.e2314.

Takebayashi-Suzuki, K. et al., 2011. The forkhead transcription factor FoxB1 regulates the dorsal-ventral and anterior-posterior patterning of the ectoderm during early Xenopus embryogenesis. *Developmental biology*, 360(1), pp.11–29.

Tan, C.M. et al., 2013. Network2Canvas: network visualization on a canvas with enrichment analysis. *Bioinformatics (Oxford, England)*, 29(15), pp.1872–8.

Tan, M.H. et al., 2013. RNA sequencing reveals a diverse and dynamic repertoire of the Xenopus tropicalis transcriptome over development. *Genome research*, 23(1), pp.201–16.

Tanaka, H. et al., 1987. Structure of FK506, a novel immunosuppressant isolated from Streptomyces. *Journal of the American Chemical Society*, 109(16), pp.5031–5033.

Tao, W. & Lai, E., 1992. Telencephalon-restricted expression of BF-1, a new member of the HNF-3/fork head gene family, in the developing rat brain. *Neuron*, 8(5), pp.957–66.

Taylor, R.W. et al., 2010. Making a difference together: reciprocal interactions in C. elegans and zebrafish asymmetric neural development. *Development (Cambridge, England)*, 137(5), pp.681–91.

Tereshina, M.B. et al., 2014. Ras-dva1 small GTPase regulates telencephalon development in Xenopus laevis embryos by controlling Fgf8 and Agr signaling at the anterior border of the neural plate. *Biology open*, (2014), pp.1–9.

Tereshina, M.B., Zaraisky, A.G. & Novoselov, V. V, 2006. Ras-dva, a member of novel family of small GTPases, is required for the anterior ectoderm patterning in the Xenopus laevis embryo. *Development (Cambridge, England)*, 133(3), pp.485–94.

Terranova, C. et al., 2015. Global Developmental Gene Programing Involves a Nuclear Form of Fibroblast Growth Factor Receptor-1 (FGFR1). *Plos One*, 10(4), p.e0123380.

Terwisscha van Scheltinga, A.F. et al., 2013. Fibroblast growth factors in neurodevelopment and psychopathology. *The Neuroscientist : a review journal bringing neurobiology, neurology and psychiatry*, 19(5), pp.479–94.

Thomas, K.R. & Capecchi, M.R., 1990. Targeted disruption of the murine int-1 proto-oncogene resulting in severe abnormalities in midbrain and cerebellar development. *Nature*, 346(6287), pp.847–50.

Trueb, B. et al., 2003. Characterization of FGFRL1, a novel fibroblast growth factor (FGF) receptor preferentially expressed in skeletal tissues. *The Journal of biological chemistry*, 278(36), pp.33857–65.

Trumpel, S., Wiedemann, L. & Krumlauf, R., 2009. *Hox genes and the segmentation of the vertebrate hindbrain* O. Pourquié, ed., Academic Press.

Tsang, M. et al., 2002. Identification of Sef, a novel modulator of FGF signalling. *Nature cell biology*, 4(February 2002), pp.165–169.

Turner, N. & Grose, R., 2010. Fibroblast growth factor signalling: from development to cancer. *Nature reviews. Cancer*, 10(2), pp.116–29.

Twigg, S. & Burns, H., 1998. Conserved use of a non-canonical 5′ splice site (/GA) in alternative splicing by fibroblast growth factor receptors 1, 2 and 3. *Human molecular …*, 7(4), pp.685–691.

Ubbels, G. a et al., 1983. Evidence for a functional role of the cytoskeleton in determination of the dorsoventral axis in Xenopus laevis eggs. *Journal of embryology and experimental morphology*, 77, pp.15–37.

Ueno, H. et al., 1992. A Truncated Form of Fibroblast Growth Factor Receptor 1 Inhibits Signal Transduction by Multiple Types of Fibroblast Growth Factor Receptor *. , 267(3), pp.1470–1476.

Umbhauer, M. et al., 1995. Mesoderm induction in Xenopus caused by activation of MAP kinase. *Nature*, 376(6535), pp.58–62.

Umbhauer, M. et al., 2000. Signaling specificities of fibroblast growth factor receptors in early Xenopus embryo. *Journal of cell science*, 113 (Pt 1, pp.2865–75.

Vandenberg, L.N. et al., 2013. Rab GTPases are required for early orientation of the left-right axis in Xenopus. *Mechanisms of development*, 130(4-5), pp.254–71.

Vassylyev, D.G. et al., 1998. Crystal structure of troponin C in complex with troponin I fragment at 2.3-A resolution. *Proceedings of the National Academy of Sciences of the United States of America*, 95(9), pp.4847–52.

Vignali, R. et al., 2000. Xotx5b, a new member of the Otx gene family, may be involved in anterior and eye development in Xenopus laevis. *Mechanisms of development*, 96(1), pp.3–13.

Vonica, A. & Gumbiner, B.M., 2002. Zygotic Wnt activity is required for Brachyury expression in the early Xenopus laevis embryo. *Developmental biology*, 250(1), pp.112–27.

Wakioka, T. et al., 2001. Spred is a Sprouty-related suppressor of Ras signalling. *Nature*, 412(6847), pp.647–51.

Walsh, S., Margolis, S.S. & Kornbluth, S., 2003. Phosphorylation of the cyclin b1 cytoplasmic retention sequence by mitogen-activated protein kinase and Plx. *Molecular cancer research : MCR*, 1(4), pp.280–9.

Wang, S. et al., 2004. QSulf1, a heparan sulfate 6- -endosulfatase, inhibits fibroblast growth factor signaling in mesoderm O induction and angiogenesis. *PNAS*, 101(14), pp.4833–4838.

Wang, T. et al., 2012. FGFR2 is associated with bipolar disorder: a large-scale case-control study of three psychiatric disorders in the Chinese Han population. *The world journal of biological psychiatry : the official journal of the World Federation of Societies of Biological Psychiatry*, 13(8), pp.599–604.

Wang, Y., Song, L. & Zhou, C.J., 2011. The canonical Wnt/ß-catenin signaling pathway regulates Fgf signaling for early facial development. *Developmental Biology*, 349(2), pp.250–260.

Wang, Z., Gerstein, M. & Snyder, M., 2009. RNA-Seq: a revolutionary tool for transcriptomics. *Nature reviews. Genetics*, 10, pp.57–63.

Webster, M.K. & Donoghue, D.J., 1997. FGFR activation in skeletal disorders: too much of a good thing. *Trends in genetics : TIG*, 13(5), pp.178–82.

Weinstein, M. et al., 1998. FGFR-3 and FGFR-4 function cooperatively to direct alveogenesis in the murine lung. *Development (Cambridge, England)*, 125(18), pp.3615–3623.

Welm, B.E. et al., 2002. Inducible dimerization of FGFR1: development of a mouse model to analyze progressive transformation of the mammary gland. *The Journal of cell biology*, 157(4), pp.703–14.

Weninger, W.J. et al., 2005. Cited2 is required both for heart morphogenesis and establishment of the left-right axis in mouse development. *Development (Cambridge, England)*, 132(6), pp.1337–1348.

Willardsen, M. et al., 2014. The ETS transcription factor Etv1 mediates FGF signaling to initiate proneural gene expression during Xenopus laevis retinal development. *Mechanisms of development*, 131, pp.57–67.

Wills, A.E. et al., 2010. BMP antagonists and FGF signaling contribute to different domains of the neural plate in Xenopus. *Developmental biology*, 337(2), pp.335–50.

Wilson, S.I. et al., 2000. An early requirement for FGF signalling in the acquisition of neural cell fate in the chick embryo. *Current biology : CB*, 10(8), pp.421–9.

Winterbottom, E.F. & Pownall, M.E., 2009. Complementary expression of HSPG 6-O-endosulfatases and 6-O-sulfotransferase in the hindbrain of Xenopus laevis. *Gene expression patterns : GEP*, 9(3), pp.166–72.

Wolda, S., Moody, C. & Moon, R., 1993. Overlapping Expression of Xwnt-3A and Xwnt-1 in Neural Tissue of Xenopus laevis Embryos. *Developmental biology*, 155(155), pp.46–57.

Wu, L., Osmani, S.A. & Mirabito, P.M., 1998. A role for NIMA in the nuclear localization of cyclin B in Aspergillus nidulans. *The Journal of cell biology*, 141(7), pp.1575–87.

Xiang, M. & Li, S., 2013. Foxn4: A multi-faceted transcriptional regulator of cell fates in vertebrate development. *Science China. Life sciences*, pp.1–9.

Xuan, S. et al., 1995. Winged helix transcription factor BF-1 is essential for the development of the cerebral hemispheres. *Neuron*, 14(6), pp.1141–1152.

Yamagishi, M. & Okamoto, H., 2010. Competition for ligands between FGFR1 and FGFR4 regulates Xenopus neural development. *The International journal of developmental biology*, 54(1), pp.93–104.

Yamaguchi, T.P. et al., 1994. Fgfr-1 Is Required for Embryonic Growth and Mesodermal Patterning During Mouse Gastrulation. *Genes and Development*, 8(24), pp.3032–3044.

Yamamoto, A. et al., 2005. Shisa promotes head formation through the inhibition of receptor protein maturation for the caudalizing factors, Wnt and FGF. *Cell*, 120(2), pp.223–35.

Yamamoto, Y., Grubisic, K. & Oelgeschläger, M., 2007. Xenopus Tetraspanin-1 regulates gastrulation movements and neural differentiation in the early Xenopus embryo. *Differentiation; research in biological diversity*, 75(3), pp.235–45.

Yan, B., Neilson, K.M. & Moody, S.A., 2009. foxD5 plays a critical upstream role in regulating neural ectodermal fate and the onset of neural differentiation. *Developmental biology*, 329(1), pp.80–95.

Yang, W. et al., 2000. Investigating protein-ligand interactions with a mutant FKBP possessing a designed specificity pocket. *Journal of medicinal chemistry*, 43(6), pp.1135–42.

Yeh, E. et al., 2013. Novel Molecular Pathways Elicited by Mutant FGFR2 May Account for Brain Abnormalities in Apert Syndrome. *PLoS ONE*, 8(4), pp.1–7.

Yoon, J. et al., 2011. xCITED2 Induces Neural Genes in Animal Cap Explants of Xenopus Embryos. *Experimental neurobiology*, 20(3), pp.123–9.

Young, J.J. et al., 2014. Spalt-like 4 promotes posterior neural fates via repression of pou5f3 family members in Xenopus. *Development (Cambridge, England)*, 141(8), pp.1683–93.

Zhang, C. & Klymkowsky, M.W., 2007. The Sox axis, Nodal signaling, and germ layer specification. *Differentiation*, 75, pp.536–545.

Zhang, X. et al., 2006. Receptor specificity of the fibroblast growth factor family. The complete mammalian FGF family. *The Journal of biological chemistry*, 281(23), pp.15694–700.

Zhang, Y. et al., 2004. Direct cell cycle regulation by the fibroblast growth factor receptor (FGFR) kinase through phosphorylation-dependent release of Cks1 from FGFR substrate 2. *Journal of Biological Chemistry*, 279(53), pp.55348–55354.

Zhao, J. et al., 2003. An SP1-like transcription factor Spr2 acts downstream of Fgf signaling to mediate mesoderm induction. *The EMBO journal*, 22(22), pp.6078–88.

Zhao, L. et al., 2013. Reptin/Ruvbl2 is a Lrrc6/Seahorse interactor essential for cilia motility. *Proceedings of the National Academy of Sciences of the United States of America*, 110(31), pp.12697–702.

Zhao, P. et al., 2006. Fgfr4 is required for effective muscle regeneration in vivo delineation of a MyoD-Tead2-Fgfr4 transcriptional pathway. *Journal of Biological Chemistry*, 281(1), pp.429–438.

Zhao, Y. et al., 2014. A novel wnt regulatory axis in endometrioid endometrial cancer. *Cancer research*, 74(18), pp.5103–17.

Zimmerman, L.B., De Jesús-Escobar, J.M. & Harland, R.M., 1996. The Spemann organizer signal noggin binds and inactivates bone morphogenetic protein 4. *Cell*, 86(4), pp.599–606.

Zuo, J. et al., 2014. An inhibitory role of NEK6 in TGFβ/Smad signaling pathway. *BMB Reports*.